Atoms and photons

J.M. Raimond
Université Pierre et Marie Curie
Laboratoire Kastler Brossel
Département de Physique de l'Ecole Normale Supérieure
jmr@lkb.ens.fr

September 6, 2016

Table des Matières

Introduction

The atom-field interaction is certainly one of the most important problems in quantum physics at low energies. Most of the information we get on the visible universe, most of the actions we may have on it are mediated by the interactions of the atoms with the electromagnetic field. The quantum theory of these interactions, the "quantum electrodynamics" is one of the key successes of last century physics. It provides an extremely detailed insight, with an impressive compatibility with the available experimental data. For instance, the spectrum of the simplest atom, hydrogen, can be computed and compared with experiments with a precision at the 10^{-12} level, only limited by our imperfect knowledge of the structure of the proton. Quantum optics, the manipulation of fields with a few light quanta only, has also led to very impressive vindications of the most intimate aspects of quantum physics, for instance with the direct evidence of quantum non-locality in the famous experiments led by A. Aspect in the 80s.

The matter-field interaction at the quantum level has also led to a flurry of important practical applications. The laser, at the heart of the modern information society (any message on the internet at one time transits as a collection of light pulses in an optical fibre), is a direct application of our understanding of the atom-field coupling. The atomic clocks are the heart of the GPS system. Their precision is considerably improved by the cold atom and trapped ions techniques, leading to an impressive stability (in the 10^{-17} range). The cold atoms science reflects our ability to use light to change the motion of atoms. It culminates in the Bose Einstein condensation, observed for the first time in 1995. This new state of matter can be used as a fully controllable prototype of a condensed matter system. The addition of a periodic potential created by a light standing wave realizes a 'quantum simulator' of various properties (quantum phase transitions, topological phases...) too complex to be computed or modelled accurately.

These lectures will not of course cover all aspects of an extremely rich problem. We will focus on the basic aspects of quantum light-matter interaction. How does a single or a few atoms interact with near-resonant light? We will pass progressively from the simplest classical or qualitative approaches to the final explicit treatment of the interaction of a quantum atom with a quantum field.

The first Chapter will be devoted to the interaction of atoms, classically modelled as a charged harmonic oscillator, with a classical field. This model is of course extraordinarily naive, but we will see in the following Chapters that its conclusions are surprisingly close to those of fuller quantum models. We will also introduce in this Chapter the Einstein coefficients describing phenomenologically the rate of energy exchange between the atoms and the field. The consistency of this model requires the introduction of a stimulated emission process, which is at the heart of the laser (or maser) principle. We will later recover these coefficients in a more rigorous way and get insight into their validity domain.

The second Chapter will be devoted to the interaction of a quantized atom with a classical field. When this field is far off-resonance from any atomic transition, we will recover, mutatis mutandis, the basic conclusions of the charged harmonic oscillator model. At resonance, we will describe the new and important phenomenon of Rabi rotation, and discuss a few of its applications such as Ramsey interferometry, a key component of high-resolution spectral measurements. This first discussion will assume that the atom is, besides its interaction with the field, isolated from the outside world. This is never the case in practice, be it only due to the spontaneous emission phenomenon, which makes

all atomic excited states unstable (the rate of this emission will be precisely computed in Chapter 4 by a fully quantum approach).

We will thus introduce in Chapter 2 the appropriate tools for the description of quantum relaxation, or decoherence, i.e. the coupling of a quantum system to a complex reservoir at thermal equilibrium. We will do so in a framework (Kraus operators) inspired by the recent developments of quantum information theory and providing a very clear and intuitive picture of the relaxation phenomenon. We will later show how this approach leads to the standard master equation, describing the time evolution of the reduced density matrix of the atom. Equipped with these equations, we will be ready to treat the interaction of a relaxing atom with a classical field, and to establish the so-called optical Bloch equations. We will discuss a variety of applications of these equations, from high-resolution spectroscopic methods based on the saturated absorption, to electromagnetically induced transparency (EIT) and slow light.

This semi-classical approach, if extremely useful, does not tell the whole story. We now need to properly quantize the electromagnetic field. We will do so in Chapter 3. The first step is to find a convenient mode basis for the classical field, solution of the Maxwell equations with appropriate limiting conditions. We will then write the Hamiltonian of these classical modes and identify them with those of 1-dimensional harmonic oscillators. The canonical quantization of the field will then be a simple problem. We will introduce the field operators, the field energy eigenstates and the coherent states, which are the closest possible analogue of a classical field. Finally we will introduce a few pictorial representations of these states in the phase plane (the so-called Fresnel plane). We will also treat the coupling of two field modes by a semi-transparent mirror (a beam-splitter) and recognize that this simple device produces extraordinarily complex entangled quantum states. The final part of this Chapter will be devoted to the exploration of field decoherence. We will in particular show that the coherent states are particularly robust with respect to decoherence.

The final Chapter will be devoted to the interaction of a quantum field with a quantum atom, completing our initial goals. We will begin with the spontaneous emission problem and show how its rate can be precisely computed. We will also guess that the coupling of the many non-resonant field modes with the atom produces a shift of the atomic levels (the Lamb-shift). The computation of this shift is a difficult problem, that jeopardized for a long time the development of quantum electrodynamics. Any simple model leads to an infinite shift value (and there are many other infinities in simple-minded QED). The regularization of these infinities, by the techniques of renormalization, is clearly beyond the scope of these lectures. Since we will focus mainly on the interaction of a few resonant modes (laser, cavity modes) with the atom, we can indeed forget these shifts or treat them phenomenologically as a slight modification of the bare atomic levels.

We will thus turn to the central part of this Chapter, the interaction of a single nearly resonant mode with a quantum two-level atom. This situation, initially explored by Jaynes and Cummings, is a rather approximate approach to the laser-atom interaction in free space. On the contrary, it is a perfectly precise description of the Cavity Quantum Electrodynamics situation, describing the coupling of a single atom with a field contained in a mode of a high quality cavity. This domain, which originates theoretically in the 40s with a seminal remark by Purcell, has and is still undergoing a remarkable development, recognised by the Nobel prize in Physics awarded in 2012 to Serge Haroche, one of the leading pioneers of CQED.

We will thus devote a rather large part of this final Chapter to CQED, first because it is a direct application of the formalism developed in these lectures, but also because it leads to many interesting quantum situations, including the realization of some of the gedankenexperiments used by the founding fathers to assess their interpretation of the formalism.

These notes will not cover all the topics related to the atom-photon interaction. There are many excellent textbooks in the field. Let us quote Cohen-Tannoudji, Dupont-Roc and Grynberg, *An introduction to quantum electrodynamics* and *Photons and atoms*, Wiley, 1992; Cohen-Tannoudji and Guery Odelin *Advances in atomic physics: an overview*, World Scientific 2012 (these three volumes

cover all the material of these lectures), but also Schleich, *Quantum optics in phase space*, Wiley 2000; Vogel, Welsch and Wallentowitz, *Quantum optics an introduction*, Wiley 2001; Meystre and Sargent *Elements of quantum optics*, Springer 1999; Barnett and Radmore *Methods in theoretical quantum optics*, OUP, 1997; Scully and Zubairy *Quantum optics*, 1997; Loudon *Quantum theory of light*, OUP 1983. A part of this document has bee extracted from Haroche and Raimond *Exploring the quantum*, OUP 2006, which covers in details all the cavity QED final part.

Last but not least, these lecture notes are in a large part directly translated from the French version written for this same course by Claude Fabre a couple of years ago.

Chapitre 1

Classical and phenomenological approach

In this Chapter, we present two simple approaches to the atom-fied interaction. First, we will describe the interaction of a classical field with an harmonically bound charge. This is admittedly a rather naive model of an atom (often called Thomson model, and proposed at the end of the 19^{th} century when the existence of the electon was first revealed). However, we will see later that it captures many essential aspects of the interaction and that its predictions coincide rather well with those of a more refined semi-classical model.

The second part of the Chapter will be devoted to the Einstein coefficients, describing in a heuristic way the energy exchanges between matter and field. They are of course essential for the description of a laser system. We will show later that the semi-classical model based on the Optical Bloch Equations indeed coincides, in the proper limits, with this simple model.

1.1 A classical model: the harmonically bound electron

1.1.1 Equations of motion

We consider thus an atom as made of a single electron (negative charge $q = -e$, mass m, bound to the origin (we assume the atom motionless) by a harmonic force[1]. The position of the electron being $\mathbf{r}$, the equation of motion is:

$$\frac{d^2\mathbf{r}}{dt^2} + \omega_0^2\mathbf{r} = 0 \ , \tag{1.1}$$

where ω_0 is the atomic resonance frequency (about 10^{15} Hz). The solution of this equation is obviously $\mathbf{r} = \mathbf{r}_0 \exp(-i\omega_0 t)$. This is not a very physical solution. We should include some damping reflecting the finite lifetime of the excited states. We will consider here only the radiative damping, corresponding to the emission of light by the accelerated, radiating electron. We will thus be able later to compare the predictions of this simple classical model to those of the full quantum approach.

The interplay between the electronic motion and the emission of radiation by the electron is a priori complex. We can simplify it a bit by noting that the radiation damping of the electronic motion is a weak perturbation. The typical lifetime of an atomic excited state is in the 10^{-8} s range, and the quality factor of the motion is thus about 10^7. We can thus use the instantaneous power radiated by the electron, given by the Larmor formula directly deduced from the Liénart-Wichert potentials (and

[1]This harmonic force derives from an early atomic model, Thomson's "plum pudding", describing the motion of electrons – the only known atomic component at the time – in the electric field of a uniformly positively charged sphere.

assuming implicitly that the motion is not strongly affected by the radiation):

$$P = \frac{q^2 a^2}{6\pi\epsilon_0 c^3} = m\tau a^2 \ , \tag{1.2}$$

where $\mathbf{a}$ is the electron acceleration and where we introduce the characteristic time τ given by:

$$\tau = \frac{1}{6\pi\epsilon_0}\frac{q^2}{mc^3} = 6.32\,10^{-24}\ \mathrm{s}\ . \tag{1.3}$$

This time is simply related to the classical radius of the electron[2]

$$r_e = \frac{q^2}{4\pi\epsilon_0 mc^2} = 3.\,10^{-15}\,\mathrm{m} \tag{1.4}$$

by

$$r_e = \frac{3}{2}c\tau\ . \tag{1.5}$$

The time τ is thus of the order of the time needed by light to cross an electron!

In order to include radiation damping in the equations on motion, we want to get an effective force acting on the electron. We will thus write the radiated power as that of a force. Integrating the power over a time interval $[t_1, t_2]$ long at the scale of τ and long compared to the electron oscillation frequency but short on the time scale of energy dissipation, we get the energy variation as

$$\Delta\mathcal{E} = m\tau\int_{t_1}^{t_2} a^2\,dt = -m\tau\int_{t_1}^{t_2}\frac{d^2\mathbf{v}}{dt^2}\cdot\mathbf{v}\,dt + m\tau\left[\mathbf{a}\cdot\mathbf{v}\right]_{t_1}^{t_2}\ , \tag{1.6}$$

where we have performed an integration per parts. For a bounded motion, the integral term over a time long compared to the period overwhelms the last integrated term on the r.h.s. We can thus neglect this last term and we get directly the radiated power as the opposite of that of a 'radiation reaction force, $\mathbf{f}_r$:

$$\mathbf{f}_r = m\tau\frac{d\mathbf{a}}{dt}\ . \tag{1.7}$$

This radiation reaction force must be taken with a grain of salt, since it does not enter in the standard Newtonian framework: it involves the derivative of the acceleration, meaning that the initial acceleration is an important inital condition for solving the equations of motions. For instance, it is quite easy to see that a particle initially at rest with a non-zero acceleration will have a velocity increasing exponentially in time with the time constant τ. These 'runaway solutions' are totally non-physical (all approximations fail in this case of course). We may use only this force when it is a small perturbation of the motion.

Even then, it is not in a very convenient form. Assuming that the motion is nearly harmonic, we get easily $\mathbf{a} \approx -\omega_0^2\mathbf{r}$ and, hence,

$$\mathbf{f}_r = -m\tau\omega_0^2\,\frac{d\mathbf{r}}{dt}\ . \tag{1.8}$$

Injecting this approximate form in the equation of motion we get:

$$\frac{d^2\mathbf{r}}{dt^2} + \gamma\frac{d\mathbf{r}}{dt} + \omega_0^2\mathbf{r} = 0\ , \tag{1.9}$$

a standard damped harmonic oscillator motion, with:

$$\gamma = \omega_0^2\tau. \tag{1.10}$$

[2]Obtained by equating the electron mass energy mc^2 with that of a uniform spherical charge distribution with radius r_e and total charge q.

being the amplitude damping coefficient (the energy damping coefficient is obviously 2γ).

Let us compute the order of magnitude of γ. We need to get a reasonable order of magnitude of ω_0. For that, let us us inject a bit of quantum mechanics in this classical model: $\omega_0 \approx R_y/\hbar$, where R is the Rydberg constant. We then note that $R = mc^2\alpha^2/2$, where

$$\alpha = \frac{e^2}{4\pi\epsilon_0\hbar c} \approx \frac{1}{137} \tag{1.11}$$

is the dimensionless fine structure constant, measuring the strength of the electromagnetic interaction in quantum units. We have then

$$\frac{\gamma}{\omega_0} = \omega_0\tau = \frac{R\tau}{\hbar} = \frac{\alpha^3}{3} \approx 1.3\,10^{-7} \ . \tag{1.12}$$

We thus get the right order of magnitude. The quality factor of the electron motion is of the order of 10^7 (note that our choice of ω_0 corresponds to a deep-UV transition for which the lifetime is notably shorter than for the ordinary optical transitions in alkali atoms for instance). Note here that γ is the damping rate for the motion amplitude. The damping rate of the mechanical energy is twice as large.

1.1.2 Polarizability

The steady state for the free evolution is clearly an electron at rest, not a very interesting situation. We thus study now how the atom responds, in the steady state, to an oscillating electric field $E_0\mathbf{u}_z\exp(-i\omega t)$ (that of a plane wave or, more realistically, of a laser beam), where we assume without real loss of generality that the incident field is polarized along the z axis and that the amplitude E_0 is real. This field can be at a frequency different from that of the atomic oscillator. The equation of motion is now:

$$\frac{d^2\mathbf{r}}{dt^2} + \gamma\frac{d\mathbf{r}}{dt} + \omega_0^2\mathbf{r} = \frac{qE_0}{m}\mathbf{u}_z e^{-i\omega t} \ , \tag{1.13}$$

In the steady state, $\mathbf{r} = \mathbf{r}_0\exp(-i\omega t)$. We can write the oscillating dipole created by the moving electron as $\mathbf{d} = \mathbf{d}_0\exp(-i\omega t)$, with

$$\mathbf{d}_0 = q\mathbf{r}_0 = \epsilon_0\alpha_c E_0\mathbf{u}_z \ , \tag{1.14}$$

where

$$\alpha_c = \frac{q^2}{m\epsilon_0}\frac{1}{\omega_0^2 - \omega^2 - i\gamma\omega} \ , \tag{1.15}$$

is the classical polarizability of the atom at the frequency ω (note that the polarizability has the dimension of a volume). This polarizability has an evident resonant behavior around the atomic resonance frequency. We will now use this classical expression of the polarizability to discuss the diffusion of radiation by an atom, an extremely important problem practically.

1.1.3 Diffusion by an atom

The electron set in motion by the field of the incoming wave. In turn, it radiates in all directions (with the emission diagram of a dipole). The total average radiated power $\mathcal{P}$ is, according to the Larmor formula, proportional to the average square acceleration $\omega^4|r_0|^2/2$. Hence

$$\mathcal{P} = \frac{1}{2}m\tau\omega^4|r_0|^2 \ , \tag{1.16}$$

or, using the polarizability and the definition of τ

$$\mathcal{P} = \frac{\epsilon_0}{12\pi c^3}|\alpha_c|^2\omega^4 E_0^2 \tag{1.17}$$

If the incoming field is close to a plane wave, the incident power per unit surface is $\mathcal{P}_i = \epsilon_0 c E_0^2/2$. We thus define a surface as the ratio $\sigma_c = \mathcal{P}/\mathcal{P}_i$, called the diffusion cross-section:

$$\sigma_c = \frac{1}{6\pi}\left(\frac{\omega}{c}\right)^4 |\alpha_c|^2 = \frac{8\pi}{3} r_e^2 \frac{\omega^4}{(\omega_0^2 - \omega^2)^2 + \gamma^2\omega^2} \ , \tag{1.18}$$

where we have introduced again the classical electron radius, r_e.

Since γ is rather small, σ_c has a sharp resonance at the atomic frequency. We may thus distinguish three important limiting cases, corresponding to three famous diffusion regimes:

- The Rayleigh diffusion, for $\omega < \omega_0$ and $\omega_0 - \omega \gg \gamma$. We then get

$$\sigma_c = \frac{8\pi}{3} r_e^2 \frac{\omega^4}{\omega_0^4} \ . \tag{1.19}$$

  The cross section is rather small, of the order of the surface of an electron, but it increases rapidly with the frequency. This is the situation encountered in the diffusion of solar light by the atmosphere. The optical resonances of the nitrogen and oxygen molecules are mainly in the UV and the visible light is thus in the Rayleigh regime. The shorter wavelengths are diffused much more efficiently than the red, because of the ω^4 dependence. This is why the sky is blue[3] and why the solar light at sunset is red, since most of the blue has been diffused out. We can easily estimate the attenuation length of visible light in the atmosphere. With $\sigma_c \approx 10^{-30}$ m^2, a numeric density of $N = 10^{25}$ m^{-3}, the attenuation length is $L = 1/N\sigma_c \approx 100$ km, a reasonable estimate for the atmosphere thickness crossed by light at sunset.

- The Thomson diffusion corresponds instead to $\omega > \omega_0$. We then get

$$\sigma_c = \frac{8\pi}{3} r_e^2 \ . \tag{1.20}$$

  The value is small and the attenuation accordingly weak. Most materials are nearly transparent above the resonance frequency.

- The most interesting regime is of course the resonant case when $\omega \approx \omega_0$. We can use this near equality to simplify the expression of the cross section, and get finally

$$\sigma_c = \frac{8\pi}{3} r_e^2 \frac{\omega_0^2}{4(\omega_0 - \omega)^2 + \gamma^2} \ . \tag{1.21}$$

  The cross section has a Lorentzian resonance, with a width γ. At exact resonance $\omega_0 = \omega$, we get

$$\frac{8\pi}{3} r_e^2 \frac{\omega_0^2}{\gamma^2} \ . \tag{1.22}$$

  Using the previous discussions, we note that

$$r_e \frac{\omega_0}{\gamma} = \frac{3}{2} c\tau \frac{1}{\omega_0 \tau} = \frac{3}{4\pi}\lambda_0 \ , \tag{1.23}$$

  where $\lambda_0 = 2\pi c/\omega_0$ is the wavelength of the resonant radiation. Hence

$$\sigma_c = \frac{3}{2\pi}\lambda_0^2 \ . \tag{1.24}$$

[3] It is not that a simple phenomenon. The short scale fluctuations of the density of air at the normal pressure play an important role to understand why the sky is diffusing at all.

The cross section is close to the square of the resonant wavelength, much larger than the size of the electron, or even than that of the atom. An atomic vapour is thus expected to be quite opaque close to resonance, since the distance between atoms is typically much less than λ_0. The present model has however a limited validity at resonance; Being purely linear, is assumes that the atom can radiate as much power as we send inside the cross section area. This is far from being true, as we will see in the next Chapter. Nevertheless, this classical order of magnitude estimate is correct as long as the radiated power remains small compared to what we will call the 'saturation power', corresponding roughly to the diffusion of photons at a rate γ. The order of magnitude of the saturation intensity is a milli-Watt per square centimetre.

1.1.4 Propagation in matter

Before switching to the Einstein's coefficients, we will use the atomic classical polarizability to discuss briefly the propagation of a field in matter. This will provide us with an insight in the loss/gain phenomenon that will be useful for the next Section. Let us first recall the basics of Maxwell equations in matter. We neglect here the magnetic properties of the matter (magnetic effects are generally quite small unless the matter is a ferromagnet, generally not very transparent). The electric displacement $\mathbf{D}$ is

$$\mathbf{D} = \epsilon_0 \mathbf{E} + \mathbf{P} \ , \tag{1.25}$$

where $\mathbf{P}$ is the density of polarization of the bound charges. For a collection of independent molecules at a low enough numerical density N (so that the field produced on each molecule by its neighbours is much smaller than the incident field), we have $\mathbf{P} = \epsilon_0 \chi_c \mathbf{E}$, where $\chi_c = N\alpha_c$ is the dimensionless susceptibility. Hence, $\mathbf{D} = \epsilon_0 \epsilon_r \mathbf{E}$ where $\epsilon_r = 1 + N\alpha_c$ is the relative permittivity (note that our expressions are only valid in the $N\alpha_c \ll 1$ regime). Injecting this relation in the Maxwell equations and playing the standard tricks, we get the modified d'Alembert equation ruling the propagation of the amplitude of a wave oscillating at frequency ω:

$$\Delta \mathbf{E} + \frac{\omega^2}{c^2} \epsilon_r \mathbf{E} = 0 \ . \tag{1.26}$$

Subsituting a plane wave $\mathbf{E} = \mathbf{E}_0 \exp(i\mathbf{k}\cdot\mathbf{r})$ in this equation, we finally obtain the dispersion relation:

$$k^2 = k_0^2 \epsilon_r \ , \tag{1.27}$$

where $k_0 = \omega/c$ is the free-space propagation wavevector. We introduce the medium's refraction index n as $n = \sqrt{\epsilon_r}$ and get $k = nk_0$. Noting the real and imaginary parts of n as $n = n' + in''$ (we will use these notations for all complex quantities), we get:

$$n' = \frac{1}{\sqrt{2}} \sqrt{\epsilon_r' + \sqrt{\epsilon_r'^2 + \epsilon_r''^2}} \quad \text{and} \quad n'' = \frac{\epsilon_r''}{\sqrt{2}} \frac{1}{\sqrt{\epsilon_r' + \sqrt{\epsilon_r'^2 + \epsilon_r''^2}}} \ . \tag{1.28}$$

The real part of the wavevector and of the index correspond to the standard dispersive phase accumulation upon propagation. The imaginary part describes the exponential attenuation (or amplification) of the amplitude of the electric field. We immediately read on the previous equations that the attenuation is directly linked to the imaginary part of the polarizability (when it is real, the index is real and the amplitude constant). We can give a simple interpretation of this observation in terms of matter-field energy exchange.

In the propagation, the density of energy (energy per unit volume) given by the field to the bound charges is the scalar product of the field by the bound current density, itself the time derivative of the polarization. Noting $\mathbf{E}_0$ and $\mathbf{P}_0$ the local amplitudes of the electric field and polarization waves,

we can write the average density of energy released to the matter, $\frac{1}{2}\mathrm{Re}\,\mathbf{j}_0 \cdot \mathbf{E}_0*$, where the current $\mathbf{j}$ is $\mathbf{j} = \partial\mathbf{P}/\partial t$ and its amplitude $\mathbf{j}_0 = -i\omega\mathbf{P}_0$:

$$\mathcal{E} = \frac{1}{2}\mathrm{Re}\,\left(-i\omega\mathbf{P}_0 \cdot \mathbf{E}_0^*\right)\ , \tag{1.29}$$

where the star indicates a complex conjugation. The real part of the susceptibility disappears from this expression, as expected, and

$$\mathcal{E} = \frac{1}{2}\epsilon_0\omega\chi''|E_0|^2 = \frac{1}{2}\epsilon_0\omega N\alpha''|E_0|^2\ . \tag{1.30}$$

As expected, the energy released by the field into the matter is proportional to the imaginary part of the polarizability. For the elastically bound electron model,

$$\alpha'' = \frac{q^2}{m\epsilon_0}\frac{\gamma\omega}{(\omega_0^2-\omega^2)^2+\gamma^2\omega^2} \tag{1.31}$$

is always positive. The energy flows from the field into the matter. The field is absorbed (and in fact diffused in other directions since γ only describes here the radiation damping). Accordingly, it propagates as an evanescent field in the medium. There is no possible amplification of a light field in the steady state in our classical mode. The Laser effect is thus, as we will see in the next Chapter, a purely quantum one.

1.2 Einstein's coefficients

We give in this Section a short account of the phenomenological coefficients proposed by Einstein to describe the matter-field energy exchanges. They predict the stimulated emission process, which permits, in special conditions, the amplification of a light field in matter and, hence, the laser effect. These coefficients are also important since we will find them again as simple limiting cases of the semi-classical model in the next Chapter.

1.2.1 The three coefficients

We plan to describe the energy exchanges between matter and field. The field is contained in a box. We will forget all about the field coherence, phase information, interferences, and assume that is has a wide spectrum. In fact, Einstein used this model to describe the matter-field thermal equilibrium. The blackbody radiation has a wide spectrum and its coherence properties are clearly of no relevance. It will be entirely described by its spectral energy density u_ν. The energy per unit volume between frequencies[4] ν and $\nu + d\nu$ is $u_\nu d\nu$, and u_ν is measured in J/m^{3}Hz. We will assume, for the sake of simplicity, that this energy density is uniform across the volume of the box. The total electromagnetic energy per unit volume is $u = \int u_\nu\, d\nu$. In qualitative quantum terms, the numerical density of photons between ν and $\nu + d\nu$ is $u_\nu/h\nu$.

The matter is made up of atoms with two levels, e above g, having respective energies E_e and E_g. We assume them first to be non-degenerate, for the sake of simplicity. These levels are coupled to the field: the atom may undergo a quantum jump from e to g and release a photon (emission process) or can absorb a photon and make the transition from g to e. The resonant frequency of this transition will be denoted as $(E_e - E_g)/h = \nu_0$. The energy difference between the two levels is thus $h\nu_0$. This will be the only quantum part in our model. The constant total number (or density) of atoms is $\mathcal{N}$, the numbers of in the upper state N_e (N_g for the lower state) are normalized to $\mathcal{N}$ so that $N_e + N_g = 1$. Note that we could use as well the total number of atoms, proportional to the density since we made an homogeneity hypothesis.

[4]For historical reasons we will use here the frequencies and not the angular frequencies.

Our goal is to write a rate equation for the time evolution of the densities N_e and N_g. We have for that to consider three processes:

- **Spontaneous emission.** The atoms in the upper state e can spontaneously decay to the lower state g by emitting a photon, as in the classical model of the last section. This process occurs with a constant probability per unit time A_{eg}, that we will also denote by Γ for consistency with the next Chapters. The rate equation for the evolution of N_e under this process is thus:

$$\frac{dN_e}{dt}\Big)_{\text{spon}} = -A_{eg}N_e \ . \tag{1.32}$$

- **Absorption of radiation.** An atom can certainly absorb radiation and make a transition from the lower to the upper state. We will use here a cross section argument and assume that the probability for this transition to occur is proportional to the total power at the atomic frequency, i.e. to the spectral density of energy at the atomic frequency. Noting B_{ge} the proportionality coefficient, we can write the rate equation of N_e due to this sole process as:

$$\frac{dN_e}{dt}\Big)_{\text{abs}} = B_{ge}u_{\nu_0}N_g \ . \tag{1.33}$$

  Einstein noticed that these two processes alone (absorption and spontaneous emission) do not tell the whole story. Imagine that the radiation is near thermal equilibrium at a very high temperature T. Whatever the atomic frequency ν_0, u_{ν_0} becomes very large. The steady state of the two rate equations written so far is $N_g = 0$. All atoms are in the upper state! This is clearly not the thermal equilibrium: at a very large temperature, we expect to find only half of the atoms in e. The matter does not get in thermal equilibrium with the field. This cannot be accepted. We must thus add a third process to our list.

- **Stimulated emission.** Einstein, for the first time, supposed that a third process may cause atomic transitions. The atom can release a photon, and jump from e to g under the influence of the already present radiation, with a rate also proportional to the energy density at the atomic frequency. This is described by an additional term in the equation for N_e:

$$\frac{dN_e}{dt}\Big)_{\text{stim}} = -B_{eg}u_{\nu_0}N_e \ . \tag{1.34}$$

The rate equation for the excited state atomic density thus writes finally:

$$\frac{dN_e}{dt} = -A_{eg}N_e - B_{eg}u_{\nu_0}N_e + B_{ge}u_{\nu_0}N_g \ . \tag{1.35}$$

In this equation, only the spontaneous emission rate can be computed easily with the classical model of the radiation reaction force. We will see, however, that the condition of the matter-field thermal equilibrium results in relations between these coefficients.

1.2.2 Relations between the coefficients

Let us thus assume that the radiation and the matter (the atoms) have reached a thermal equilibrium at temperature T. The densities of atoms in e and g must thus obey the Boltzmann statistics:

$$\frac{N_e}{N_g} = e^{(E_g - E_e)/k_bT} = e^{-h\nu_0/k_bT} \ , \tag{1.36}$$

where k_b is the Boltzmann constant.

The spectral density of radiation is given at the same time by the Planck law[5]:

$$u_{\nu_0} = \frac{8\pi h {\nu_0}^3}{c^3} \frac{1}{\exp(h\nu_0/k_bT) - 1} \ . \tag{1.37}$$

In the steady state, these two equilibrium conditions plugged in Eq.(1.35) should lead to $dN_e/dt = 0$. In order to make the algebra simpler, let us first consider the $T \to \infty$ limit. Then, $u_{\nu_0} \to \infty$ and $N_e/N_g \to 1$. The spontaneous transitions are negligible in this high radiation power limit, and we immediately get that the absorption and stimulated emission coefficients are equal:

$$B_{ge} = B_{eg} = B \tag{1.38}$$

Noting for simplicity $A_{eg} = A$, we get the steady state at a finite temperature T when:

$$A + Bu_{\nu_0} = Bu_{\nu_0} e^{h\nu_0/k_bT} \tag{1.39}$$

and hence

$$u_{\nu_0} = \frac{A}{B} \frac{1}{\exp(h\nu_0/k_bT) - 1} \tag{1.40}$$

A mere comparison with Planck law immediately leads to

$$\frac{A}{B} = \frac{8\pi h {\nu_0}^3}{c^3} = \frac{8\pi h}{\lambda_0^3} \ , \tag{1.41}$$

where $\lambda_0 = c/\nu_0$ is the resonant wavelength of the transition. All the Einstein's coefficients can be deduced simply from the spontaneous emission one, a quite remarkable result.

Let us now briefly evoke the case of degenerate atomic levels. It happens quite often in atomic structure that a few quantum levels have the same energy. This is for instance the case for all magnetic sublevels of an atomic state, when no external static electric or magnetic field is applied. Let us denote by g_e and g_g the degeneracies (dimension of the energy eigenspaces) of energies E_e and E_g. The Boltzmann thermal equilibrium condition now reads $N_e/N_g = (g_e/g_g)\exp(-h\nu_0/k_bT)$. Getting to the infinite temperature limit, we find $B_{ge}/B_{eg} = g_e/g_g$. Assuming then (sometimes a gross approximation) that we can define a single spontaneous emission rate from e to g, we can compute the B coefficients from A_{eg}. We leave this to the reader as an exercise. We will not consider this purely algebraic complication any further and assume that all levels are non-degenerate in the following.

1.2.3 Stimulated emission: the laser

The novelty of Einstein's approach is the introduction of the stimulated emission. This leads naturally to the possibility of amplifying radiation by the propagation in a medium, an impossible feat in the harmonically bound charge model. Let us consider thus a plane wave at the resonant frequency ν_0 impinging on a thin slice of atoms, with the densities N_e and N_g. Let $\mathcal{P}$ be the incident power per unit surface. At the exit of the medium, the power is $\mathcal{P} + d\mathcal{P}$. The increment $d\mathcal{P}$ reflects the matter-field energy exchange. Let us assume (a good approximation for most lasers) that spontaneous emission is negligible (that u_ν is large enough so that the absorption and stimulated emission processes rule the evolution). The power increment δP is thus proportional to the difference between the stimulated emission and absorption rates. Since u_ν is obviously proportional[6] to $\mathcal{P}$, we get finally

$$d\mathcal{P} \propto \mathcal{P}(N_e - N_g) = \mathcal{P}\, D \ , \tag{1.42}$$

[5]It will be derived later in Chapter 3. We take it here as granted.

[6]In this simple model, we will give explicitly the proportionality coefficients.

where we introduce the population inversion density $D = N_e - N_g$. For a constant D, we thus find for the propagation through a macroscopic thickness of material either an exponential decrease of the power (evanescent wave) or an exponential increase (gain!).

A medium with a gain, an amplifier for light, naturally leads to the idea of a light oscillator. In the electronic realm, an amplifier can be turned into an oscillator by connecting the input to the (non-inverting) input. The same applies for Light Amplification by Stimulated Emission of Radiation (LASER). A gain medium placed between two highly reflecting mirrors (an optical cavity) will sustain a steady state oscillation as soon at the single-pass gain through the medium exceeds the round-trip losses of the cavity. Provided this threshold condition is met, the laser can produce an intense field in the steady state.

The condition to obtain a gain is that the population inversion D should be positive, i.e. that the upper level should be more populated than the lower one. It is quite clear that this population inversion condition is never met at thermal equilibrium[7]. The laser can thus operate only if we provide a fast pumping mechanism of the upper level, together with a fast drain of the population in the lower one.

There is no way to achieve that in the steady-state with a two-level structure. The most common situation is to use a four-level structure. The lower level g is then above the real ground state f and connected to it by a fast (radiative or non-radiative) damping mechanism. From the real ground state f, a pumping process (excitation by light, electronic collisions...) populates an excited state i, lying above e. A fast relaxation empties i into e. When the relaxation processes are faster than the laser-field induced transition, and when the pumping from f to i is fast enough, the level e may reach a steady-state population above that of g, achieving the condition for laser amplification. Other schemes are possible, with a three-level structure (as in the He-Ne laser), with unstable ground states (excimer lasers), or with excitations made up of annihilating particles (semiconductor lasers)

1.2.4 A simple model of laser radiation

We give here a simple model of the operation of a four-level laser. We will omit all the hairy proportionality factors and concentrate on the physical contents. The variables of interest are the population inversion D and the intra-cavity intensity I, measured for instance in terms of the volumic density of photons in the cavity, and obviously proportional to u_ν. In a four-level configuration, the level g is strongly damped and practically empty at all times. We thus have to a good approximation $D \simeq N_e$. The rate equation for the intensity is of the form:

$$\frac{dI}{dt} = -\kappa I + gID \ , \tag{1.43}$$

where the term κI models the cavity losses (for instance through one of the cavity mirrors used as an output coupler). The gain term is proportional to I (through u_{ν_0}) and to the population inversion D. The gain coefficient g encapsulates the geometry of the medium, the Einstein coefficients a.s.o. In the same vein, we can put the equation of motion of D under the form:

$$\frac{dD}{dt} = \Lambda - \Gamma D - gID \ . \tag{1.44}$$

In this equation, the first term Λ describes the pumping mechanism that populates the upper level e. The last term expresses that any gain in intensity is made at the expense of the population inversion. Finally, the mid term $-\Gamma D$ reflects the spontaneous damping of the population inversion under the action of the e state relaxation (including spontaneous emission outside of the cavity).

We thus have two coupled equations of motion and we look for a steady state. The equation for I always admits $I = 0$ as a solution. The 'laser off' condition is always possible. If $I = 0$, we get from

[7]The level degeneracies, when taken into account, do not change this fundamental conclusion.

Eq.(1.44) $D = \Lambda/\Gamma$. The population inversion rises linearly with the pumping rate Λ, an intuitive result

This operating point is fortunately not the only one. The equation of evolution of I admits a non-zero solution if $D = \kappa/g$. Plugged in the population inversion equation, this leads to:

$$I = \frac{1}{\kappa}\left(\Lambda - \frac{\Gamma\kappa}{g}\right) . \tag{1.45}$$

This solution is physically relevant only if $I \geq 0$ i.e. if

$$\Lambda \geq \Lambda_t = \frac{\Gamma\kappa}{g} . \tag{1.46}$$

For $\Lambda < \Lambda_t$, the only solution is thus $I = 0$. Above the 'laser threshold' i.e. for $\Lambda > \Lambda_t$, two solutions coexist, $I = 0$ and $I \neq 0$. A simple stability analysis shows that the $I = 0$ solution is unstable above threshold. Any small intensity fluctuations (for instance those due to the few spontaneous emission photons trapped in the cavity mode) will trigger an evolution towards the high intensity solution. It is clear that the threshold condition expresses that the laser gain exceeds the losses (due to the Γ and κ coefficients). Above the threshold, the laser intensity grows proportionally to the pumping rate. The population inversion remains constant, 'clamped' at the value $D_t = \kappa/g$. Note that our model is oversimplified. A practical laser unfortunately cannot give an infinite power when pumped infinitely strongly!

1.2.5 Properties of laser radiation

In this Einsteinian approach, we have only thought in terms of energies, in terms of number of photons. We have not taken into account the coherence properties of the light field, i.e. the phase information. This is not a lecture on lasers and we will refer the reader to the many textbooks on lasers for a more complete description. Let us just get a qualitative insight. The stimulated emission process, interpreted in terms of photons, corresponds to an atom in e emitting a photon under the influence of an incoming, 'triggering' photon. The two photons must belong to the same field mode. We will define the notion of field mode properly in Chapter 3. Let us just say that if the incoming photon is in a plane wave, the stimulated photon is also in the same plane wave. It has, whatever it means, the same frequency, phase, direction of propagation and polarization as the incoming photon. This is, by the way, a simple example of 'bosonic amplifications'. Photons are bosons and love to share the same quantum state.

The laser radiation is thus (the 'thus' is somewhat a short-cut through the complete theory) coherent. It is spatially coherent: different points in the laser beam have fixed phase relationships. The beam can thus be extremely directive, be focused in tiny spots with a size of the order of the wavelength, much smaller than those obtained with incoherent sources. The beam is also coherent in time. The optical phase can be stable over very long times, making it possible, for instance, to realize interferometers with extraordinarily long optical path differences (tens of thousand of kilometres for the gravitational wave antennas).

The lasers are powerful, up to 100s of kW for the welding and cutting lasers. Ultra-short pulses can be generated, in the fs range, with peak powers reaching in the PW range (10^{15}). WIth such powers, the atoms are immediately ionized and the electrons reach relativistic velocities in one optical period. This leads to the efficient generation of very high harmonics, due to the non-linearity of the relativistic motion.

Lasers can be ultra-stable, with linewidths now in the mHz range. This is of course instrumental for the realization of clocks based on the measurement of a very narrow optical transition. The best clock in 2014 is based on cold atoms in an optical lattice, interrogated by ultrastable lasers. It provides a frequency stability of 10^{-17} (a couple of seconds over the age of the Universe!).

Finally, semi-conductor diode laser are everywhere in our lifes, in the CD or DVD players but also in the optical fibre communication systems. Without them, there would be no internet!

Chapitre 2

Semi-classical approach

The first part of the previous Chapter proposed a classical model of atom-field interaction. It is of course quite limited and, for instance, does not predict or support the possibility of light amplification. We will go one step beyond in this Chapter by studying a semi-classical model for the matter-field coupling. We will use a classical radiation model, entirely described by the electric and magnetic time and space-dependent fields, ruled by Maxwell's equations. But we will treat the atom as a quantum object, whose energy levels are solution of the Schrödinger equation. We will obtain with this model many important results, which are valid provided the quantum nature of the field can be neglected. In a nutshell, they are valid as long as the number of photons in the field is very large and as long as the field quantum state is close to a classical one (a coherent state in technical terms, much more on that later).

The first point in this Chapter will be to get the atom-field interaction Hamiltonian. We will propose two equivalent forms, equally useful in the following. We will then briefly describe the interaction of an atom with a weak non-resonant field (whose frequency is different from that of all the atomic transitions). We will see that we recover in this way most of the results of the harmonically bound model, renewing the interest of this simple approach.

We will then turn to the more important problem of an atom interacting with a resonant field, when the atom can be safely assimilated to a two-level system. We will explore first the case of a free atom, without relaxation, and investigate the Rabi oscillation mechanism and its applications to high-precision spectroscopy and atomic interferometry (Ramsey method). We will then learn how to describe atomic relaxation, either due to spontaneous emission or to other perturbing effects.

The last part of the Chapter will then be devoted to an in-depth analysis of the interaction of an relaxing atom with a resonant field. We will derive the Optical Bloch equations (OBE) describing the evolution of the atomic density operator and review briefly a few applications.

2.1 Interaction Hamiltonian

We consider here, for the sake on simplicity, a one-electron atom (the hydrogen atom). The results we will get, for most of them, do not depend upon this assumption. They hold, within some algebraic variations, for many-electron atoms. They also hold perfectly for alkali atoms, whose outer electron is the only one taking part in optical transitions. The Hamiltonian of the free atom is

$$H_0 = \frac{P^2}{2m} + qU(\mathbf{R}) \ , \tag{2.1}$$

where $\mathbf{P}$ and $\mathbf{R}$ are the momentum and position operators of the electron (mass m, charge q)[1]. The potential U is the electrostatic Coulomb potential binding the electron to the nucleus or to the

[1] As much as possible, we will use upper case letters for the operators in the Hilbert space, and lower-case letters for the positions and momentum eigenvalues. With this convention, the definition of the position eigenstates reads $\mathbf{R}\,|\mathbf{r}\rangle = \mathbf{r}\,|\mathbf{r}\rangle$.

core (nucleus and other electrons). The eigenstates $|i\rangle$ of H_0 are defined by the eigenvalue equation $H_0 |i\rangle = E_i |i\rangle$. The ground state will be called $|g\rangle$.

We place this atom in a radiation field defined by its potential vector $\mathbf{A}(\mathbf{r}, t)$, its electric potential $\mathbf{V}(\mathbf{r}, t)$, its electric and magnetic fields $\mathbf{E}$ and $\mathbf{B}$. Obtaining the complete atom-field Hamiltonian is as simple as replacing all positions and momenta by operators in the expression of the classical Hamiltonian of a charge in an electromagnetic field, and hence:

$$H = \frac{1}{2m} \left(\mathbf{P} - q\mathbf{A}(\mathbf{R}, t)\right)^2 + qU(\mathbf{R}) + qV(\mathbf{R}) \ , \tag{2.2}$$

where $\mathbf{A}(\mathbf{R}, t)$ is the electron Hilbert space operator obtained by merely replacing $\mathbf{r}$ by $\mathbf{R}$ in the classical vector potential (there is no commutation relation problem involved in this operation). Note that we neglect, in all these expressions, the electron spin and its interaction with the incoming magnetic field. The effects of spins and magnetic fields are generally quite negligible when there is a resonance between an atomic transition and the incoming electric field.

2.1.1 Gauge choice

The Hamiltonian given by Eq.(2.2) is rather impractical. We will start simplifying it by making a proper gauge choice for the electromagnetic field.

Let us recall briefly that the fields only are physical quantities. The potentials can be changed in a gauge transformation:

$$\begin{aligned} \mathbf{A}' &\rightarrow \mathbf{A} = \mathbf{A}' + \boldsymbol{\nabla}\chi(\mathbf{r}, t) \\ V' &\rightarrow V = V' - \frac{\partial \chi}{\partial t} \ , \end{aligned} \tag{2.3}$$

where χ is an arbitrary function of space and time, without altering the physical fields. We can thus impose for our benefit an extra condition to the vector potential. In electromagnetism, it is customary to use the Lorentz gauge condition $\boldsymbol{\nabla} \cdot \mathbf{A} + (1/c^2)\partial V/\partial t$, since it is manifestly invariant in a Lorentz transformation. It is an easy exercise in vector calculus to show that whatever $\mathbf{A}', V'$, χ can be chosen to satisfy this condition.

We are dealing here with non-relativistic quantum mechanics. We do not care about Lorentz invariance and we are thus free to use the much simpler Coulomb gauge:

$$\boldsymbol{\nabla} \cdot \mathbf{A} = 0 \ , \tag{2.4}$$

(note that χ is obtained in this case by solving a Laplacian equation).

In order to explore the benefits of this gauge choice, we will introduce the time-space Fourier transform of the vector potential, $\boldsymbol{\mathcal{A}}(\mathbf{k}, \omega)$, defined by:

$$\mathbf{A}(\mathbf{r}, t) = \frac{1}{4\pi^2} \int \boldsymbol{\mathcal{A}}(\mathbf{k}, \omega) e^{i(\mathbf{k}\cdot\mathbf{r} - \omega t)} \, d\mathbf{k} d\omega \ . \tag{2.5}$$

The vector field $\boldsymbol{\mathcal{A}}(\mathbf{k}, \omega)$ can always be decomposed in a component parallel to $\mathbf{k}$, $\boldsymbol{\mathcal{A}}_\parallel$, and one perpendicular to it, $\boldsymbol{\mathcal{A}}_\perp$. The potential vector can thus itself be decomposed in a 'longitudinal' component, $\mathbf{A}_\parallel(\mathbf{r}, t)$, Fourier transform of $\boldsymbol{\mathcal{A}}_\parallel$, and a 'transverse component, $\mathbf{A}_\perp(\mathbf{r}, t)$, Fourier transform of $\boldsymbol{\mathcal{A}}_\perp$[2].

With this definition, the space-time Fourier transform of $\boldsymbol{\nabla} \cdot \mathbf{A}$ is obviously $i\mathbf{k} \cdot \boldsymbol{\mathcal{A}}$. Since it is identically zero, we deduce that the potential vector is 'transverse', its Fourier transform reducing to the $\boldsymbol{\mathcal{A}}_\perp$ component and that the vector potential is purely transverse: $\mathbf{A} = \mathbf{A}_\perp$. The electric field is a transverse vector also (in terms of its space-time Fourier transform $\boldsymbol{\mathcal{E}}$), since its divergence is zero

[2]Note that the 'longitudinal' or 'transverse' nature applies to the Fourier transforms, but has no direct simple geometrical consequence for the transverse and longitudinal potential vectors themselves.

in a place free of charge (the incoming wave is external to the electron, and the electron does not participate to it as a source).

Using the expression of the electric field:

$$\mathbf{E} = -\frac{\partial \mathbf{A}}{\partial t} - \boldsymbol{\nabla} V \ , \tag{2.6}$$

and noting that the gradient of V has a Fourier transform parallel to $\mathbf{k}$ (longitudinal), we get obviously $\boldsymbol{\nabla} V = 0$ in the Coulomb gauge. Since a constant potential does not imply any physical effect, we can finally set the potential V to zero: the electrostatic potential of an electromagnetic wave is identically zero in the Coulomb gauge.

2.1.2 $\mathbf{A} \cdot \mathbf{P}$ interaction

We now proceed to expand the $(\mathbf{P} - q\mathbf{A}(\mathbf{R}, t))^2$ quadratic term in the full Hamiltonian (2.2). We have to take care that $\mathbf{P}$ does not commute with $\mathbf{A}$, which is a function of the position operator $\mathbf{R}$. Here also, the Coulomb gauge will help us.

It is easy to show indeed that

$$[P_i, f(\mathbf{R})] = -i\hbar \frac{\partial f}{\partial R_i} \ , \tag{2.7}$$

where i stands for x, y or z. Hence,

$$\sum_i [P_i, A_i] = -i\hbar \sum_i \frac{\partial A_i}{\partial R_i} = -i\hbar \boldsymbol{\nabla} \cdot \mathbf{A} = 0 \ . \tag{2.8}$$

and

$$\mathbf{P} \cdot \mathbf{A} = \sum_i P_i A_i = \sum_i A_i P_i = \mathbf{A} \cdot \mathbf{P} \ . \tag{2.9}$$

The complete Hamiltonian can thus be written exactly as:

$$H = \frac{P^2}{2m} + qU(\mathbf{R}) - \frac{q}{m}\mathbf{P} \cdot \mathbf{A} + \frac{q^2}{2m}\mathbf{A} \cdot \mathbf{A} \ . \tag{2.10}$$

The remaining quadratic term is quite an annoyance and makes the problem extremely difficult. Fortunately, it is generally quite small compared to the term linear in $\mathbf{A}$ if the incoming wave electric field is small as compared to the static field binding the electron on its orbit (one atomic unit of electric field, about 10^{11} V/m). This is nearly always the case, except with the very high intensity lasers that we evoked in the end of the previous Chapter. We will thus, for all practical interactions of an atom with a reasonable laser, neglect the quadratic terms and write the Hamiltonian as:

$$H = H_0 - \frac{q}{m}\mathbf{P} \cdot \mathbf{A}(\mathbf{R}, t) \ . \tag{2.11}$$

The coupling term remains quite complex, since it involves both the momentum and the position operators. We can make a further simplification by performing the 'dipole approximation'. It relies on the fact that the resonant wavelength of an optical atomic transition, of the order of the micrometer, is much larger that the size of the atom itself, a fraction of a nanometre. Hence, we can assimilate the potential vector at the position of the electron to that at the centre of the atom, that we take from now on as the origin. We then get the final Hamiltonian in the in the '$\mathbf{A} \cdot \mathbf{P}$' form:

$$H = H_0 - \frac{q}{m}\mathbf{P} \cdot \mathbf{A}(0, t) \ , \tag{2.12}$$

where the coupling term is now simply proportional to the momentum operator. Note that the dipole approximation might not be valid if we study the interaction of non-resonant light with an atom. Diffusion of a X-ray radiation by an atom cannot be treated in this way, since the wavelength is of the order of the size of the atom itself.

2.1.3 D · E interaction

In the previous paragraph, we have obtained the coupling Hamiltonian in a simple form. However, it is not the most intuitive one. We are used, since the previous Chapter, to think of the atom as an electric dipole. A dipole interacts with the field by a $-\mathbf{d}\cdot\mathbf{E}$ energy. Moreover, this form of the interaction Hamiltonian would be manifestly gauge-invariant since it only involves the 'physical' field $\mathbf{E}$ and not the vector potential as before. Is there a simple way to cast the full quantum Hamiltonian under this form? In fact, there are two ways that we will expose now since they shed complementary light onto the problem.

The Göppert-Mayer transformation

We restart from the full Hamiltonian of Eq.(2.2) before switching to the Coulomb gauge, including thus the scalar potential of the incoming wave and we perform the dipole approximation on this Hamiltonian before all other operations. We thus replace the vector potential by its value at the origin, $\mathbf{A}(0,t)$[3]. We also neglect the quadratic terms.

We will be a bit more careful with the static potential, and expand it to the first order in $\mathbf{R}$ as $V = V(0,t) + \mathbf{R}\cdot\boldsymbol{\nabla}V(0,t)$. We have to include this first order terms, since the potential vector acts to order zero in $\mathbf{R}$, while a uniform electric potential (at order zero) has no effect. We can forget the uniform term in the potential, and write the electric dipole approximation Hamiltonian as:

$$H = H_0 - \frac{q}{m}\mathbf{P}\cdot\mathbf{A}(0,t) + \mathbf{D}\cdot\boldsymbol{\nabla}V \ , \tag{2.13}$$

where we introduce the dipole operator $\mathbf{D} = q\mathbf{R}$.

By choosing at this point the Coulomb gauge, we could cancel the electric potential and its gradient and recover the $\mathbf{A}\cdot\mathbf{P}$ interaction. We make instead, following Maria Göppert-Mayer, a different choice of gauge. We replace $\mathbf{A}$ by $\mathbf{A}'$ and V by V', using the gauge transformation expression Eq.(2.3) (and exchanging the roles of $\mathbf{A}$ and $\mathbf{A}'$). We chose $\chi(\mathbf{r},t)$ so that the new vector potential $\mathbf{A}'(0)$ cancels at the origin. The gauge function $\chi(\mathbf{r},t) = -\mathbf{r}\cdot\mathbf{A}(0,t)$ does the job since its gradient is precisely $-\mathbf{A}(0,t)$. The new scalar potential is then given by:

$$V' = V + \mathbf{r}\cdot\frac{\partial\mathbf{A}(0,t)}{\partial t} \ , \tag{2.14}$$

Its gradient at the origin is then simply:

$$\boldsymbol{\nabla}V'(0) = \boldsymbol{\nabla}V(0) + \frac{\partial\mathbf{A}(0,t)}{\partial t} = -\mathbf{E}(0) \ , \tag{2.15}$$

the actual electric field at the origin. In this new gauge the Hamiltonian just writes:

$$H = H_0 - \mathbf{D}\cdot\mathbf{E}(0) \ , \tag{2.16}$$

the required form for the interaction of a dipole with a field. This is the form that we will mostly use in the following (it is often more intuitive to work in terms of the position operator than in terms of the momentum one). Note that this expression is not valid outside the dipole approximation that we made at an early stage of the calculation. In the frame of this approximation, it is, once again, clearly gauge invariant.

[3]Note that the vector potential at the origin is a scalar in the atomic Hilbert space and thus commutes with the electron momentum.

Unitary transform approach

The other path to the $\mathbf{D}\cdot\mathbf{E}$ interaction does not use a gauge transformation, but a unitary basis change in the atom's Hilbert space. We start from the general Hamiltonian Eq.(2.2), switch to the Coulomb gauge (this cancels the incoming wave scalar potential), and perform the dipole approximation by replacing $\mathbf{A}(\mathbf{r},t)$ by $\mathbf{A}(0,t)$. We get finally the Hamiltonian:

$$H = \frac{1}{2m}\left(\mathbf{P} - q\mathbf{A}(0,t)\right)^2 + qU(\mathbf{R}) \ . \tag{2.17}$$

We then perform a time-dependent basis change in the Hilbert space, defined by the unitary operator $T(t)$ ($T^\dagger T = \mathbb{1}$) and changing $|\Psi\rangle$ into $\left|\widetilde{\Psi}\right\rangle = T\,|\Psi\rangle$. It is easy to show, by a mere substitution in the original Schrödinger equation, that the new wavevector evolves under the Hamiltonian:

$$\widetilde{H} = THT^\dagger + i\hbar\frac{dT}{dt}T^\dagger \tag{2.18}$$

We now choose $T(t)$ so that:

$$T\mathbf{P}T^\dagger = \mathbf{P} + q\mathbf{A}(0,t) \ , \tag{2.19}$$

which defines T as a time-dependent translation of the electron's momentum. The unitary T is thus an exponential function of the position operator:

$$T = e^{-\frac{i}{\hbar}q\mathbf{R}\cdot\mathbf{A}(0,T)} = e^{-\frac{i}{\hbar}\mathbf{D}\cdot\mathbf{A}(0,T)} \ , \tag{2.20}$$

where we get back the dipole operator. We note that

$$T\left(\mathbf{P} - q\mathbf{A}(0,t)\right)^2 T^\dagger = \mathbf{P}^2 \ , \tag{2.21}$$

and that

$$i\hbar\frac{dT}{dt}T^\dagger = \mathbf{D}\cdot\frac{d\mathbf{A}(0,T)}{dt} = -\mathbf{D}\cdot\mathbf{E}(0,t) \ , \tag{2.22}$$

since the scalar potential vanishes in the Coulomb gauge. We also observe that T does not change $U(\mathbf{R})$ since T and $\mathbf{R}$ commute. We finally obtain:

$$\widetilde{H} = H_0 - \mathbf{D}\cdot\mathbf{E}(0) \ , \tag{2.23}$$

where H_0 is the field-free Hamiltonian. We get once again the interaction in the gauge-invariant electric dipole form. We did not use here the weak field approximation (we did not neglect explicitly the A^2 term in the expansion of the Hamiltonian) and our expression is exact in the frame of the dipole approximation. It should be noted however that the unitary basis change also entails a change of all physical observables in order to predict the same measurable quantities ($O \to TOT^\dagger$) and that the non-linear terms in the potential are a priori present in these transformations. In the case of weak fields, these corrections do not contribute and we are left with an Hamiltonian fully equivalent to that of the previous paragraph.

2.2 Non-resonant interaction: Perturbative approach

Before turning to the resonant atom-field interaction, we will study in this section the interaction of the atom with a non-resonant field in a perturbative regime. We thus assume that the atom is initially ($t = 0$) in its ground state $|g\rangle$. It interacts with a weak harmonic field, whose angular frequency ω is very different from that of all transitions to excited states connected to $|g\rangle$. The population of the excited states will thus remain at all times much lower than that in $|g\rangle$. Without loss of generality,

we can assume that the incoming wave is polarized along the $\mathbf{u}_z$ axis (we can use the superposition principle to treat other polarization states) and write:

$$\mathbf{E}(0,t) = E_0 \mathbf{u}_z \cos \omega t \ . \tag{2.24}$$

Using the electric dipole form for the interaction Hamiltonian, we get $H = H_0 + H_1$ with $H_1 = -qZE_0 \cos \omega t$ (Z being the $\mathbf{u}_z$ component of the position operator). We now switch to an interaction representation with respect to H_0, defined by the free evolution operator $U_0 = \exp(-iH_0 t/\hbar)$. The Hamiltonian in this representation is $\widetilde{H} = U_0^\dagger H_1 U_0$. Let us decompose the interaction representation state vector, $\left|\widetilde{\Psi}\right\rangle$, on the basis $\{|j\rangle\}$ of the H_0 eigenstates:

$$\left|\widetilde{\Psi}\right\rangle = \sum_j \beta_j \left|j\right\rangle \ . \tag{2.25}$$

Injecting this expansion in the Schrödinger equation and taking the scalar product of both sides with a bra $\langle k|$ (also an eigenstate of H_0), we get:

$$i\hbar \frac{d\beta_k}{dt} = \sum_j \left\langle k\right| U_0^\dagger H_1 U_0 \left|j\right\rangle \beta_j \ . \tag{2.26}$$

Noting that $U_0 \left|j\right\rangle = \exp(-i\omega_j t) \left|j\right\rangle$, where $\omega_j = E_j/\hbar$ is the Bohr frequency of level $|j\rangle$, and setting $\omega_{kj} = \omega_k - \omega_j$, we get:

$$\frac{d\beta_k}{dt} = -\frac{qE_0}{i\hbar} \sum_j \ e^{i\omega_{kj}t} \left\langle k\right| Z \left|j\right\rangle \beta_j \cos \omega t \ . \tag{2.27}$$

We have thus transformed our problem in a mere set of coupled first-order differential equations. However, this is a rather impractical infinite set (and even a continuous set is we include the continuum eigenstates of H_0).

We now proceed to a first order approximation, a priori valid within our hypotheses. We assume that all the amplitudes are small, except β_g, which is close to one (and can always be assumed to be real by a proper phase choice). Thus, only one term remains in the r.h.s of the previous equation and:

$$\frac{d\beta_k}{dt} \approx -\frac{qE_0}{i\hbar} e^{i\omega_{kg}t} \left\langle k\right| Z \left|g\right\rangle \cos \omega t \ , \tag{2.28}$$

a simple differential equation whose evident solution is:

$$\beta_k(t) = \frac{qE_0}{2\hbar} \left\langle k\right| Z \left|g\right\rangle \left[\frac{e^{i(\omega_{kg}+\omega)t} - 1}{\omega_{kg} + \omega} + \frac{e^{i(\omega_{kg}-\omega)t} - 1}{\omega_{kg} - \omega} \right] \ . \tag{2.29}$$

We get the complete solution to the problem, with clear resonances at $\omega = \pm\omega_{kg}$ i.e. at all the Bohr frequencies connecting $|g\rangle$ to another level $|k\rangle$, provided that the matrix element $\langle k| Z |g\rangle$ does not vanish (selection rules).

It is instructive to compare this result with that of the classical model derived in Section 1.1. We had then computed the steady state dipole amplitude, $\mathbf{d}$, for the harmonically bound electron and defined the classical polarizability α_c by $\mathbf{d} = \epsilon_0 \alpha_c(\omega) E$. In order to compare α_c with our quantum calculation, we will estimate the average value of the dipole operator $\mathbf{D} = qZ\mathbf{u}_z = D\mathbf{u}_z$ (by symmetry the dipole operator has only a component along $\mathbf{u}_z$) in the state:

$$\left|\Psi\right\rangle = \sum_k \beta_k e^{-i\omega_k t} \left|k\right\rangle \ . \tag{2.30}$$

Note that we should quit the interaction representation for this calculation in order to get the time evolution right. We get:

$$\langle D \rangle = \sum_{\ell,k} \beta_\ell^* \beta_k e^{-i\omega_{k\ell}t} \left\langle \ell\right| qZ \left|k\right\rangle \ . \tag{2.31}$$

Keepîng only the first oder terms, including at least one β_g, this reduces to:

$$\langle D \rangle = \sum_k \beta_k e^{-i\omega_{kg}t} \langle g| qZ |k\rangle + \text{c.c.} \ . \tag{2.32}$$

Injecting finally the explicit expression of β_k and after a bit of algebra, we have:

$$\langle D \rangle = \frac{q^2 E_0}{2\hbar} \sum_k |\langle g| Z |k\rangle|^2 \left[\frac{e^{i\omega t} - e^{-i\omega_{kg}t}}{\omega_{kg} + \omega} + \frac{e^{-i\omega t} - e^{-i\omega_{kg}t}}{\omega_{kg} - \omega} + \text{c.c.} \right] \tag{2.33}$$

We get a quite complex expression, with terms evolving at the drive frequency ω and other oscillating at all the atomic Bohr frequencies ω_{kg}. The latter are clearly an artefact in our calculation. We have not introduced any damping and, hence, the excited states of our atom are everlasting. Even if we do not yet know how to treat it (much more on that later), there is a damping and the Bohr frequency terms must vanish, leaving us with an evolution only at the drive frequency, as in the classical model. This evolution is simply given by:

$$\langle D \rangle = \frac{q^2 E_0}{2\hbar} \sum_k |\langle g| Z |k\rangle|^2 \left[\frac{e^{i\omega t}}{\omega_{kg} + \omega} + \frac{e^{-i\omega t}}{\omega_{kg} - \omega} + \text{c.c.} \right] \ . \tag{2.34}$$

We define the real quantum polarizability at frequency ω, $\alpha_Q(\omega)$, by $\langle D \rangle = \epsilon_0 \alpha_Q(\omega) E_0 \cos \omega t$ and get:

$$\alpha_Q(\omega) = \frac{2q^2}{\hbar \epsilon_0} \sum_k |\langle g| Z |k\rangle|^2 \frac{\omega_{kg}}{\omega_{kg}^2 - \omega^2} \ . \tag{2.35}$$

Let us recall here the classical polarizability in the case of a non-resonant frequency and negligible damping γ (and hence in a situation where the polarizability is real):

$$\alpha_c(\omega, \omega_0) = \frac{q^2}{m\epsilon_0} \frac{1}{\omega_0^2 - \omega^2} \ , \tag{2.36}$$

where ω_0 is the classical resonance frequency.

The two expressions are very similar. In fact, the quantum polarizability appears as a weighted sum of classical polarizabilities for resonant frequencies equal to the Bohr frequencies:

$$\alpha_Q(\omega) = \sum_k f_{kg} \alpha_c(\omega, \omega_{kg}) \ , \tag{2.37}$$

where we introduce the real, positive, dimensionless 'oscillator strength':

$$f_{kg} = \frac{2m\omega_{kg}}{\hbar} |\langle g| Z |k\rangle|^2 \ . \tag{2.38}$$

In this picture, an atomic medium of numeric density N appears a a mixture of classical harmonically bound electrons with resonance frequencies ω_{kg} and densities $N f_{kg}$. All our conclusions on the propagation of light in the classical medium thus retain their validity in this perturbative semi-classical model. This picture holds, in particular, because the oscillator strengths obey the important sum rule:

$$\sum_k f_{kg} = 1 \ , \tag{2.39}$$

that we now proceed to establish. Let us rewrite f_{kg} as

$$f_{kg} = \frac{2m\omega_{kg}}{\hbar} \langle g| Z |k\rangle \langle k| Z |g\rangle \ . \tag{2.40}$$

Noting that

$$[Z, H_0] = \frac{i\hbar}{m} P_z \ , \tag{2.41}$$

(since only the momentum term in H_0 contributes to the commutator), we have

$$\langle k| P_z |g\rangle = \frac{m}{i\hbar} \langle k| ZH_0 - H_0 Z |g\rangle = -\frac{m\omega_{kg}}{i} \langle k| Z |g\rangle \ . \tag{2.42}$$

Using this relation to replace the matrix element $\langle k| Z |g\rangle$ in the oscillator strength, we get

$$f_{kg} = \frac{2}{i\hbar} \langle g| Z |k\rangle \langle k| P_z |g\rangle \ . \tag{2.43}$$

The sum over k introduces a closure relation and:

$$\sum_k f_{kg} = \frac{2}{i\hbar} \langle g| ZP_z |g\rangle \ . \tag{2.44}$$

The oscillator strength being real, the r.h.s of this equation is also real and equal to half the sum of it with its complex conjugate. Hence

$$\sum_k f_{kg} = \frac{1}{i\hbar} \langle g| ZP_z - P_z Z |g\rangle = 1 \ , \tag{2.45}$$

completing the sum rule demonstration.

2.3 Free atom and resonant field

The perturbative approach of the last Section only holds when the incoming radiation has a low intensity and is non resonant (the results boldly diverge when the incoming field hits an atomic resonance). We will now consider the experimentally very important case of a monochromatic field whose frequency ω is extremely close to that, $\omega_0 = \omega_{eg}$ of one atomic transition, between the two levels $|g\rangle$ (lower, possibly ground level) and $|e\rangle$. We will assume that these two levels are non degenerate to extract the physics without the algebraic complications of a multi-level structure.

In this situation, assuming furthermore that the atom is initially either in $|g\rangle$ or in $|e\rangle$, it is clear that all the other atomic levels play a minute role, the main effect of the incoming wave being to induce transitions between the two levels. We will first consider in this paragraph an ideal two-level atom, undergoing no relaxation mechanism and no perturbation from the outside world, besides the incoming wave of course.

2.3.1 Atomic system and interaction

Spin-$1/2$

Let us first briefly remind the notations for the quantum description of this simplified two-level atom. The Hilbert space is of dimension 2, and the system isomorphic to a spin-1/2 system placed in a constant magnetic field. We will thus assimilate $|e\rangle$ and $|g\rangle$ with the eigenstates $|+\rangle$ and $|-\rangle$ of the Pauli σ_z operator. A basis of the real vector space of Hermitian operators for the spin is the set of Pauli operators which write in matrix form in the $\{|+\rangle, |-\rangle\}$ basis:

$$\sigma_x = \begin{pmatrix} 0 & 1 \\ 1 & 0 \end{pmatrix} \ ; \qquad \sigma_y = \begin{pmatrix} 0 & -i \\ i & 0 \end{pmatrix} \ ; \qquad \sigma_z = \begin{pmatrix} 1 & 0 \\ 0 & -1 \end{pmatrix} \ ; \qquad \mathbb{1} \ . \tag{2.46}$$

Note that, in quantum information science, a quite active field worldwide, a spin-1/2 is the elementary information carrier, a qubit. In this context, the $|+\rangle$ and $|-\rangle$ states are the 'logical' states of the qubit

and are often referred to as $|0\rangle$ and $|1\rangle$. We will use from time to time these quantum information notations when useful.

All the Pauli matrices are hermitian, with square equal to $\mathbb{1}$ and are thus also unitary. They obey the standard commutation relation of angular momentum operators:

$$[\sigma_x, \sigma_y] = 2i\sigma_z \ , \tag{2.47}$$

and all the similar commutations rules obtained by a circular permutation of the indices.

We will also make use of the spin lowering and raising operators;

$$\sigma_+ = |+\rangle\langle -| = \frac{\sigma_x + i\sigma_y}{2} = \begin{pmatrix} 0 & 1 \\ 0 & 0 \end{pmatrix}; \qquad \sigma_- = |-\rangle\langle +| = \sigma_+^\dagger = \frac{\sigma_x - i\sigma_y}{2} = \begin{pmatrix} 0 & 0 \\ 1 & 0 \end{pmatrix} \ , \tag{2.48}$$

whose square is zero. They do not commute with σ_z and we have:

$$[\sigma_z, \sigma_\pm] = \pm 2\sigma_\pm \ . \tag{2.49}$$

The most general observable (within a dimensional factor), $\sigma_{\mathbf{u}}$, corresponds to the measurement of the spin component along an arbitrary direction defined by the unit vector $\mathbf{u}$ and the associate spherical coordinates angles θ and ϕ: $\mathbf{u} = (\sin\theta\cos\phi, \sin\theta\sin\phi, \cos\theta)$. It reads in matrix form:

$$\sigma_{\mathbf{u}} = \begin{pmatrix} \cos\theta & \sin\theta e^{-i\phi} \\ \sin\theta e^{i\phi} & -\cos\theta \end{pmatrix} \ , \tag{2.50}$$

and obviously coincides with the three first Pauli matrices when $\mathbf{u}$ is along one of the axes. It also squares to unity and has thus the eigenvalues ± 1 like all Pauli matrices. The corresponding eigenvectors are, within a global phase choice:

$$|+_{\mathbf{u}}\rangle = |0_{\mathbf{u}}\rangle = \cos\frac{\theta}{2}|+\rangle + \sin\frac{\theta}{2}e^{i\phi}|-\rangle \tag{2.51}$$

$$|-_{\mathbf{u}}\rangle = |1_{\mathbf{u}}\rangle = -\sin\frac{\theta}{2}e^{-i\phi}|+\rangle + \cos\frac{\theta}{2}|-\rangle \ , \tag{2.52}$$

where we have recalled the quantum logic notations.

When $\mathbf{u}$ spans all the directions, $|+_{\mathbf{u}}\rangle$ spans all accessible normalized states in the Hilbert space, within a global irrelevant phase. In fact, the most general state of a spin-1/2 is defined by two complex number, i.e. 4 real parameters. Normalization and the possibility to change at will the global phase make two of these parameters irrelevant. Only two are free, and we can use θ and ϕ. There is thus a bijection between the points on a unit sphere, the Bloch sphere, and the state of a spin-1/2 (see Fig. 2.1).

A rotation on the Bloch sphere by an angle θ around the axis defined by $\mathbf{v}$ maps a state onto another one. The corresponding unitary operator can be expressed as:

$$R_{\mathbf{v}}(\theta) = e^{-i(\theta/2)\sigma_{\mathbf{v}}} = \cos\frac{\theta}{2}\mathbb{1} - i\sin\frac{\theta}{2}\sigma_{\mathbf{v}} \ , \tag{2.53}$$

where we made use for the rightmost part that the Pauli matrices square to unity. For instance, a rotation by an angle θ around the $\mathbf{u}_z$ axis is represented by the matrix:

$$R_z(\theta) = \begin{pmatrix} e^{-i\theta/2} & 0 \\ 0 & e^{i\theta/2} \end{pmatrix} \ , \tag{2.54}$$

with the immediate and intuitive consequence that $R_z(\pi/2)|+_x\rangle = |+_y\rangle$. Note that $R_{\mathbf{v}}(2\pi) = -\mathbb{1}$, a remarkable feature of spin-1/2 systems.

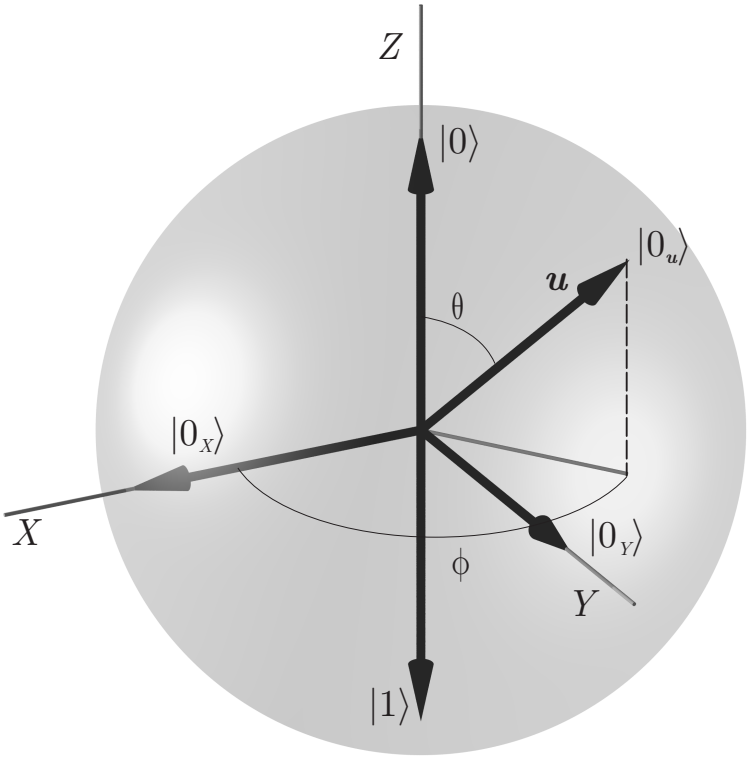

Figure 2.1: Representation of the Hilbert space of a two-level system on the Bloch sphere. Using the quantum logics notations, the $|0\rangle$ and $|1\rangle$ states correspond to the 'north' and 'south' poles respectively. The $|0_x\rangle$ and $|0_y\rangle$ states are mirrored on the 'equator' of the sphere, at its intersection with the x and y axes. The most general spin state corresponds to a point on the sphere of angular coordinates θ and ϕ.

Atomic Hamiltonian and observables

With these notations, and choosing the energy origin midway between levels $|e\rangle$ and $|g\rangle$, the atomic Hamiltonian is:

$$H_0 = \frac{\hbar\omega_{eg}}{2}\sigma_z \ . \tag{2.55}$$

The dipole operator $\mathbf{D} = q\mathbf{R}$ has no average value in the $|e\rangle$ or $|g\rangle$ state ($\mathbf{R}$ has odd parity and the atomic levels have a well-defined parity). The matrix representing $\mathbf{D}$ in the atomic Hilbert space thus reduces to non-diagonal elements (which are vectors in the real space):

$$\mathbf{D} = \begin{pmatrix} 0 & \mathbf{d} \\ \mathbf{d}^* & 0 \end{pmatrix} \ , \tag{2.56}$$

where $\mathbf{d}$ is a vector with a priori complex components describing the polarization coupled to the transition (linear, circular or elliptical in the general case). In order to keep things simple, we assume that $\mathbf{d}$ is real (corresponding, to the coupling of the transition to linearly polarized light in an arbitrary direction). The dipole thus writes

$$\mathbf{D} = \mathbf{d}\sigma_x = \mathbf{d}(\sigma_+ + \sigma_-) \ , \tag{2.57}$$

a superpositions of the atomic raising and lowering operators as we could have expected.

The incoming wave has a field $\mathbf{E}(0,t) = \mathbf{E}_0\cos(\omega t + \varphi)$ at the position of the atom, where $\mathbf{E}_0$ is a real vector amplitude. We note the complex amplitude of this field as

$$E_1 = E_0 e^{-i\varphi} \ . \tag{2.58}$$

The atom-field coupling Hamiltonian is thus, in the $\mathbf{D}\cdot\mathbf{E}$ representation:

$$H_1 = -\mathbf{d}\cdot\mathbf{E}_0\cos(\omega t + \varphi)\sigma_x \ . \tag{2.59}$$

Defining the "Rabi frequency" Ω by:

$$\Omega = \frac{\mathbf{d}\cdot\mathbf{E}_0}{\hbar} \ , \tag{2.60}$$

we get:

$$H_1 = -\hbar\Omega\cos(\omega t + \varphi)\sigma_x \ . \tag{2.61}$$

2.3.2 Rabi precession

Let us now study the evolution of the atomic system under the complete $H_0 + H_1$ Hamiltonian. The first step is to get rid of the explicit time dependence of the electric field at frequency ω. For this purpose, we first switch to an interaction representation with respect to the Hamiltonian $H_0' = \hbar\omega\sigma_z/2$. Note that this Hamiltonian differs from the atomic one by $\hbar\Delta\sigma_z/2$, with

$$\Delta = \omega_{eg} - \omega \ , \tag{2.62}$$

being the angular frequency difference between the atomic transition and the field. With these notations, the full Hamiltonian is:

$$H = H_0' + \frac{\hbar\Delta}{2}\sigma_z + H_1 \ . \tag{2.63}$$

The interaction representation is defined by the evolution operator $U'_0 = \exp(-iH'_0 t/\hbar)$. The new Hamiltonian is $\widetilde{H} = U'^{\dagger}_0 H_1 U'_0$. The σ_z part of H_1 is unchanged, since it commutes with the evolution operator. We only have thus to compute the new spin raising and lowering operators $\widetilde{\sigma}_\pm = U'^{\dagger}_0\sigma_\pm U'^0$.

Using the Baker-Hausdorff lemma:

$$e^B A e^{-B} = A + [B, A] + \frac{1}{2!}[B, [B, A]] + \dots \tag{2.64}$$

and expanding the commutators of σ_z (proportional to B) with those of $\sigma_+ = A$, we get

$$\widetilde{\sigma}_+ = \sigma_+ + i\omega t\sigma_+ + (i\omega t)^2\sigma_+ + \dots = e^{i\omega t}\sigma_+ \ , \tag{2.65}$$

a remarkably simple result. By a mere hermitian conjugation, we get:

$$\widetilde{\sigma}_- = e^{-i\omega t}\sigma_- \ , \tag{2.66}$$

The interaction representation Hamiltonian is thus

$$\widetilde{H} = \frac{\hbar\Delta}{2}\sigma_z - \frac{\hbar\Omega}{2}\left(e^{i(\omega t+\varphi)} + e^{-i(\omega t+\varphi)}\right)\left(e^{i\omega t}\sigma_+ + e^{-i\omega t}\sigma_-\right) \ . \tag{2.67}$$

Embarrassingly, it still contains a time dependence. However, when expanding the product of exponentials, we see that we get two constant terms and two terms evolving at the frequencies $\pm 2\omega$. We can thus perform a secular approximation, that will be valid as long as the Rabi frequency Ω, describing the atom-field coupling, is much smaller than the field frequency, close to the atomic transition one. We merely neglect the fast oscillating terms that, intuitively, average to zero in the Schrödinger equation. This approximation, that we will meet in a variety of contexts, is also called the "rotating wave approximation" (RWA). The name derives from the Nuclear Magnetic Resonance context. A spin rotates in a constant magnetic field at the Larmor frequency. A linearly polarized transverse magnetic field at the same frequency can induce a flip of the spin, but only the circularly polarized component rotating together with the spin is efficient in producing the effect. The other can be merely neglected[4].

With the RWA, we finally arrive at a time-independent Hamiltonian:

$$\widetilde{H} = \frac{\hbar\Delta}{2}\sigma_z - \frac{\hbar\Omega}{2}\left(\sigma_+ e^{-i\varphi} + \sigma_- e^{i\varphi}\right) = \frac{\hbar\Delta}{2}\sigma_z - \frac{\hbar\Omega}{2}\left(\sigma_x\cos\varphi + \sigma_y\sin\varphi\right) \ . \tag{2.68}$$

From the second form of the total Hamiltonian, we see clearly that it is proportional to the spin operator $\sigma_{\mathbf{n}}$ is a well defined direction:

$$H = \frac{\hbar\Omega'}{2}\sigma_{\mathbf{n}} \ , \tag{2.69}$$

with

$$\mathbf{n} = \frac{\Delta\mathbf{u}_z - \Omega\cos\varphi\mathbf{u}_x - \Omega\sin\varphi\mathbf{u}_y}{\Omega'} \ , \tag{2.70}$$

and

$$\Omega' = \sqrt{\Omega^2 + \Delta^2} \ . \tag{2.71}$$

The evolution operator $U(t)$ for a time interval t is thus

$$U(t) = e^{-i(\Omega' t/2)\sigma_{\mathbf{n}}} = R_{\mathbf{n}}(\theta) \ , \tag{2.72}$$

with

$$\theta = \Omega' t \ . \tag{2.73}$$

On the Bloch sphere, the evolution is thus simply a rotation around $\mathbf{n}$ at the angular frequency Ω', a quite simple result.

[4] In a more refined approximation, it induces a slight shift of the spin's Larmor frequency.

When the detuning Δ is much larger than the Rabi frequency Ω, the rotation axis coincides nearly with the z axis, and the rotation frequency Ω' with the detuning. If we start in one of the energy eigenstates $|e\rangle$ or $|g\rangle$, we remain there. A widely non resonant field cannot induce an atomic transfer, a quite intuitive result.

When $\Delta = 0$, the rotation frequency coincides with the Rabi frequency and the rotation axis lies in the equatorial plane of the Bloch sphere. The Bloch vector rotates on a great circle going through the two poles. When starting in $|g\rangle$, for instance, the probability for finding the atom in $|e\rangle$ at time t, $p_e(t)$, oscillates between zero and one according to:

$$p_e(t) = \frac{1 - \cos(\Omega t)}{2} \ . \tag{2.74}$$

This is the Rabi oscillation phenomenon, discovered by I.I. Rabi, immediately after WWII, in one of the first atomic radio-frequency spectroscopy experiments.

The state transformations have simple expressions for well-chosen interaction times. Let us consider for instance a so-called '$\pi/2$ pulse', i.e. $t = \pi/2\Omega$. The rotation of the Bloch vector is by $\pi/2$ around the vector:

$$\mathbf{n} = -\cos\varphi \mathbf{u}_x - \sin\varphi \mathbf{u}_y \ , \tag{2.75}$$

at an angle $\pi + \varphi$ with the Ox axis in the equatorial plane of the Bloch sphere. The evolution operator is thus the rotation:

$$R_{\mathbf{n}}(\pi/2) = \frac{1}{\sqrt{2}}(\mathbb{1} - i\sigma_{\mathbf{n}}) = \frac{1}{\sqrt{2}} \begin{pmatrix} 1 & ie^{-i\varphi} \\ ie^{i\varphi} & 1 \end{pmatrix} \ . \tag{2.76}$$

It performs the state transformations:

$$\begin{aligned} |g\rangle &\longrightarrow \frac{1}{\sqrt{2}} \left(|g\rangle + ie^{-i\varphi} |e\rangle \right) \\ |e\rangle &\longrightarrow \frac{1}{\sqrt{2}} \left(|e\rangle + ie^{i\varphi} |g\rangle \right) \ . \end{aligned} \tag{2.77}$$

This transformation prepares a superposition of $|g\rangle$ and $|e\rangle$ with equal weights and a phase defined by that of the incoming field.

For $\Omega t = \pi$ (π-pulse), we perform, within phases, an exchange of the $|e\rangle$ and $|g\rangle$ level. Finally, for $\Omega t = 2\pi$ (2π pulse), we leave the atomic state unchanged, besides the global $-$ sign associated to a 2π rotation of a spin-1/2.

When Δ and Ω are comparable, the rotation is around an axis making a non-trivial angle α (given by $\tan\alpha = \Omega'/\Delta$) with the downwards z axis and the rotation around this axis is faster than in the resonant case. It does not mean that the incident wave is more efficient in inducing transitions. Starting from $|g\rangle$, we cannot reach exactly state $|e\rangle$ whatever the interaction time.

The Bloch vector in its rotation generates a cone with an opening angle α and its maximum angle with respect to the downwards z axis is 2α. The maximum probability $p_{e,m}$ for finding the atom in $|e\rangle$ is thus $\sin^2\alpha$ and we get:

$$p_{e,m} = \frac{\Omega^2}{\Omega^2 + \Delta^2} \ . \tag{2.78}$$

The maximum transfer probability has a Lorentzian dependence versus the detuning Δ. This stresses the resonant nature of the interaction. Most spectroscopic methods are based on it, either optical spectroscopy or radiofrequency extensions, such as EPR or RMN. The width of the resonance is entirely determined by the Rabi frequency Ω and can, in principle, be made arbitrarily small.

To get an appreciable transfer from $|g\rangle$ to $|e\rangle$ at resonance, we need to perform a π pulse ($\Omega t = \pi$). For a given interrogation time τ, this leads to $\Omega = \pi/\tau$ and thus to a resonance width of the order of π/τ. We recover here a very simple Fourier analysis result: it is impossible to determine a frequency with a precision larger than π/τ for a given interrogation time τ. Translated in terms of the energy of

the transition, $\hbar\omega_{eg}$, this remark boils down to the time-energy Heisenberg uncertainty relations. Of course, in real life, relaxation process contribute to the linewidth and this optimal cannot be reached for long interaction times.

2.3.3 Ramsey separated oscillatory fields method

In order to perform a high-resolution spectroscopy experiment, the previous results suggest to apply a long interrogation pulse to the system. This method is nevertheless often quite impractical, particularly when the atoms are moving at the typical velocities of room-temperature, as in most atomic clocks.It requires a very large atom-field interaction zone and puts severe constraints on the homogeneity of the probe field.

In 1949, N. Ramsey proposed a method that circumvents most of these difficulties. It has been instrumental in the development of high-resolution atomic spectroscopy and of atomic clocks. The principle of the method is to divide a π Rabi pulse into two identical $\pi/2$ pulses, with a very short duration τ, separated by a long time interval T of free atomic evolution. Each pulse alone would result in a low resolution but their combination results in a spectroscopic resolution only limited by the total interrogation time T.

Principle of the method

We will assume that the $\pi/2$ pulses are identical and are obtained with a driving field phase $\varphi = -\pi/2$, Since their duration is very short, they are nearly resonant over a wide frequency range and we can thus assume $\Delta = 0$ to treat them. These "Ramsey pulses" induce thus, using Eq.(2.77), the state transformations:

$$|e\rangle \longrightarrow \frac{1}{\sqrt{2}}\left(|e\rangle + |g\rangle\right) \tag{2.79}$$

$$|g\rangle \longrightarrow \frac{1}{\sqrt{2}}\left(-|e\rangle + |g\rangle\right) \tag{2.80}$$

Let us now follow the atomic state through time, assuming that we initially start in the lower state $|g\rangle$. After the first pulse (duration τ), the state is $|\Psi(\tau)\rangle = (1/\sqrt{2})(-|e\rangle + |g\rangle)$. During the time T, the atomic state evolves freely. For this long duration, we cannot neglect the detuning Δ as is the case during the short Ramsey pulses. The atom evolves during this time interval under the Hamiltonian $(\hbar\Delta/2)\sigma_z$, producing the state transformations $|e\rangle \rightarrow \exp(-i\Phi/2)\,|e\rangle$ and $|g\rangle \rightarrow \exp(i\Phi/2)\,|g\rangle$, with $\Phi = \Delta t$. Within an irrelevant global phase, the state at time $T + \tau \approx T$ is thus

$$|\Psi(T)\rangle = \frac{1}{\sqrt{2}}\left(-|e\rangle + e^{i\Phi}\,|g\rangle\right) \tag{2.81}$$

The final $\pi/2$ pulse performs the same state transformations as the first. We are thus left with the final state:

$$|\Psi_f\rangle = -\frac{1}{2}\left[\left(1 + e^{i\Phi}\right)|e\rangle + \left(1 - e^{i\Phi}\right)|g\rangle\right) \tag{2.82}$$

The final probability for finding the atom in the upper state $|e\rangle$ is thus:

$$p_e = \frac{1}{4}\left(1 + e^{i\Phi}\right)^2 = \frac{1}{2}\left(1 + \cos\Delta T\right)\ . \tag{2.83}$$

It is oscillates between zero and one as a function of Δ, with a period $2\pi/T$. The spectroscopic resolution on the measurement of the atomic frequency ω_{eg} is thus of the order of $1/T$, as if a single π pulse with duration T would have been applied on the atom. This clever trick makes it possible to achieve interrogation-time limited resolution in all atomic clocks. It also allows for a precise measurement of perturbations acting on the atom during the free evolution time. The phase of the

p_e oscillations is determined by the time integral of the atom-probe field detuning over time T and reflects any shift, even a transient one, acting on the atom in-between the two Ramsey pulses.

The Ramsey method can also be viewed as an atomic interference process. The first pulse creates an atomic state superposition, and the second mixes again the two atomic levels. This is reminiscent of a Mach-Zehnder light interferometer, in which a first beam-splitter coherently splits the incoming light into two beams, later recombined by a second beam-splitter. The final interference of the two beams reflects any phase shift they undergo in their separated paths though the interferometer. Here, the paths are not separated in space, but in atomic states. There are two quantum paths leading the atom from $|g\rangle$ to $|e\rangle$, in which it makes the transition either during the first pulse or during the second. The Ramsey signal results from the quantum interference of these two paths. The names "Ramsey interferometer" and "Ramsey fringes" are thus often used to describe the method.

Signal to noise ratio

We have qualitatively estimated the precision of the atomic frequency measurement to be of the order of $1/T$ in the Ramsey interferometer. Let us make this argument more precise by considering in more details the detection statistical noise problem.

We will assume that we send N independent atoms through the interferometer. Let us call N_e the number of atom detected in $|e\rangle$, an obviously random quantity. The mean number of atoms detected in $|e\rangle$ is

$$\langle N_e \rangle = \frac{N}{2}(1 + \cos\Phi) \ , \tag{2.84}$$

with $\Phi = \Delta T$. The variance of N_e is given by:

$$\Delta^2 N_e = N p_e (1 - p_e) = \frac{N}{4} \sin^2 \Phi \ , \tag{2.85}$$

and hence

$$\Delta N_e = \frac{\sqrt{N}}{2} \sin\Phi \ . \tag{2.86}$$

This variance, associated to the random nature of N_e is called "projection noise".

In order to assess the resolution of the method, we perform two measurements of N atoms, with two different settings of the interrogation source frequency, corresponding to Δ and $\Delta + \delta$. Assuming that the detuning increment δ is small, we get

$$\langle N_e(\Delta + \delta) \rangle = \langle N_e(\Delta) \rangle - \frac{NT}{2} \delta \sin \Delta T \ . \tag{2.87}$$

We will be able to distinguish the two values of the detunings provided the variation of the mean is greater than the square root of the variance multipled by $\sqrt{2}$ (the statistical errors on two independent measurements add quadratically), i.e. provided

$$\frac{NT}{2} \delta \sin \Delta T > \sqrt{2} \frac{\sin \Delta T}{2} \sqrt{N} \ , \tag{2.88}$$

or

$$\delta > \frac{\sqrt{2}}{T\sqrt{N}} \ . \tag{2.89}$$

We thus get a more precise expression of the spectroscopic sensitivity of the method. The first observation is that it is independent upon the Ramsey interferometer phase Φ. When N_e is maximum or minimum (top or bottom of the Ramsey fringes signal), the noise on it is minimal but the derivative of the signal versus the detuning is also minimal. At a mid-fringe setting, where $p_e = 1/2$, the sensitivity to the detuning variation is optimal, but the statistical noise is also high. We also observe that the sensitivity ranges like $\sqrt{N}$, a typical feature for N independent measurements of the same quantity. Using more sophisticated entangled atomic states makes it possible in principle to reach a much higher sensitivity, ranging like N (Heisenberg limit).

2.4 Relaxing atom and resonant field

The model developed in the previous section is quite unrealistic. We have assumed that the atomic states are stationary, including the upper state $|e\rangle$ of the transition. We should at least take into account the spontaneous emission from this level. In realistic situations, all kinds of random fields may also act on the atoms (fluctuations of the local electric or magnetic fields, inducing random Stark or Zeemann effects). These fields may spoil the atomic levels coherence and will certainly contribute to a limitation of the spectroscopic resolution.

Introducing these effects will lead us to the famous Optical Bloch Equations describing the atom-field interaction is a realistic way in a wide variety of situations. We will extensively describe some of their main applications. This Section will also be the opportunity to review first the description of 'open' quantum systems coupled to a complex environment.

2.4.1 Description of the atomic relaxation

We consider the rather general problem of a quantum system $\mathcal{S}$ (the atom here) coupled to an environment $\mathcal{E}$. By 'environment' we mean a large collection of systems or degrees of freedom, with a continuous and wide spectrum of characteristic frequencies, in thermal equilibrium at some temperature T (possibly zero).

The environment and the system are together a closed quantum system, described by a pure state $|\Psi_{\mathcal{SE}}\rangle$. The environment being fantastically complex, we are not interested in this state but only in the reduced system state described by the density operator $\rho_{\mathcal{S}}$, obtained by tracing the projector $|\Psi_{\mathcal{SE}}\rangle\langle\Psi_{\mathcal{SE}}|$ over the environment.

We are thus seeking an equation of evolution for ρ_s (that we will now note ρ since there is no ambiguity). The standard approach[5] starts from a model of the environment. The equation of motion of ρ is obtained by a complex procedure (some 20 pages), involving two stages of approximation. The Born approximation amounts to treating the system-environment interaction to the lowest significant order. Physically it means that any excitation which the system looses in the environment will be lost forever, and never comes back in the system. This is clearly highly valid for thermodynamics reservoirs, made of infinitely many degrees of freedom. The Markov approximation neglects the memory of the reservoir: it assumes that all its observables have, in the Heisenberg picture, an extremely small correlation time τ_c. This is also very well verified for all reasonable reservoir models. It is particularly the case for spontaneous emission. The reservoir is then the continuum of all optical modes of the field, with a width of the order of the optical frequencies themselves, and thus a correlation time in the 10^{-15} s range. The equation of motion of ρ is then obtained. Its form finally does not depend about the detailed structure of the reservoir. Only the numerical values of the relaxation times involved in the dynamics do depend a priori on the details of the model. This is not a serious concern, though, since these times can also be measured independently in dedicated experiments.

We will follow here a much more intuitive and direct path. It will provide us easily with the equation of motion of ρ by considering the "quantum jumps" that the system may undergo under the influence of its coupling with the environment[6]

Kraus operators

We thus consider a short time interval τ and consider the transformation of the system's density matrix from time t to time $t+\tau$:

$$\rho(t) \longrightarrow \rho(t+\tau) \ . \tag{2.90}$$

[5] See for instance S. Barnett's *Theoretical methods in Quantum Physics*, Oxford University Press.

[6] More details on this approach are in Haroche and Raimond *Exploring the quantum* and in the course by Preskill on quantum information, freely available on the Web at http://www.theory.caltech.edu/people/preskill/ph229/#lecture.

The time interval τ is chosen to be small at the scale of the system's dynamics (i.e. small compared to all characteristic frequencies and relaxation times), so that the modification of ρ is only incremental. On the other hand, we chose it much longer than the correlation time of the environment, $\tau \gg \tau_c$, so that there are no coherent effects in the system-reservoir interaction. For spontaneous emission, for instance, the dynamics occurs at the time scale of the spontaneous emission lifetime $1/\Gamma \simeq 10^{-9}$ s and $\tau_c \simeq 10^{-15}$. There is thus a wide possible range for the time increment τ. Since the environment is a very large system, with a very short memory time, we can assume that it is always disentangled with the system and in some reference state, for instance reflecting its thermal equilibrium at temperature T.

The transformation (2.90) is an example of a "quantum map" operation: $\mathcal{L}(\rho(t)) = \rho(T+\tau)$. This quantum map operation should obey some important mathematical rules:

- It should be a linear operation, i.e. a super-operator acting in the Hilbert space of operators. This operator space is of dimension $N_{\mathcal{S}}^2$ if the system's Hilbert space of $\mathcal{S}$ is of dimension $N_{\mathcal{S}}$.
- It should preserve the unit trace of the density operator, as well as its positivity (a density operator does not have any negative eigenvalue).
- It should be "completely positive". If, at a time t, $\mathcal{S}$ is entangled with another system $\mathcal{S}'$, the application of the quantum map $\mathcal{L}$ to $\mathcal{S}$ should lead to a completely positive density operator for the entangled state of $\mathcal{S}$ and $\mathcal{S}'$ at time $t+\tau$. Let us only mention at this stage that there are quantum maps, which obey the first two properties but which are not completely positive (the partial transpose is an example).

When $\mathcal{L}$ checks these three properties, it is possible to show (the mathematical derivation is a bit longish and will not be reproduced here) that there are at most $N_{\mathcal{S}}^2$ operators M_μ acting on the system's Hilbert space (not necessarily Hermitian or unitary) such that the map can be written in the Kraus form:

$$\mathcal{L}(\rho) = \sum_\mu M_\mu \rho M_\mu^\dagger \ , \tag{2.91}$$

with the normalization condition

$$\sum_\mu M_\mu^\dagger M_\mu = \mathbb{1} \ . \tag{2.92}$$

The Kraus operators M_μs are not unique. Any linear unitary transformation mixing them leaves the quantum map unchanged. There are thus many ways in which the same quantum map can be described. This is a very simple and powerful mathematical result. It also brings a considerable simplification, since all the action of the formidably complex environment $\mathcal{E}$ can be "wrapped" in the M_μ operators.

Note that the evolution of $\mathcal{S}$ under the Hamiltonian H can be cast in this form also, since $\rho(t+\tau) = U(\tau)\rho U^\dagger(\tau)$, where U is the unitary evolution operator. A generalized measurement of $\mathcal{S}$ cannot be cast in this form. It is described by at most $N_{\mathcal{S}}^2$ arbitrary operators O_μ but the map is non linear:

$$\rho \longrightarrow \frac{O_\mu \rho O_\mu^\dagger}{\mathrm{Tr}\rho O_\mu^\dagger O_\mu} \ , \tag{2.93}$$

where the denominator is simply the probability p_μ for getting μ as the result of the measurement. If we do not take notice of the measurement result, we should average the final density matrix over all possible results weighed by their occurrence probabilities. The mapping due to an unread measurement thus writes:

$$\rho \longrightarrow \sum_\mu O_\mu \rho O_\mu^\dagger \ , \tag{2.94}$$

and appears in the Kraus form. The Kraus process encapsulates thus most quantum processes.

Lindblad equation

We can write the quantum map $\mathcal{L}$ leading from the density operator at time t to that at time $t+\tau$, but we are obviously more interested in a differential "master" equation for the evolution of ρ. We will now show that it can be straightforwardly derived from the Kraus operators.

Since the environment is at all times close to its thermal equilibrium and does not take part in the dynamics, it is natural to assume that the Kraus operators M_μ do not depend upon time. They, however, depend clearly upon the tiny time interval τ.

If the density operator evolves smoothly, we have:

$$\rho(t+\tau) = \sum_\mu M_\mu \rho M_\mu^\dagger \approx \rho(t) + \frac{d\rho}{dt}\tau \ . \tag{2.95}$$

One and only one of the M_μs is thus of the order of unity and all others must then be of order $\sqrt{d\tau}$. We will write, without loss of generality:

$$M_0 = \mathbb{1} - iK\tau \tag{2.96}$$

$$M_\mu = \sqrt{\tau} L_\mu \qquad \text{for } \mu \neq 0 \ , \tag{2.97}$$

Note that M_0 might a priori include corrections at order $\sqrt{\tau}$. These corrections can nevertheless be removed from M_0 and incorporated in one of the M_μs.

The operator K, which has no particular a priori mathematical properties, can be split in its hermitian and anti-hermitian parts:

$$K = \frac{H}{\hbar} - iJ \ , \tag{2.98}$$

where

$$H = \frac{\hbar}{2}\left(K + K^\dagger\right) \tag{2.99}$$

$$J = \frac{i}{2}\left(K - K^\dagger\right) \tag{2.100}$$

are both hermitian. With these notations:

$$M_0 = \mathbb{1} - \frac{i\tau}{\hbar}H - J\tau \ . \tag{2.101}$$

To first order in τ, we now have:

$$M_0 \rho M_0^\dagger = \rho - \frac{i\tau}{\hbar}\left[H, \rho\right] - \tau\left[J, \rho\right]_+ \ , \tag{2.102}$$

where $\left[J, \rho\right]_+ = J\rho + \rho J$ is an anti-commutator. The commutator in the r.h.s. of the above equation clearly evokes the Hamiltonian evolution of the density operator. We also have to the same order:

$$M_0^\dagger M_0 = \mathbb{1} - 2J\tau \ . \tag{2.103}$$

The normalization condition $\sum_\mu M_\mu^\dagger M_\mu = \mathbb{1}$ thus writes simply:

$$J = \frac{1}{2}\sum_{\mu\neq 0} L_\mu^\dagger L_\mu \ . \tag{2.104}$$

Injecting these expressions in the Kraus map, we finally get the density matrix master equation in the so-called "Lindblad form":

$$\frac{d\rho}{dt} = -\frac{i}{\hbar}\left[H, \rho\right] + \sum_{\mu\neq 0}\left(L_\mu \rho L_\mu^\dagger - \frac{1}{2}L_\mu^\dagger L_\mu \rho - \frac{1}{2}\rho L_\mu^\dagger L_\mu\right) \ . \tag{2.105}$$

Note that the last two terms in the r.h.s. sum are included to preserve the trace of the density matrix. The dynamics is in fact mostly governed by the first term in the sum, Since the M_μs are not uniquely defined, there is also a considerable freedom in the way we can write the same master equation.

2.4.2 Quantum jumps

Let us now get an insight into the physical interpretation of the L_μ operators appearing in the Lindblad master equation. For this purpose, let us consider a simple situation, in which the initial density matrix is a pure state $\rho(0) = |\Psi\rangle\langle\Psi|$ and let us assume that there is no Hamiltonian evolution (or that we use a proper interaction representation cancelling H). After a small time interval τ, the un-normalized density operator[7] is:

$$\rho(\tau) = |\Psi\rangle\langle\Psi| + \tau \sum_\mu \left(L_\mu |\Psi\rangle\right)\left(\langle\Psi| L_\mu^\dagger\right) \ . \tag{2.106}$$

Either, with a probability of order one, the quantum state of the system is unchanged, or, with probabilities of order one in τ, the system undergoes a large evolution described by one of the L_μ operators.

We are thus lead to interpret the L_μs as 'jump operators' which describe a random (perhaps large) evolution of the system which suddenly (at the time scale of the evolution) changes under the influence of the environment. Of course the density operator evolves slowly, since these quantum jumps occur with a small probability, at the first order in τ.

The interest of the method is that, in many cases, the nature of the quantum jumps can be guessed from the mere nature of the system. Anticipating a lot, we for instance guess that a field cavity losses are represented by a jump operator proportional to the annihilation operator a, describing the loss of a single photon. We also guess that, for an atom, the jump operator should be proportional to the lowering spin operator σ_-. The proportionality factors (the actual relaxation rates) cannot be obtained in this way, but they can at least be measured. We have thus a very simple path to guide us in writing the proper Lindblad master equation for any system.

Once again, the jump operators are not uniquely defined. The same relaxation process can be modeled in different ways, different 'unravelings' of the master equation. In some situations, the nature of the system privileges one of these unravelings. For instance, with an emitting atom completely surrounded by a photo-detector array. The quantum jump then corresponds to a click of one detector. Different unravelings may then correspond to different ways of monitoring the environment, in this case to different detectors (photon counters, homodyne recievers...). In other situations, the quantum jumps are an abstract representation of the system+environment evolution.

Even when the environment is not explicitly monitored, one may imagine that it is done. We then imagine we have full information about which quantum jump occurs when. The system is thus, at any time, in a pure state, which undergoes a stochastic trajectory in the Hilbert space, made up of continuous Hamiltonian evolutions interleaved with sudden quantum jumps. However, since we only imagine the information is available, we should describe the evolution of the density operator by averaging the system evolution over all possible trajectories.

The 'environment simulator' concept provides a simple recipe to perform this averaging. We introduce a system $\mathcal{B}$, much simpler than the formidably complex environment $\mathcal{E}$ and couple it to $\mathcal{S}$ in such a way that the reduced dynamics of $\mathcal{S}$ is exactly ruled by the Lindblad equation (2.105). For this, it is enough to check that $\mathcal{S}$ undergoes the same quantum map during the time interval τ as with its interaction with $\mathcal{E}$. We also assume that $\mathcal{B}$ is prepared at the beginning of all time intervals τ in the same reference state $|0\rangle$, reflecting the fact that in the real situation $\mathcal{E}$ never gets modified by $\mathcal{S}$.

We assume that $\mathcal{S}$ and $\mathcal{B}$ undergo an Hamiltonian evolution during τ, resulting in the global unitary evolution operator $U_{\mathcal{SB}}$ such that:

$$U_{\mathcal{SB}} |\Psi\rangle \otimes |0\rangle = M_0 |\Psi\rangle \otimes |0\rangle + \sum_\mu \left(M_\mu |\Psi\rangle\right) \otimes |\mu\rangle \ , \tag{2.107}$$

where the first ket refers to $\mathcal{S}$ and the second to $\mathcal{B}$, and $M_\mu = \sqrt{\tau} L_\mu$ are the Kraus operators. The $|\mu\rangle$ states of $\mathcal{B}$ are assumed to be orthogonal. Defining an Hamiltonian leading to this action of the

[7] We do not take into account the last two terms in the r.h.s. sum of Eq.(2.105).

evolution operator is always possible, provided the dimension of the Hilbert space of $\mathcal{B}$ is at least as large as the number of Kraus operators, at most $N_{\mathcal{S}}^2$. The 'environment simulator' is thus much simpler than the actual environment.

At the end of the time interval τ an unspecified observer performs a measurement of an observable $O_{\mathcal{B}}$ having the $|\mu\rangle$s as non degenerate eigenstates, with μ as the eigenvalue. Applying the measurement postulates, we immediately find that

- With a probability $p_0 = \langle\Psi| M_0^\dagger M_0 |\Psi\rangle = \mathrm{Tr}(\rho M_0^\dagger M_0) = 1 - \tau \sum_{\mu\neq 0} \mathrm{Tr}(\rho L_\mu^\dagger L_\mu) = 1 - \sum_{\mu\neq 0} p_\mu$, the result is 0, no jump occurs and the system's state is finally left in the normalized state

$$\frac{M_0 |\Psi\rangle}{\sqrt{p}_0} = \frac{1 - iH\tau/\hbar - J\tau}{\sqrt{p}_0} |\Psi\rangle \ . \tag{2.108}$$

  Note that the state vector evolution involves an Hamiltonian part, $iH\tau/\hbar$, (resulting alone in a unitary evolution) and a part reflecting normalization whose evolution operator is non-unitary. This no-jump evolution can be interpreted as resulting from the non-hermitian effective Hamiltonian:

$$H_{eff} = H - i\hbar J \ . \tag{2.109}$$

- With a probability $p_\mu = \tau \mathrm{Tr}(\rho L_\mu^\dagger L_\mu)$, the result is μ and the system's state is accordingly projected onto $\frac{M_\mu|\Psi\rangle}{\sqrt{p_\mu}} = \frac{L_\mu|\Psi\rangle}{\sqrt{p_\mu/\tau}}$. Note that the mere definition of the probabilities ensures that $\sum_{\mu=0} p_\mu = 1$.

Of course, the information provided by the unspecified observer of the environment simulator is not available (in most cases, we do not have any information about what happens in the environment). We have thus to assume that the measurement at the end of the time interval τ is unread. This results in a quantum map acting on the system state that is precisely expressed by $\sum_\mu M_\mu \rho M_\mu^\dagger$, identical to the environment-induced quantum map. The evolution of the system coupled to $\mathcal{B}$ is thus the same as when it is coupled to $\mathcal{E}$.

The different unravelings of the master equation obviously correspond to the measurement of another observable in the environment simulator $\mathcal{B}$, whose eigenvectors are linear combinations of the $|\mu\rangle$s, defined by a unitary basis change matrix.

2.4.3 Quantum Monte Carlo

The quantum jump approach also leads to a very efficient method for computing numerically the evolution of the system: the 'quantum Monte Carlo' method.

Computing a solution to the Lindblad master equation is complex, because the density operator involves a number of parameters of order $N_{\mathcal{S}}^2$. Direct integration, straightforwardly feasible for an Hilbert space dimension of a few hundreds, becomes nearly intractable for much larger Hilbert spaces. This is a very strong limitation for many practical problems, such as those involved in cold atoms physics.

The above discussion nevertheless provides us with a useful approach. Instead of assuming that the measurement performed by the unspecified observer of $\mathcal{B}$ is unread, we will take it as a projective measurement whose result is known to us. In this case, the system initially in a pure state is still in a pure state at the end of the time interval τ and thus remains forever in a pure state. We can compute, by throwing the dice to determine the result of each measurement, the time evolution of this pure state over a particular 'trajectory'. Of course, a single trajectory does not tell the whole story. It can be shown easily that the density operator obtained by averaging the projector on this pure state over many realisations of individual trajectories, determined by different dice throwing for each time interval, is the solution of the Lindblad equation with the initial pure state as initial condition. When

the initial state is not a pure state, we can obviously diagonalize the density operator, evolve each of its pure state components and finally average the result.

The quantum Monte Carlo algorithm is thus quite simple

- Choose a time interval τ short on the time scale of the relaxation, but long compared to the reservoir correlation time.
- Initialize the state to its initial value, or to a randomly chosen eigenstate of the density operator (if the initial state is not pure).
- For each time interval τ over the total evolution time evolve the quantum state $|\Psi\rangle$ according to the rules:
  - Compute the probabilities $p_\mu = \tau \langle\Psi| L_\mu^\dagger L_\mu |\Psi\rangle$ and $p_0 = 1 - \sum_{\mu\neq 0} p_\mu$.
  - Use a (good) random number generator to decide upon the result of the measurement of the environment simulator $\mathcal{B}$.
  - If the result of the measurement is zero, evolve $|\Psi\rangle$ with
$$|\Psi\rangle \longrightarrow \frac{1 - iH\tau/\hbar - J\tau}{\sqrt{p_0}} |\Psi\rangle \ . \tag{2.110}$$
  - If the result of the measurement is $\mu \neq 0$, evolve $|\Psi\rangle$ by the jump operator L_μ:
$$|\Psi\rangle \longrightarrow \frac{L_\mu}{\sqrt{\langle\Psi| L_\mu^\dagger l_\mu |\Psi\rangle}} |\Psi\rangle = \frac{L_\mu}{\sqrt{p_\mu/\tau}} |\Psi\rangle \ . \tag{2.111}$$
- Repeat the procedure for a large number (a few hundreds is most often enough) of trajectories
- Average the projectors on the states and obtain an estimate of the time-dependent density operator solution of the Lindblad equation
$$\rho(t) = \overline{|\Psi(t)\rangle \langle\Psi(t)|} \ . \tag{2.112}$$

This procedure allows to compute only state vectors with $N_\mathcal{S}$ parameters. It is thus much faster than the direct integration of the Lindblad equation, as soon as the Hilbert space dimension is greater than a few hundreds. It is now widely used in a variety of contexts.

Spontaneous emission

Let us now turn to the focus of this Chapter and examine the master equation describing the spontaneous emission by a single two-level atom in which $|g\rangle$ is the ground state. We assume here a zero-temperature environment. This is an excellent approximation for optical transitions at room temperature, since the average thermal energy, $k_b T$ (about 1/40 eV), is much smaller than the transition energy (at least 1 eV).

It is easy to identify the jump operators. Let us for that consider a simple environment simulator, that corresponds to an experiment in which the atom would be totally enclosed in unit detection efficiency photo-counters. Then, either nothing happens in a time interval τ (the counters remain inactive), or one of the counters clicks. This reveals the emission of a photon while the atom makes the transition from $|e\rangle$ to $|g\rangle$, described by the atomic lowering operator σ_-. We can thus guess that the emission can be modelled by a single jump operator L:

$$L = \sqrt{\Gamma}\sigma_- \ , \tag{2.113}$$

where Γ is the spontaneous emission rate. The Lindblad master equation thus writes (we assume that the Hamiltonian term cancels or that we use a proper interaction representation):

$$\frac{d\rho}{dt} = \Gamma\left(\sigma_-\rho\sigma_+ - \frac{1}{2}\sigma_+\sigma_-\rho - \frac{1}{2}\rho\sigma_+\sigma_-\right) , \tag{2.114}$$

where we have used $\sigma_-^\dagger = \sigma_+$ (note also that $\sigma_+\sigma_- = |e\rangle\langle e|$).

Writing ρ in matrix form as:

$$\rho = \begin{pmatrix} \rho_{ee} & \rho_{eg} \\ \rho_{ge} & \rho_{gg} \end{pmatrix} , \tag{2.115}$$

(the first index in the subscripts being the line index as usual), where $\rho_{ee} + \rho_{gg} = 1$ and $\rho_{eg} = \rho_{ge}^*$, we get the only two relevant equations:

$$\frac{d\rho_{ee}}{dt} = -\Gamma\rho_{ee} , \tag{2.116}$$

$$\frac{d\rho_{eg}}{dt} = -\frac{\Gamma}{2}\rho_{eg} . \tag{2.117}$$

We thus obtain the simple result that the population of level $|e\rangle$, ρ_{ee}, is exponentially damped with a time constant $T_1 = 1/\Gamma$, whereas the coherence between the levels is damped with a time constant $2T_1$. Note that at a finite environment temperature, we should add a σ_+ jump operator, describing the absorption of a thermal photon by the atom, making in the process a transition from $|g\rangle$ to $|e\rangle$.

Let us analyse the spontaneous emission process in terms of Monte Carlo trajectories. The atom is assumed to be initially in $|e\rangle$, At each time step, either there is no jump or there is one. In the first case, only the normalization operator $J \propto \sigma_+\sigma_-$ acts on the wavefunction. Since $|e\rangle$ is an eigenvector of this operator, the atomic state does not change when the no-jump option is selected, a rather intuitive result. When a jump occurs, it is described by σ_- which turns the state into $|g\rangle$. From this time on, no jump can act. It is easy to show that the jump probability cancels when the atom is in $|g\rangle$, a fortunate fact to keep normalization since $\sigma_-|g\rangle = 0$.

A quantum Monte Carlo trajectory is thus a 'telegraphic' signal, where the atom remains in $|e\rangle$ for some time and suddenly jumps into $|g\rangle$. The time of the jump is random (we leave to the reader as an exercise in probabilities to compute its statistical distribution). Of course, a single trajectory does not tell the whole story. We have to average many of these telegraphic trajectories. In this way, we recover the average exponential damping, solution of the Lindblad equation.

We can get a bit more insight by considering as initial state a superposition of $|e\rangle$ and $|g\rangle$: $|\Psi_0\rangle = (1/\sqrt{2})(|e\rangle + |g\rangle)$. Let us follow a trajectory. Before the jump (only one allowed of course), the wavefunction evolves due to the non-hermitian Hamiltonian H_{eff} which writes here:

$$H_{eff} = -\frac{i\hbar}{2}\Gamma\sigma_+\sigma_- = -\frac{i\hbar}{2}\Gamma|e\rangle\langle e| . \tag{2.118}$$

Writing the state at time t as the un-normalized ket $c_e|e\rangle + c_g|g\rangle$, a mere substitution leads to:

$$i\hbar\frac{dc_e}{dt} = -\frac{i\hbar}{2}\Gamma c_e , \tag{2.119}$$

whose solution is

$$c_e(t) = e^{-\Gamma t/2} . \tag{2.120}$$

The normalized wavefunction is then

$$|\Psi(t)\rangle = \frac{1}{1+e^{-\Gamma T}}\left(e^{-\Gamma t/2}|e\rangle + |g\rangle\right) . \tag{2.121}$$

When the quantum jump occurs, at a random time, the state is suddenly projected onto $|g\rangle$ and no further evolution takes part, since $|g\rangle$ is an eigenstate of H_{eff} with eigenvalue 0.

Now the state evolves even before the quantum jump, the probability for being in $|e\rangle$ being exponentially damped with the rate Γ. We can understand that in terms of the measurements in the environment simulator. When no photon is detected for a while, it provides information on the system state. It tells that it is less likely that the atom is excited, since it does not emit. It is important to recognize here that an experiment with a negative result (no photon counted) does indeed change the state of the system, not as brutally though as a quantum jump. In the limit where no photon has been observed for a very long time, it is clear that the system must be in state $|g\rangle$. Observing no photon at any time is performing a projective measurement of the atomic state.

Phase damping

Spontaneous emission is not the only relaxation process than can affect an atom. It can also be submitted to random fields that modify in an uncontrolled way its resonant frequency. In an intuitive picture, these fields will not affect the states population, but they will provoke random dephasings of the coherence between $|e\rangle$ and $|g\rangle$ and finally damp these coherences. Let us add the corresponding terms in the Lindblad equation.

The extreme event on the phase of the atomic coherence is a π phase shift, represented by the σ_z operator. We will thus use $\sqrt{\gamma/2}\sigma_z$ as the jump operator, where $\gamma = 1/T_2$ is a 'transverse' relaxation rate and T_2 the associated transverse relaxation time constant. We call them transverse because they describe a process affecting only the transverse components of the Bloch vector representing the density operator. By opposition we will call T_1 a 'longitudinal' relaxation time.

After a little bit of algebra, that we leave to the reader as an exercise on Pauli matrices, we obtain the master equations for the populations, which remain constant as expected, and for the coherence ρ_{eg}, which is exponentially damped with a rate γ.

Adding the spontaneous emission and the phase damping in the same Lindblad equation, we get the complete master equation for the density matrix elements:

$$\frac{d\rho_{ee}}{dt} = -\Gamma\rho_{ee} \tag{2.122}$$

$$\frac{d\rho_{eg}}{dt} = -\frac{\Gamma}{2}\rho_{eg} - \gamma\rho_{eg} = -\gamma'\rho_{eg} \ , \tag{2.123}$$

where we define the total relaxation rate of the coherence by:

$$\gamma' = \gamma + \frac{\Gamma}{2} \ . \tag{2.124}$$

At finite temperature, the Lindblad master equation would include all the operators σ_z and $\sigma_\pm$. They are, with the trivial unity, a basis of all possible spin operators. There is thus no new relaxation process that we could add by making the Lindblad equation more complex.

2.5 Optical Bloch equations

We now turn to the core of this Chapter on the semi-classical approach, by writing the Optical Bloch equations that describe the evolution of the atomic field operator under the joint influence of an external classical driving field and of a general (zero temperature) relaxation process, described by the transverse and longitudinal relaxation times introduced in the previous Section. We first write the equations, revisit in this frame the Rabi oscillations phenomenon. We examine it in two limiting cases (strong transverse relaxation or stochastic driving field). In both cases we will recover, mutatis mutandis, the phenomenological Einstein's coefficients model and get an insight into their validity range.

2.5.1 The equations

OBE

Let us recall here that the Hamiltonian (2.68) describing the action of the classical field is, in the interaction representation with respect to the field frequency:

$$H = \frac{\hbar\Delta}{2}\sigma_z - \frac{\hbar\Omega}{2}\left(\sigma_+ e^{-i\varphi} + \sigma_- e^{i\varphi}\right) \ , \tag{2.125}$$

with $\Omega = dE_0/\hbar$ and $\Delta = \omega_{eg} - \omega$ being the angular frequency difference between the atom and the field (we assume throughout this Section that d is real). We omit here the tildes for the interaction representation that we will always use from now on. We will note E_1 the complex amplitude of the driving field:

$$E_1 = E_0 e^{-i\varphi} \ . \tag{2.126}$$

The Schrödinger equation describing the coherent evolution of ρ, $i\hbar d\rho/dt = [H, \rho]$ leads, after evaluation of the commutators, to the two coupled equations which together entirely determine the evolution of the density matrix:

$$\begin{aligned} \frac{d\rho_{ee}}{dt} &= \Omega \mathrm{Im}\left(\rho_{eg} e^{i\varphi}\right) \\ &= \frac{d}{\hbar}\mathrm{Im}\left(\rho_{eg} E_1^*\right) \ , \end{aligned} \tag{2.127}$$

and

$$\begin{aligned} \frac{d\rho_{eg}}{dt} &= -i\Delta\rho_{eg} + i\frac{\Omega}{2}e^{-i\varphi}(\rho_{gg} - \rho_{ee}) \\ &= -i\Delta\rho_{eg} - i\frac{d}{2\hbar}E_1(\rho_{ee} - \rho_{gg}) \end{aligned} \tag{2.128}$$

The electric field couples the populations (precisely the population inversion) and the coherences.

We now add relaxation in the Lindblad form, taking into account both the longitudinal (spontaneous emission) and the transverse (dephasing) mechanisms. We must take care that we are now in an interaction representation at the driving field frequency ω, which has changed $\sigma_\pm$ into $\sigma_\pm \exp(\pm i\omega t)$ and leaved σ_z unchanged. However, all terms in the relaxation part of the Lindblad equation involve products of the form $\sigma_-\sigma_+$ which are left unchanged. The coupled equations of motion of the population and coherences, the Optical Bloch Equations are thus:

$$\frac{d\rho_{ee}}{dt} = \frac{d}{\hbar}\mathrm{Im}\left(\rho_{eg} E_1^*\right) - \Gamma\rho_{ee} \tag{2.129}$$

$$\frac{d\rho_{eg}}{dt} = -i\Delta\rho_{eg} - i\frac{d}{2\hbar}E_1(\rho_{ee} - \rho_{gg}) - \gamma'\rho_{eg} \ , \tag{2.130}$$

where once again $\Gamma = 1/T_1$ and $\gamma' = (1/2T_1) + 1/T_2$.

We now proceed to put these important equations under equivalent and equally useful forms. Noting $N_e = \rho_{ee}$ and $N_g = \rho_{gg}$ the populations of the states and introducing the complex dipole amplitude $\mathcal{D}$ [8]

$$\mathcal{D} = 2d\rho_{eg} \ , \tag{2.131}$$

so that the average value of the hermitian dipole operator in state ρ is $\mathrm{Re}\,\mathcal{D}$, we put the OBE under a form frequently encountered in literature:

$$\frac{dN_e}{dt} = \frac{1}{2\hbar}\mathrm{Im}\left(\mathcal{D}E_1^*\right) - \Gamma N_e \tag{2.132}$$

$$\frac{d\mathcal{D}}{dt} = -i\Delta\mathcal{D} - \gamma'\mathcal{D} - i\frac{d^2 E_1}{\hbar}(N_e - N_g) \tag{2.133}$$

[8] $\mathcal{D}$, should not be mistaken for the population inversion $D = N_e - N_g$ introduced in the previous Chapter.

Let us introduce the Cartesian coordinates of the Bloch vector $\mathbf{r} = (x, y, z)$ (often noted $\mathbf{r} = (u, v, w)$ in the NMR context) defined by:

$$\rho = \frac{1 + \mathbf{r} \cdot \boldsymbol{\sigma}}{2} \tag{2.134}$$

or equivalently by:

$$\rho = \frac{1}{2} \begin{pmatrix} 1+z & x-iy \\ x+iy & 1-z \end{pmatrix} , \tag{2.135}$$

i.e. by

$$x = 2\mathrm{Re}\,\rho_{eg} \qquad y = -2\mathrm{Im}\,\rho_{eg} \qquad z = 2\rho_{ee} - 1 \ . \tag{2.136}$$

with the notation $E_1 = E_x + iE_y$ (where both E_x and E_y are real) we finally arrive at the three real coupled equations:

$$\frac{dz}{dt} = -\frac{d}{\hbar}(xE_y + yE_x) - \Gamma(1+z) \tag{2.137}$$

$$\frac{dx}{dt} = -\Delta y + \frac{d}{\hbar} z E_y - \gamma' x \tag{2.138}$$

$$\frac{dy}{dt} = +\Delta x + \frac{d}{\hbar} z E_x - \gamma' y \ . \tag{2.139}$$

The interpretation of these equations is straightforward. The detuning Δ results in a rotation of the Bloch vector around the z axis. The E_x component of the electric field induces a rotation of the Bloch vector around the x axis, coupling the y and z components, and the E_y component a simultaneous rotation around the y axis coupling x and z. Relaxation leads z to the -1 point corresponding to the atomic ground state, while the transverse relaxation damps the x and y coordinates.

Rabi oscillations Revisited

In this section, we revisit the Rabi oscillation phenomenon in the frame of the OBEs, including relaxation. In order to make the algebra a bit simpler without losing the main features, we will make the following assumptions:

- The initial state is the ground state $|g\rangle$ corresponding to $z = -1$ and $x = y = 0$.
- The field is purely real: $E_y = 0$, $E_x = +E_0$
- Atom and field are at resonance: $\Delta = 0$.

From these hypotheses, it is clear that x remains zero at any time and that the whole dynamics is contained in the xOz plane. The corresponding equations of motion are, in terms of the Rabi frequency $\Omega = dE_0/\hbar$:

$$\frac{dz}{dt} = -\Omega y - \Gamma(1+z) \tag{2.140}$$

$$\frac{dy}{dt} = \Omega z - \gamma' y \ . \tag{2.141}$$

We can extract a single second-order differential equation for z from this system. We derive the first with respect to time, replace dy/dt using the second. We are left with an y term in the equation that we can eliminate by getting y as a function of z and dz/dt from the first equation. After a bit of rearranging, we get finally:

$$\frac{d^2z}{dt^2} + (\Gamma + \gamma')\frac{dz}{dt} + \left(\Omega^2 + \gamma'\Gamma\right) z = -\gamma'\Gamma \ . \tag{2.142}$$

This equation can be solved by standard methods and exhibits a transient behaviour [lasting a time of the order of $1/(\Gamma+\gamma')$] towards a steady state point, instead of the permanent Bloch vector rotation obtained in the relaxation-free case. The final steady state point coordinates, z_s and y_s can be obtained easily from the equations:

$$z_s = -\frac{\gamma'\Gamma}{\Omega^2+\gamma'\Gamma} \ , \tag{2.143}$$

and

$$y_s = \frac{\Omega}{\gamma'}z = -\frac{\Omega\Gamma}{\Omega^2+\gamma'\Gamma} \ , \tag{2.144}$$

Not surprisingly, we find $y_s = 0$ and $z_s = -1$ in the limit of a vanishing driving field $\Omega \to 0$. In the opposite limit, $\Omega \to \infty$, we get instead $z_s = y_s = 0$. The Bloch vector is in the centre of the sphere, corresponding to an equal weight mixture of $|e\rangle$ and $|g\rangle$. In an intuitive picture, a fast oscillating spin is in such a mixture of the two levels.

The transient regime is algebraically complicated. In order to get a simpler picture, let us assume that we have no transverse relaxation (pure spontaneous emission) and, hence, that $\gamma' = \Gamma/2$. Let us furthermore assume $\Omega \gg \Gamma$ (strong driving of the transition). We can thus write the evolution equation as:

$$\frac{d^2z}{dt^2} + \frac{3\Gamma}{2}\frac{dz}{dt} + \Omega^2 z = 0 \ , \tag{2.145}$$

where we have neglected the constant term since, in this regime, the asymptotic value z_s is nearly zero. The solution, with the initial condition $z(0) = -1$ is:

$$z(t) = -\cos(\Omega t)e^{-3\Gamma t/2} \ , \tag{2.146}$$

an exponentially damped Rabi oscillation at the frequency Ω.

We can get a qualitative insight into the nature of the Rabi oscillation damping by returning to the quantum Monte Carlo trajectory picture. The non-hermitian part of the Hamiltonian can be neglected as compared to the strong driving. The no-jump evolution is thus an unchanged Rabi oscillation at frequency Ω starting from $|g\rangle$. Jumps occur in this case at an average rate $\Gamma/2$ since, on the average, the atom is in $|e\rangle$ half of the time. A strongly driven atom emits on the average one photon each $2T_1$, a simple result that will be useful later. After a jump, the atom is projected in the lower state $|g\rangle$ and the Rabi oscillation restarts. However, its phase has changed, since the quantum jump never occurs when the atom is in $|g\rangle$. The oscillation continues with this phase up to the next quantum jump, that changes again randomly the oscillation phase. An average over many trajectories thus results in a progressive washing out of the oscillations.

Oscillator strength

Let us, mostly for the sake of completeness, briefly compare the results of this Section to those of the perturbative model introduced in Section 2.2, in the case where the atom is initially in state $|g\rangle$, driven by a widely detuned field $\Delta \gg \Gamma, \gamma'$. Obviously, the atom remains at any time close to its initial state and we can assume that $N_g = 1$. The steady-state value of the complex dipole amplitude $\mathcal{D} = 2d\rho_{ge}$, where $d = \langle e|\, z\, |g\rangle$, is given by Eq. (2.133):

$$\mathcal{D}_s = \frac{d^2}{\hbar\Delta}E_1 = \frac{q^2|\,\langle e|\, z\, |g\rangle\,|^2}{\hbar(\omega_{eg}-\omega)}E_1 \ . \tag{2.147}$$

Since $\mathcal{D}_s$ is proportional to the complex electric field amplitude, this defines a quantum polarizability α_Q by $\mathcal{D}_s = \epsilon_0\alpha_Q E_1$. We get

$$\alpha_Q = \frac{q^2}{\hbar(\omega_{eg}-\omega)}|\,\langle e|\, z\, |g\rangle\,|^2 \ . \tag{2.148}$$

Comparing it to the classical polarizability in similar conditions:

$$\alpha_c = \frac{q^2}{2m\epsilon_0\omega_{eg}}\frac{1}{\omega_{eg}-\omega} \ , \tag{2.149}$$

we get an expression of the 'oscillator strength' of the atomic transition:

$$f = \frac{2m\omega_{eg}}{\hbar}|\langle e|\, z\, |g\rangle|^2 \ , \tag{2.150}$$

which coincides obviously with that obtained in Section 2.2.

2.5.2 Two limit cases: back to Einstein's coefficients

We consider in this paragraph two limit cases in which the Einstein's coefficients model can be directly retrieved from the OBEs.

Strong transverse relaxation

The first case is that of a strong transverse relaxation. We thus assume that the damping rate $\gamma' \approx \gamma$ is very large compared to all other rates and frequencies appearing in the OBEs (2.132) and (2.133). In the evolution equation for $\mathcal{D}$, we thus neglect $d\mathcal{D}/dt$ as compared to $\gamma'\mathcal{D}$. This amounts to assuming that $\mathcal{D}$ is at any time in its steady state value. The remaining equation is merely algebraic and we can solve it after this 'adiabatic elimination' as:

$$\mathcal{D} = \frac{i}{\gamma'+i\Delta}\frac{d^2E_1}{\hbar}(N_g-N_e) \ , \tag{2.151}$$

(note that this expression is valid in the steady state for all γ' values – we will use it later in this context). We then inject this expression in the equation of evolution of N_e (in which dN_e/dt cannot be neglected in front of ΓN_e since $\Gamma \ll \gamma'$):

$$\begin{aligned}\frac{dN_e}{dt} &= -\Gamma N_e + \frac{1}{2\hbar}\mathrm{Im}\left[\frac{i}{\gamma'+i\Delta}\frac{d^2E_1}{\hbar}(N_g-N_e)E_1^*\right] \\ &= -\Gamma N_e + \frac{d^2E_0^2}{2\hbar^2}(N_g-N_e)\frac{\gamma'}{\gamma'^2+\Delta^2}\end{aligned} \tag{2.152}$$

The squared field amplitude, E_0^2, is proportional to the energy density of the field, u. Since the field is in principle strictly monochromatic, we cannot attribute to it a regular spectral energy density u_ν. We can nevertheless assume that the field has a finite, if small width and that we can make use of a spectral density of energy, u_ν, obviously proportional to E_0^2.

We will assume furthermore that the field is resonant with the atomic transition ($\Delta = 0$). We can then rewrite the master equation for N_e as:

$$\frac{dN_e}{dt} = -\Gamma N_e + \frac{d^2E_0^2}{2\hbar^2\gamma'}(N_g-N_e) = -\Gamma N_e + \frac{\Omega^2}{2\gamma'}(N_g-N_e) \ , \tag{2.153}$$

and cast it straightforwardly in terms of the Einstein's transition rates:

$$\frac{dN_e}{dt} = A_{eg}N_e + (B_{ge}u_\nu N_g - B_{eg}u_\nu N_e) \ , \tag{2.154}$$

with the evident correspondence $A_{eg} = \Gamma$.

This shows that the OBEs lead to an Einstein coefficients master equation when the transverse relaxation is large, even tough the driving field is nearly monochromatic (let us recall that the Einstein argument a priori holds for a stochastic field with a large spectral bandwidth).

This is particularly reassuring for the laser theory that we briefly outlined. When a laser operates, the intra-cavity field is intense and nearly monochromatic. We would expect thus a regime of Rabi oscillations. The Einstein coefficients provide a precise description of the laser operation, precisely because, in most laser media, the transverse relaxation is intense. In gaz lasers, the collisions damp efficiently the laser coherence. In solid-state lasers, inhomogeneous broadening causes a rapid relaxation of the transverse components of the polarization, equivalent to a strong transverse relaxation. In simple words, something must have a large spectrum for the Einstein coefficients approach to be valid, either the field as in the previous Chapter, or the atom, due to a strong transverse relaxation.

It should be noted that, in the case of some lasers, the transverse relaxation is smaller or much smaller than the Rabi oscillation. This is for instance the case in the micromaser, that will be briefly discussed in the last Chapter. The dynamics of these lasers is then radically different from that of the ordinary ones (in particular the notion of threshold must be radically modified), and it cannot be described in terms of Einstein's coefficients.

Stochastic fields

We now show how the OBEs lead to the Einstein's coefficients in the case when the field has a large spectral width. We thus consider the case of a field with a stochastic amplitude and phase, whose average frequency $\overline{\omega}$ is nevertheless close to that of the atomic transition. Such a field can be written in terms of a slowly variable stochastic complex amplitude $E_1(t)$[9]:

$$E(t) = E_1(t)e^{-i\overline{\omega}t} \ . \tag{2.155}$$

Such a field would, for instance, be quite appropriate for describing the radiation of a spectral lamp. This radiation is made of small pulses of light, corresponding to emission by individual atoms, all close to the atomic transition frequency, with random phases between them. It is furthermore possible to assume that each of these tiny pulses has an exponentially decaying amplitude.

The properties of stochastic fields are described by the autocorrelation function $\Gamma_E(\tau)$, defined as:

$$\Gamma_E(\tau) = \lim_{T\to\infty} \frac{1}{T} \int_t^{t+T} E_1^*(t')E_1(t'-\tau)\, dt' \ , \tag{2.156}$$

where the integral depends only upon τ in the limits of large Ts for stationary stochastic processes, whose statistical properties are time invariant.

There is a useful alternative formulation of the autocorrelation function that holds provided we make an ergodic hypothesis. Instead of taking the average of the fields product over a long time period, we can equivalently take an ensemble average at a given time over a large number of realizations of the source (a large ensemble of spectral lamps for instance). We thus assume that:

$$\Gamma_E(\tau) = \overline{E_1^*(t)E_1(t-\tau)} \ , \tag{2.157}$$

where the overline symbol denotes the ensemble average. Note that:

$$\Gamma_E(-\tau) = \overline{E_1^*(t)E_1(t+\tau)} = \overline{E_1^*(t'-\tau)E_1(t')} = \Gamma_E^*(\tau) \ . \tag{2.158}$$

For zero time intervals, $\tau = 0$, the autocorrelation function reduces to a term proportional to the intensity of the source. At long times, Γ_E goes towards zero since the fields radiated at the two times do not have fixed phase relations. In between, $\Gamma_E(\tau)$ is generally a decreasing function of τ, with a characteristic width τ_c measuring the correlation time of the source.

[9] We of course consider here a single spatial point, where the atom is located. A full study of the spatio-temporal correlations properties is beyond the scope of this course. See the Born and Wolf Optics textbook for further information.

The spectral density of radiation, $S_E(\omega)$, (the quantity of energy in a narrow band $d\omega$ around the frequency ω) is defined as the Fourier transform of the autocorrelation function[10]:

$$S_E(\omega) = \frac{1}{2\pi}\int_{-\infty}^{\infty} d\tau\, \Gamma_E(\tau) e^{-i\omega\tau} \ , \tag{2.159}$$

which is real due to the relation (2.158). The spectral density is centred around zero frequency, with a width of the order of $1/\tau_c$. The spectrum of the source is the spectral density translated in the frequency space by $\overline{\omega}$.

Assuming that E_1 varies slowly at the scale of the optical frequency (the field is close to being monochromatic), we can just insert this time-dependent amplitude in the OBEs for the density matrix elements and write:

$$\frac{d\rho_{eg}}{dt} = -i\Delta\rho_{eg} - \gamma'\rho_{eg} - \frac{id}{2\hbar}E_1(t)(\rho_{ee}-\rho_{gg}) \ , \tag{2.160}$$

where Δ is now $\omega_{eg} - \overline{\omega}$.

In order to get rid of the first two trivial terms in the above equation, we define:

$$\widetilde{\rho_{eg}} = \rho_{eg} e^{(i\Delta+\gamma')t} \ . \tag{2.161}$$

This is equivalent to an interaction representation (albeit with a complex evolution frequency). We can then formally integrate the evolution equation, with the initial condition $\rho_{eg}(0) = 0$ since we assume as usual that the atom is initially in $|g\rangle$. We then get:

$$\widetilde{\rho_{eg}}(t) = -\frac{id}{2\hbar}\int_0^t E_1(t')(\rho_{ee}-\rho_{gg})(t') e^{(i\Delta+\gamma')t'}\, dt' \ . \tag{2.162}$$

Returning to the $\rho_{eg} = \widetilde{\rho_{eg}} \exp[-(i\Delta+\gamma')t]$ variable, we get

$$\rho_{eg}(t) = -\frac{id}{2\hbar}\int_0^t E_1(t')(\rho_{ee}-\rho_{gg})(t') e^{(-i\Delta-\gamma')(t-t')}\, dt' \ . \tag{2.163}$$

We then plug this formal expression in the evolution equation of the populations and use $\mathrm{Im}\, i = \mathrm{Re}$:

$$\frac{d\rho_{ee}}{dt} = -\Gamma\rho_{ee} - \frac{d^2}{2\hbar^2}\mathrm{Re}\int_0^t E_1^*(t)E_1(t')(\rho_{ee}-\rho_{gg})(t') e^{(-i\Delta-\gamma')(t-t')}\, dt' \ . \tag{2.164}$$

Settting $t - t' = \tau$, or $t' = t - \tau$ $(0 \le \tau \le t)$, this can be rewritten as

$$\frac{d\rho_{ee}}{dt} = -\Gamma\rho_{ee} - \frac{d^2}{2\hbar^2}\mathrm{Re}\int_0^t E_1(t-\tau)E_1^*(t)(\rho_{ee}-\rho_{gg})(t-\tau) e^{(-i\Delta-\gamma')\tau}\, d\tau \ . \tag{2.165}$$

We now perform an ensemble average of this equation over many realizations of the source. Obviously, the density matrix should be invariant in this operation, since its predictions are relative to a collection of very many identical systems. The averaging makes the field autocorrelation function appear in the r.h.s. and we get:

$$\frac{d\rho_{ee}}{dt} = -\Gamma\rho_{ee} - \frac{d^2}{2\hbar^2}\mathrm{Re}\int_0^t \Gamma_E(\tau)(\rho_{ee}-\rho_{gg})(t-\tau) e^{(-i\Delta-\gamma')\tau}\, d\tau \ . \tag{2.166}$$

The autocorrelation function has a width τ_c. We assume this time scale to be the shortest in the problem (it is of course nevertheless long compared to the optical frequency). In the above integral, we can thus replace $(\rho_{ee}-\rho_{gg})(t-\tau)$ by $(\rho_{ee}-\rho_{gg})(t)$. Moreover, since the times τ much greater

[10]Note that we use here an asymmetric definition of the Fourier transform with a $1/2\pi$ factor instead of the standard $1/\sqrt{2\pi}$.. This is the most commonly used convention in this domain.

than τ_c do not contribute significantly to the integral, we can extend the upper bound to infinity. We finally get:

$$\frac{d\rho_{ee}}{dt} = -\Gamma\rho_{ee} - C(\rho_{ee} - \rho_{gg}) \ , \tag{2.167}$$

where

$$C = \frac{d^2}{2\hbar^2}\mathrm{Re}\int_0^\infty \Gamma_E(\tau)e^{(-i\Delta-\gamma')\tau}\,d\tau \ . \tag{2.168}$$

In order to relate C to the incoming field spectral density, we first neglect the transverse relaxation rate γ' in this equation (we assume in the present regime that the dominant cause of spectral broadening is the spectral width of the field, and we can thus safely neglect that of the atomic transition):

$$C = \frac{d^2}{2\hbar^2}\mathrm{Re}\int_0^\infty \Gamma_E(\tau)e^{-i\Delta\tau}\,d\tau \ . \tag{2.169}$$

The worrying point is that the integral only extends from zero to infinity. It is thus not exactly identical to that giving the spectral density of the field at the detuning frequency Δ. We can nevertheless write:

$$2\pi S_E(\Delta) = \int_{-\infty}^0 \Gamma_E(\tau)e^{-i\Delta\tau}\,d\tau + \int_0^\infty \Gamma_E(\tau)e^{-i\Delta\tau}\,d\tau \ . \tag{2.170}$$

With a change of sign of the integration variable and using $\Gamma_E(-\tau) = \Gamma_E^*(\tau)$:

$$\int_{-\infty}^0 \Gamma_E(\tau)e^{-i\Delta\tau}\,d\tau = \int_0^\infty \Gamma_E(-\tau)e^{i\Delta\tau}\,d\tau = \left(\int_0^\infty \Gamma_E(\tau)e^{-i\Delta\tau}\,d\tau\right)^* \ . \tag{2.171}$$

Hence,

$$2\pi S_E(\Delta) = 2\mathrm{Re}\int_0^\infty \Gamma_E(\tau)e^{-i\Delta\tau}\,d\tau \ . \tag{2.172}$$

and, finally

$$C = \frac{\pi d^2}{2\hbar^2}S_E(\Delta) \ , \tag{2.173}$$

a very simple result indeed.

The spectral density is obviously proportional to the spectral energy density u_v at the atomic frequency $\overline{\omega} + \Delta$. Including the proper factors,

$$u_\nu = 2\pi^2\epsilon_0 S_E(\Delta) \ . \tag{2.174}$$

We can thus write

$$C = B_{eg}u_\nu \ , \tag{2.175}$$

with

$$B_{eg} = \frac{d^2}{4\pi\epsilon_0\hbar^2} \tag{2.176}$$

and recover for the population equations those of the Einstein model:

$$\frac{dN_e}{dt} = -A_{eg}N_e + B_{eg}u_\nu(N_g - N_e) \ . \tag{2.177}$$

The B_{eg} value obtained here is somewhat different from that that can be deduced from the link between the A_{eg} and the B_{eg} Einstein's coefficients and from the precise quantum value of the quantum spontaneous emission rate (see Chapter 4):

$$A_{eg} = \frac{d^2\omega^3}{3\pi\epsilon_0\hbar c^3} \ , \tag{2.178}$$

leading to:

$$B_{eg} = \frac{d^2}{6\pi\epsilon_0\hbar^2} \ , \tag{2.179}$$

a factor 2/3 off from the expression above. The difference is due in part to the fact that, here, we have considered an incoming wave with a well defined polarization. In order to get the proper Einstein coefficient, we should average the result over all possible polarizations (the Einstein approach deals with a disordered radiation).

As an exercise on correlation functions, let us now compute that of the field emitted by a spectral lamp. We thus consider emissions by independent atoms. In a semi-classical approach, guided by the charged oscillator model, we will assume that each atom emits at a random time a field pulse at the atomic frequency $\overline{\omega}$, with an exponentially damped amplitude and a random phase. The global field of the source is the sum of these independent pulses:

$$E_1(t) = \sum_{i=-\infty}^{\infty} E_0 e^{i\phi_i} e^{-(t-t_i)/\tau_e} \Theta(t-t_i) \ , \tag{2.180}$$

where the index i enumerates all the individual pulses. The Heavyside function Θ ensures that each pulse has a zero field before it starts. The real E_0 is the common amplitude of all the field pulses, which have phases ϕ_i, start at time t_i and are damped with an emission time constant τ_e (which is clearly a priori of the order of the source correlation time τ_c. We note N_p the number of pulses per unit time.

The correlation function $\Gamma_E(\tau)$ is given by the equation (2.156). Expanding the two fields at different times, we find square terms describing the autocorrelation of an individual pulse and cross terms involving the product of fields generated in different pulses. Since the pulses have random relative phases, it is quite clear that the cross terms average out to zero and that only the square terms contribute to the final result. The autocorrelation function is proportional to that of a single pulse:

$$\Gamma_E = N_p T \gamma_e \ , \tag{2.181}$$

with

$$\gamma_E(\tau) = \frac{1}{T} E_0^2 \int_0^T e^{-t/\tau_e} e^{-(t-\tau)/\tau_e} \Theta(t-\tau)\, dt \ . \tag{2.182}$$

We will take the $T \to \infty$ limit at the end of the calculation. We set $\tau > 0$ and will use the symmetry of the correlation function to get the values for $\tau < 0$. We have assumed without loss of generality that the pulse starts at time $t = 0$. The delayed field is a damped exponential starting at time τ (hence the $\Theta(t-\tau)$ function. During a time interval T, we have $N_p T$ contributing pulses and we thus have $\Gamma_E(\tau) = N_p T \gamma_E(\tau)$.

The computation of $\gamma_E(\tau)$ is then a simple integration exercise. We get rid of the Θ function by changing the lower integral bound from 0 to τ, extend the other bound to ∞ since $T \gg \tau_e$ and get:

$$\begin{aligned} \gamma_E(\tau) &= \frac{1}{T} E_0^2 \left[\int_\tau^\infty e^{-2t/\tau_e}\, dt \right] e^{\tau/\tau_e} \\ &= \frac{1}{T} E_0^2 \frac{\tau_e}{2} e^{-|\tau|/\tau_e} \ , \end{aligned} \tag{2.183}$$

where we introduce a $|\tau|$ to make the expression correct for negative τ values as well. Introducing the normalization factor $N_p T$ and recognizing that the $T \to \infty$ limit is trivial, we get finally:

$$\Gamma_E(\tau) = N_p E_0^2 \frac{\tau_e}{2} e^{-|\tau|/\tau_e} \ , \tag{2.184}$$

which allows us to identify the emission time τ_e with the source's correlation time τ_c. The correlation function has a bi-exponential shape that reflects the envelope of the individual pulses. A simple Fourier

transform leads to the spectral density:

$$S_E(\omega) = \frac{N_p E_0^2}{\pi} \frac{1}{\omega^2 + (1/\tau_e)^2} \ . \tag{2.185}$$

We should remind ourselves that the actual spectrum of the source is this spectral density translated by the average emission frequency $\overline{\omega}$. The source has thus a Lorentzian spectrum, whose width is limited by the pulse emission time, a rather direct consequence of the Fourier transform properties, or, in more shiny worlds, of the Heisenberg time-energy uncertainty relations. For a typical optical transition, the emission time is in the 10 ns range and the spectrum width is thus in the 16 MHz range.

Note that we have assumed here that all atoms in the source emit pulses at the same frequency. This is far from being the case in most actual atomic sources. First, inhomogeneous emission line shifts, due for instance to electric fields in discharge lamps, may contribute to a broadening of the spectrum. Most importantly, we have not taken into account here the Doppler effect due to atomic motion if the emitting atoms are in a gas phase. It is of the order of a few hundred MHz for an optical transition and atoms in a vapour at room temperature.

Doppler effect could be taken into account in our calculations by adding a slow oscillatory component (at the typical Doppler shift frequency) in all pulses and by computing the resulting autocorrelation. Since the cross terms between different pulses do not contribute, we should get, for each velocity class in the sample, the same correlation function as above, centred at the Doppler-shifted frequency. The total correlation function is thus the average of these shifted bi-exponential correlation functions, weighted by the velocity distribution.

The spectrum is thus a convolution of the Lorentzian emission-time limited shape by the Gaussian distribution of Doppler shifted frequencies (a Voigt profile). There are two simple limiting cases. When $1/\tau_e$ is much smaller than the Doppler width, the spectrum is a Gaussian. This is for instance the case in the very low pressure spectral lamps, such as the historical Geissler tube. The other limit is when τ_e is very short. The spectrum is then Lorentzian, and its width dominated by the emission time broadening. This occurs in two limiting cases. The first occurs when the Doppler effect is very small, either because the atomic velocities are small (emission by an ensemble of laser cooled atom) or because one observes the fluorescence of an atomic beam at a right angle with respect to its mean velocity. The second limiting case occurs when the coherence time of the source, τ_e is reduced, for instance because of collisions between excited atoms or between excited atoms and a background gas. This is the case in most high-pressure gas lamps (sodium lamps for street lightning) in which the discharge operates at very high pressures. The spectrum is then again mostly Lorentzian, with a width in the GHz range or above.

2.6 Applications of the optical Bloch equations

We now focus on a few direct applications of the Optical Bloch equations. We first examine the saturation of an optical transition by a strong field in the high-transverse relaxation regime, leading to features absent from the classical model of the first Chapter. We describe optical pumping, which allows one to act on the internal state of a multi-level atom through its interaction with a laser field. We then turn to coherent excitation phenomena, dark resonance and eletromagnetically-induced transparency (EIT). They rely on subtle quantum interference phenomena and lead to interesting applications such as slow light propagation and coherent transfer of quantum information between light and atomic ensembles. We finally supplement the OBEs with the classical Maxwell equations and write the full equations of propagation of a classical light in a quantum atomic medium.

2.6.1 Steady-state and saturation

We consider first the simple problem of the energy exchange between matter and field. We have already, in the first Chapter, written the power delivered to the matter by the field, in the harmonically bound electron model. We recall here the main result [see Eq.(1.30)]: the density of energy released by the field in the matter is $\mathcal{E} = \frac{1}{2}\epsilon_0\omega\chi''|E_1|^2 = \frac{1}{2}\epsilon_0\omega\mathcal{N}\alpha''|E_1|^2$, where $\mathcal{N}$ is the number (or density) of atoms, ω the incoming field frequency, E_1 its complex amplitude and α'' the imaginary part of the atomic polarizability. We plan to compare this simple expression to the predictions of the OBEs.

Let us first turn the expression of $\mathcal{E}$ in a slightly different form. Noting that the complex dipole amplitude is $D = \epsilon_0\alpha E_1$, we can write $\mathcal{E}$ as:

$$\mathcal{E} = \mathcal{N}\frac{\omega E_1}{2}\mathrm{Im}\, D \ , \tag{2.186}$$

where we assume in the following for the sake of simplicity, without real loss of generality, that E_1 is real. The power released is proportional to the incoming intensity. Classical atoms can radiate arbitrary power levels. This should not be the case for a quantized two-level atom.

In the semi-classical model, we will replace in the above expression of $\mathcal{E}$ the dipole by $\mathcal{D}$ [Eq.(2.133)]. Whatever the precise values of the relaxation coefficients are, the atom will reach after some time a steady state. The corresponding dipole value is given by Eq.(2.151):

$$\mathcal{D} = \frac{\Delta + i\gamma'}{\Delta^2 + \gamma'^2}\frac{d^2E_1}{\hbar}(N_g - N_e) \ . \tag{2.187}$$

In this regime, the steady state value of the upper state population[11] is:

$$N_e = \frac{d^2E_1^2}{2\hbar^2\Gamma}(N_g - N_e)\frac{\gamma'}{\Delta^2 + \gamma'^2} \ , \tag{2.188}$$

and, from $N_g + N_e = 1$:

$$N_e = \frac{s/2}{1+s} \tag{2.189}$$

$$N_g - N_e = \frac{1}{1+s} \ , \tag{2.190}$$

where we define the 'saturation parameter', s by:

$$s = \frac{\Omega^2}{\Gamma\gamma'}\frac{1}{1 + \Delta^2/\gamma'^2} \ , \tag{2.191}$$

and making finally use of the Rabi frequency $\Omega = dE_1/\hbar$. Note that in this regime (with no external pumping on the atoms), $N_g - N_e$ is always positive as in the classical case. The medium is always absorptive. The saturation parameter varies, as a function of the detuning Δ as a Lorentzian, whose width is given by γ', a rather intuitive result. We get from there finally the average value of the dipole D, whose square modulus $|D|^2$ in the steady state is:

$$|D|^2 = d^2\frac{\Gamma}{\gamma'}\frac{s}{(1+s)^2} \ . \tag{2.192}$$

Using the expression of $N_g - N_e$ and plugging that of D into $\mathcal{E}$, we finally arrive at :

$$\mathcal{E} = \frac{\mathcal{N}\hbar\omega\Gamma}{2}\frac{s}{1+s} \ , \tag{2.193}$$

[11] We deal here with the OBE populations (which sum to one), not to be mistaken with the total number of atoms $\mathcal{N}$

Clearly, s is large when the Rabi frequency dominates the evolution, small when the Rabi frequency is small compared to the relaxation rates. For small values of Ω, the shape of the absorption curve versus Δ follows that of the saturation parameter s and is thus also a Lorentzian. For high intensities, the width of the resonance curve increases and its top flattens, since $\mathcal{E}$ cannot exceed $N\hbar\omega\Gamma/2$ (see below). At resonance ($\Delta = 0$), we have:

$$s = s_0 = \frac{\Omega^2}{\Gamma\gamma'} \ . \tag{2.194}$$

For low input powers,the power absorbed by the matter is proportional to s_0, i.e. to the square of the incoming field amplitude. We thus basically recover the results of the classical model. For large s_0 values, the power saturates to a finite value. This saturation in stark contradiction with the predictions of the classical model. The limit for very large s_0 is:

$$\mathcal{E}_s = \mathcal{N}\hbar\omega\frac{\Gamma}{2} \ . \tag{2.195}$$

It has a simple interpretation. The power radiated by atom is one photon ($\hbar\omega$) each time interval $2/\Gamma$. At saturation, the populations of the two levels are equal and, hence, both 0.5 on the average. An atom in $|e\rangle$ radiates one photon in a time $1/\Gamma$. Hence a saturated atom radiates at a rate $2/\Gamma$.

The transition between the classical linear regime and the saturation regime occurs for $s_0 \approx 1$. Let us discuss the physical signification of this $s = 1$ condition. Noting that $s_0 = d^2E_1^2/\hbar^2\Gamma\gamma'$ and that the incident power per unit surface is $I = \epsilon_0 c E_1^2/2$, we can write

$$s_0 = \frac{d^2E_1^2}{\hbar^2\Gamma\gamma'} = \frac{I}{I_s} \ , \tag{2.196}$$

where the saturation intensity I_s is defined as

$$I_s = \frac{\Gamma\gamma'}{d^2}\frac{\epsilon_0 c}{2}\hbar^2 \ . \tag{2.197}$$

In order to estimate the order of magnitude of the saturation intensity, we will consider the case $\gamma' = \Gamma/2$ (no additional transverse damping):

$$I_s = \frac{\Gamma^2}{4}\frac{\epsilon_0 c}{d^2}\hbar^2 \ . \tag{2.198}$$

Let us plug in the exact quantum expression of the spontaneous emission rate (see Chapter 4) $\Gamma = \omega^3 d^2/3\pi\epsilon_0\hbar c^3$, After a bit of algebra, and noting that $\omega^2/c^2 = 4\pi^2/\lambda^2$, where λ is the transition wavelength, we get:

$$I_s = \frac{\pi}{3}\hbar\omega\Gamma\frac{1}{\lambda^2} = \hbar\omega\frac{\Gamma}{2}\frac{1}{\sigma_c} \ , \tag{2.199}$$

where we have introduced again the classical resonant absorption cross section $\sigma_c = 3\lambda^2/2\pi$. The saturation intensity corresponds thus to a classical absorption on one photon at a rate $\Gamma/2$, the maximum power a quantum atom can diffuse

Taking a typical atomic transition, with $\Gamma = 3.10^7$ s^{-1} i.e. an excited lifetime of 30 ns, a photon energy of 1.5 eV, corresponding to a 1 μm wavelength (these orders of magnitude are relevant for the principal line of the Caesium atom), we get $I_s = 6$ W/m^2 or $I_s = 0.6$ mW/cm^2. This is a rather low power, easily reached with standard laser sources. Driving such a line far above saturation is easy. It shows that the classical model is inappropriate in most cases, not a surprising result.

When the saturation parameter is large, the absorbed power (of the order of I_s) is much lower than the input one. A strong drive makes an atomic medium nearly transparent. This leads to quite interesting applications, in particular saturated absorption spectroscopy.

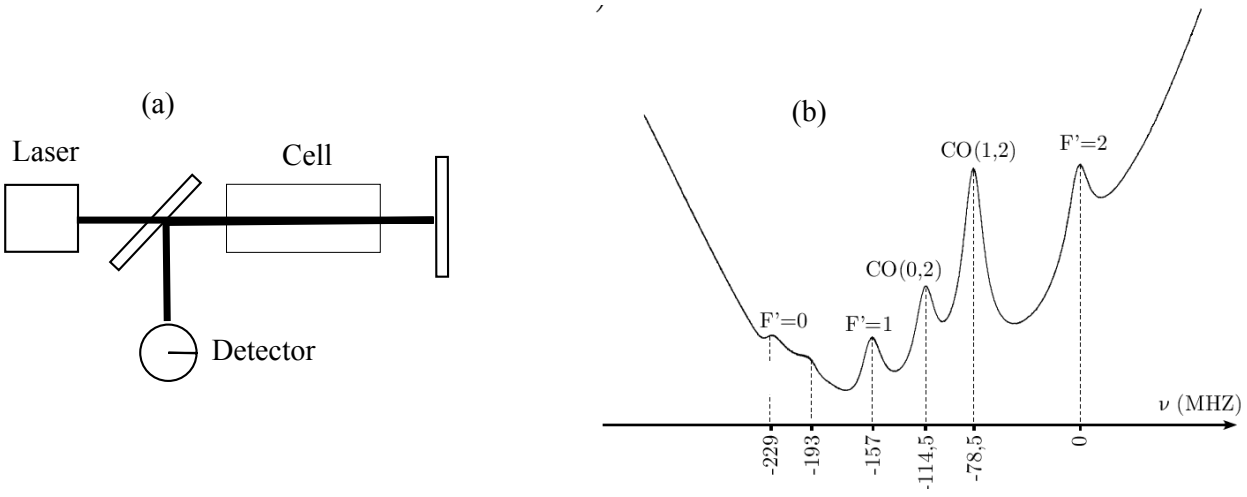

Figure 2.2: (a) Typical saturated absorption set-up. (b) Saturated absorption spectrum on the transition between the $F = 1$ ground state and the $F' = 0, 1, 2$ excited levels. The signal is proportional to the detected intensity.

Laser spectroscopy in a vapour has to face the problem of the Doppler broadening, a few hundred MHz at room temperature for a gas. This is much more than many interesting structures, such as the hyperfine splittings in excited states. This is of course also much larger than the spectral width, of the order of $1/\Gamma$, due to the finite lifetime of the excited states.

Doppler-free spectroscopy is thus badly needed. There are a few techniques available. The most ancient ones rely on atomic beam technology, the interrogation laser propagating then at a right angle with the beam. Only the second-order relativistic Doppler effect is left, much less important in magnitude (being of order $v^2/c^2 \approx 10^{-12}$ for thermal velocities). Laser cooling can also be used, but these two methods imply rather large and complex apparatus. For simple experiments, compatible with atoms contained in a small cell at room temperature, Doppler-free two photon and saturated absorption are to be preferred. The second is most widely used, since it can be applied to almost any atomic transition.

The typical set-up for saturated absorption is shown on figure 2.2(a). A cell contains the resonant atoms. The laser beam at frequency ω propagates through the cell, is reflected back onto a mirror and the returning beam is separated from the incoming one by a beam-splitter (in most cases, one uses polarizing beam-splitter and wave-plates to separate the incoming and outgoing lases without signal losses). The final power of the outgoing laser is measured with a quadratic detector.

It is important to realize that, due to the Doppler effect, only one velocity class is exactly resonant with the incoming laser. Calling z the propagation axis (oriented in the direction of the incoming laser), the resonance condition is obtained when $\Delta = \omega_{eg} - \omega = -kv_z$, where k is the laser wave-vector and v_z the z component of the atomic velocity.

In a first qualitative picture, all velocity classes are impervious to the incoming laser, but the one that is on resonance. A part of the incoming laser is absorbed. Close to saturation, it is proportional to the density of atoms in the velocity class. Measuring the single pass absorption clearly leads to the Doppler-broadened spectrum.

Let us now consider the return beam. It is also resonant with a single velocity class, with a velocity v'_z given by the resonance condition $\Delta = kv'_z$ (note that this laser propagates in an opposite direction). If the resonant classes for the two lasers are different, the absorption on the return path adds to the absorption on the incoming path. However, when the two paths address the same velocity class, the absorption of the return beam is reduced due to the saturation induced by the first. Because of saturation, the absorptions do no simply add as in the linear classical model. Hence, one should

observe a narrow reduction of the overall absorption when the two beams address the same velocity class, i.e. when $v_z = 0$, and hence $\Delta = 0$. This saturated absorption transmission peak is centred precisely on the atomic frequency and appears on the wide background of the Doppler-broadened absorption [figure 2.2(b)].

More quantitatively, out of resonance (Δ much larger than Ω and Γ), the two counterpropagating beams interact with different velocity classes due to the Doppler effect. The absorptions are independent and equivalent to one path in a medium with a double density $2\mathcal{N}$. The absorbed energy is

$$\mathcal{E} = 2 \times \frac{\mathcal{N}\hbar\Omega\Gamma}{2} \frac{s_0}{1+s_0} \tag{2.200}$$

At resonance ($\Delta = 0$), the two beams interact with the $v_z = 0$ class. The saturation parameter is doubled (twice the intensity) but the density is twice lower (only one class). The absorbed energy is then:

$$\mathcal{E}_0 = \frac{\mathcal{N}\hbar\Omega\Gamma}{2} \frac{2s_0}{1+2s_0} \tag{2.201}$$

Hence, the 'dip depth' is

$$\frac{\mathcal{E}_0}{\mathcal{E}} = \frac{1+s_0}{1+2s_0} \tag{2.202}$$

and its width is $\gamma'\sqrt{1+s_0}$.

To observe the peak, one should be in a moderate saturation regime. For too low s_0 parameters, the absorptions add linearly, even when the two paths address the same velocity class. For too high s_0 parameters, the medium is basically transparent and no absorption can be detected. The best compromise corresponds to $s_0 \approx 1$, with a dip depth of 1/3 and a width of $2\gamma'$).

This simple picture does not give us the frequency resolution of the method. By considering equation (2.193), we see that the width of the absorption line in the absence of Doppler effect is $\gamma'\sqrt{1+s_0}$. This is also of course the order of magnitude of the saturated absorption transmission peak. For s of the order of unity, the width of the peak is thus set by the total transverse relaxation rate γ', equal to $\Gamma/2$ when no other phenomenon than spontaneous emission contributes to the linewidth. The saturated absorption method thus reaches nearly the limit set by the excited level lifetime.

Saturated absorption spectroscopy has been widely used for high-resolution atomic and molecular spectroscopy. It is particularly interesting for infrared molecular lines, which can have extremely small intrinsic linewidths. Saturated spectroscopy is also often used to lock lasers to atomic lines for long-term stability. The simple arrangement (one cell, one mirror, one beamsplitter and a detector) makes it very appealing for extensive use. A modern cold atom experiment optical table may contain up to ten lasers, all locked to saturated absorption lines of an alkali atom.

In most cases, the atoms have more than two levels. This is particularly the case for most alkalis, who have a rich hyperfine structure. In this case the saturated spectrum may exhibit a more complex structure, due to the presence of crossover resonances.

In order to understand them, we qualitatively consider a simple three level model. Our atom has two nearly degenerate ground states, $|g\rangle$ and $|f\rangle$, and an excited state $|e\rangle$ coupled to both ground levels by dipole transitions at the respective frequencies ω_{ge} and ω_{fe}.

The saturated absorption spectrum will obviously present transmission peaks at both ω_{ge} and ω_{fe}. There is another additional feature. Let us consider the velocity class resonant on the ω_{fe} frequency for the first pass in the cell. Its velocity is given by the resonance condition $kv_z = \omega - \omega_{fe}$. The laser being at saturation, it promotes a large fraction of the atoms initially in $|f\rangle$ into the excited level $|e\rangle$. Hence, for this velocity class, the absorption of a laser resonant on the $|g\rangle \to |e\rangle$ transition will be reduced. The return path is resonant on this latter transition and this velocity class provided $kv_z = -(\omega - \omega_{ge})$. Hence, we get a 'cross-over' transmission peak if $\omega - \omega_{fe} = -(\omega - \omega_{ge})$ i.e. if

$$\omega = \frac{\omega_{fe} + \omega_{ge}}{2} \ , \tag{2.203}$$

at the middle between the two standard saturated absorption features. There are three lines in the spectrum.

2.6.2 Optical pumping

Optical pumping covers a rather large variety of techniques whose aim is to use light to control the internal state of the atoms. For instance, it is used to prepare the atoms in a single magnetic quantum number state, i.e. to control the internal angular momentum of the atoms. It has been originally proposed by A. Kastler in 1950. It has been observed for the first time in 1952 by J. Brossel on a sodium atomic beam, and in a cell by B. Cagnac in 1961. It led since then to considerable experimental developments. Optical pumping is still an important tool for laser manipulation of atoms and plays a key role in atomic cooling, whose aim is to control also the external degrees of motion of the atom, i.e. its motion.

The general theory of optical pumping occupies entire books. We will limit ourselves to a simple model, with a three-level atom as above. The excited level $|e\rangle$ may decay by spontaneous emission towards both the ground state levels $|g\rangle$ and $|f\rangle$ with respective rates Γ_{eg} and Γ_{ef}. We start from a situation in which both ground levels are populated and want to reach one in which only level $|f\rangle$ is populated.

The simple idea of optical pumping is to drive selectively with a light source (a laser or, in the early days of optical pumping, a spectral lamp) the $|g\rangle \rightarrow |e\rangle$ transition. From $|e\rangle$ either the atom falls back into $|g\rangle$ by spontaneous emission, and nothing has been done, or it falls back to $|f\rangle$ and stays there since the excitation source is selective. It is clear that, after a few absorption/emission cycles, the atom will eventually end up in $|f\rangle$.

The excitation selectivity on the $|g\rangle \rightarrow |e\rangle$ transition can be achieved through the source frequency, if the difference between ω_{ge} and ω_{fe} is large enough. This is for instance the case when pumping in one of the hyperfine ground state sublevels of an alkali atom. The typical hyperfine splitting being of a few GHz, the structure can be resolved with a laser or even with a spectral lamp. When the two frequencies are too close, one can use instead the polarization selectivity of the atomic transitions. This is the case for the optical pumping of the magnetic sublevels. Then, the polarization of the source is chosen to couple to a single transition.

Let us make this simple model more quantitative with an Einstein coefficient approach (strong transverse relaxation). We need to generalize equation (2.153) in the large γ' limit for this three level situation. It is not too difficult to guess the right form of the rate equations for the three levels populations:

$$\frac{dN_e}{dt} = -(\Gamma_{eg} + \Gamma_{ef})N_e + \frac{\Omega^2}{2\gamma'}(N_g - N_e) \tag{2.204}$$

$$\frac{dN_g}{dt} = \Gamma_{eg}N_e - \frac{\Omega^2}{2\gamma'}(N_g - N_e) \tag{2.205}$$

$$\frac{dN_f}{dt} = \Gamma_{ef}N_e \ , \tag{2.206}$$

with $1 = N_e + N_f + N_g$, where Ω is the Rabi frequency on the driven transition.

The steady state can be obtained easily. From the last equation, we get $N_e = 0$. Plugging in the second, it leads to $N_g = 0$ and, hence, to $N_f = N$. In the steady state, all the atoms are in level $|f\rangle$ as intuitively expected.

Let us now examine the dynamics towards the steady state. We take as initial condition $N_g = N$, without loss of generality (if some atoms are already in $|f\rangle$, they will not take part in the dynamics). We also assume, for the sake of simplicity, a weak pumping limit:

$$\frac{\Omega^2}{\gamma'} \ll \Gamma_{eg},\ \Gamma_{ef} \ . \tag{2.207}$$

The population in level $|e\rangle$ is thus low. We can treat it as being at any time in a steady-state given by the first equation:

$$N_e = \frac{\Omega^2/2\gamma'}{\Gamma_{eg} + \Gamma_{ef} + \Omega^2/2\gamma'} N_g \approx \frac{\Omega^2/2\gamma'}{\Gamma_{eg} + \Gamma_{ef}} N_g \ . \tag{2.208}$$

Plugging this result in the equation of evolution for N_g, we get:

$$\frac{dN_g}{dt} = -\Gamma_p N_g \ , \tag{2.209}$$

where we define the optical pumping rate Γ_p by:

$$\Gamma_p = \frac{\Gamma_{ef}}{\Gamma_{eg} + \Gamma_{ef}} \frac{\Omega^2}{2\gamma'} \ . \tag{2.210}$$

The population of level $|g\rangle$ decreases exponentially with a rate Γ_p, proportional to the source intensity, as expected in this rate equation model.

2.6.3 Dark resonances and EIT

In the previous paragraphs, we have considered multi-level systems in the simple case when the interaction with light can be described in terms of rate equations. We now scrutinize in more details this situation in the coherent evolution case. We will show that new and interesting phenomena arise, due to a quantum interference process between the competing atomic transitions. We will discuss the important phenomenon of electromagnetically induced transparency. We will also finally outline the study the atomic levels modifications by a resonant (Autler Townes effect) or non-resonant light field (light shift, which play an important role in laser spectroscopy).

Dark states or coherent population trapping

We consider again the three-level structure described above. We assume that two input fields at frequencies ω_1 and ω_2, $\mathbf{E}_1$ and $\mathbf{E}_2$, couple separately (due to selection rules) to the two $|g\rangle \to |e\rangle$ and $|f\rangle \to |e\rangle$ transitions. The total interaction Hamiltonian is $H_i = -\mathbf{d} \cdot (\mathbf{E}_1 + \mathbf{E}_2)$, where $\mathbf{d}$ is the dipole operator (back to the basics). We set

$$d_{eg} = \langle e|\mathbf{d} \cdot \mathbf{E}_1|g\rangle; \qquad d_{ef} = \langle e|\mathbf{d} \cdot \mathbf{E}_2|f\rangle \tag{2.211}$$

We now show that one can define a superposition $|\Psi_-\rangle$ of $|g\rangle$ and $|f\rangle$ that is not coupled to the field. Let $|\Psi_-\rangle = c_g\,|g\rangle + c_f\,|f\rangle$. It decouples from the field if $\langle e|H_i\,|\Psi_-\rangle = 0$ or $c_g d_{eg} + c_f d_{ef} = 0$ i.e.

$$c_g = \frac{d_{ef}}{d} \qquad \text{and} \qquad c_f = -\frac{d_{eg}}{d} \tag{2.212}$$

or

$$|\Psi_-\rangle = \frac{d_{ef}}{d}\,|g\rangle - \frac{d_{eg}}{d}\,|f\rangle \tag{2.213}$$

with

$$d = \sqrt{|d_{eg}|^2 + |d_{ef}|^2} \ . \tag{2.214}$$

The decoupling of the 'dark' state $|\Psi_-\rangle$ with the field is clearly due to a quantum interference phenomenon: excitation can occur either through the $|g\rangle$ component or through the $|f\rangle$ component and these two competing excitation paths have amplitudes, proportional to the Rabi frequencies, which interfere destructively, leading to a vanishing probability for making the transition to $|e\rangle$.

Obviously the orthogonal state (in the $\{|g\rangle, |f\rangle\}$ subspace):

$$|\Psi_+\rangle = \frac{d_{eg}^*}{d}\,|g\rangle + \frac{d_{ef}^*}{d}\,|f\rangle \ , \tag{2.215}$$

is coupled to the driving field.

If we switch to the $\{|\Psi_+\rangle, |\Psi_-\rangle\}$ basis in the ground state manifold, we are left with one level coupled to the excited state and another uncoupled. We are thus back very much in the optical pumping situation. If we now include the relaxation from the excited level into both ground states ones and switch on the driving field, the atom will be rapidly pumped into the dark state which is decoupled to the field. The fluorescence emission by the atom will stop and it will remain impervious to the incoming light.

We have here written the states and the fields at a given time. The dark state condition will be independent of time if the two lower levels are exactly degenerate and it the lasers are both at exact resonance. When $|g\rangle$ and $|f\rangle$ have different energies, or Bohr frequencies, ω_g and ω_f, the dark state superposition evolves in time as well as the electric fields. The dark state condition will be maintained for every time provided:

$$|\Psi_-\rangle(t) = \frac{d_{ef}}{d} e^{-i\omega_1 t} e^{-i\omega_g t} |g\rangle - \frac{d_{eg}}{d} e^{-i\omega_2 t} e^{-i\omega_f t} |f\rangle \tag{2.216}$$

is, within a global phase, independent of time i.e; if $\omega_1 + \omega_g = \omega_2 + \omega_f$ or

$$\omega_1 - \omega_2 = \omega_{fg} \ , \tag{2.217}$$

if the difference of the fields frequencies is equal to the Bohr frequency between the two ground states. This is nothing but a Raman resonance condition.

The first evidence of dark resonances has been obtained in 1976 by Gozzini and his group in Pisa. They illuminated by two laser modes an atomic vapor placed in a gradient of magnetic field sweeping the transition frequency with the position, and observed a narrow dark spot in the fluorescence induced by the lasers where the Zeeman level splitting exactly matched the frequency difference of the two modes.

Note that the dark resonances are closely related to the STIRAP technique, which allows a fast and efficient transfer from $|g\rangle$ to $|f\rangle$ by modulating with time the relative amplitudes of the two lasers. Using a counter intuitive sequence in which the laser coupled to $|f\rangle$ is switched off while the other has a raising intensity, one can achieve the transfer by remaining at any time in the Dark state, avoiding thus any noise due to spontaneous emission from $|e\rangle$.

Electromagnetically induced transparency

We now examine another important quantum interference situation, where the interference is now the competition between two excitation paths driven by two classical fields. We thus return the the non-degenerate case ($\omega_{ge} \neq \omega_{fe}$) and assume that we drive the $|f\rangle \rightarrow |e\rangle$ transition with a strong pump field E at frequency ω (resulting Rabi frequency Ω) and simultaneously the $|g\rangle \rightarrow |e\rangle$ transition with a weaker proble field E' at frequency ω', and a Rabi frequency Ω'. We assume here that the laser on the $|f\rangle \rightarrow |e\rangle$ transition is resonant, while the other may be detuned from exact resonance by $\Delta' = \omega_{eg} - \omega'$.

The OBE equations, including the spontaneous emission relaxation, cannot be obtained in a completely trivial way. We would have to return to the basic Hamiltonian and Liouvillian ant to redo all the initial derivations of this Chapter from the very start. We leave this lengthy path to the reader as an exercise and only give here the final result.

With self-explanatory notations, the equations of motion of the atomic density matrix relevant elements read:

$$\frac{d\rho_{ee}}{dt} = -(\Gamma_{ef} + \Gamma_{eg})\rho_{ee} - \Omega \mathrm{Im}\, \rho_{ef} - \Omega' \mathrm{Im}\, \rho_{eg} \tag{2.218}$$

$$\frac{d\rho_{ff}}{dt} = \Gamma_{ef}\rho_{ee} + \Omega \mathrm{Im}\, \rho_{ef} \tag{2.219}$$

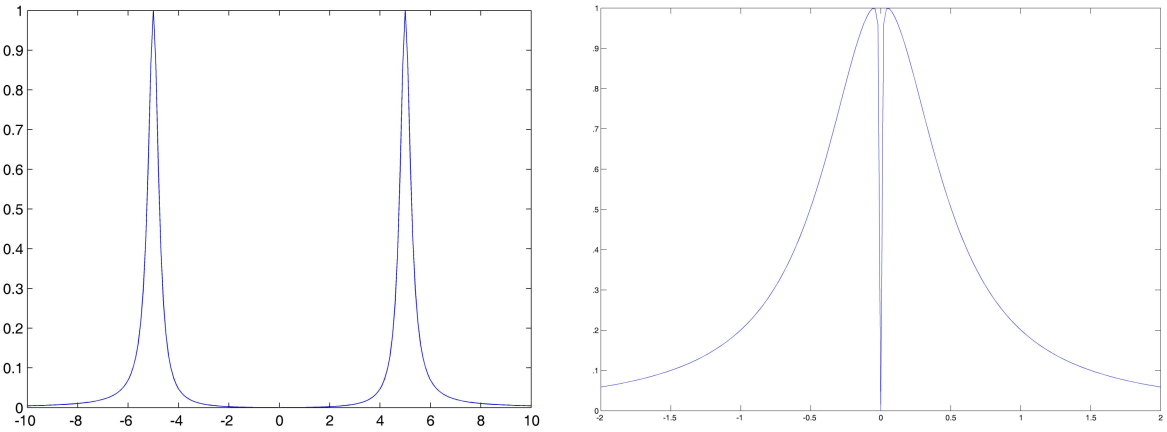

Figure 2.3: EIT signals. Absorption of the probe field as a function of the detuning Δ for $\Omega = 10\Gamma$ (left) or $\Omega = 0.1\Gamma$ (right). The unit of the horizontal axis is Γ.

$$\frac{d\rho_{gg}}{dt} = \Gamma_{eg}\rho_{ee} + \Omega' \mathrm{Im}\,\rho_{eg} \tag{2.220}$$

$$\frac{d\rho_{ef}}{dt} = -\frac{\Gamma_{ef}}{2}\rho_{ef} + i\frac{\Omega}{2}(\rho_{ee} - \rho_{ff}) + i\frac{\Omega'}{2}\rho_{gf} \tag{2.221}$$

$$\frac{d\rho_{eg}}{dt} = -\left(\frac{\Gamma_{eg}}{2} + i\Delta'\right)\rho_{eg} + i\frac{\Omega'}{2}(\rho_{gg} - \rho_{ee}) + i\frac{\Omega}{2}\rho_{fg} \tag{2.222}$$

$$\frac{d\rho_{gf}}{dt} = -i\Delta'\rho_{gf} + i\frac{\Omega}{2}\rho_{ge} - i\frac{\Omega'}{2}\rho_{ef} \tag{2.223}$$

It is clear that the structure of these equations cannot be guessed easily from that of the standard two-level OBEs; In particular the coupling of the coherences to the populations contain non trivial terms, and the coherence between the two ground levels plays an important role.

Simplifying a bit these equations by assuming $\Gamma_{ef} = \Gamma_{eg} = \Gamma$, it is possible to extract the absorption of the probe field E' (proportional to $\mathrm{Im}\,\rho_{eg}$ in the steady state. The absorbed energy $\mathcal{E}'$ is found to be proportional to:

$$\mathcal{E}' \propto \frac{\Gamma^2\Delta'^2}{\Gamma^2\Delta'^2 + 4\left(\Delta'^2 - \Omega^2/4\right)^2} \tag{2.224}$$

This rather complex expression is plotted in figure 2.3 in two simple limiting cases.

When the pump field Rabi frequency Ω is large compared to the excited level width, we get two lines separated by the Rabi frequency. This is the Autler-Townes splitting whose physical significance will be discussed in more details in the next paragraph. When Ω is very small as compared to Γ, we find an absorption profile with a width Γ (as for a two-level atom) with a dip in the centre, going all the way to zero absorption. The width of this dip is of the order of Ω, and can be made nearly arbitrarily small by reducing the pump laser power (not all the way to zero, since the approximations performed to derive the above expression of the absorption would not apply any longer for very low Ωs).

At exact resonance of the probe field, the pump field create a near zero absorption gap, hence the name Electromagnetically Induced Transparency coined for the phenomenon. It results from a subtle quantum interference between the absorption processes of the two lasers.

In these conditions, a narrow hole is created in the absorption profile. This makes EIT a useful spectroscopic tool on the one hand. On the other hand, since absorption is proportional to the

imaginary part of the susceptibility χ, it has a fast variation in a narrow frequency range around resonance. In fact, the real part of χ has also a rapid variation in the transparency gap, which can either be computed directly from the OBEs or through the Kramers Kronig relations relating the real and imaginary parts of the susceptibility.

A medium made of atoms in the EIT configuration has thus a refraction index for the probe beam, $n(\omega')$, which varies extremely rapidly with the frequency. In particular, at exact resonance, n is a rapidly growing function of ω'. Reminding ourselves that the group velocity, v_g, for light propagating in a medium is:

$$v_g = \frac{c}{n + \omega' \, dn/d\omega'} \ , \tag{2.225}$$

we recognize that, close to resonance, the velocity of light is considerably reduced with respect to c.

This 'slow light' phenomenon has been observed in a variety of media, such as transparent solids doped with optically active ions, and in particular in cold atomic samples or Bose Einstein condensates. Considerable velocity reductions can be obtained, down to the m/s range. It is even possible, by switching off the pump laser intensity while the light is inside the medium, to stop the light altogether. It restarts again at low speed when the pump intensity is restored.

Note that the conditions for the observation of the slow light effect are demanding. The whole light pulse should fit in the medium (with an extension of a few hundred microns for BECs). It should thus be short enough in time. But the pulse spectrum should also be all contained in the EIT transparency window and inside the high index variation region, which is as narrow as Ω, much lower than the optical frequency. A careful optimization of the parameters is thus mandatory.

What does a stopped light (or such slow light) really means? In fact, the thing that propagates is not pure light, but a complex mixture of light together with atomic spin coherence. In the stopped light case, the wave is stored in the medium as a spin wave, a coherent spatial arrangement of atomic coherences.

Slow and stopped light can be used for the storage of quantum information carried by light into the atomic medium for later retrieval. This is an important step for quantum key distribution or quantum teleportation operations for instance. These memories can now store individual photons and retrieve them later with a reasonable fidelity.

Of course the storage time is limited. In the cold atom case one of the main limitations, leading to a storage time in the ms range, is the residual atomic motion. This motion blurs the spin pattern which store the incoming light and the retrieval becomes impossible. Of course this effect does not exist in doped crystals, but other sources of inhomogeneous broadening also contribute to limiting the memory lifetime.

Light shifts and Autler Townes splitting

We turn for this paragraph only to a ladder configuration, with $|g\rangle$ as the ground state, $|f\rangle$ being more excited, and $|e\rangle$ even more so. We strongly drive the $|f\rangle \rightarrow |e\rangle$ transition at or close to resonance and we probe with a weak drive the $|g\rangle \rightarrow |f\rangle$ one at ω_{gf}. When the strong drive is off-resonance, there is still a single resonance close to ω_{gf}, but it is shifted with respect to the bare atomic frequency, by an amount proportional to the strong drive intensity. This is the light-shift effect, well known in laser spectroscopy.

When the strong drive is at resonance, the $|g\rangle \rightarrow |f\rangle$ transition is split in two lines, separated by the Rabi frequency Ω of the strong drive, as in the EIT situation for strong drive. This Autler-Townes splitting can be understood in qualitative terms. The strong drive results in a fast oscillation on the $|f\rangle \rightarrow |e\rangle$ transition at frequency Ω. The population in $|f\rangle$ is thus modulated at Ω and, hence, the absorption from $|g\rangle$ also modulated. This modulation creates sideband o the absorption, which are precisely the Autler-Townes lines.

This discussion is obviously utterly qualitative. It can be studied in more details by the OBEs using the formalism of the last paragraph,*mutatis mutandis*. However, the computations are complex

and we will see in Chapter 4 that the dressed atom picture provides a much more detailed and more economic insight into these problems, by coupling a quantum atom to a quantum field. We will thus defer their detailed study to the end of these lectures.

2.6.4 Maxwell-Bloch equations

We have up to now considered the driving field as imposed externally on the system. We now take into account the atomic medium response itself and write the equations for the propagation of light in a medium of two-level atom whose density matrix obeys the OBEs.

We start by recalling a few results about propagation in dielectric matter. The Maxell equations read:

$$\boldsymbol{\nabla} \times \mathbf{E} = -\frac{\partial \mathbf{B}}{\partial t} \tag{2.226}$$

$$\boldsymbol{\nabla} \cdot \mathbf{D} = 0 \tag{2.227}$$

$$\boldsymbol{\nabla} \cdot \mathbf{B} = 0 \tag{2.228}$$

$$\boldsymbol{\nabla} \times \mathbf{B} = \mu_0 \epsilon_0 \frac{\partial \mathbf{E}}{\partial t} + \mu_0 \frac{\partial \mathbf{P}}{\partial t} \ , \tag{2.229}$$

where $\mathbf{E}$ and $\mathbf{B}$ are the electric and magnetic field, $\mathbf{P}$ the density of polarization in the medium and $\mathbf{D}$ the electric displacement $\mathbf{D} = \epsilon_0 \mathbf{E} + \mathbf{P}$. The last term in the last equation corresponds to the bound charges current.

We study the propagation of a transverse wave. All the fields are then divergence-free. By taking the rotational of the first equation an using a standard vector calculs formula, we arrive at the equation of propagation of $\mathbf{E}$:

$$\Delta \mathbf{E} - \frac{1}{c^2} \frac{\partial^2 \mathbf{E}}{\partial t^2} = \mu_0 \frac{\partial^2 \mathbf{P}}{\partial t^2} \ . \tag{2.230}$$

This equation determines the propagation and the dispersion relation if $\mathbf{P}$ can be expressed as a function of $\mathbf{E}$. The standard approach is to use the linear response theory and to introduce the electric susceptibility of the medium. We will use the OBEs instead to compute the polarizability.

Before doing that, we will simplify a bit this equation before proceeding further. We will consider only a nearly monochromatic plane wave at frequency ω, propagating, without loss of generality, along the z axis. Assuming that the medium is isotropic and, thus, that $\mathbf{P}$ and $\mathbf{E}$ are collinear, we can write them as:

$$\mathbf{P} = P_0(z,t) e^{i(kz-\omega t)} \mathbf{u}_x \qquad \text{and} \qquad \mathbf{E} = E_0(z,t) e^{i(kz-\omega t)} \mathbf{u}_x \ , \tag{2.231}$$

where P_0 and E_0 are slowly varying envelopes (their variation describes slow phase or amplitude changes of the wave due to the propagation). We set in these equations $k = \omega/c$ as for free space propagation (the phase shifts due to the index of refraction will be encapsulated in the slowly varying envelope).

We plug these expressions in the wave equation. The second derivatives of the field in z and t cancel due to our choice of dispersion relation. Noting that:

$$\frac{\partial P_0}{\partial t} \ll \omega P_0 \ , \tag{2.232}$$

we can neglect the time derivatives of $\mathbf{P}_0$ in the r.h.s.. We get then, for the slow envelopes:

$$\frac{\partial E_0}{\partial z} + \frac{1}{c} \frac{\partial E_0}{\partial t} = i \frac{\mu_0 \omega^2}{2k} P_0 \ . \tag{2.233}$$

We can compute the local atomic density matrix as a function of $\mathbf{E}$, or more simply as a function of the local field amplitude E_0 by solving the OBEs. From that, we compute the density of polarization.

It is quite clear that, provided the density is large enough (many atoms contribute), it is proportional to $\mathcal{D}$ and thus to the coherence of the atomic density matrix:

$$\mathbf{P}_0 = N\mathcal{D} = 2Nd\rho_{eg} \ , \tag{2.234}$$

where N is the numerical density and where we assume again d real. We thus arrive at the 'Maxwell-Bloch equations', combining the OBEs with the propagation relation:

$$\frac{\partial E_0}{\partial z} + \frac{1}{c}\frac{\partial E_0}{\partial t} = i\frac{\omega N d}{\epsilon_0 c}\rho_{eg} \ . \tag{2.235}$$

These coupled equations are rather complex and must generally be solved numerically. There are some situations in which they can be simplified. We will describe one of them as an exercise.

We consider the propagation of a laser pulse in a medium of atoms, where we can neglect all relaxation phenomena. The OBEs then describe only the Rabi oscillation of the atom between its two levels. Note that this approximation, very rough in most cases, is appropriate, for instance, to describe the propagation of a very short laser pulse (whose duration is much shorter than the spontaneous emission lifetime). The atoms are assumed to be all initially in their ground state $|g\rangle$.

In this simple situation, the atomic state is described entirely by the angle $\phi(z,t)$ of the Bloch vector with the vertical axis (the axis of the Bloch sphere should not be confused with those of the real space in which the wave propagates). This angle rotates at the local Rabi frequency and thus:

$$\frac{d\phi(z,t)}{dt} = \frac{dE_0(z,t)}{\hbar} = \Omega(z,t) \ . \tag{2.236}$$

In order to avoid any difficulty, we shall define in z and at time t the phase of the atomic levels such that the Rabi frequency defined here, and accordingly the angle ϕ are real. This is always possible, since E_0 varies slowly. We then have

$$\rho_{eg} = -i\sin\frac{\phi}{2} \ . \tag{2.237}$$

Plugging this in the propagation equation, we can write the Maxell-Bloch equations as a simple equation for ϕ:

$$\frac{\partial^2\phi}{\partial z\partial t} + \frac{1}{c}\frac{\partial^2\phi}{\partial t^2} = -\mu\sin\phi \ , \tag{2.238}$$

where

$$\mu = \frac{\omega N d^2}{2\epsilon_0\hbar c} \ . \tag{2.239}$$

We can even further simplify this equation by using as independent variables z and the 'retarded time' $\tau = t - z/c$:

$$\frac{\partial^2\phi}{\partial z\partial\tau} - \mu\sin\phi \ , \tag{2.240}$$

This is the Sine-Gordon equation, a well-known non-linear propagation equation.

The propagation in an atomic medium is thus a highly non-linear process. It is only the the limit of a very low intensity, a very small angle of the Bloch vector, that we would recover an ordinary index of refraction. This non-linearity has many interesting properties. In particular, the Sine-Gordon equation sustains solitonic solutions.

Chapitre 3

Field quantization

3.1 Introduction

In this essential Chapter, we give a quantum nature to the field, before treating in the next and final Chapter the interaction of a quantum atom and a quantum field, completing our programme. We start in this short introductory section by recalling the original Planck and Einstein arguments used to quantize the field energy and to built a consistent theory of the blackbody radiation. We then perform the field quantization itself. The first stage in field quantization is in fact a classical electromagnetic problem. We need to define independent, canonical variables for the field dynamics. We will thus devote a long section to the decomposition of the electromagnetic field in orthogonal modes. We will write all the essential quantities, the field energy, the field momentum and the field angular momentum in terms of the dynamical variables of these modes.

We will then be ready to proceed to the field quantization. The analogy between the dynamics of one mode and a one-dimensional harmonic oscillator will help us greatly, by making this quantization a nearly trivial process. We will define the field operators, and examine in detail some interesting field states. We will also define pictorial representations of the quantum field states in the phase space.

In the last two sections, we will supplement the elementary field dynamics, first by coupling two modes with a simple beam-splitter. We will be able to unveil some interesting and deeply quantum phenomena such as the Hong Ou Mandel quantum interference process. The last Section of this Chapter will be devoted to field relaxation. We will guess the quantum jump operators for the field, write the Lindblad master equation and derive a few important consequences.

3.1.1 Planck 1900

The first apparition of the concept of field quantization dates from a communication by Planck at the Berlin Academy of sciences, in December 1900. The interested reader should consult an history of physics treaty to fully understand the problem, Planck's position and the impact of his paper. We will only here give the standard vulgate of the physics textbooks.

Planck's aim was to compute the spectrum of the blackbody field. A blackbody is fully absorbing at any wavelength. When heated to a non-zero temperature T, it emits radiation, as we all can experience. Of course, the blackbody is an idealization. There is no such material that can be fully absorbing for all frequencies (be it only due to the Kramers Kronig relations). However, a good approximation of the blackbody radiation can be obtained by taking that emitted by a small hole pierced in a closed oven, with black diffusive coating on its inner walls. In other words, calculating the blackbody spectrum amounts to computing the thermal equilibrium of the field at a temperature T inside a large closed envelope.

This problem is not only of academic nature. It has also, and already had in Planck's time, considerable industrial applications. Measuring the blackbody radiation is nearly the only way to

get information on the temperature of a furnace or of a melting metal. A great deal was known experimentally at Planck's time. The spectrum had been carefully measured and calibrated in the visible and in the near-infrared. The radiation spectral density, u_ν (see Chapter 1) starts as ν^2 for small frequencies, reaches a maximum and finally decays exponentially at high frequencies. The maximum of the intensity is in the 10 μm wavelength region for room temperature. Its frequency is proportional to the temperature. It is thus in the visible for the solar chromosphere temperature (6000 K).

This density of radiation is universal. It does not depend upon the detailed nature of the envelope containing the radiation. A simple classical thermodynamics argument can be used to show it. Assume that, for at least one frequency ν_0, we could build two ovens such that they do not have the same density of radiation at the same temperature T. Joining the two ovens by a small channel (connected through filters allowing only the frequency ν_0 to flow freely), we would establish a constant flow of energy from one oven to the other. This flow can produce work, and we have thus built an engine working with a single temperature source, an impossibility due to the second principle.

The total power radiated by a surface S was also well known to be proportional to the fourth power of the temperature. This is the Stefan's law:

$$\mathcal{P} = \sigma S T^4 \ , \tag{3.1}$$

where

$$\sigma = 5.67\,10^{-8}\ \mathrm{W/m^2K^4} \ . \tag{3.2}$$

As an order of magnitude, one square centimetre of blackbody at room temperature radiates about 56 mW, a quite appreciable amount. The radiation of the blackbody obeys Lambert's law. The power $d\mathcal{P}$ radiated in the solid angle $d\Omega$ making the angle θ with the normal to the surface is:

$$d\mathcal{P} = LS\cos\theta\, d\Omega \ , \tag{3.3}$$

where the luminance L is related to the total density of energy in the oven, $u = \int u_\nu\, d\nu$, by:

$$L = \frac{cu}{4\pi} \tag{3.4}$$

By a simple integration, we thus get

$$\mathcal{P} = \frac{cSu}{4} \ , \tag{3.5}$$

and hence

$$u = \frac{4}{c}\sigma T^4 \ . \tag{3.6}$$

On the theoretical side, little was known, even though statistical physics and electromagnetism were already quite mature at this time. The difficulty is that classical statistical physics fails to compute the equilibrium state of the field. In a nutshell (more on that in a second), we should attribute an energy $k_b T$ to each degree of freedom, i.e. to each field mode (to each plane wave, or to each standing wave pattern). But there is an infinity of modes and their number raises with the frequency. Classical statistical physics thus predicts boldly that the energy density is infinite, an embarrassing conclusion.

Using careful considerations on the entropy of the radiation (which will be extremely useful for Einstein in his 1905 paper, see next paragraph), Wien had show his 'displacement law', a scaling law for the spectral density:

$$u_\nu = \nu^3 f\left(\frac{\nu}{T}\right) \ , \tag{3.7}$$

where f is a function that Wien could not explicit. He also proposed a semi-phenomenological model for high frequencies:

$$u_v = \alpha\nu^2 e^{-\gamma\nu/T} \ , \tag{3.8}$$

where α and γ could be fitted to the exponentially decreasing part of the spectrum at high frequencies.

Let us reproduce (more or less) Planck's computation of the statistical equilibrium of the field. As will be explained in much more details in the following Section, the field should be expanded on modes, orthogonal harmonic solutions of the Maxwell equations with boundary conditions, such that the total field energy is the sum of the energy of the modes.

For a simple approach, we will here assume that the oven is rectangular, with lengths L_x, L_y and L_z along the three axes and a volume $\mathcal{V} = L_x L_y L_z$. We use periodic boundary conditions on the walls of the oven. The field can only be expanded on plane waves whose wavevector $\mathbf{k} = (k_x, k_y, k_z)$ is such that

$$k_x = \frac{2\pi}{L_x} n_x \ , \tag{3.9}$$

and similar relations for the other components, where $n_{x,y,z}$ is a set of positive or negative integers. Each set of $n_{x,y,z}$ values is associated to two modes, two plane waves with orthogonal polarizations.

This set of plane waves is a basis for all solutions of the Maxwell equations. Moreover, since the scalar product of modes with different $n_{x,y,z}$ values (volume integral of the product of one mode by the complex conjugate of the other) is zero, the energy of the field is the sum of the energies stored in all the modes (this derivation will be performed in great details in the next Section).

We note N_ν the total number of modes with frequency between 0 and ν, i.e. with a wavevector $k < 2\pi\nu/c$. We introduce the spectral density of modes ρ_ν. The number of modes per unit volume between ν and $\nu + d\nu$ is then $\rho_\nu \, d\nu$. Hence,

$$\rho_\nu = \frac{1}{\mathcal{V}} \frac{dN_\nu}{d\nu} \ . \tag{3.10}$$

The total number of modes N_ν is simply, within the factor of 2 due to the polarization, the number of points with integer coordinates inside a sphere with a radius $2\pi\nu/c$. The unit cell of this cubic lattice of points has a volume $8\pi^3/\mathcal{V}$. It contains 8 vertices, but each vertex is shared by 8 adjacent cells. The volume occupied by a point is thus also $8\pi^3/\mathcal{V}$. We thus have:

$$N_\nu = 2 \frac{\frac{4\pi}{3}\left(\frac{2\pi\nu}{c}\right)^2}{\frac{8\pi^3}{\mathcal{V}}} = \frac{8\pi}{3}\frac{\nu^3}{c^3}\mathcal{V} \ , \tag{3.11}$$

and hence

$$\rho_\nu = \frac{8\pi}{c^3}\nu^2 \ . \tag{3.12}$$

The spectral density of modes is proportional to ν^2.

If we apply then the standard statistical physics approach, we will attribute an average energy $k_b T$ to each mode. The spectral density of radiation is then:

$$u_\nu = k_b T \rho_\nu \ . \tag{3.13}$$

This is the Rayleigh-Jeans law. The onset at low frequency fits rather well with the observed spectrum, but the high-frequency part is totally irrelevant, since u_ν diverges as already explained.

In order to circumvent this difficulty, Planck uses a state counting ansatz. He assumes that the matter-field energy exchanges in the oven are quantized and only proceed at frequency ν in integer multiples of a quantity, the light quantum $h\nu$. The field energy at frequency ν is then $E = nh\nu$, where the 'hilfe'constant h has the dimension of an action and n is the integer number of light quanta. It is a simple exercise in statistical physics to compute the average number $\overline{n}$ of these elementary excitations and hence the spectral density.

The average energy per mode $\overline{E}$ is given by the Boltzmann distribution:

$$\overline{E} = h\nu \frac{\sum_{n=0}^{\infty} n e^{-nh\nu/k_b T}}{\sum_{n=0}^{\infty} e^{-nh\nu/k_b T}} \ . \tag{3.14}$$

Setting the shorthand notations $\beta = 1/k_bT$ and $\chi = \beta h\nu$, we note that $\sum \exp(-\chi n) = 1/[1-\exp(-\chi)]$ and $\sum n\exp(-\chi n) = -(d/d\chi)1/[1-\exp(-\chi)] = \exp(-\chi)/[1-\exp(-\chi)]^2$. Hence

$$\overline{E} = h\nu\overline{n} = h\nu\frac{1}{e^{\chi}-1} \ . \tag{3.15}$$

Inserting this in the expression of the spectral density, we finally get the Planck's law:

$$u_\nu = \frac{8\pi h\nu^3}{c^3}\frac{1}{e^{h\nu/k_bT}-1} \ , \tag{3.16}$$

whose form agrees with the Wien's displacement law. Setting

$$h = 6.62\,10^{-34}\ \mathrm{J/s} \ , \tag{3.17}$$

Planck obtained a perfect agreement with the available experimental spectra, a considerable breakthrough.

For small frequencies, the Planck law reduces to

$$u_\nu = \frac{8\pi\nu^2}{c^3}k_bT \ , \tag{3.18}$$

the Rayleigh-Jeans law. For low frequencies, the energy of the light quantum (let us call it anachronistically a photon) is small as compared to the thermal energy and the quantization ansatz of Planck plays no role. We recover the standard statistical physics result.

At large frequencies, the spectral density decreases exponentially. It writes

$$u_\nu = \frac{8\pi h\nu^3}{c^3}e^{-h\nu/k_bT} \ , \tag{3.19}$$

in agreement with the phenomenological Wien's law.

From the spectral density, we can compute the total power radiated by the unit surface of the blackbody. The integration is tedious (use Mathematica!), but gives the theoretical value of the Stefan's constant:

$$\sigma = \frac{2\pi^5}{15}\frac{k_b^4}{c^2h^3} \ , \tag{3.20}$$

whose numerical value agrees remarkably with the experimental one.

Planck thought his quantization ansatz was only a way to compute in a proper way the spectral density. He did not take seriously the fact that the field energy itself could indeed be quantized, that the field might exhibit a corpuscular nature. This point was convincingly made 5 years later by Einstein.

3.1.2 Einstein 1905

In one of the three famous 1905 papers, Einstein tackles the problem of the thermal equilibrium of the field. He starts equipped with the Wien's phenomenological law, in which, according to Planck, $\gamma = h/k_b$:

$$u_\nu = \alpha\nu^3e^{-h\nu/k_bT} = \alpha\nu^3e^{-\gamma\nu T} \ , \tag{3.21}$$

with $\gamma = h/k_b$. This leads by a simple inversion to:

$$T = -\frac{\gamma\nu}{\ln u_\nu/\alpha\nu^3} \ . \tag{3.22}$$

He introduces then the density of entropy of the field s. Since, for all systems, $1/T = \partial S/\partial U$, $ds/du = 1/T$. Replacing T by the expression deduced from the Wien's law and performing the integration, he finds:

$$\begin{aligned} s &= -\int_0^\infty du' \, \frac{\ln u'/\alpha\nu^3}{\gamma\nu} \\ &= -\frac{u}{\gamma\nu}\left[\ln\frac{u}{\alpha\nu^3} - 1\right] . \end{aligned} \tag{3.23}$$

The total entropy $S = s\mathcal{V}$ (including only the contribution from the radiation at frequency ν) is linked thus to the total energy $E = u\mathcal{V}$ by:

$$S = -\frac{E}{\gamma\nu}\left[\ln\frac{E}{\mathcal{V}\alpha\nu^3} - 1\right] . \tag{3.24}$$

Einstein now considers the variation of the entropy with the total volume $\mathcal{V}$. Calling S_0 the entropy for the volume $\mathcal{V}_0$, he writes:

$$S - S_0 = \frac{E}{\gamma\nu}\ln\frac{\mathcal{V}}{\mathcal{V}_0} . \tag{3.25}$$

This compares directly to the variation of the entropy of a perfect gas in an isothermal compression:

$$S - S_0 = k_b N \ln\frac{\mathcal{V}}{\mathcal{V}_0} , \tag{3.26}$$

where N is the total number of particles. It is thus quite tempting to identify the two expressions and to say that the radiation is indeed composed of elementary particles, light quanta or photons, whose number at frequency ν is such that $Nk_b = Ek_b/h\nu$. The energy of each particle is thus $E/N = h\nu$. This sets a clear physical meaning to the Planck's ansatz.

In the last paragraph of this paper, Einstein uses the light quantum concept to shed light on the photoelectric effect, whose theoretical interpretation was also impossible in the frame of classical electromagnetism. This led him to the Nobel ceremony, in 1922. This historical paper marks the real beginning of quantum theory. We will now use the modern formalism to quantify properly the field.

3.2 Field eigenmodes

As shown in the introductory section, the first step in field quantization is to identify properly a set of orthogonal modes on which any solution of the Maxwell equations can be expanded. We will do that in this Section is a quite systematic way. This is a section on classical electromagnetism, but the work done here will make most of the quantization a trivial process. We first define the modes and then turn to the field energy. The last paragraph will be devoted to the field momentum and angular momentum.

3.2.1 Mode decomposition of the electromagnetic field

We set up some limiting conditions. This can be a fictitious box, as the one we used for the Planck calculus, or a real cavity with mirrors surrounding an empty space. The electric field $\mathbf{E}(\mathbf{r}, t)$ and the magnetic field $\mathbf{B}(\mathbf{r}, t)$ obey Maxwell equations and the limiting conditions. We are interested in the field only and there will thus be no sources in the box. We shall use the Coulomb gauge, and the electric potential is thus identically zero. Of course, it is of interest to introduce the Fourier transforms of the fields.

Positive frequency field

We thus define the elecric field time Fourier transform by

$$\mathbf{E}(\mathbf{r},t) = \frac{1}{\sqrt{2\pi}} \int_{-\infty}^{\infty} \widetilde{\mathbf{E}}(\mathbf{r},\omega) e^{-i\omega t}\, d\omega \ . \tag{3.27}$$

Since $\mathbf{E}$ is a real field,

$$\widetilde{\mathbf{E}}^*(\mathbf{r},\omega) = \widetilde{\mathbf{E}}(\mathbf{r},-\omega) \ . \tag{3.28}$$

We can thus split the Fourier transform in two parts and define the 'positive frequency field', integral over only positive frequencies:

$$\mathbf{E}^+(\mathbf{r},t) = \frac{1}{\sqrt{2\pi}} \int_{0}^{\infty} \widetilde{\mathbf{E}}(\mathbf{r},\omega) e^{-i\omega t}\, d\omega \ . \tag{3.29}$$

and the 'negative frequency field':

$$\mathbf{E}^-(\mathbf{r},t) = \frac{1}{\sqrt{2\pi}} \int_{-\infty}^{0} \widetilde{\mathbf{E}}(\mathbf{r},\omega) e^{-i\omega t}\, d\omega = \left(\mathbf{E}^+(\mathbf{r},t)\right)^* \ . \tag{3.30}$$

Note that the positive frequency field is not real in the general case. The real field is the sum of its parts

$$\mathbf{E}(\mathbf{r},t) = \mathbf{E}^+(\mathbf{r},t) + \mathbf{E}^-(\mathbf{r},t) \ . \tag{3.31}$$

This splitting into positive and negative frequency components can of course be extended to all relevant fields and potentials.

Eingenmode basis

We thus set a 'box' of limiting conditions with a total volume $\mathcal{V}$. These conditions can be the cancellation of field components (reflecting boundary conditions) or, as above, periodic boundary conditions (more appropriate for practical use). Inside the box, we look for a solution of the Maxwell equation. All fields are divergence-free (no sources).

Mathematicians show that the ensemble of solutions *for the electric field* with limiting conditions form a Hilbert space, on which we can always define an orthogonal basis. The basis vectors are harmonic and evolve with a positive frequency[1]. They can be written as:

$$\mathbf{f}_\ell(\mathbf{r}) e^{-i\omega_\ell t} \ , \tag{3.32}$$

where the dimensionless amplitude $\mathbf{f}_\ell$ is divergence-free and obeys the Helmholtz equation:

$$\Delta \mathbf{f}_\ell + \frac{\omega_\ell^2}{c^2} \mathbf{f}_\ell = 0 \ . \tag{3.33}$$

The index ℓ enumerates all these solutions that we will call 'modes' from now on. Of course, ℓ may be a set of indices and not a single integer (see the Planck calculation above). Note also that the frequencies ω_ℓ are generally quantized due to the limiting conditions imposed onto the $\mathbf{f}_\ell$s.

This mode basis can be chosen to be orthogonal:

$$\int_{\mathcal{V}} d^3\mathbf{r}\, \mathbf{f}_\ell^*(\mathbf{r}) \cdot \mathbf{f}_{\ell'}(\mathbf{r}) = \delta_{\ell,\ell'} \mathcal{V} \ , \tag{3.34}$$

the normalization condition being:

$$\int_{\mathcal{V}} d^3\mathbf{r}\, |\mathbf{f}_\ell(\mathbf{r})|^2 = \mathcal{V} \ . \tag{3.35}$$

[1] With the simple relation between the positive and negative frequency parts of the field, we need only to expand it on a basis of positive frequency solutions.

We have used here a standard scalar product definition for complex vector functions. We operate in a finite volume. All integrals are thus convergent if the functions are not singular. Note that other normalization choices would be possible. For instance, when studying cavity quantum electrodynamics in Chapter 4, we will normalize the modes with another condition, better adapted to a problem with real limiting conditions. This normalization choice only entails numerical factors here and there and do not, of course, alter the final physical results.

The positive frequency field can be expanded onto this basis according to:

$$\mathbf{E}^+(\mathbf{r},t) = \sum_\ell \mathcal{E}_\ell(t)\mathbf{f}_\ell(\mathbf{r}) \ , \tag{3.36}$$

where the amplitude $\mathcal{E}_\ell$ (which has the dimension of an electric field) can be written, using the mode basis orthogonality as:

$$\mathcal{E}_\ell(t) = \frac{1}{\mathcal{V}} \int \mathbf{E}^+(\mathbf{r},t)\cdot\mathbf{f}_\ell^*(\mathbf{r})\, d^3\mathbf{r} \ . \tag{3.37}$$

Of course the time evolution of the amplitude $\mathcal{E}_\ell$ is harmonic:

$$\mathcal{E}_\ell(t) = \mathcal{E}_\ell(0)e^{-i\omega_\ell t} \ . \tag{3.38}$$

This results directly from the definition of the basis. It can also be recovered by plugging the expansion of $\mathbf{E}^+$ into the d'Alembert equation for the field and observing that $\mathbf{f}_\ell$ obeys the Helmholtz equation. We leave this as an exercise to the reader. Finally,

$$\mathbf{E}^+(\mathbf{r},t) = \sum_\ell \mathcal{E}_\ell(0)e^{-i\omega_\ell t}\mathbf{f}_\ell(\mathbf{r}) \ . \tag{3.39}$$

Plane wave basis

Let us now give a practical example of mode decomposition. We consider, as in the introductory Section, a rectangular box with dimensions L_x, L_y and L_z and chose periodic boundary conditions. A set of solutions of the Maxwell equations is made up of plane waves with a wavevector indexed by a set of three integers $\mathbf{n} = (n_x, n_y, n_z)$ $\mathbf{k_n} = (k_x, k_y, k_z) = (n_x 2\pi/L_x, n_y 2\pi/L_y, n_z 2\pi/L_z)$.

For each set of indices $\mathbf{n}$ we must chose two orthogonal polarizations $\boldsymbol{\epsilon}_1$ and $\boldsymbol{\epsilon}_2$, perpendicular to $\mathbf{k}$. In most cases, we shall take linear polarizations. The first polarization $\boldsymbol{\epsilon}_1$ can be constructed by taking the vector product of $\mathbf{k}$ with a fixed vector (not collinear with any $\mathbf{k}$) and by imposing $\boldsymbol{\epsilon}_1 \times \boldsymbol{\epsilon}_2 = \mathbf{u_k}$, where $\mathbf{u_k}$ is the unit vector in the direction of $\mathbf{k}$.

The index ℓ has thus four components: $\ell = (n_x, n_y, n_z, \epsilon)$ where $\epsilon = 1, 2$. With these notations, the basis vectors are:

$$\mathbf{f}_\ell(\mathbf{r}) = \boldsymbol{\epsilon}_\ell e^{i\mathbf{k}_\ell\cdot\mathbf{r}} \ , \tag{3.40}$$

which have modulus one, ensuring that the normalization condition $\int |f_e ll|^2 = 1$ is automatically fulfilled. The positive frequency field is written as:

$$\mathbf{E}^+(\mathbf{r},t) = \sum_\ell \mathcal{E}_\ell(0)\boldsymbol{\epsilon}_\ell e^{-i\omega_\ell t}e^{i\mathbf{k}_\ell\cdot\mathbf{r}} \ , \tag{3.41}$$

a sum of plane waves.

In a few instances (discussion of the field angular momentum) it is fruitful to use a basis of circularly polarized waves. The corresponding unit vectors can be defined from the linear basis by;

$$\boldsymbol{\epsilon}_\pm = \frac{\boldsymbol{\epsilon}_1 \pm i\boldsymbol{\epsilon}_2}{\sqrt{2}} \ , \tag{3.42}$$

with the obvious relation $\boldsymbol{\epsilon}_+ = \boldsymbol{\epsilon}_-^*$. We introduce one useful relations which can be obtained by expanding the circular polarizations on the linear ones in the vector products and using the linear polarizations geometry:

$$\boldsymbol{\epsilon}_+ \times \boldsymbol{\epsilon}_- = -i\mathbf{u_k} \ . \tag{3.43}$$

Mode basis change

The mode basis is not determined in a unique way. For instance, the basis for the polarizations can be changed, we can turn a plan wave basis into a standing wave basis, or we can use Gaussian laser modes instead of plane waves. We will consider in this paragraph such basis changes. We have two sets of mode functions, $\mathbf{f}_\ell$ and $\mathbf{g}_p$. The 'old' basis $\mathbf{f}_\ell$ can be expanded on the other one according to

$$\mathbf{f}_\ell = \sum_p U_{\ell p} \mathbf{g}_p \ . \tag{3.44}$$

We should not forget at this point that the modes have well defined frequency. We shall thus restrict ourselves to a situation in which the modes coupled by the basis change have the same frequencies (if the sum runs on all modes, all elements $U_{\ell p}$ connecting modes with different frequencies should be zero).

The base orthonormality allows us to write:

$$U_{\ell p} = \frac{1}{\mathcal{V}} \int \mathbf{f}_\ell \cdot \mathbf{g}_p^* \, d^3\mathbf{r} \ . \tag{3.45}$$

The basis change matrix must be a unitary: $U^\dagger U = \mathbb{1}$. We can check that by an explicit calculation as an exercise. Let us write the scalar product of two $\mathbf{f}$ modes:

$$\delta_{\ell,\ell'} = \frac{1}{\mathcal{V}} \int \mathbf{f}_\ell^* \cdot \mathbf{f}_{\ell'} \, d^3\mathbf{r} = \sum_{p,p'} U_{\ell p}^* U_{\ell' p'} \frac{1}{\mathcal{V}} \int \mathbf{g}_p^* \cdot \mathbf{g}_{p'} \, d^3\mathbf{r} \ . \tag{3.46}$$

Using the orthonormality of the $\mathbf{g}$ basis, we get

$$\delta_{\ell,\ell'} = \sum_p U_{\ell p}^* U_{\ell' p} = \sum_p U_{\ell' p} U_{p\ell}^\dagger \ , \tag{3.47}$$

and hence $\mathbb{1} = UU^\dagger$ as expected.

3.2.2 Normal variables

We need now to chose a simple set of dynamical variables to describe the evolution of all fields and in terms of which we can write the system's Hamiltonian. We will use for that purpose the coefficients of the mode expansion of the potential vector.

Potential vector

The potential vector $\mathbf{A}$ is divergence free and, in the Coulomb gauge, $\mathbf{E} = -\partial\mathbf{A}/\partial t$. It is thus, for harmonic modes, proportional to the electric field and can be used as a convenient dynamical variable. We also expand $\mathbf{A}$ in a positive and a negative frequency part and expand the positive part on the same mode basis as $\mathbf{E}$ (they obviously verify the same limiting conditions and the same Helmholtz equation):

$$\mathbf{A}^+(\mathbf{r}, t) = \sum_\ell \mathcal{A}_\ell(t) \mathbf{f}_\ell(\mathbf{r}) \ . \tag{3.48}$$

Of course, for the free field we are considering here, the $\mathcal{A}_\ell$ function evolve at the mode frequency ω_ℓ. The set of the scalar $\mathcal{A}(t)$ functions will be called the 'normal variables'. We show now that all fields and relevant quantities can be expressed as a functions of them.

For energy calculations, it is preferable to use real fields. We will thus define the real and imaginary parts of $\mathcal{A}_\ell$ by:

$$\mathcal{A}_\ell(t) = \mathcal{A}_\ell(0) e^{-i\omega t} = x_\ell(t) + i p_\ell(t) \ . \tag{3.49}$$

All fields

From $\mathbf{E}^+ = -\partial\mathbf{A}^+/\partial t$ (it is easy to show that the relation holds separately for the positive and negative frequencies), we get:

$$\mathcal{E}_\ell(t) = -\frac{d\mathcal{A}_\ell}{dt} = i\omega_\ell \mathcal{A}_\ell \ , \tag{3.50}$$

and hence

$$\mathbf{E}^+(\mathbf{r},t) = \sum_\ell i\omega_\ell \mathcal{A}_\ell(t)\mathbf{f}_\ell(\mathbf{r}) \ . \tag{3.51}$$

The magnetic field is the rotational of $\mathbf{A}$. Hence

$$\mathbf{B}^+(\mathbf{r},t) = \sum_\ell \mathcal{A}_\ell(t)\mathbf{h}_\ell(\mathbf{r}) \ , \tag{3.52}$$

where

$$\mathbf{h}_\ell(\mathbf{r}) = \boldsymbol{\nabla} \times \mathbf{f}_\ell(\mathbf{r}) \ . \tag{3.53}$$

We note immediately that the mode basis for the magnetic field is not the same as for the electric field. Obviously, both fields share the same propagation equation and, when harmonic, obey the same Helmholtz equation. However, the limiting conditions are generally quite different (for instance on conductors, where the tangential component of the electric field vanishes while that of the magnetic field is maximum). The passage from $\mathbf{f}$ to $\mathbf{h}$ is not a mode basis change! The electric potential vanishes. We have now expressed all fields in terms ot the normal variables and we can deduce the expression of the field energy, which will be the field Hamiltonian in the quantum realm.

3.2.3 Field energy: canonical variables

The total field energy H is simply given by:

$$H = \frac{\epsilon_0}{2}\int E^2 + \frac{1}{2\mu_0}\int B^2 \ . \tag{3.54}$$

Let us write it in terms of the normal variables.

The energy must be written in terms the real fields, for instance:

$$\mathbf{E} = 2\mathrm{Re}\,\mathbf{E}^+ = 2\mathrm{Re}\sum_\ell i\omega_\ell \mathcal{A}_\ell \mathbf{f}_\ell \ , \tag{3.55}$$

and a similar expression for $\mathbf{B}$. When inserting these mode sums in the energy and expanding the squares, we will get two types of terms. A first class involves scalar products of different field mode functions. They identically cancel since we use and orthonormal mode basis. Only the square terms remain, which imply one and the same mode. It means that the total field energy is the direct sum of the energies of each mode considered separately, a considerable simplification:

$$H = \sum_\ell H_\ell \ . \tag{3.56}$$

We are left with the much simpler problem to compute the total energy stored in a single mode with index ℓ. In order to make the notations more compact, we will for a time omit the index ℓ in the calculations, since it is shared by all quantities.

Let us start with the electric energy H_e. The real field is

$$\mathbf{E} = i\omega\left[\mathcal{A}\mathbf{f} - \mathcal{A}^*\mathbf{f}^*\right] \ . \tag{3.57}$$

Separating the real and imaginary parts of $\mathcal{A}$ and introducing those of $\mathbf{f}$ defined by:

$$\mathbf{f} = \mathbf{f}' + i\mathbf{f}'' \ , \tag{3.58}$$

we get, after a little bit of algebra:

$$\mathbf{E} = -2\omega \left[x\mathbf{f}'' + p\mathbf{f}' \right] \ . \tag{3.59}$$

Inserting that in the expression of H_e and noting that the x and p variables are independent of $\mathbf{r}$, we get finally

$$H_e = 2\omega^2 \epsilon_0 \left[x^2 \int (\mathbf{f}'')^2 + p^2 \int (\mathbf{f}')^2 + 2xp \int \mathbf{f}' \cdot \mathbf{f}'' \right] \ . \tag{3.60}$$

Let us now proceed with the magnetic energy H_b. In the same vein, we write

$$\mathbf{B} = \mathcal{A}\mathbf{h} + \mathcal{A}^* \mathbf{h}^* = 2x\mathbf{h}' - 2p\mathbf{h}'' \ , \tag{3.61}$$

where we have also separated $\mathbf{h}$ in its real and imaginary parts. Plugging in the energy, we get:

$$H_b = \frac{2}{\mu_0} \left[x^2 \int (\mathbf{h}')^2 + p^2 \int (\mathbf{h}'')^2 - 2xp \int \mathbf{h}' \cdot \mathbf{h}'' \right] \ . \tag{3.62}$$

The expressions of the electric and magnetic energies are very similar and it is quite tempting to group them. In addition we are in classical electromagnetism and we know that, in free space, the electric and magnetic average energies are the same. There must be thus simple relations between the integrals of $\mathbf{f}$ and those of $\mathbf{h}$. We need a bit of vector calculus to check that.

Let us start with the integral of $(\mathbf{h}')^2$, with $\mathbf{h} = \boldsymbol{\nabla} \times \mathbf{f}$. Reminding ourselves that:

$$\boldsymbol{\nabla} \cdot (\mathbf{a} \times \mathbf{b}) = \mathbf{b} \cdot (\boldsymbol{\nabla} \times \mathbf{a}) - \mathbf{a} \cdot (\boldsymbol{\nabla} \times \mathbf{b}) \ , \tag{3.63}$$

we can write

$$\boldsymbol{\nabla} \cdot [\mathbf{f}' \times (\boldsymbol{\nabla} \times \mathbf{f}')] = (\boldsymbol{\nabla} \times \mathbf{f}')^2 - \mathbf{f}' \cdot (\boldsymbol{\nabla} \times \boldsymbol{\nabla} \times \mathbf{f}') \ . \tag{3.64}$$

Since $\mathbf{f}'$ is, as $\mathbf{f}$, divergence-free, the double rotational in the r.h.s. reduces to the opposite of the Laplacian of $\mathbf{f}'$, and, thanks to the Helmholtz equation verified by $\mathbf{f}'$ (both the real and imaginary parts of $\mathbf{f}$ verify this equation), we get

$$\boldsymbol{\nabla} \cdot [\mathbf{f}' \times (\boldsymbol{\nabla} \times \mathbf{f}')] = (\mathbf{h}')^2 - \frac{\omega^2}{c^2} (\mathbf{f}')^2 \ . \tag{3.65}$$

Integrating over the whole space (beyond the box used to defined the modes), we cancel the divergence term since the mode functions cancel identically outside the box, and we get finally:

$$\int (\mathbf{h}')^2 = \frac{\omega^2}{c^2} \int (\mathbf{f}')^2 \tag{3.66}$$

a remarkably simple result. The same derivation applies without modification to the imaginary part of the $\mathbf{f}$ and $\mathbf{h}$ functions:

$$\int (\mathbf{h}'')^2 = \frac{\omega^2}{c^2} \int (\mathbf{f}'')^2 \tag{3.67}$$

The last term we must examine is $\int \mathbf{h}' \cdot \mathbf{h}''$. We start in a similar way from the vector identity:

$$\boldsymbol{\nabla} \cdot [\mathbf{f}' \times (\boldsymbol{\nabla} \times \mathbf{f}'')] = (\boldsymbol{\nabla} \times \mathbf{f}) \cdot (\boldsymbol{\nabla} \times \mathbf{f}'') - \mathbf{f}' \cdot (\boldsymbol{\nabla} \times \boldsymbol{\nabla} \times \mathbf{f}'') \ . \tag{3.68}$$

The double rotational transforms as above and the integral over the whole space of the divergence cancels as well. After a little work, we find:

$$\int \mathbf{h}' \cdot \mathbf{h}'' = \frac{\omega^2}{c^2} \int \mathbf{f}' \cdot \mathbf{f}'' \ . \tag{3.69}$$

We can thus rewrite the magnetic energy as:

$$H_b = 2\omega^2 \epsilon_0 \left[x^2 \int (\mathbf{f}')^2 + p^2 \int (\mathbf{f}'')^2 - 2xp \int \mathbf{f}' \cdot \mathbf{f}'' \right] \ . \tag{3.70}$$

When summing with the electric energy, we observe that the xp terms cancel. Using the normalization,

$$\int (\mathbf{f}')^2 + \int (\mathbf{f}'')^2 = \mathcal{V} \ , \tag{3.71}$$

we get finally:

$$H = 2\omega^2 \epsilon_0 \mathcal{V} \left[x^2 + p^2 \right] \ . \tag{3.72}$$

This is obviously the energy of a one-dimensional harmonic oscillator, where the real and imaginary parts of the normal variable $\mathcal{A}$ play the role of the position and momentum respectively. Quantizing the field is as simple as quantizing an harmonic oscillator!

Of course, when returning to the full multi-mode problem, we get a collection of independent oscillators and a total energy

$$H = \sum_\ell H_\ell = \sum_\ell 2\omega_\ell^2 \epsilon_0 \mathcal{V} \left[x_\ell^2 + p_\ell^2 \right] \ . \tag{3.73}$$

We must perform a last step to put the problem in terms that can be directly quantized. We need x and p variables (we drop again the mode index), which are canonically conjugate quantities (their Poisson bracket is one and their commutator in the quantum realm will be $i\hbar$).

For this, we need to perform a little bit of normalisation (we could have made the right choices before, but they had looked very artificial at the time). The proper canonical (in the meaning of analytical mechanics) variables x_c and p_c should verify the Hamilton equations of motion:

$$\frac{dx_c}{dt} = \frac{\partial H}{\partial p_c} \qquad \text{and} \qquad \frac{dp_c}{dt} = -\frac{\partial H}{\partial x_c} \ . \tag{3.74}$$

The variables x and p are not canonical, since

$$\frac{dx}{dt} = \omega p \neq \frac{\partial H}{\partial p} = 4\omega^2 \epsilon_0 \mathcal{V} p \ . \tag{3.75}$$

We thus define a canonical amplitude for each mode

$$\alpha(t) = 2\sqrt{\epsilon_0 \omega \mathcal{V}} \mathcal{A}(t) \tag{3.76}$$

and the canonical position and momentum as its real and imaginary parts:

$$\alpha(t) = x_c + i p_c \ , \tag{3.77}$$

i.e.

$$x_c = 2\sqrt{\epsilon_0 \omega \mathcal{V}} x \qquad \text{and} \qquad p_c = 2\sqrt{\epsilon_0 \omega \mathcal{V}} p \ . \tag{3.78}$$

In these terms, the mode energy is

$$H = \frac{\omega}{2} \left[x_c^2 + p_c^2 \right] \ . \tag{3.79}$$

Note that the x_c and p_c coordinates are not dimensionless. They are homogeneous to the square root of an action, i.e. to the square root of the Planck's constant. They are thus not in direct correspondence with the position and momentum of a mechanical harmonic oscillator. This is only a matter of normalization choices and of numerical factors.

It is easy now to check that the canonical position and momentum indeed verify the Hamilton equations of motion (3.74). They are thus the right variables to perform the canonical quantization of the field. Before performing this quantization, we will remain classical for a moment and examine the field momentum and angular momentum.

3.2.4 Field momentum and angular momentum

Total momentum

That an electromagnetic field carries a momentum is evident, particularly in the relativistic frame as expressed by the Maxwell stress tensor. The density of momentum is found to be proportional to the Poynting vector:

$$\mathbf{g} = \frac{\mathbf{\Pi}}{c^2} \qquad \text{with} \qquad \mathbf{\Pi} = \frac{\mathbf{E} \times \mathbf{B}}{\mu_0} \ . \tag{3.80}$$

Note that this proportionality is evident in terms of photons. Each photon having an energy $h\nu$ must have a momentum $h\nu/c$ since it propagates at light velocity. Hence, the density of momentum is directly proportional to the flux of energy.

In order to make the calculations, we shall use the plane wave mode basis. This is the most adapted to describe the momentum, since all photons in a plane wave have the same direction and hence the same momentum. We therefore write:

$$\mathbf{E}^+(\mathbf{r},t) = \sum_\ell \mathbf{E}_\ell^+ = \sum_\ell \ i\omega_\ell \mathcal{A}_\ell(t) \boldsymbol{\epsilon}_\ell e^{i\mathbf{k}_\ell \cdot \mathbf{r}} \ , \tag{3.81}$$

and

$$\mathbf{B}^+(\mathbf{r},t) = \sum_\ell \mathbf{B}_\ell^+ = \sum_\ell \ \mathcal{A}_\ell(t)(i\mathbf{k}_\ell \times \boldsymbol{\epsilon}_\ell) e^{i\mathbf{k}_\ell \cdot \mathbf{r}} \ , \tag{3.82}$$

since the rotational of $\mathbf{f}_\ell$ is trivial in the plane wave case.

We inject these expressions in the Poynting vector and sum over all space to find the total momentum $\mathbf{P}$ of the field[2]. There are in the expansion square terms involving a single mode and cross terms between two modes. When the two modes have different $\mathbf{k}$ wavevectors, it is clear that the integral over space cancels.

Let us examine in more details the cross terms between the two polarization modes associated to the same wavevector. Assuming linear polarizations for the sake of simplicity, the first mode has an electric field along $\boldsymbol{\epsilon}_1$ and thus a magnetic field along $\boldsymbol{\epsilon}_2$. This is reversed for the other mode. The electric field of one mode is always aligned with the magnetic field of the other, canceling the cross terms in the Poynting vector.

The total momentum is thus the sum of the momenta stored in all modes: $\mathbf{P} = \sum_\ell \mathbf{P}_\ell$ with:

$$\mathbf{P}_\ell = \epsilon_0 \int (\mathbf{E}_\ell^+ + \mathbf{E}_\ell^-) \times (\mathbf{B}_\ell^+ + \mathbf{B}_\ell^-) \ . \tag{3.83}$$

We then plug the expression of the fields and expand all the terms. Some contain phase factors of the form $\exp(2i\mathbf{k}_\ell \cdot \mathbf{r})$. They integrate to zero. Only the terms independent of $\mathbf{r}$ can survive in the integration. This computation is painful and we only give the final result:

$$\mathbf{P}_\ell = 2\epsilon_0 \mathcal{V} \omega_\ell |\mathcal{A}_\ell|^2 \boldsymbol{\epsilon}_\ell \times (\mathbf{k}_\ell \times \boldsymbol{\epsilon}_\ell) \ . \tag{3.84}$$

The double vector product is simply equal to $\mathbf{k}_\ell$ since the polarizations are transverse. Finally, introducing the canonical amplitude α_ℓ (whose modulus square has the dimension of $\hbar$) we can write

$$\mathbf{P} = \frac{1}{2} \sum_\ell |\alpha_\ell|^2 \mathbf{k}_\ell \ . \tag{3.85}$$

The interpretation of this expression is simple. The momentum of a plane wave mode is in the direction of its wavevector and its is proportional to the square modulus of the canonical amplitude. Note that this square modulus is a constant of motion. The momentum is thus a constant of motion, a logical result for an isolated system.

[2] We use the same notation, $\mathbf{P}$, for the total field momentum and the density of polarization in matter. There is little risk of confusion.

Angular momentum

We now examine the field's total angular momentum. The task is more demanding and we will not complete it fully. The density of angular momentum with respect to the origin is simply $\mathbf{r} \times \mathbf{g}$ and we can write the total angular momentum $\mathbf{J}$ as:

$$\mathbf{J} = \epsilon_0 \int \mathbf{r} \times (\mathbf{E} \times \mathbf{B})\, d^3\mathbf{r} \ . \tag{3.86}$$

Simplifying this integral is quite difficult and we will only give the final result in the Coulomb gauge:

$$\mathbf{J} = \mathbf{L} + \mathbf{S} \ , \tag{3.87}$$

where

$$\mathbf{S} = \epsilon_0 \int \mathbf{E} \times \mathbf{A}\, d^3\mathbf{r} \tag{3.88}$$

is called the field's 'intrinsic angular momentum' and

$$\mathbf{L} = \epsilon_0 \int d^3\mathbf{r} \sum_j E_j (\mathbf{r} \cdot \nabla) A_j \ , \qquad j = (x, y, z) \ , \tag{3.89}$$

is the field's 'orbital angular momentum'. The reference to the electron angular momentum in these denominations is obvious, but we should not forget we are here treating a classical field.

Let us discuss a bit the intrinsic angular momentum $\mathbf{S}$, since its expression is relatively simple. We perform a plane wave mode expansion, but choose the circular polarization basis (for reasons that will be evident soon). When expanding the modes sum, the cross terms with different wavevectors cancel. However, it is necessary to keep all terms with the same $\mathbf{k}$ and the two circular polarizations. We thus distinguish the index n enumerating the wavevector and the $\pm$ index of the polarizations. One notes that the cross terms between the two circular polarizations also cancel, due to the relation $\boldsymbol{\epsilon}_+ \times \boldsymbol{\epsilon}_-^* = 0$ demonstrated above. After some work, we arrive at

$$\mathbf{S} = i\epsilon_0 \mathcal{V} \sum_n \omega_n \left[\mathcal{A}_{n+} \mathcal{A}_{n+}^* (\boldsymbol{\epsilon}_+ \times \boldsymbol{\epsilon}_+^*) + \mathcal{A}_{n-} \mathcal{A}_{n-}^* (\boldsymbol{\epsilon}_- \times \boldsymbol{\epsilon}_-^*) - \text{c.c.} \right] \ , \tag{3.90}$$

where we have used the fact that the frequency of the mode is independent of the polarization.

Using now $\boldsymbol{\epsilon}_+ \times \boldsymbol{\epsilon}_+^* = \boldsymbol{\epsilon}_+ \times \boldsymbol{\epsilon}_- = -i\mathbf{u}_\mathbf{k}$ and its complex conjugate $\boldsymbol{\epsilon}_- \times \boldsymbol{\epsilon}_-^* = i\mathbf{u}_\mathbf{k}$, and introducing again the canonical amplitude, we arrive at a simple form:

$$\mathbf{S} = \frac{1}{2} \sum_n \left[|\alpha_{n+}|^2 - |\alpha_{n-}|^2 \right] \mathbf{u}_\mathbf{k} \ . \tag{3.91}$$

The interpretation of this form is far simpler than the calculation leading to it. Each circularly polarized mode contribute to the intrinsic angular momentum, by a quantity aligned with the wavevector and proportional to the mode intensity. The right-circular polarized modes have a positive contribution, the left-handed ones a negative contribution. We guess that the interpretation of this result in terms of the intrinsic angular momentum of the light quanta will be straightforward.

Of course, the modes intensities are constant and the intrinsic angular momentum is also a constant of motion. Since $\mathbf{J}$ should be constant as for any isolated system, $\mathbf{L}$ is bound to be constant too.

This is almost the only property of $\mathbf{L}$ that we can deduce with simple calculations. Expanding it over the mode basis is extremely cumbersome. The orbital momentum depends upon the precise spatial configuration of the field. It is in particular non-zero for laser beams tailored to have an helical phase, with a potential vector of the form $U(r, z) \exp(im\phi) \exp(i(kz - \omega t))$ in the cylindrical coordinates r, ϕ, z (with of course $U(r = 0) = 0$). The phase rotation around the axis confers angular momentum to these modes, and $\mathbf{L} = (H/\omega) m \mathbf{u}_z$. Here also the interpretation in terms of photons will be simple, each photon in this beam having an orbital angular momentum $m\hbar$.

3.3 Field quantization

We can now take the final step and quantize the field. Each mode being totally independent from the others, we can treat their quantization separately. We will thus drop the mode index ℓ when there is no possible confusion. We assume of course that the quantization of a one-dimensional harmonic oscillator is well known.

3.3.1 Creation and annihilation operators, Hamiltonian

The classical field energy of one mode is, within a factor $\omega/2$, equal to $x_c^2 + p_c^2$, where x_c and p_c are conjugate canonical variables. The quantization of such a 'mechanical' problem dates from the very early days of quantum mechanics. The conjugate classical variables should be replaced by two operators X and P (position and momentum operators) acting in an infinite dimension Hilbert space, with the commutation rule:

$$[X, P] = i\hbar \ . \tag{3.92}$$

From X and P, we can build quantum analogues of the complex classical oscillation amplitude, proportional to $x_c + ip_c$. Let us thus define the non-hermitian operator a by:

$$a = \frac{1}{\sqrt{2\hbar}}(X + iP) \ , \tag{3.93}$$

whose ajoint is

$$a^\dagger = \frac{1}{\sqrt{2\hbar}}(X - iP) \ , \tag{3.94}$$

It is easy to compute the commutator of a with $a^\dagger$ from the commutation relation of X and P:

$$\left[a, a^\dagger\right] = \mathbb{1}. \tag{3.95}$$

We can invert the definition of a and $a^\dagger$ and get

$$X = \sqrt{\frac{\hbar}{2}}\left(a + a^\dagger\right) \ , \tag{3.96}$$

and

$$P = i\sqrt{\frac{\hbar}{2}}\left(a^\dagger - a\right) \ . \tag{3.97}$$

It is often useful to introduce reduced units for the position and momentum operators. We thus define here the field quadratures X_0 and P_0 by:

$$X_0 = \frac{X}{\sqrt{2\hbar}} \qquad \text{and} \qquad P_0 = \frac{P}{\sqrt{2\hbar}} \ . \tag{3.98}$$

With these definitions:

$$[X_0, P_0] = \frac{i}{2} \tag{3.99}$$

$$a = X_0 + iP_0 \ , \qquad a^\dagger = X_0 - iP_0 \ , \qquad X_0 = \frac{a + a^\dagger}{2} \ , \qquad P_0 = i\frac{a^\dagger - a}{2} \ . \tag{3.100}$$

The quantum mode Hamiltonian is in direct correspondence with the classical one, by replacing the canonical variables by the position and momentum operators (no commutation problem occurs in this replacement. Hence

$$H = \frac{\omega}{2}(X^2 + P^2) = \hbar\omega(X_0^2 + P_0^2) \ . \tag{3.101}$$

Let us express it in terms of the a and $a^\dagger$ operators:

$$H = \frac{\hbar\omega}{4}\left[(a+a^\dagger)^2 - (a^\dagger - a)^2\right] \ . \tag{3.102}$$

The square terms cancel. Using the commutation relation of a and $a^\dagger$ to put the double products in the so-called 'normal order' (all $a^\dagger$s on the left of the as, we finally arrive at

$$H = \hbar\omega\left(a^\dagger a + \frac{1}{2}\right) \ . \tag{3.103}$$

Diagonalizing this Hamiltonian is a simple procedure, described in all textbooks. It amounts do diagonalizing the 'number operator'

$$N = a^\dagger a \ , \tag{3.104}$$

which has the following commutation relations:

$$[N, a] = -a \qquad \text{and} \qquad \left[N, a^\dagger\right] = a^\dagger \ . \tag{3.105}$$

It is easy to show that the spectrum of N is the set of positive or zero integers. The eigenstates of N defined by

$$N\,|n\rangle = n\,|n\rangle \ , \tag{3.106}$$

are non-degenerate and called the Fock states. They are also the eigenstates of the Hamiltonian H with an eigenvalue

$$E_n = \left(n + \frac{1}{2}\right)\hbar\omega \ . \tag{3.107}$$

The ground state is the 'vacuum state', $|0\rangle$, with a non-zero $\hbar\omega/2$ energy. This 'vacuum energy' is of course a totally non-classical effect linked to the Heisenberg uncertainty relations.

The Fock states form an equidistant ladder of levels, separated by the energy of a photon $\hbar\omega$. We can thus interpret the Fock states as states with a well-defined number of photons. They are thus also called 'photon-number states'. Of course, the Fock states are an orthonormal basis in the Hilbert space with:

$$\langle n\,|p\rangle = \delta_{n,p} \ . \tag{3.108}$$

The a operator transforms $|n\rangle$ into $|n-1\rangle$ according to:

$$a\,|n\rangle = \sqrt{n}\,|n-1\rangle \ , \tag{3.109}$$

and, similarly

$$a^\dagger\,|n\rangle = \sqrt{n+1}\,|n+1\rangle \ , \tag{3.110}$$

The operator a is thus called the 'annihilation' operator since it removes one photon, and $a^\dagger$ is called the 'creation' operator. All Fock states can thus be generated from the vacuum by:

$$|n\rangle = \frac{(a^\dagger)^n}{\sqrt{n!}}\,|0\rangle \ . \tag{3.111}$$

Note also that

$$a\,|0\rangle = 0 \ , \tag{3.112}$$

an essential property of the vacuum state.

Let us now return to the full multi-mode case. The total Hilbert space is the tensor product of all spaces associated to the separate modes. Its dimension is thus quite infinite. Since the modes are dynamically uncoupled, the operators of one mode commute with all the other modes operators.

The vacuum $|0\rangle$ is the tensor product of the vacuum states of all modes. The eigenstates of the total Hamiltonian H are the tensor products of Fock states of each mode:

$$H\,|n_1,\ldots,n_\ell\ldots\rangle = E_n\,|n_1,\ldots,n_\ell\ldots\rangle \ , \tag{3.113}$$

with

$$E_n = \sum_\ell \left(n_\ell \hbar\omega_\ell + \frac{\hbar\omega_\ell}{2}\right) \ . \tag{3.114}$$

and

$$|n_1,\ldots,n_\ell\ldots\rangle = \prod_\ell \frac{(a_\ell^\dagger)^{n_\ell}}{\sqrt{n_\ell!}}\,|0\rangle \ . \tag{3.115}$$

We note that the vacuum has an infinite energy. This is the harbinger of a considerable difficulty in this simple approach to field quantization. The zero-point energy is quite harmful for some problems, leading to infinities in many calculations, such as the atomic energy level shifts due to the continuum of empty field modes (Lamb shift effect). We will discuss this matter a bit further in the next Chapter and see how we can in most cases circumvent the difficulty without getting in the technically complex renormalization procedures of QED.

3.3.2 Field operators

We now proceed to express all the relevant field operators in terms of the annihilation and creation operators, in correspondence with the classical fields. The normal variables for the classical fields are the vector potential amplitudes $\mathcal{A}$, which are expressed in terms of the canonical variables by:

$$\mathcal{A} = \frac{1}{2\sqrt{\epsilon_0\omega\mathcal{V}}}(x_c + ip_c) \ . \tag{3.116}$$

The corresponding quantum mechanical operator is thus, reintroducing the modes indices:

$$A_\ell = \frac{1}{2\sqrt{\epsilon_0\omega_\ell\mathcal{V}}}(X_\ell + iP_\ell) = \sqrt{\frac{\hbar}{2\epsilon_0\omega_\ell\mathcal{V}}}a_\ell \ , \tag{3.117}$$

and is simply proportional to the annihilation operator. We just need to replace, within this factor, in all the classical fields $\mathcal{A}_\ell$ by a_ℓ and $\mathcal{A}_\ell^*$ by $a_\ell^\dagger$.

Fields

The positive-frequency vector potential is now a non-hermitian operator in the field Hilbert space and depends upon the classical position $\mathbf{r}$:

$$\mathbf{A}^+(\mathbf{r}) = \sum_\ell \sqrt{\frac{\hbar}{2\epsilon_0\omega_\ell\mathcal{V}}}a_\ell\mathbf{f}_\ell(\mathbf{r}) \ . \tag{3.118}$$

The hermitian full vector potential is the sum of $\mathbf{A}^+$ and of its complex conjugate:

$$\mathbf{A}(\mathbf{r}) = \sum_\ell \sqrt{\frac{\hbar}{2\epsilon_0\omega_\ell\mathcal{V}}}\left(a_\ell\mathbf{f}_\ell(\mathbf{r}) + a_\ell^\dagger\mathbf{f}_\ell^*(\mathbf{r})\right) \ . \tag{3.119}$$

The hermitian electric field is similarly:

$$\mathbf{E}(\mathbf{r}) = i\sum_\ell \mathcal{E}_\ell\left(a_\ell\mathbf{f}_\ell(\mathbf{r}) - a_\ell^\dagger\mathbf{f}_\ell^*(\mathbf{r})\right) \ , \tag{3.120}$$

where we define the 'field per photon in mode ℓ' by

$$\mathcal{E}_\ell = \sqrt{\frac{\hbar\omega_\ell}{2\epsilon_0 \mathcal{V}}} \ . \tag{3.121}$$

The magnetic field is:

$$\mathbf{B}(\mathbf{r}) = \sum_\ell \sqrt{\frac{\hbar}{2\epsilon_0\omega_\ell \mathcal{V}}} \left(a_\ell \mathbf{h}_\ell(\mathbf{r}) + a_\ell^\dagger \mathbf{h}_\ell^*(\mathbf{r}) \right) \ , \tag{3.122}$$

with $\mathbf{h}_\ell = \boldsymbol{\nabla} \times \mathbf{f}_\ell$.

In all these expressions, all the details of the field geometry (mode structure, polarization...) are encapsulated in the classical mode functions. The only quantum parts are the creation and annihilation operators. A photon can thus be defined as an elementary excitation of a classical field mode, solution of Maxwell equations with limiting conditions. As such, a photon has a polarization, a mode structure. It can inhabit a plane wave, a standing wave pattern or a propagating Gaussian beam. In this point of view, of course, the photon cannot be pictured as a localized particle. It is everywhere in the mode at the same time (the relative mode amplitude modulus square giving the probability to detect the photon at a point – see the paragraph on photodetection in Chapter 4).

If we use the plane-wave basis, we can write (we give only the positive frequency parts of the field operators to save space):

$$\mathbf{A}^+(\mathbf{r}) = \sum_\ell \sqrt{\frac{\hbar}{2\epsilon_0\omega_\ell \mathcal{V}}} a_\ell \boldsymbol{\epsilon}_\ell e^{i\mathbf{k}_\ell \cdot \mathbf{r}} \ , \tag{3.123}$$

$$\mathbf{E}^+(\mathbf{r}) = i \sum_\ell \mathcal{E}_\ell a_\ell \boldsymbol{\epsilon}_\ell e^{i\mathbf{k}_\ell \cdot \mathbf{r}} \ , \tag{3.124}$$

$$\mathbf{B}^+(\mathbf{r}) = \sum_\ell \sqrt{\frac{\hbar}{2\epsilon_0\omega_\ell \mathcal{V}}} a_\ell (i\mathbf{k}_\ell \times \boldsymbol{\epsilon}_\ell) e^{i\mathbf{k}_\ell \cdot \mathbf{r}} \ . \tag{3.125}$$

Note that there is no explicit time dependence, since we have replaced the time-dependent amplitudes by operators. We are in the Schrödinger picture and all time dependence is encapsulated in the state. We can recover time-varying fields, close to the classical picture, by switching to the Heisenberg representation. The evolution equation for a_H, the annihilation operator in the Heisenberg picture is

$$i\hbar \frac{da_H}{dt} = [a_H, H] \qquad \text{i.e.} \qquad \frac{da_H}{dt} = -i\omega a_H \ , \tag{3.126}$$

whose immediate solution is

$$a_H(t) = a_H(0) e^{-i\omega t} = a e^{-i\omega t} \ . \tag{3.127}$$

Substituting this in the field operators, we get the fields in the Heisenberg picture, which have the same time dependence as their classical counterparts.

Momentum, angular momentum

The momentum[3] has been expressed in terms of the canonical classical amplitude α_l, which is proportional to $\mathcal{A}_\ell$. Its quantum counterpart is just $a_\ell\sqrt{2\hbar}$. Substituting $|\alpha_\ell|^2$ by $\alpha_\ell^* \alpha_\ell$ in the expression of the momentum, we get

$$\mathbf{P} = \sum_\ell \hbar \mathbf{k}_l \, a_\ell^\dagger a_\ell \ . \tag{3.128}$$

[3]The momentum of the field and the momentum associated to the fictitious unidimensional harmonic oscillator equivalent to a field mode are not related at all!

Note that we have an ordering problem for a and $a^\dagger$ in the transformation of the quadratic classical quantity into a quantum operator. We have here made implicitly the only reasonable choice, that of normal ordering, since the momentum cancels in the vacuum state for this form only. Changing the ordering would add an infinite constant terms ($\sum_\ell \hbar \mathbf{k}_\ell$) to the momentum.

The interpretation of this expression of the momentum is evident. Each photon in the plane-wave mode ℓ has a momentum $\hbar\mathbf{k}_\ell$, the modulus of which is $h\nu/c$, and the total momentum is the sum of all the photons momenta.

The same simple reasoning applies to the intrinsic angular momentum of the field. We get:

$$\mathbf{S} = \sum_n \hbar \mathbf{u}_{\mathbf{k}_n} [N_{n+} - N_{n-}] \ . \tag{3.129}$$

each right (left) circularly polarized photon has an intrinsic angular momentum $\hbar$ ($-\hbar$) along its direction of propagation. The photon thus appears as a spin-1 particle. However, the photons never have a zero intrinsic angular momentum along their direction of propagation, an immediate consequence of the transverse nature of the electromagnetic waves. A linearly polarized wave corresponds to photons in a quantum superpositions of having a $\pm\hbar$ angular momentum.

Field quadratures

Let us return to the two field quadratures X_0 and P_0. We can define their eigenstates which correspond to the position or momentum eigenstates of the harmonic oscillator:

$$X_0 \left|x\right\rangle = x \left|x\right\rangle \qquad \text{and} \qquad P_0 \left|p\right\rangle = p \left|p\right\rangle \ . \tag{3.130}$$

Note that these states, which are a basis of the Hilbert space, cannot be properly normalized, a standard pathology in infinite dimensional Hilbert spaces. The position x and momentum p define a classical phase space for the mode's harmonic oscillator, equivalent to the Fresnel plane for the electric field.

With these states, we can define wavefunctions for the field either in the X_0 or P_0 representation. For instance, let:

$$\Psi(x) = \left\langle x \right| \left.\Psi\right\rangle \ . \tag{3.131}$$

The wavefunction of the vacuum state $|0\rangle$ is found to be

$$\Psi_0(x) = \left(\frac{2}{\pi}\right)^{1/4} e^{-x^2} \tag{3.132}$$

a simple Gaussian with a width 1. The wavefunction of the same state in the P_0 representation is thus the same Gaussian, since both wavefunctions are linked by a Fourier transform relation. We can thus view the ground state in the phase space as a unit radius blob centred at the origin. We will give later a much more precise representation of this fact.

The Fock state wavefunction is then:

$$\Psi_n(x) = \left(\frac{2}{\pi}\right)^{1/4} \frac{1}{\sqrt{2^n n!}} e^{-x^2} H_n(x\sqrt{2}) \ , \tag{3.133}$$

where H_n is the nth Hermite polynomial defined by

$$H_n(u) = (-1)^n e^{u^2} \frac{d^n}{du^n} e^{-u^2} \ . \tag{3.134}$$

These wavefunctions have $n-1$ nodes and a a parity $(-1)^n$. They are plotted in all textbooks.

We define now a more general field quadrature by:

$$X_\phi = \frac{a e^{-i\phi} + a^\dagger e^{i\phi}}{2} \ , \tag{3.135}$$

with the evident identification of X_0 with the $\phi = 0$ quadrature. We also have $X_{\pi/2} = P_0$. It can be easily shown that:

$$\left[X_\phi, X_{\phi+\pi/2}\right] = \frac{i}{2} \ , \tag{3.136}$$

resulting in the Heisenberg uncertainty relations

$$\Delta X_\phi \Delta X_{\phi+\pi/2} \geq \frac{1}{4}. \tag{3.137}$$

The eigenstates of the quadratures are defined by $X_\phi \left|x_\phi\right\rangle = x_\phi \left|x_\phi\right\rangle$ and are linked by Fourier transformations;

$$\left|x_{\phi+\pi/2}\right\rangle = \frac{1}{\sqrt{\pi}} \int dy_\phi e^{2ix_{\phi+\pi/2}y_\phi} \left|y_\phi\right\rangle \tag{3.138}$$

Mode basis change

We now examine the quantum version of the mode basis change described in the last Section. We change from the mode functions $\mathbf{f}_\ell$ to the mode functions $\mathbf{g}_p$, with

$$\mathbf{f}_\ell = \sum_p U_{\ell p} \mathbf{g}_p \ , \tag{3.139}$$

where $U_{\ell p}$ is a unitary matrix that connects only the modes with identical frequencies.

The positive frequency part of the electric field can be written as:

$$\begin{aligned} \mathbf{E}^+ &= i \sum_\ell \mathcal{E}_\ell \mathbf{f}_\ell(\mathbf{r}) a_\ell \\ &= i \sum_{\ell,p} \mathcal{E}_\ell U_{\ell p} a_\ell \mathbf{g}_p(\mathbf{r}) \\ &= \sum_p \mathcal{E}_p \mathbf{g}_p(\mathbf{r}) b_p \ , \end{aligned} \tag{3.140}$$

with

$$b_p = \sum_\ell U_{\ell p} a_\ell \ , \tag{3.141}$$

The last relation defines the annihilation operator b_p of the 'new' modes as a linear combination of the 'old' modes annihilation operators. A mode basis change thus reflects on the field operators. Note that the fact that $U_{\ell p}$ connects only modes with the same frequency plays an essential role in this computation, when it comes to identifying the fields per photon $\mathcal{E}_\ell$ and $\mathcal{E}_p$. The conjugate of the previous equation leads, since $U^*_{\ell p} = U^\dagger_{p\ell}$, to

$$b^\dagger_p = \sum_\ell U^\dagger_{p\ell} a^\dagger_\ell \ , \tag{3.142}$$

where we make use of $U^*_{\ell p} = U^\dagger_{p\ell}$. As an exercise, we can check that the bosonic commutation relations of the annihilation and creation operators is preserved in this transformation:

$$\begin{aligned} \left[b_p, b^\dagger_q\right] &= \sum_{\ell,m} U_{\ell p} a_\ell U^\dagger_{qm} a^\dagger_m - U^\dagger_{qm} a^\dagger_m U_{\ell p} a_\ell \\ &= \sum_{\ell,m} U_{\ell p} U^\dagger_{qm} \left[a_\ell, a^\dagger_m\right] \\ &= \sum_\ell U^\dagger_{q\ell} U_{\ell p} \\ &= \delta_{p,q} \ , \end{aligned} \tag{3.143}$$

where we take care that, for the field modes, the matrix U is made up of numbers, not of operators and where we use $\left[a_\ell, a^\dagger_m\right] = \delta_{\ell,m}$.

3.4 Field quantum states

We now examine in more details the field quantum states. We have already introduced the Fock states, eigenstates of the field Hamiltonian. We will show that they are utterly non-classical in nature. We will thus introduce also the coherent states,

3.4.1 Fock states

We have already given most of the properties of these eigenstates of the field Hamiltonian. They are a convenient basis of the Hilbert space and any field state can be written as:

$$|\Psi\rangle = \sum_n c_n |n\rangle \ . \tag{3.144}$$

The 'photon number distribution' for state $|\Psi\rangle$, p_n, i.e. the probability for finding n photons in an ideal photon counting experiment is:

$$p_n = |c_n|^2 \ . \tag{3.145}$$

The mean number of photons in state $|\Psi\rangle$ is thus:

$$\overline{n} = \sum_n n p_n \ , \tag{3.146}$$

and the photon number variance is:

$$\begin{aligned} \Delta N^2 &= \left\langle N^2 \right\rangle - \langle N \rangle^2 \\ &= \sum_n (n - \overline{n})^2 p_n \ . \end{aligned} \tag{3.147}$$

The average values of a and $a^\dagger$ in a Fock state vanish, since $a|n\rangle$ and $a^\dagger|n\rangle$ are both orthogonal to $|n\rangle$. It results that the average value of all fields cancel in a Fock state. This reveals the non-classical nature of these states. They have a finite, possibly large energy, but they correspond to zero electric and magnetic fields! This is due to the fact that the Fock states bear no phase information. In a classical picture, they represent a field with a totally random phase.

In most cases, the field states are not pure states, but statistical mixtures. This is particularly the case when field relaxation is involved, as described in the end of this Chapter. In this situation, the field state must be described by a density operator:

$$\rho = \sum_{n,p} \rho_{np} |n\rangle \langle p| \ . \tag{3.148}$$

The diagonal elements of the density matrix correspond to the photon number distribution:

$$\rho_{nn} = p_n \ . \tag{3.149}$$

The non-diagonal elements describe the phase information contents of the state. We will examine the importance of these coefficients in the next paragraph.

Let us mention finally that the Fock states with at least one photon are of course not invariant under a change of the mode basis. The state with n photons in the mode b_p can be expressed as:

$$|n_p\rangle = \frac{(b_p^\dagger)^{n_p}}{\sqrt{n!}} |0\rangle = \frac{\left(\sum_\ell U_{p\ell}^\dagger a_\ell^\dagger\right)^{n_p}}{\sqrt{n!}} |0\rangle \tag{3.150}$$

The total number of photons is the same in both cases, but the n_p photons stored in mode b_p are shared by all the coupled a_ℓ modes. We will see a more practical example of this situation when treating the beam-splitter later in this Chapter.

3.4.2 Coherent states

We introduce in this paragraph the coherent states of the field, which are much closer to the classical picture of non-zero oscillating electric and magnetic fields than the non-classical Fock states. These states are quite important, since they are produced by all classical field sources (electronic oscillators or lasers) involving a large, coherent emitting system (either a classical oscillating current or a large collection of atoms).

Definition

Let us first define the unitary 'displacement' operator:

$$D(\alpha) = e^{\alpha a^\dagger - \alpha^* a} \ , \tag{3.151}$$

where α is an arbitrary complex amplitude, which can be split in its real and imaginary parts according to:

$$\alpha = \alpha' + i\alpha'' \ . \tag{3.152}$$

The displacement operator is obviously unitary :

$$D(\alpha)^\dagger D(\alpha) = \mathbb{1} \ . \tag{3.153}$$

We also note that

$$D(\alpha)^\dagger = D(-\alpha) \ . \tag{3.154}$$

The coherent state $|\alpha\rangle$ is defined as the action of the displacement operator on the vacuum:

$$|\alpha\rangle = D(\alpha)\,|0\rangle \ . \tag{3.155}$$

Since $D(0) = \mathbb{1}$, we observe that the vacuum state $|0\rangle$ is also the coherent state with zero amplitude. Let us examine in more details the action of the displacement operator. We separate the real and imaginary parts of α and write

$$D(\alpha) = e^{2i\alpha'' X_0 - 2i\alpha' P_0} \ . \tag{3.156}$$

We now make use of the Glauber relation:

$$e^A e^B = e^{A+B} e^{[A,B]/2} \ , \tag{3.157}$$

valid when both A and B commute with their commutator:

$$[A,[A,B]] = [B,[A,B]] = 0 \ . \tag{3.158}$$

It thus applies above since $[X_0, P_0] = i/2$ is proportional to the identity. We thus get:

$$D(\alpha) = e^{-i\alpha'\alpha''} e^{2i\alpha'' X_0} e^{-2i\alpha' P_0} \ . \tag{3.159}$$

The last operator is obviously a translation operator for the position of the harmonic oscillator, by an amount α'. The next operator is a translation in momentum by an amount α'':

$$e^{-2i\alpha' P_0}\,|x\rangle = |x+\alpha'\rangle \tag{3.160}$$

$$e^{2i\alpha'' X_0}\,|p\rangle = |p+\alpha''\rangle \ . \tag{3.161}$$

The coherent state appears thus, within a global phase factor, as the vacuum state translated by α' in position and α'' in momentum. This justifies fully the name 'displacement operator' coined for

$D(\alpha)$. This simple feature provides in a simple way the wavefunction of the coherent state in the X_0 representation:

$$\Psi_\alpha(x) \propto e^{-(x-\alpha')^2} \ , \tag{3.162}$$

and in the P_0 representation:

$$\widetilde{\Psi}_\alpha(x) \propto e^{-(p-\alpha'')^2} \ . \tag{3.163}$$

Let us now examine the action of the displacement operator on the annihilation operator by computing $D(\alpha)aD(-\alpha)$. Using the Baker-Hausdorff lemma:

$$e^A a e^{-A} = a + [A,a] + \frac{1}{2!}[A,[A,a]] + \dots \ , \tag{3.164}$$

for $A = \alpha a^\dagger - \alpha^* a$ and noting that $[A,a] = -\alpha$ and, hence, that all higher order commutators cancel, we get immediately:

$$D(\alpha)aD(-\alpha) = a - \alpha\mathbb{1} \ . \tag{3.165}$$

The displacement operator thus performs a translation on the annihilation operator.

We can also compute the combination of displacements. Using again the Glauber relations, it is easy to show that

$$D(\alpha)D(\beta) = e^{(\alpha\beta^* - \alpha^*\beta)/2} D(\alpha+\beta) \ . \tag{3.166}$$

Within a phase factor, the displacement operators add as the classical fields. Let us interpret the phase factor $i\Phi = (\alpha\beta^* - \alpha^*\beta)/2$, where Φ is obviously a real phase. Separating the real and imaginary parts of the displacements amplitudes, we get:

$$\Phi = \frac{\alpha''\beta' - \alpha'\beta''}{2} \ . \tag{3.167}$$

This is precisely half the vector product of the two vectors α and β in the phase plane. The phase Φ is thus simply the surface of the triangle with sides α and β. This phase is of a geometrical, topological nature. This is a simple example of a Berry's phase observed when a quantum state is displaced.

Properties of the coherent states

Let us examine now the main properties of the coherent states. First, they are right-eigenstates of the annihilation operator:

$$a\,|\alpha\rangle = aD(\alpha)\,|0\rangle = D(\alpha)D(-\alpha)aD(\alpha)\,|0\rangle = (a+\alpha\mathbb{1})\,|0\rangle = \alpha\,|\alpha\rangle \ , \tag{3.168}$$

since $a\,|0\rangle = 0$. The annihilation operator a being non-hermitian, there are no restriction on its spectrum, which appears here as made of all complex numbers. Hence:

$$\langle\alpha|\,a^\dagger = \alpha^*\,\langle\alpha| \ , \tag{3.169}$$

and the coherent states are left-eigenstates of the creation operator. Note that there is no simple expression for $a^\dagger\,|\alpha\rangle$.

This property entails that the annihilation and creation operators have an non-zero expectation value in the coherent states:

$$\langle\alpha|\,a\,|\alpha\rangle = \alpha \qquad \text{and} \qquad \langle\alpha|\,a^\dagger\,|\alpha\rangle = \alpha^* \tag{3.170}$$

The average values of all fields are thus also non zero and, for instance:

$$\langle\mathbf{E}\rangle = i\mathcal{E}\left(\mathbf{f}(\mathbf{r})\alpha - \mathbf{f}^*(\mathbf{r})\alpha^*\right) \tag{3.171}$$

$$\langle\mathbf{A}\rangle = \frac{\mathcal{E}}{\omega}\left(\mathbf{f}(\mathbf{r})\alpha + \mathbf{f}^*(\mathbf{r})\alpha^*\right) \ , \tag{3.172}$$

a result very close to the expressions of the classical fields.

The average number of photons in the coherent state is simply:

$$\overline{n} = \langle\alpha| a^\dagger a |\alpha\rangle = |\alpha|^2 \ . \tag{3.173}$$

We can also compute easily the variance of the photon number, using $N^2 = a^\dagger a a^\dagger a = (a^\dagger)^2 a^2 + a^\dagger a$. Hence:

$$\left\langle N^2 \right\rangle = |\alpha|^4 + |\alpha|^2 \ , \tag{3.174}$$

and

$$\Delta N^2 = |\alpha|^2 = \overline{n} \ . \tag{3.175}$$

The variance of the photon number is equal to its average, a characteristic feature of the Poisson distribution. We observe that:

$$\frac{\Delta N}{\overline{n}} = \frac{1}{\sqrt{\overline{n}}} \ . \tag{3.176}$$

The larger the energy of the coherent state, the less is the relative uncertainty on this energy and the more the coherent state looks like a classical field.

We can make this observation more precise by computing the expansion of the coherent states on the Fock state basis. Using once again the Glauber relation to expand the displacement operator as:

$$D(\alpha) = e^{-|\alpha|^2/2} e^{\alpha a^\dagger} e^{-\alpha^* a} \ , \tag{3.177}$$

and noting that $e^{-\alpha^* a} |0\rangle = |0\rangle$ (in the power expansion of the exponential, all terms cancel but the identity one), we get:

$$|\alpha\rangle = e^{-|\alpha|^2/2} e^{\alpha a^\dagger} |0\rangle \ . \tag{3.178}$$

We expand the exponential operator in power series and note that $(a^\dagger)^n |0\rangle$ is proportional to $|n\rangle$. We finally get:

$$|\alpha\rangle = \sum_n c_n |n\rangle \ , \tag{3.179}$$

with

$$c_n = e^{-|\alpha|^2/2} \frac{\alpha^n}{\sqrt{n!}} \ . \tag{3.180}$$

This expression shows that $|0\rangle$ is indeed the only state which is, at the same time, a photon number state and a coherent state.

The photon number distribution of the coherent state $|\alpha\rangle$ is thus given by:

$$p_n = e^{-|\alpha|^2} \frac{|\alpha|^{2n}}{n!} = e^{-\overline{n}} \frac{\overline{n}^n}{n!} \ , \tag{3.181}$$

a Poisson distribution as expected. For very large average photon numbers, this distribution is nearly Gaussian, with

$$p_n \propto e^{-(n-\overline{n})^2/\overline{n}} \ . \tag{3.182}$$

The larger the photon number, the more peaked (in relative value) is this distribution. We recover the fact that a large coherent field has a well-defined energy, as a classical field.

We can now finally compute the scalar product of two coherent states:

$$\begin{aligned} \langle\alpha|\beta\rangle &= e^{-(|\alpha|^2+|\beta|^2)/2} \sum_{n,p} \frac{(\alpha^*)^n \beta^p}{\sqrt{n!p!}} \langle n|p\rangle \\ &= e^{-(|\alpha|^2+|\beta|^2)/2} e^{\alpha^*\beta} \end{aligned} \tag{3.183}$$

and its square modulus

$$|\langle\alpha\,|\beta\rangle\,|^2 = e^{-|\alpha-\beta|^2}\ . \tag{3.184}$$

Two coherent states are thus never orthogonal. Nevertheless, when the difference of their amplitudes has a modulus much larger than one, they can be considered as nearly orthogonal for all practical purposes.

We have seen that the coherent states are displaced vacuum states. The vacuum can be visualized as a radius unity blob around the origin of phase space. The coherent state $|\alpha\rangle$ can thus be also visualized as a blob, centred on the complex amplitude α. The scalar product of $|\alpha\rangle$ and $|\beta\rangle$ nearly cancels as soon as the two blobs no longer overlap.

These non-orthogonal states form an over-complete basis of the Hilbert space:

$$\mathbb{1} = \frac{1}{\pi}\int d^2\alpha\ |\alpha\rangle\,\langle\alpha|\ . \tag{3.185}$$

In order to establish this important property, we expand in the integral the ket and the bra over the Fock states basis:

$$\int d^2\alpha\ |\alpha\rangle\,\langle\alpha| = \sum_{n,p}\frac{1}{\sqrt{n!p!}}\,|n\rangle\,\langle p|\int d^2\alpha\, e^{-|\alpha|^2}\alpha^n(\alpha^*)^p\ . \tag{3.186}$$

We compute the integral over the phase plane in polar coordinates, with $\alpha = \rho\exp(i\theta)$. The integral is then:

$$\int \rho d\rho d\theta\, e^{-\rho^2}\rho^{n+p}e^{i\theta(n-p)}\ , \tag{3.187}$$

and obviously cancels when $n \neq p$. For $n = p$, the integral reduces, with $u = \rho^2$, to:

$$I_n = \pi\int du\, u^n e^{-u}\ . \tag{3.188}$$

An integration per parts gives $I_n = nI_{n-1}$. Since $I_0 = \pi$, we get $I_n = \pi n!$ and hence:

$$\int d^2\alpha\ |\alpha\rangle\,\langle\alpha| = \pi\sum_n\ |n\rangle\,\langle n|\ , \tag{3.189}$$

completing the demonstration.

The coherent state basis being over-complete, the expansion of a quantum state onto it is not unique. This is particularly the case for the vacuum. On the one hand, it is itself a coherent state. On the other hand, using the generalized closure relation above:

$$|0\rangle = \frac{1}{\pi}\int d^2\alpha\, e^{-|\alpha|^2/2}\,|\alpha\rangle\ . \tag{3.190}$$

Let us finally note that the Fock state can (non uniquely) be expanded on the coherent states as:

$$|n\rangle = \frac{1}{\pi\sqrt{n!}}\int d^2\alpha\, e^{-|\alpha|^2/2}(\alpha^*)^n\,|\alpha\rangle\ . \tag{3.191}$$

Evolution

The coherent states are not eigenstates of the mode's Hamiltonian. They thus evolve with time in a non-trivial way. Let

$$|\Psi(0)\rangle = |\alpha\rangle = e^{-|\alpha|^2/2}\sum_n\ \frac{\alpha^n}{\sqrt{n!}}\,|n\rangle\ . \tag{3.192}$$

Then

$$\begin{aligned}|\Psi(t)\rangle &= e^{-|\alpha|^2/2}\sum_n\ \frac{\alpha^n}{\sqrt{n!}}e^{-in\omega t}e^{-i\omega t/2}\,|n\rangle\\ &= e^{-i\omega t/2}\left|\alpha e^{-i\omega t}\right\rangle\ .\end{aligned} \tag{3.193}$$

Within a phase factor (that could be eliminated in a single mode problem by a convenient interaction representation i.e. by choosing the vacuum energy as being zero), the coherent state remains coherent and the amplitude evolves as the classical complex field amplitude:

$$\alpha(t) = \alpha(0)e^{-i\omega t} \ . \tag{3.194}$$

The wavefunction of the coherent state is thus a Gaussian which oscillates around the origin without deformation. Coherent states escape the dispersion of the wave-packet that affects free space propagation. Accordingly, all the average values of the field operators oscillate at the frequency ω as their classical counterparts. The coherent state are thus clearly the 'most classical' states and retain their features throughout their evolution.

Let us conclude this paragraph by a note on the creation of the coherent states. We will treat it in details when we will have a proper interaction Hamiltonian for charges coupled to the field. We will show that a classical oscillating current, resonantly coupled to the mode, produces an interaction proportional to $a + a^\dagger$. It is clear that the evolution operator associated to this interaction is a displacement. Thus, a classical oscillating current creates a coherent state. Not only are the coherent states blessed with remarkable properties, but they are also the easiest to produce experimentally. On the contrary, the Fock states, excluding the vacuum of course, are rather difficult to obtain and have only been produced in relatively recent quantum optics experiments.

3.4.3 Phase space representations

Phase space distributions[4] are fundamental tools in classical statistical physics. For a particle undergoing a one-dimensional motion, the phase space is a plane, with the position x and conjugate momentum p as coordinates. A point in this plane defines the mechanical state of the particle. In the case of a field mode, equivalent to a one-dimensional oscillator, the two orthogonal field quadratures play the role of position and momentum, and a point in the Fresnel plane defines a classical field state. Statistical uncertainties or lack of knowledge about the system are accounted for by replacing the Dirac distribution associated to this point by a positive and normalized density of probability, $f(x,p)$, which takes non-vanishing values in a limited region of phase space. The statistical average $\overline{o}$ of any observable quantity, $o(x,p)$, is given by:

$$\overline{o} = \int f(x,p)o(x,p)\,dxdp \ . \tag{3.195}$$

The system's evolution due to external forces and to the coupling with the environment is described by a diffusion equation for f, relating its temporal and spatial derivatives.

The extension of this phase space representation to quantum states was discussed for the first time by Wigner in 1932. A difficulty has immediately arisen because Heisenberg uncertainty relations forbid, even in the absence of any statistical indeterminacy, the precise and simultaneous determination of conjugate variables. In other words, a fundamental quantum blurring adds to the classical uncertainties. In spite of this problem, it remains possible to define a real phase space function for a quantum particle, which retains some of the essential characteristic features of the classical probability distribution. This quantum distribution is called the Wigner function W. Its definition and main properties are recalled in this Section.

We will see that W is naturally defined from its Fourier transform, the system's symmetrical characteristic function $C_s(\lambda)$. Introducing C_s will lead us to consider two simply related characteristic functions, $C_n(\lambda)$ and $C_{an}(\lambda)$, and we will see that their Fourier transforms define two phase space distributions different from W, the Husimi-Q function and the Glauber–Sudarshan P distribution. The latter, which is highly singular, is of difficult mathematical use and we will not say much about it. Here, we will discuss the connexions between W and Q, compare them and explain why W is more useful than Q for the analysis of the quantum features of a system.

[4]This Section is reproduced from Haroche and Raimond, 'Exploring the quantum', OUP, 2006

Characteristic functions

The three simple characteristic functions depend upon the choice made for the ordering when expanding in power series a function of the annihilation and creation operators a and $a^\dagger$. In the 'normal' order, all creation operators are placed to the left of the annihilation ones (the photon number operator $N = a^\dagger a$ is in normal order). The 'anti-normal' order puts all the a's on the left. Finally, the 'symmetric' order produces expressions in which all products of operators are symmetrized. For instance, the direct power series expansion of the displacement operator:

$$D(\lambda) = e^{\lambda a^\dagger - \lambda^* a} = \mathbb{1} + \lambda a^\dagger - \lambda^* a + \lambda^2 a^{\dagger 2} - \lambda\lambda^*(a^\dagger a + a a^\dagger) + \lambda^{*2} a^2 + \dots \ , \tag{3.196}$$

is naturally in symmetric order.

We now introduce three characteristic functions of the state of the system corresponding to these orders. The symmetric-order characteristic function, $C_s^{[\rho]}(\lambda)$, is the average of $D(\lambda)$ in the state described by the density operator ρ:

$$C_s^{[\rho]}(\lambda) = \langle D(\lambda) \rangle = \mathrm{Tr}\left[\rho e^{\lambda a^\dagger - \lambda^* a}\right] \ . \tag{3.197}$$

The operator $D(\lambda)$ being unitary, all its eigenvalues have a unit modulus. The modulus of its average is thus always bounded by one:

$$|C_s^{[\rho]}(\lambda)| \leq 1 \ . \tag{3.198}$$

Note also the identity:

$$C_s^{[\rho]}(0) = \mathrm{Tr}(\rho) = 1 \ . \tag{3.199}$$

The upper bound of $C_s^{[\rho]}(\lambda)$ is thus reached at the origin. In addition, $C_s^{[\rho]}(\lambda)$ obeys the conjugation relation:

$$C_s^{[\rho]}(-\lambda) = \left[C_s^{[\rho]}(\lambda)\right]^* \ . \tag{3.200}$$

Let us finally give the expression of the symmetric characteristic function for a pure state $|\Psi\rangle$:

$$C_s^{[|\Psi\rangle\langle\Psi|]} = \langle\Psi| \, D(\lambda) \, |\Psi\rangle \ . \tag{3.201}$$

It is merely the overlap between $|\Psi\rangle$ and the state obtained by translating $|\Psi\rangle$ in phase space by $D(\lambda)$. It is thus an autocorrelation function of the quantum state in phase space.

The normal- and anti-normal-order characteristic functions are likewise defined as:

$$C_n^{[\rho]}(\lambda) = \mathrm{Tr}\left[\rho e^{\lambda a^\dagger} e^{-\lambda^* a}\right] \ , \tag{3.202}$$

and:

$$C_{an}^{[\rho]}(\lambda) = \mathrm{Tr}\left[\rho e^{-\lambda^* a} e^{\lambda a^\dagger}\right] \ . \tag{3.203}$$

These functions can be related to each other with the help of the Glauber identity. We obtain immediately:

$$C_n^{[\rho]}(\lambda) = e^{|\lambda|^2/2} C_s^{[\rho]}(\lambda) \ ; \quad C_{an}^{[\rho]}(\lambda) = e^{-|\lambda|^2/2} C_s^{[\rho]}(\lambda) \ . \tag{3.204}$$

Any couple of characteristic functions can thus be determined from the knowledge of the third one by a mere multiplication by $e^{\pm|\lambda|^2/2}$ or $e^{\pm|\lambda|^2}$.

As a simple example, let us determine the characteristic functions for a coherent state $|\alpha\rangle$. We have:

$$C_s^{[|\alpha\rangle\langle\alpha|]}(\lambda) = \langle\alpha| \, D(\lambda) \, |\alpha\rangle \, . \tag{3.205}$$

Recalling that:

$$D(\lambda) \, |\alpha\rangle = \exp[(\lambda\alpha^* - \lambda^*\alpha)/2] \, |\alpha + \lambda\rangle \ , \tag{3.206}$$

we get:

$$C_s^{[|\alpha\rangle\langle\alpha|]}(\lambda) = e^{(\lambda\alpha^* - \lambda^*\alpha)/2} \langle\alpha\,|\alpha+\lambda\rangle = e^{-|\lambda|^2/2} e^{\alpha^*\lambda - \lambda^*\alpha}\ , \tag{3.207}$$

a complex Gaussian function from which we derive:

$$C_n^{[|\alpha\rangle\langle\alpha|]} = e^{\alpha^*\lambda - \lambda^*\alpha}\ , \tag{3.208}$$

and:

$$C_{an}^{[|\alpha\rangle\langle\alpha|]} = e^{-|\lambda|^2} e^{\alpha^*\lambda - \lambda^*\alpha}\ . \tag{3.209}$$

The characteristic functions of a Fock state $|n\rangle$ are obtained in a similar way, by expanding the normal-ordered displacement operator in powers of $a^\dagger$ and a, retaining terms with the same number of creation and annihilation operators which are the only ones to have non-vanishing expectation values in an $|n\rangle$ state . The final result for C_s is:

$$C_s^{[|n\rangle\langle|n\rangle|]} = e^{-|\lambda|^2/2} \mathcal{L}_n(|\lambda|^2)\ , \tag{3.210}$$

where $\mathcal{L}_n$ is the nth Laguerre polynomial:

$$\mathcal{L}_n(x) = \sum_{p=0}^{n} (-1)^p \frac{n!}{p!^2(n-p)!} x^p\ . \tag{3.211}$$

Let us finally mention the symmetric-order characteristic function for a thermal field, obtained by summing the Fock state result over a thermal distribution (more on the thermal field equilibrium in the last Section of this Chapter):

$$\rho_{\rm th} = \sum_n \frac{n_{\rm th}^n}{(n_{\rm th}+1)^{n+1}} |n\rangle\langle n|\ , \tag{3.212}$$

where $n_{\rm th}$ is the average number of thermal photons. We get a remarkably simple result:

$$C_s^{[\rho_{\rm th}]}(\lambda) = e^{-(n_{\rm th}+1/2)|\lambda|^2}\ . \tag{3.213}$$

The Husimi-Q distribution

The Q distribution is the Fourier transform of the anti-normal-order characteristic function:

$$Q^{[\rho]}(\alpha) = \frac{1}{\pi^2} \int d^2\lambda\, e^{(\alpha\lambda^* - \alpha^*\lambda)} C_{an}^{[\rho]}(\lambda)\ . \tag{3.214}$$

This expression looks formidable, but in fact, $Q^{[\rho]}(\alpha)$ is simply related to the expectation value of the density operator ρ in state $|\alpha\rangle$. To show this, let us write Q as:

$$Q^{[\rho]}(\alpha) = \frac{1}{\pi^3} {\rm Tr}\left[\rho \int d^2\lambda d^2\beta\, e^{(\alpha\lambda^* - \alpha^*\lambda)} e^{-\lambda^* a} |\beta\rangle\langle\beta| e^{\lambda a^\dagger}\right]\ , \tag{3.215}$$

where we have used the definition (3.203) of C_{an} and the closure relation on coherent states:

$$\frac{1}{\pi} \int d^2\beta\ |\beta\rangle\langle\beta| = \mathbb{1}\ . \tag{3.216}$$

The coherent state $|\beta\rangle$ being an eigenstate of $\exp(-\lambda^* a)$, Q reduces to:

$$Q^{[\rho]}(\alpha) = \frac{1}{\pi^3} {\rm Tr}\left[\rho \int d^2\lambda d^2\beta\, e^{\lambda^*(\alpha-\beta) - \lambda(\alpha^* - \beta^*)} |\beta\rangle\langle\beta|\right]\ , \tag{3.217}$$

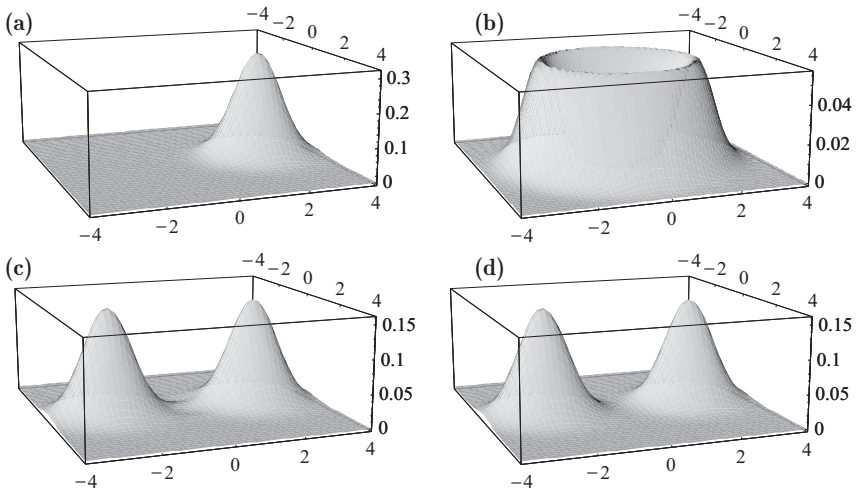

Figure 3.1: Husimi-Q distributions. (a) Coherent state $|\beta\rangle$, with $\beta = \sqrt{5}$. (b) Five-photon Fock state. (c) Schrödinger cat state, superposition of two coherent fields $|\pm\beta\rangle$, with $\beta = \sqrt{5}$. (d) Statistical mixture of the same coherent components.

and the integration over λ leads to a Dirac distribution $\delta(\alpha - \beta)$ according to the standard Fourier transform[5] relation:

$$\frac{1}{\pi^2}\int d^2\lambda\, e^{\lambda\beta^* - \lambda^*\beta} = \delta(\beta)\ . \tag{3.218}$$

We thus finally get:

$$Q^{[\rho]}(\alpha) = \frac{1}{\pi}\mathrm{Tr}\left[\rho\,|\alpha\rangle\,\langle\alpha|\right] = \frac{1}{\pi}\,\langle\alpha|\,\rho\,|\alpha\rangle\ , \tag{3.219}$$

which can also be written as:

$$Q^{[\rho]}(\alpha) = \frac{1}{\pi}\,\langle 0|\,D(-\alpha)\rho D(\alpha)\,|0\rangle = \frac{1}{\pi}\mathrm{Tr}[|0\rangle\,\langle 0|\,D(-\alpha)\rho D(\alpha)]\ . \tag{3.220}$$

The Q function is thus the average of the projector onto the vacuum state, $|0\rangle\,\langle 0|$, in the field displaced in phase space by $-\alpha$. Being the expectation value of an observable, it is thus a directly measurable quantity.

The Q distribution is positive, bounded by $1/\pi$ and normalized ($\int d^2\alpha\, Q(\alpha) = 1$), this last property resulting directly from eqn. (3.216). Using eqn. (3.219), it is easy to compute the Q functions of our favourite classical and non-classical states.

The Q distribution of a coherent state $|\beta\rangle$ is:

$$Q^{[|\beta\rangle\langle\beta|]}(\alpha) = \frac{1}{\pi}|\,\langle\alpha\,|\beta\rangle\,|^2 = \frac{1}{\pi}e^{-|\alpha-\beta|^2}\ . \tag{3.221}$$

It is plotted in Fig. 3.1(a) for $\beta = \sqrt{5}$. It is a Gaussian, with a width 1, reaching for $\alpha = \beta$ the maximum allowed value $1/\pi$. Note that the pictorial representation of coherent states as an uncertainty disk superposed on a classical amplitude corresponds to a cut at $1/e\pi$ in the $Q^{[|\beta\rangle\langle\beta|]}(\alpha)$ distribution.

Expanding $|\alpha\rangle$ on the Fock state basis, it is easy to find the Q function for an n-photon Fock state:

$$Q^{[|n\rangle\langle n|]}(\alpha) = \frac{1}{\pi}\frac{|\alpha|^{2n}}{n!}e^{-|\alpha|^2}\ . \tag{3.222}$$

[5]That the integral written in this equation is a bidimensional Fourier transform appears when separating the real and imaginary parts of the complex quantities.

Represented in Fig. 3.1(b) for $n = 5$, it appears as a single circular rim around the origin, which peaks for $|\alpha|^2 = n$, an intuitive result.

An interesting example of non-classical state is given by the 'phase cat states', which are superposition of two coherent fields with opposite phases:

$$\left|\Psi^{\pm}_{\rm cat}\right\rangle = \frac{1}{\sqrt{\mathcal{N}_{\pm}}}\left(|\beta\rangle \pm |-\beta\rangle\right) \ , \tag{3.223}$$

where:

$$\mathcal{N}_{\pm} = 2\left(1 \pm e^{-2|\beta|^2}\right) \ , \tag{3.224}$$

is a normalization factor resulting from the finite overlap of $|\beta\rangle$ and $|-\beta\rangle$. The density matrix is $\rho^{\pm}_{\rm cat} = \left|\Psi^{\pm}_{\rm cat}\right\rangle\left\langle\Psi^{\pm}_{\rm cat}\right|$.

Assuming again β real, and expanding coherent states scalar products, we get:

$$Q^{[\rm cat,\pm]}(\alpha) = \frac{1}{\pi\mathcal{N}_{\pm}}\left[e^{-|\alpha-\beta|^2} + e^{-|\alpha+\beta|^2} \pm 2e^{-(|\alpha|^2+|\beta|^2)}\cos(2\beta\alpha'')\right] \ . \tag{3.225}$$

The cat's Husimi distributions are made up of two Gaussians [first two terms in the right-hand side of eqn. (3.225)], corresponding to the field components and of an interference term, a Gaussian around the origin multiplied by a modulated cosine function. The maximum amplitude of the interference term, $\sim e^{-|\beta|^2}/\pi$ at $\alpha = 0$, is exponentially small for large β values. The Q function of the $\left|\Psi^{+}_{\rm cat}\right\rangle$ cat state, plotted in Fig. 3.1(c) for $\overline{n} = 5$, is thus almost identical to that of a statistical mixture, represented in Fig. 3.1(d). The Q function is not able to display the quantum coherence of such a state superposition. We thus introduce in the next paragraph the Wigner function that is much more suited to the pictorial representation of the coherence of such cat states.

The Wigner function

The Wigner function is defined as the two-dimensional Fourier transform of the symmetric order characteristic function:[6]

$$W(\alpha) = \frac{1}{\pi^2}\int d^2\lambda\, C_s(\lambda) e^{\alpha\lambda^* - \alpha^*\lambda} \ . \tag{3.226}$$

Separating the real and imaginary parts and setting $\alpha = \alpha' + i\alpha'' = x + ip$, we can also write:

$$W(x,p) = \frac{1}{\pi^2}\int d^2\lambda\, C_s(\lambda) e^{2i(p\lambda' - x\lambda'')} \ . \tag{3.227}$$

The Wigner function is real, as a direct consequence of the conjugate property of its Fourier transform (eqn. 3.200). It is also normalized, which results from the identity:

$$\int d^2\alpha\, W(\alpha) = \frac{1}{\pi^2}\int d^2\alpha d^2\lambda\, C_s(\lambda) e^{\alpha\lambda^* - \alpha^*\lambda} = \int d^2\lambda\, C_s(\lambda)\delta(\lambda) = C_s(0) = 1 \ , \tag{3.228}$$

where we have used again the integral definition of the two-dimensional Dirac distribution. Before exploring further the properties of W, we will write it in two other equivalent and useful forms.

We first make explicit the trace operation in the definition of $C_s(\lambda)$, by using the continuous eigenbasis $\{|x\rangle\}$ of the quadrature operator $X_0 = (a + a^\dagger)/2$:

$$C_s(\lambda) = \int dx' \ \langle x'|\, \rho D(\lambda)\, |x'\rangle \ . \tag{3.229}$$

[6] To simplify the notation, we omit for the time being, since no confusion is possible, the indication of the state in the expression of the C_s function and its Fourier transform. We write here $C_s(\lambda)$ instead of $C_s^{[\rho]}(\lambda)$ and $W(\alpha)$ instead of $W^{[\rho]}(\alpha)$. We come back later to the complete notation.

Using the Glauber identity, we can write:

$$D(\lambda) = e^{-i\lambda'\lambda''} e^{2i\lambda'' X_0} e^{-2i\lambda' P_0} \ , \tag{3.230}$$

It follows that:

$$D(\lambda) \left|x'\right\rangle = e^{i\lambda'\lambda''} e^{2i\lambda'' x'} \left|x' + \lambda'\right\rangle \ . \tag{3.231}$$

Hence:

$$W(\alpha) = W(x,p) = \frac{1}{\pi^2} \int d\lambda' d\lambda'' dx' \, e^{2i(p\lambda' - x\lambda'')} e^{i\lambda'\lambda''} e^{2i\lambda'' x'} \left\langle x'\right| \rho \left|x' + \lambda'\right\rangle \ . \tag{3.232}$$

The integral over λ'' is a one-dimensional Dirac function:

$$\int d\lambda'' \, e^{i\lambda''(\lambda' + 2x' - 2x)} = 2\pi\delta(\lambda' + 2x' - 2x) \ . \tag{3.233}$$

The integration over λ' is then simple, leading to:

$$W(x,p) = \frac{2}{\pi} \int dx' \, e^{4ip(x-x')} \left\langle x'\right| \rho \left|2x - x'\right\rangle \ . \tag{3.234}$$

Setting finally $u = 2(x' - x)$, we obtain an important form for the Wigner function:

$$W(x,p) = \frac{1}{\pi} \int du \, e^{-2ipu} \left\langle x + u/2\right| \rho \left|x - u/2\right\rangle \ , \tag{3.235}$$

which is the Fourier transform of non-diagonal density matrix elements in the position eigenstates basis. The function W is clearly sensitive to quantum coherence in the field state. The Fourier transform can be inverted yielding the matrix elements of ρ in terms of W as:

$$\left\langle x + u/2\right| \rho \left|x - u/2\right\rangle \ = \int dp \, e^{2ipu} W(x,p) \ . \tag{3.236}$$

This equation shows that the knowledge of W is equivalent to that of the density operator, and hence that the Wigner function contains all information needed to compute the expectation value of any observable in the state of the system. We come back to this point below.

An even simpler expression for W can be derived from eqn. (3.235). We start from the translation relation:

$$\left|x - \frac{u}{2}\right\rangle = e^{-i(x-u)p} D(x + ip) \left|-\frac{u}{2}\right\rangle \ , \tag{3.237}$$

[which follows directly from eqn. (3.231) in which we set $x' = -u/2$ and $\lambda = x + ip$] and from the conjugate relation, in which we change u into $-u$:

$$\left\langle x + \frac{u}{2}\right| = \left\langle \frac{u}{2}\right| D(-x - ip) e^{i(x+u)p} \ . \tag{3.238}$$

We then replace $|x - u/2\rangle$ and $\langle x + u/2|$ by their expressions (3.237) and (3.238) in eqn. (3.235) and we introduce the hermitian parity operator $\mathcal{P}$ which performs a symmetry around the phase space origin according to:

$$\mathcal{P} \left|x\right\rangle = \left|-x\right\rangle \ ; \quad \mathcal{P} \left|p\right\rangle = \left|-p\right\rangle \ . \tag{3.239}$$

We finally get:

$$W(x,p) = \frac{1}{\pi} \int du \left\langle \frac{u}{2}\right| D(-\alpha) \rho D(\alpha) \mathcal{P} \left|\frac{u}{2}\right\rangle = \frac{2}{\pi} \mathrm{Tr}[D(-\alpha) \rho D(\alpha) \mathcal{P}] \ . \tag{3.240}$$

The Wigner function is thus the average value of $2\mathcal{P}/\pi$ in the state obtained by displacing the oscillator in phase space by the amount $-\alpha$, transforming its density operator according to $\rho \to D(-\alpha)\rho D(\alpha)$.

It is easy to show that the $\mathcal{P}$ operator is the photon number parity observable. The $|n\rangle$ Fock state wave functions in the $|x\rangle$ and $|p\rangle$ representations are a product of an even parity Gaussian multiplied by a Hermite polynomial which has the parity of n. Reversing the sign of x or p in these functions thus amounts to a multiplication by $(-1)^n$, so that we can write:

$$\mathcal{P} = e^{i\pi a^\dagger a} \ . \tag{3.241}$$

The parity operator is clearly hermitian and unitary, with the Fock states as eigenvectors and eigenvalues ± 1:

$$\mathcal{P}\,|n\rangle = (-1)^n\,|n\rangle \ . \tag{3.242}$$

Being the expectation value of an observable, W is thus a directly measurable quantity. The eigenvalues of the parity operator being $+1$ and -1, its expectation lies between these values. It follows that the Wigner function is bounded:

$$-2/\pi \leq W(\alpha) \leq 2/\pi \ . \tag{3.243}$$

As noted above, the average value of any observable can be obtained from the knowledge of the Wigner distribution. There is in fact a very simple recipe to express this average by a simple integral, provided the observable, considered as a function of a and $a^\dagger$, has been cast in the symmetric order. The relation (3.226) defining W can be written:

$$W(\alpha) = \frac{1}{\pi^2}\mathrm{Tr}\left[\rho \int d^2\lambda\, e^{\lambda^*(\alpha - a) - \lambda(\alpha^* - a^\dagger)}\right] \ , \tag{3.244}$$

in which the integral is reminiscent of the two-dimensional Dirac distribution. We can then formally write:

$$W(\alpha) = \mathrm{Tr}\left[\rho_c \delta(\alpha - a)\right] \ . \tag{3.245}$$

The Wigner function is thus the average value of the operator-Dirac distribution of $\alpha - a$. Obviously, such a formal derivation has to be taken with care. We do not enter here in the mathematical justification of this expression, which is valid provided all quantum operators are put in the symmetric order.

Consider now an observable O of the field mode. It can be expanded as a power series of a and $a^\dagger$ and cast in the symmetric order by repeated commutations of these operators. Let us note $O_s(a, a^\dagger)$ the resulting expression. Formally, we can write:

$$O_s(a, a^\dagger) = \int d^2\alpha\, o_s(\alpha, \alpha^*)\delta(\alpha - a) \ , \tag{3.246}$$

where $o_s(\alpha, \alpha^*)$ is the complex function of α obtained by replacing a by α and $a^\dagger$ by α^* in $O_s(a, a^\dagger)$. The average value of O_s is then:

$$\langle O_s \rangle = \mathrm{Tr}\left[\rho O_s\right] = \int d^2\alpha\, o_s(\alpha, \alpha^*)\mathrm{Tr}\left[\rho_c \delta(\alpha - a)\right] = \int d^2\alpha\, o_s(\alpha, \alpha^*) W(\alpha) \ . \tag{3.247}$$

This simple expression reminds us of eqn. (3.195) giving the average value of any classical observable as an integral over the probability density in phase space. The real and normalized Wigner function plays in this respect the role of $f(x, p)$ in classical physics. We will see however that, contrary to f, W can take negative values which are a signature of the oscillator's quantum behaviour.

The analogy between $f(x, p)$ and $W(x, p)$ can be pushed further by considering the marginal distributions of x and p, obtained by integrating the distribution over the conjugate variable. Setting $u = 0$ in eqn. (3.236), we get immediately the probability density of finding the value x of the oscillator's position (or field quadrature X_0) as:

$$P(x) = \langle x|\,\rho\,|x\rangle = \int dp\, W(x, p) \ . \tag{3.248}$$

A simple calculation involving changes between the $|x\rangle$ and $|p\rangle$ bases shows that the integration of W over x yields likewise the probability density of finding the value p of the oscillator's momentum (or field quadrature $X_{\pi/2}$):

$$P(p) = \langle p|\,\rho\,|p\rangle = \int dx\, W(x,p)\ . \tag{3.249}$$

More generally, the Wigner distribution can be expressed as a function of a any couple of orthogonal field quadratures x_ϕ and p_ϕ defined by:

$$x_\phi = x\cos\phi + p\sin\phi\ ; \quad p_\phi = -x\sin\phi + p\cos\phi\ , \tag{3.250}$$

and corresponding to axes rotated in the phase plane by an angle ϕ with respect to the x and p coordinate directions. The marginal distributions properties apply to any such couple of conjugate quadratures:

$$P(p_\phi) = \int dx_\phi\, W(x_\phi, p_\phi)\ . \tag{3.251}$$

It can be shown that W is the only quantum phase space distribution obeying this interesting property, on which the 'quantum tomographic' methods for the reconstruction of W are based.

For many quantum states, the probability distributions $P(x)$ or $P(p)$ present nodes. This is, for instance, the case for the x distribution of the excited Fock states. When $P(x_0) = 0$, it follows that:

$$\int dp\, W(x_0, p) = 0\ . \tag{3.252}$$

Hence, W cannot be everywhere positive. When it takes negative values, it cannot be assimilated to a genuine probability distribution. In fact, as we now show, negativities in W are clear-cut indicators of the non-classical nature of a field state. We now examine the Wigner functions of a few simple quantum states.

Let us consider first a coherent state $|\beta\rangle$ (including obviously the vacuum state). Using the symmetric-order characteristic function [eqn. (3.207), in which we replace α by β], the corresponding Wigner function, $W^{[|\beta\rangle\langle\beta|]}(\alpha)$ is:

$$\begin{aligned} W^{[|\beta\rangle\langle\beta|]}(\alpha) &= \frac{1}{\pi^2}\int d^2\lambda\, e^{-|\lambda|^2/2} e^{\lambda(\beta^*-\alpha^*)-\lambda^*(\beta-\alpha)} \\ &= \frac{2}{\pi} e^{-2|\beta-\alpha|^2}\ . \end{aligned} \tag{3.253}$$

It is a Gaussian, with a width $1/\sqrt{2}$, centred on the classical amplitude β and taking for $\alpha = \beta$ its maximum allowed value, $2/\pi$. Figure 3.2(a) and (b) present the Wigner functions of the vacuum ($\beta = 0$) and of a coherent state with $\beta = \sqrt{5}$ ($\overline{n} = 5$ photons on the average).

The Wigner function of a thermal field, with $n_{\rm th}$ photons on the average is derived also from the corresponding Gaussian characteristic function (eqn. 3.213):

$$W^{[\rho_{\rm th}]}(\alpha) = \frac{2}{\pi}\frac{1}{2n_{\rm th}+1} e^{-2|\alpha|^2/(2n_{\rm th}+1)}\ . \tag{3.254}$$

It is again a Gaussian, centred at the origin and represented in Fig. 3.2(c) for $n_{\rm th} = 1$. The width is now $\sqrt{n_{\rm th}+1/2}$ and the peak value is reduced to $1/\pi(n_{\rm th}+1/2)$

Let us examine also the case of a squeezed vacuum state, often considered in quantum optics as 'non-classical'. It is obtained by the action on the vacuum of the 'squeezing' operator:

$$S(\xi) = e^{(\xi^* a^2 - \xi {a^\dagger}^2)/2}\ , \tag{3.255}$$

where we assume for the sake of this simple discussion that ξ is real. The squeezed states are minimal uncertainty states satisfying the Heisenberg uncertainty relation $\Delta X_0 \Delta P_0 = 1/4$. For a coherent

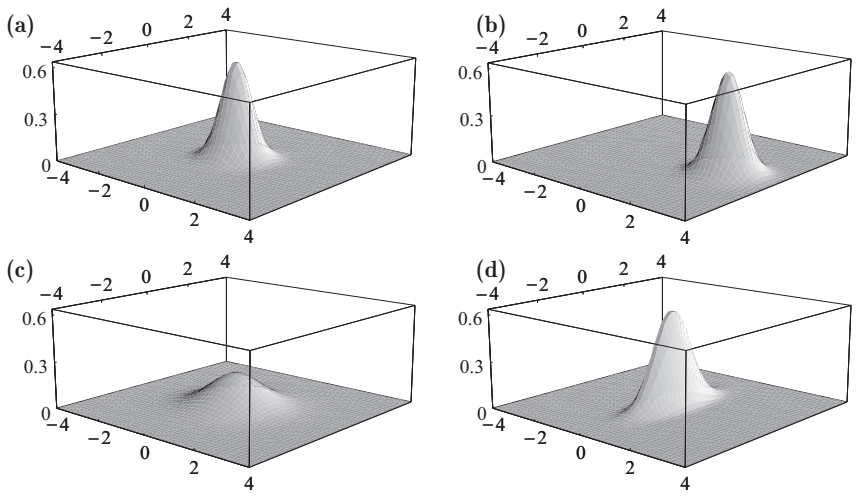

Figure 3.2: Classical state Wigner functions. (a) Vacuum state. (b) Coherent state with $\beta = \sqrt{5}$. (c) Thermal field with $n_{\rm th} = 1$ photon on the average. (d) A squeezed vacuum state, with a squeezing parameter $\xi = 0.5$. The vertical scales are from 0 to $2/\pi$.

state, the variances of X_0 and P_0 are equal. For a squeezed state the standard deviation of the X_0 quadrature is reduced to:

$$\Delta X_0 = \tfrac{1}{2} e^{-\xi} \ , \tag{3.256}$$

and the fluctuations of P_0 accordingly increased:

$$\Delta P_0 = \tfrac{1}{2} e^{\xi} \ . \tag{3.257}$$

Note that the limit of infinite squeezing corresponds to the position eigenstate $|x = 0\rangle$, with no position fluctuations and infinite momentum uncertainty. The Wigner function of a squeezed vacuum is a non-degenerate Gaussian:

$$W^{[sq,\xi]}(x,p) = \frac{2}{\pi} e^{-2\exp(2\xi)x^2} e^{-2\exp(-2\xi)p^2} \ , \tag{3.258}$$

represented in Fig. 3.2(d) for $\xi = 0.5$. A general squeezed state corresponds to a complex ξ parameter and to a displacement towards a non-vanishing classical amplitude in phase space. Its Wigner function is also a non-degenerate Gaussian, centred on the classical amplitude, whose principal axis (minimum and maximum fluctuations) are tilted with respect to x and p.

For all states considered so far, including the squeezed ones, the Wigner function is definite and positive. It has all the properties of a classical probability distribution in phase space. For the computation of any observable eigenvalue, these states can be considered as classical fields with a stochastic complex amplitude whose probability distribution over phase space is given by W. This is not the case for the states we consider below.

The Fock state Wigner function can be derived from the corresponding characteristic function (eqn. 3.210):

$$W^{[|n\rangle\langle n|]}(\alpha) = \frac{2}{\pi}(-1)^n e^{-2|\alpha|^2} \mathcal{L}_n(4|\alpha|^2) \ . \tag{3.259}$$

Note that $W^{[|n\rangle\langle n|]}$ does not depend upon the phase of α, which depicts the complete phase indeterminacy in Fock states. Since $\mathcal{L}_n(0) = 1$:

$$W^{[|n\rangle\langle n|]}(0) = \frac{2}{\pi}(-1)^n \ . \tag{3.260}$$

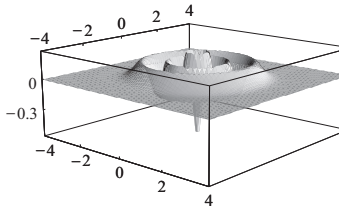

Figure 3.3: Wigner function of a five-photon Fock state.

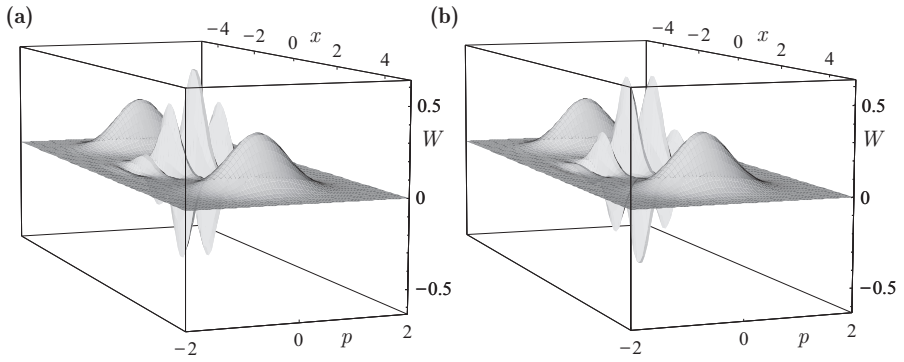

Figure 3.4: Wigner functions of even (a) and odd (b) 10-photon π-phase cats

The Wigner function of odd photon number states takes the minimal value $-2/\pi$ at the origin of phase space. It cannot thus be interpreted as a probability distribution of classical field fluctuations, as was the case for the states considered above. In fact, all photon number states, but $|0\rangle$, present negativities in some region of phase space. The single-photon Wigner function:

$$W^{[|1\rangle\langle 1|]}(\alpha) = -\frac{2}{\pi}(1-4|\alpha|^2)e^{-2|\alpha|^2} \ , \tag{3.261}$$

has a Mexican-hat shape. As another example, we present in Fig. 3.3 the five-photon state Wigner function. It presents circular rims around the origin, with alternating negative and positive values. Note that this representation does not coincide with the intuitive picture of a Fock state, better depicted by the Husimi-Q function. The inner rims in $W^{[|n\rangle\langle n|]}$ correspond to quantum interference features, revealing the non-classical nature of the Fock states.

Finally, a cat state Wigner function is:

$$W^{[\mathrm{cat},\pm]} \ = \ \frac{1}{\pi^2\mathcal{N}_\pm}\int d^2\lambda\, e^{(\alpha\lambda^*-\alpha^*\lambda)}\Big[\,\langle\beta|\,D(\lambda)\,|\beta\rangle + \langle-\beta|\,D(\lambda)\,|-\beta\rangle$$

$$\pm \langle\beta| D(\lambda) |-\beta\rangle \pm \langle-\beta| D(\lambda) |\beta\rangle \Big] \ . \tag{3.262}$$

The first line in this equation corresponds to the weighted sum of the Wigner functions of the coherent states $|\beta\rangle$ and $|-\beta\rangle$. The second line corresponds to non-diagonal terms involving the quantum coherence between the two components. These terms are absent in the case of a statistical mixture $(|\beta\rangle\langle\beta| + |\beta\rangle\langle\beta|)/2$. Assuming, for the sake of simplicity, that β is real we get:

$$\langle-\beta| D(\lambda) |\beta\rangle = e^{i\beta\lambda''} \langle-\beta \,|\beta+\lambda\rangle = e^{-2\beta(\beta+\lambda)-|\lambda|^2/2} \ . \tag{3.263}$$

The coherence terms also correspond to Gaussian integrations which can be performed explicitly, leading finally to:

$$W^{[\mathrm{cat},\pm]}(\alpha) = \frac{1}{\pi(1 \pm e^{-2|\beta|^2})} \Big[e^{-2|\alpha-\beta|^2} + e^{-2|\alpha+\beta|^2} \pm 2e^{-2|\alpha|^2} \cos(4\alpha''\beta)\Big] \ . \tag{3.264}$$

The cat Wigner function is represented in Fig. 3.4(a). It exhibit large negative values near the phase-space origin, a clear signature of non-classical behaviour of a cat, depicted in a more vivid way that through the Q distribution. Fig. 3.4(b) presents the Wigner function of an 'odd' cat, $|\beta\rangle - |-\beta\rangle$. The only difference is a π shift of the phase of the interference pattern.

We can discuss in more quantitative terms why is it that W is better adapted to the cat states than Q. The W and Q functions are connected in reciprocal space by the relation (3.204) between their Fourier transforms, $C_s(\lambda)$ being obtained from $C_{an}(\lambda)$ by a multiplication by $e^{|\lambda|^2/2}$. We have seen that this coherence is described by vanishingly small terms in Q around the phase space origin. The value of Q at $\alpha = 0$ is equal to the integral over the λ plane of its Fourier transform $C_{an}(\lambda)$. This integral is thus very small for a cat. The same integral, performed on the Fourier transform of W, yields a much larger result since $C_s(\lambda)/C_{an}(\lambda)$ diverges for $|\lambda| \to \infty$, entailing $W(0) \gg Q(0)$. The features of the phase space distribution around $\alpha = 0$, critical to the description of the coherence, are thus greatly amplified by the $e^{|\lambda|^2/2}$ multiplication transforming Q into W in reciprocal space.

As a final remark, we have defined W and Q as the Fourier transforms of C_s and C_{an}. What about C_n? Its Fourier transform is yet another phase space density function, the Glauber–Sudarshan-P distribution. It turns out to be highly singular. For instance, the P distribution of the coherent state $|\beta\rangle$ is a Dirac distribution centred at β and the P distribution of an $|n\rangle$ Fock state involves the n first derivatives of δ. In spite of their mathematical interest, these distributions do not provide a very practical representation of quantum states.[7]

3.5 Coupling field modes: the beamsplitter

We now explore the quantum dynamics of coupled field modes, providing an useful insight into the physics of beam-splitters, which are essential tools in quantum optics experiments[8]. We present a simple model of the beam-splitter, a device coupling linearly two modes of the field and examine the transformations of a few simple imput state in this device.

3.5.1 Hamiltonian approach

Two possible realizations of a beamsplitter are shown in Fig. 3.5. On the left, two modes (a) and (b) of the radiation field with the same frequency propagate at right angles. At their intersection, there is a partially transmitting, partially reflecting dielectric slab inclined at 45 degrees with respect

[7] One can in fact consider a wide range of quasi-probability distributions, by defining the s-order of operators (s being a continuous parameter), whose symmetric, normal and anti-normal orders are limiting cases. None of these 'exotic' distributions is as useful as W or Q.

[8] Once again, this Section is derived from Haroche and Raimond, Exploring the quantum, OUP, 2006.

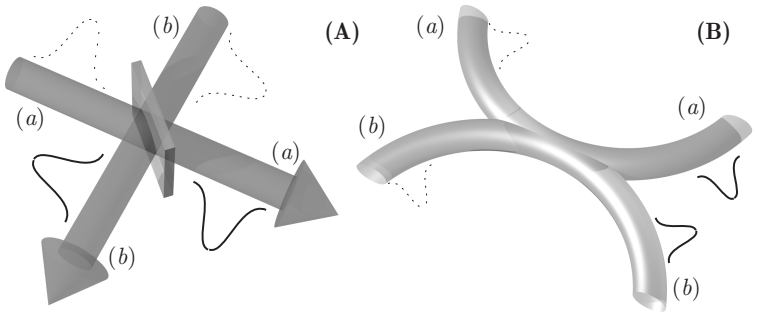

Figure 3.5: Two beam-splitter models. (A) Two freely propagating modes coupled by a semi-transparent mirror. (B) Two modes guided in single-mode fibres coupled in a fibre coupler. Incoming wave packets (dotted lines) and outgoing ones (solid lines) are represented pictorially in both cases.

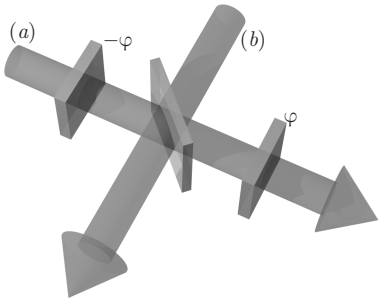

Figure 3.6: Principle of a generalized beam-splitter with adjustable phase φ. A semi-reflecting plate, inclined at 45° with the (a) and (b) beams, is sandwiched between two retarding plates inducing opposite phase shifts on beam (a).

to the beam directions. We assume that the modes are geometrically matched: they have the same polarization (orthogonal to the incidence plane) and the spatial structure of mode (b) reflected by the slab exactly matches the transmitted mode (a). Figure 3.5(b) represents an optical fibre coupler realizing the same mode mixing. The upper fibre, (a), and the lower fibre, (b), are placed side by side over some length,[9] so that light is coupled from one mode into the other.

In both cases, the two field-mode amplitudes are classically mixed. In the case of a lossless dielectric slab, for instance, the emerging electric field amplitudes, E'_a and E'_b, are linked to the incoming ones, E_a and E_b, by a unitary and symmetrical[10] matrix relation:

$$\begin{pmatrix} E'_a \\ E'_b \end{pmatrix} = U_c \begin{pmatrix} E_a \\ E_b \end{pmatrix} = \begin{pmatrix} t(\omega) & r(\omega) \\ r(\omega) & t(\omega) \end{pmatrix} \begin{pmatrix} E_a \\ E_b \end{pmatrix} , \tag{3.265}$$

where $t(\omega)$ and $r(\omega)$ are complex transmission and reflection coefficients, functions of the frequency ω of the field modes, which satisfy the unitarity conditions $|t(\omega)|^2+|r(\omega)|^2 = 1$ and $t(\omega)r^*(\omega)+t^*(\omega)r(\omega) = 0$. The general relation (3.265) holds for any kind of lossless symmetrical semi-reflecting device, whether dielectric or metallic, and for a fibre coupler as well. By choosing properly the phase origin of the transmitted field, one can always assume that $t(\omega)$ is real positive, which entails that $r(\omega)$ is purely imaginary. We then introduce a mixing angle θ characterizing the beam-splitter operation at

[9] In practical couplers, the cladding around the fibre core is partially removed. The modes' evanescent waves around both fibre cores are thus superposed and directly coupled.

[10] The unitarity is imposed by energy conservation, while the symmetry of the matrix reflects the invariance of optics laws when propagation directions are reversed.

frequency ω, set $t(\omega) = \cos\theta/2$, $r(\omega) = i\sin\theta/2$, and for a monochromatic field U_c is:

$$U_c(\theta) = \begin{pmatrix} \cos(\theta/2) & i\sin(\theta/2) \\ i\sin(\theta/2) & \cos(\theta/2) \end{pmatrix} . \tag{3.266}$$

This description of classical mode mixing is valid for monochromatic fields interacting continuously with the beam-splitter. In general, a realistic experiment involves time-limited wave packets propagating in modes (a) and (b) and 'colliding' on the beam-splitter during a time τ, as illustrated on Fig. 3.5. These transient fields are developed over a collection of field modes spanning a small frequency interval $\Delta\omega = 1/\tau$. To avoid complications arising from the spectral analysis of this time-dependent problem, we take the limit in which $\Delta\omega$ is very small and τ very long yet finite, so that we can define a 'before' and an 'after' for the collision. We assume that the time envelopes of the wave packets are identical and thus overlap perfectly on the beam-splitter. We consider also that the r, t and φ parameters do not vary over the narrow spectrum of the wave packets, so that we can define a single matrix (3.266) or (**??**) describing the same mixing process for all the frequency components of the light field.

What is the action of this beam-splitter on the quantum states and observables of the field? We now show that it is described by an interaction Hamiltonian H_{ab}, which, at the classical limit of large numbers of photons, has the same effect on the field operators as the transformation (**??**) on the classical fields. This Hamiltonian acts transiently on the fields, coupling the two quantum oscillators during the finite time τ corresponding to the simultaneous passage of the wave packets on the beam-splitter. Since it describes a linear interaction, H_{ab} is made of two terms associated to single-photon exchange between the two modes:

$$H_{ab}(t) = -\hbar\frac{g(t)}{2}(ab^\dagger + a^\dagger b) , \tag{3.267}$$

where a and b are the annihilation operators in the modes and $g(t)$ is a slowly varying real function of time, switching adiabatically the coupling on and off for the time interval τ around $t = 0$. In the following, we consider the action of H_{ab} alone. This implicitly assumes that we use an interaction representation with respect to the Hamiltonians of the free modes.[11]

The operation of the beam-splitter can be analyzed either in the Schrödinger or Heisenberg point of views. In the first case, the quantum states of both modes evolve due to the coupling Hamiltonian H_{ab}. This approach is used in the next section to describe the evolution of some special quantum states.

We focus here on the Heisenberg point of view, which lends itself to a direct comparison between the classical and quantum descriptions. The quantum states are constant and the dynamical variables are the field operators. In the interaction picture with respect to the free mode Hamiltonians, these operators are time-independent before and after the 'collision' with the beam-splitter. We can thus identify them, for $t \ll -\tau$ and $t \gg \tau$, with the a and b operators of the Schrödinger picture. The beam-splitter transforms the input operator a into the output operator a':

$$a' = U^\dagger a U , \tag{3.268}$$

where U is the evolution operator:

$$U = e^{-(i/\hbar)\int H_{ab}(t)\,dt} , \tag{3.269}$$

the integral being carried over the whole duration τ of the coupling. The evolution operator can be rewritten as:

$$U(\theta) = e^{-iG\theta/2} , \tag{3.270}$$

[11] To simplify the notation, we will omit the tilde that we should use in an interaction representation.

where:

$$G = -(ab^\dagger + a^\dagger b) \quad \text{and} \qquad \theta = \int g(t)\, dt \ . \tag{3.271}$$

Note that we omit the θ and φ arguments in U when no confusion is possible. We now have:

$$\begin{aligned} a' &= U^\dagger a U = e^{iG\theta/2} a e^{-iG\theta/2} = a + \frac{i\theta}{2}\,[G,a] \\ &\quad + \frac{i^2\theta^2}{2!2^2}\,[G,[G,a]] + \cdots + \frac{i^n\theta^n}{n!2^n}\,[G,[G,[\cdots,[G,a]]]] + \cdots \ , \end{aligned} \tag{3.272}$$

where we have used again the Baker–Hausdorff lemma to develop the exponentials. The nested commutators on the right-hand side can be easily computed: $[G,a] = b$ and $[G,[G,a]] = a$. All the odd-order terms in the development are proportional to b, while the even-order ones are proportional to a. The coefficients of a and ib thus coincide with the series expansion of $\cos\theta/2$ and $\sin\theta/2$ respectively:

$$a' = U^\dagger a U = \cos(\theta/2)\, a + i \sin(\theta/2)\, b \ , \tag{3.273}$$

and similarly:

$$b' = U^\dagger b U = i \sin(\theta/2)\, a + \cos(\theta/2)\, b \ . \tag{3.274}$$

The output mode operators are a linear (unitary) combination of the input ones [12]. These relations are formally identical to the input–output matrix relations (3.266) for the classical electric field amplitudes. This identity, which justifies the expression (3.267) of H_{ab}, expresses the correspondence principle. When the fields involve many photons, the annihilation operators behave as the classical field complex amplitudes. The mixing parameter θ is directly related to the transmission and reflection coefficients of the beam-splitter, which can be measured in a classical optics experiment. These results are independent of the precise details of the model.

Taking the hermitian conjugate of the previous relations and noting that $U^\dagger(\theta) = U(-\theta)$, we find similarly:

$$U a^\dagger U^\dagger = \cos(\theta/2)\, a^\dagger + i \sin(\theta/2)\, b^\dagger \ ; \qquad U b^\dagger U^\dagger = i \sin(\theta/2)\, a^\dagger + \cos(\theta/2)\, b^\dagger \ . \tag{3.275}$$

3.5.2 State transformations

We now analyse the action of the beam-splitter on selected initial states in the Schrödinger point of view. The final state $|\Psi'\rangle$ is given in terms of the input state $|\Psi\rangle$ by $|\Psi'\rangle = U\,|\Psi\rangle$.

No photons

The first trivial case corresponds to the vacuum impinging in both modes, $|\Psi\rangle = |0,0\rangle$. This state is invariant under the action of U. A beam-splitter has no effect in the dark.

One photon

Let us consider now a single photon impinging in mode (a), the initial state being $|1,0\rangle$ [in the following, the first and second labels in the kets refer to (a) and (b) respectively]. The sequence of equalities:

$$U\,|1,0\rangle = U a^\dagger\,|0,0\rangle = U a^\dagger U^\dagger U\,|0,0\rangle = U a^\dagger U^\dagger\,|0,0\rangle \ , \tag{3.276}$$

leads, using eqn. (3.275), to:

$$U\,|1,0\rangle = \left[\cos(\theta/2)\, a^\dagger + i \sin(\theta/2)\, b^\dagger\right]|0,0\rangle = \cos(\theta/2)\,|1,0\rangle + i \sin(\theta/2)\,|0,1\rangle \ . \tag{3.277}$$

[12] We should by the way obtain similar expressions in a mode basis change involving only two modes. This paragraph on the beamsplitter operation is thus also appropriate for the description of field state modifications in a mode basis change.

For a single photon impinging on the beam-splitter in mode (b), we get:

$$U\,|0,1\rangle = \left[i\sin(\theta/2)\,a^\dagger + \cos(\theta/2)\,b^\dagger\right]|0,0\rangle = i\sin(\theta/2)\,|1,0\rangle + \cos(\theta/2)\,|0,1\rangle \ . \tag{3.278}$$

A single photon is thus in general dispatched in a coherent superposition between the two modes, with a final probability distribution corresponding to the classical light intensity transmission and reflection coefficients $\cos^2(\theta/2)$ and $\sin^2(\theta/2)$. In particular, for $\theta = \pi/2$, we have:

$$U(\pi/2)\,|1,0\rangle = (|1,0\rangle + i\,|0,1\rangle)/\sqrt{2}\ . \tag{3.279}$$

Is this an entangled state? If we define the system as two oscillators (a) and (b) coupled by the beam-splitter, the answer is definitely 'yes'. The two parts of this bipartite entity are entangled by sharing in an ambiguous way a quantum of excitation. Correlations between measurements performed independently on the two modes could reveal this entanglement. If we renounce to perform such independent measurements, though, we can define two new modes ($\pm$), linear combinations of (a) and (b) corresponding to the photon creation operators $(a^\dagger \pm ib^\dagger)/\sqrt{2}$. The state (3.279) then represents a single photon in the ($+$) mode with the vacuum in the ($-$) mode and, in this point of view, it is not entangled. This example shows that the notion of entanglement depends upon the basis in which we choose to describe the system (this choice being in turn determined by the kind of measurements we intend to perform on it). The unitary transformation changing the tensor products of Fock states in modes (a) and (b) into those of photon number states in modes ($\pm$) is non-local with respect to the (a)-(b) partition since it mixes the two modes. Such a non-local operation can result in different degrees of entanglement in the two representations, turning an entangled state into a separate one.[13]

Adding, by means of a mere dephaser in one of the modes, an adjustable phase φ between the two-components of the single-photon state (3.277), we can explore, when θ and φ are tuned, the whole two-dimensional Hilbert space spanned by $|1,0\rangle$ and $|0,1\rangle$. We note the formal analogy between a single photon 'suspended' between the two modes and a spin on the Bloch sphere. It has been suggested to exploit this analogy and to code information into the path of single-photon bimodal states, $|1,0\rangle$ and $|0,1\rangle$, playing the roles of logical $|0\rangle$ and $|1\rangle$ qubit states. In this context, the beam-splitter which transforms the logical qubit states into their most general superpositions realizes a one-qubit quantum gate.

n photons

Let us now consider the action of the beam-splitter on fields containing many photons. Assume first that n-photons impinge in (a), the initial state being $|n,0\rangle$. A calculation similar to the single-photon one yields:

$$U\,|n,0\rangle = U\frac{(a^\dagger)^n}{\sqrt{n!}}\,|0,0\rangle = \frac{1}{\sqrt{n!}}U(a^\dagger)^n U^\dagger U\,|0,0\rangle \ . \tag{3.280}$$

Noting that $U(a^\dagger)^n U^\dagger = (Ua^\dagger U^\dagger)^n$, and using again eqn. (3.275):

$$U\,|n,0\rangle = \frac{1}{\sqrt{n!}}\left[\cos\frac{\theta}{2}\,a^\dagger + i\sin\frac{\theta}{2}\,b^\dagger\right]^n |0,0\rangle \ . \tag{3.281}$$

The right-hand side can be expanded according to the binomial law:

$$U\,|n,0\rangle = \sum_{p=0}^{n}\binom{n}{p}^{1/2}[\cos(\theta/2)]^{n-p}\,[i\sin(\theta/2)]^p\,|n-p,p\rangle \ . \tag{3.282}$$

[13] Note that the notion of entanglement is here independent of the number of particles in the system. A single photon can be in an entangled state or not, depending upon the basis choice.

The final quantum state is a coherent superposition of terms corresponding to all possible partitions of the n incoming photons between the two modes. If we describe the system as a bipartite (a)-(b) entity, the final state is thus in general massively entangled. When θ is an even multiple of π, the output state is disentangled, in fact identical to the initial one [all photons in mode (a)]. When θ is an odd multiple of π, all photons are channelled in mode (b) (again a disentangled situation).

To be specific, let us consider in more detail a balanced beam-splitter ($\theta = \pi/2$). The output state is:

$$U\left(\pi/2, 0\right)|n, 0\rangle = \frac{1}{\sqrt{2^n}} \sum_{p=0}^{n} \binom{n}{p}^{1/2} (i)^p \, |n-p, p\rangle \ . \tag{3.283}$$

The probability of getting $n-p$ photons in (a) and p in (b) is proportional to $\binom{n}{p}$, the number of partitions of the incoming photons into the two outputs. From the photon counting point of view, the quantum beam-splitter behaves as a random device. Each photon 'freely chooses' to emerge either in (a) or (b), with equal probabilities. The average photon number in each output mode is thus $n/2$. The photon number in one mode obeys, in the limit of large incoming photon numbers $n \gg 1$, Gaussian statistics with a width $\sqrt{n}/2$. The relative fluctuations, proportional to $1/\sqrt{n}$, are negligible for large fields and the two output energies are balanced according to the correspondence principle. This simple picture, treating photons as billiard balls, is valid because we consider only the output energies. It is not sufficient to account for the massive entanglement between the two modes, which would be revealed by more complex photon coincidence experiments.

Coherent states

Suppose now that the impinging field in mode (a) is in a coherent state $|\alpha\rangle$ with $\overline{n} = |\alpha|^2$ photons on the average, while mode (b) is in vacuum. The output state of the beam-splitter is now:

$$U\,|\alpha, 0\rangle = U D_a(\alpha) U^\dagger \, |0, 0\rangle \ , \tag{3.284}$$

where $D_a(\alpha)$ is the displacement operator in mode (a). Using the operator identity $U f(A) U^\dagger = f(UAU^\dagger)$, which holds whenever f can be expanded in power series, we get:

$$U D(\alpha) U^\dagger = e^{\alpha U a^\dagger U^\dagger - \alpha^* U a U^\dagger} \ . \tag{3.285}$$

Using eqn. (3.275) and its hermitian conjugate, and separating the commuting contributions of a and b in the exponentials, we get:

$$U\,|\alpha, 0\rangle = D_a\left[\alpha \cos(\theta/2)\right] D_b\left[i\alpha \sin(\theta/2)\right] |0, 0\rangle \ , \tag{3.286}$$

where D_b is the displacement operator acting on mode b. The output state is thus:

$$U\,|\alpha, 0\rangle = |\alpha \cos(\theta/2), i\alpha \sin(\theta/2)\rangle \ . \tag{3.287}$$

It is an unentangled tensor product of coherent states in the two modes, with amplitudes obeying the same relations as the classical fields (eqn. 3.266). The coherent state dynamics, entirely classical even for small photon numbers, is thus very different from that of Fock states. The non-entanglement of coherent states involved in linear coupling operations is a very basic feature of these states, with far-reaching consequences, as we will see below when discussing relaxation and decoherence.

Let us note also that the two modes exchange periodically their energies as a function of the mixing angle θ or, equivalently, as a function of the coupling time. This periodic energy exchange is the counterpart of the classical beating phenomenon for two coupled mechanical oscillators.

Photon collision on a beamsplitter

A beam-splitter can also be used to mix two excited modes. As a simple example, suppose that (a) and (b) initially contain a single photon. The output state is then:

$$U\left|1,1\right\rangle = Ua^{\dagger}b^{\dagger}\left|0,0\right\rangle = Ua^{\dagger}U^{\dagger}Ub^{\dagger}U^{\dagger}\left|0,0\right\rangle \ . \tag{3.288}$$

Using eqn. (3.275), we get:

$$U\left|1,1\right\rangle = \frac{i\sin\theta}{\sqrt{2}}\left[\left|2,0\right\rangle + \left|0,2\right\rangle\right] + \cos\theta\left|1,1\right\rangle \ , \tag{3.289}$$

which is, in general, an entangled state. In the case of a balanced beam-splitter ($\theta = \pi/2$):

$$U(\pi/2,0)\left|1,1\right\rangle = \left(\left|2,0\right\rangle + \left|0,2\right\rangle\right)/\sqrt{2} \ , \tag{3.290}$$

which is a superposition of two photons propagating together in mode (a) or (b). The two photons are bunched in the same mode after the beam-splitter. This can be seen as a consequence of the bosonic nature of the photons. It is also a quantum interference effect. The probability amplitude of getting one photon in each mode cancels, because of the exact destructive interference between two indistinguishable quantum paths. In one of the paths, both photons are transmitted, with a probability amplitude $t \times t = 1/2$. In the other, they are both reflected, with the quantum amplitude $ir \times ir = -1/2$.

This process and the resulting state are non-classical. A superposition of two photons either in mode (a) or in mode (b) is the simplest example of a multi-particle quantum state superposition. This photon 'bunching' effect has been observed by the first time by Hong, Ou and Mandel in the early times of quantum optics. It is generally considered as one of the key phenomena exhibiting field quantization.

It is obtained here because the polarizations of the two photons are the same. Photons with orthogonal polarizations behave differently. If they are initially in an entangled polarization state, anti-symmetric versus photon exchange, they emerge 'anti-bunched' in different spatial modes. This is required to preserve the overall state symmetry versus photon exchange. Photon entanglement and Bell states analysis techniques are based on this feature. Let us add that these photon coincidence experiments are technically difficult, since the wave packets must be well-matched, both in space (mode matching) and in time (coherence length overlap).

3.6 Field relaxation

We now treat the important problem of the coupling of a mode, not to a single other one as in the beamsplitter case, but to a continuum of modes playing the role of an environment. We describe in this way for instance the quantum field state transformation due to the attenuation in an optical fibre. The diffusion on the silica defects, after a long path, couples photons to the outside. We also describe with this situation the important case of Cavity Quantum Electrodynamics, when the box limiting the field is not a virtual one, but a real cavity made up of mirrors. The residual losses or diffusion on these mirrors also induce a damping of the quantum states of the field.

3.6.1 Lindblad equations

The system $\mathcal{S}$ (in the terms used to discuss relaxation in Chapter 2) is a field mode at frequency ω, coupled to the environment $\mathcal{E}$. What are the possible jump operators? Assuming, reasonably, that the coupling with the environment is linear in the cavity field amplitude, there are only two possible jumps. The mode may lose a photon in the environment or gain a photon from it.

The environment simulator $\mathcal{B}$ has, accordingly, three different states, the initial one, $\left|0^{(\mathcal{B})}\right\rangle$, $\left|-^{(\mathcal{B})}\right\rangle$ and $\left|+^{(\mathcal{B})}\right\rangle$, corresponding respectively to the loss or to the gain of a photon by the cavity field. These latter states are associated to the jump operators L_- and L_+. The first, L_-, is proportional to the annihilation operator a: $L_- = \sqrt{\kappa_-}a$. The second, L_+, is proportional to the photon creation operator: $L_+ = \sqrt{\kappa_+}a^\dagger$.

We can relate the rates κ_- and κ_+ by a general thermodynamical argument, independent of the specifics of $\mathcal{E}$. Any process in which $\mathcal{S}$ loses (or gains) a quantum must be accompanied by a correlated jump of the environment in the opposite direction, a transition upwards (or downwards) on the energy ladder of $\mathcal{E}$. The probabilities for these transitions to occur are proportional to those for finding in $\mathcal{E}$ an initial state linked to a final state having with it an energy difference $\pm\hbar\omega_c$, necessary to conserve the energy of the $\mathcal{S}+\mathcal{E}$ system. A given transition in the environment will thus contribute to the gain and loss of photons in a ratio equal to the probability of finding $\mathcal{E}$ in the upper state of this transition divided by the probability of finding it in its lower state. Assuming that the environment is in thermal equilibrium at temperature T, this ratio is simply equal to $\exp(-\hbar\omega/k_bT)$ (Boltzmann law). We thus have:

$$\kappa_+ = \kappa_- e^{-\hbar\omega/k_bT} \ . \tag{3.291}$$

The relation between the loss and gain rates can be expressed in a more transparent form, by introducing the average number $n_{\rm th}$ of thermal photons per mode at frequency ω_c, given by Planck's law:

$$n_{\rm th} = \frac{1}{e^{\hbar\omega/k_bT}-1} \ . \tag{3.292}$$

Equation (3.291) can then be rewritten as:

$$\frac{\kappa_-}{\kappa_+} = \frac{1+n_{\rm th}}{n_{\rm th}} \ , \tag{3.293}$$

which leads us to define κ_- and κ_+ in term of a unique damping rate κ as:

$$\kappa_- = \kappa(1+n_{\rm th}) \ ; \qquad \kappa_+ = \kappa n_{\rm th} \ , \tag{3.294}$$

and to write the Lindblad equation for the field state ρ as:

$$\begin{aligned}\frac{d\rho}{dt} &= -i\omega_c\left[a^\dagger a,\rho\right] - \frac{\kappa(1+n_{\rm th})}{2}\left(a^\dagger a\rho + \rho a^\dagger a - 2a\rho a^\dagger\right) \\ &\quad -\frac{\kappa n_{\rm th}}{2}\left(aa^\dagger\rho + \rho aa^\dagger - 2a^\dagger\rho a\right) \ .\end{aligned} \tag{3.295}$$

The commutator term in this equation can be removed by switching to an interaction representation with respect to the field Hamiltonian, that we chose here as $H_0' = \hbar\omega a^\dagger a$ (we get rid of the vacuum energy term). The relaxation terms are not modified, since a is changed into $a\exp(-i\omega t)$ while $a^\dagger$ becomes $a^\dagger\exp(i\omega t)$.

3.6.2 Evolution of some states

Fock states

The field master equation turns into a simple rate equation for the photon number distribution $p(n) = \rho_{nn} = \langle n|\,\rho\,|n\rangle$. Using eqn. (3.295) and the action of a and $a^\dagger$ on Fock states, we obtain a closed set of equations for $p(n)$:

$$\frac{dp(n)}{dt} = \kappa(1+n_{\rm th})(n+1)p(n+1) + \kappa n_{\rm th} np(n-1) - [\kappa(1+n_{\rm th})n + \kappa n_{\rm th}(n+1)]p(n) \ . \tag{3.296}$$

The first two terms on the right-hand side describe the transitions towards the n-photons state $|n\rangle$, increasing its occupation probability. They originate either from the upper state $|n+1\rangle$, at a rate $\kappa(1+n_{\rm th})(n+1)$ or from the lower level $|n-1\rangle$, with a rate $\kappa n_{\rm th} n$. The last term describes the transition out of state $|n\rangle$, towards $|n+1\rangle$ or $|n-1\rangle$. At zero temperature, the damping rate of the Fock state $|n\rangle$ is $n\kappa$.

These rates can be used to determine the photon statistics in the steady-state solution of the master equation. We invoke a 'detailed balance argument', stating that the transfer rates from $|n\rangle$ to $|n-1\rangle$ and from $|n-1\rangle$ to $|n\rangle$ are equal when the system A ceases to evolve:

$$\kappa(1+n_{\rm th})np(n) = \kappa n_{\rm th} np(n-1) \ , \tag{3.297}$$

which leads immediately to:

$$\frac{p(n)}{p(n-1)} = \frac{n_{\rm th}}{1+n_{\rm th}} = e^{-\hbar\omega/k_b T} \ . \tag{3.298}$$

We thus find, not unexpectedly, that the mode $\mathcal{S}$ ends up in the Boltzmann equilibrium distribution at the temperature T. The average steady-state photon number is then given by Planck's law (3.292).

It is also instructive to determine how the average photon number $\langle N\rangle = \sum_n np(n)$ reaches this equilibrium. Calculating the rate $d\langle N\rangle/dt = \sum_n n\, dp(n)/dt$ with the help of eqn. (3.296) leads to:

$$\frac{d\langle N\rangle}{dt} = -\kappa(\langle N\rangle - n_{\rm th}) \ . \tag{3.299}$$

The κ coefficient is the exponential decay rate of the field mean energy towards its thermal equilibrium, a quantity which is classically denoted as ω/Q, where Q is the dimensionless mode quality factor. In spite of the obvious environment's complexity, mode relaxation depends only upon two simple dimensionless parameters, Q and $n_{\rm th}$. It is interesting to note that the damping rate of the Fock state $|n\rangle$ is n times larger than that of the energy in the mode. This is a typical decoherence effect. As illustrated by the negativities in their Wigner functions, the Fock states are non-classical. The larger they are, the more fragile with respect to the coupling with the environment.

It is very instructive to apply the quantum Monte Carlo approach to mode relaxation. We start by considering the evolution from an initial Fock state $|n\rangle$. Consider first an environment at zero temperature. The single jump operator, $L_- = \sqrt{\kappa}a$, describes the loss of a photon by the cavity mode. The non-hermitian part of the Hamiltonian describing the 'no-jump' evolution reduces to

$$H_e = -i\hbar J = -i\hbar\kappa a^\dagger a/2 \ . \tag{3.300}$$

The effective Hamiltonian is proportional to the mode one $H_0' = \hbar\omega a^\dagger a$. The no-jump evolution is thus formally obtained by setting the mode frequency at the complex value $\omega - i\kappa/2$.

During the first time interval τ, the probability of a jump is $p_1 = \tau\kappa\,\langle n|\, a^\dagger a\,|n\rangle = \kappa\tau n$, an intuitive result, which could have been guessed from eqn. (3.296). Being an eigenvector of H_0', $|n\rangle$ is also an eigenvector of the non-hermitian 'no-jump' Hamiltonian. Besides an irrelevant phase factor, the state thus does not evolve in the no-jump case. When a jump occurs, $|n\rangle$ is transformed into $|n-1\rangle$. Throughout the evolution, the mode thus remains in a Fock state, the photon number decreasing by one unit at each jump. The field energy is a staircase function of time. The jump rate is the largest at the start, when the photon number is maximum. The last photon is lost at a rate κ, which is also the classical energy damping rate.

Figure 3.7 presents simulations of a 10-photon Fock state decay. The staircase curves correspond to random individual quantum trajectories. All eventually end up in the vacuum state $|0\rangle$. The evolution of the standard deviation, ΔN, of the photon number can be guessed from these curves. Zero in the initial and final states, it reaches a maximum during the evolution. The solid line presents the evolution of the average photon number obtained from 10 000 such trajectories. It is in agreement

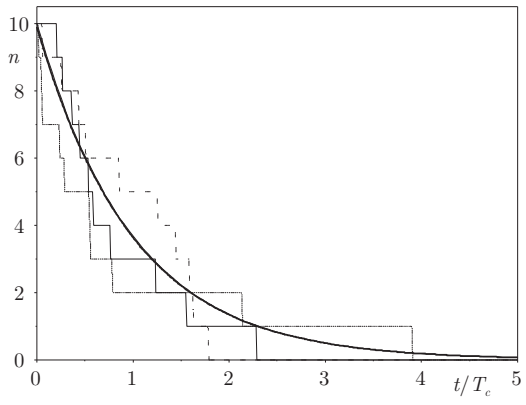

Figure 3.7: Quantum Monte Carlo simulation of a 10-photon Fock state relaxation in a $T = 0$ K environment. Photon number n as a function of time in units of the mode damping time $T_c = Q/\omega$. Thin lines (solid, dashed and dotted): three individual staircase trajectories. Thick line: average over 10 000 trajectories corresponding to the usual exponential decay.

with the exponential decay with a rate κ predicted by the density matrix approach, which cannot be distinguished from the statistical average at this scale.

For a finite environment temperature T, L_- is multiplied by $\sqrt{1+n_{\rm th}}$ and another jump operator $L_+ = \sqrt{n_{\rm th}}\kappa a^\dagger$ must be considered. The two possible jumps lower or increase the photon number by one. The field is again at any time in a Fock state, but there is no stationary final state for any trajectory. After a transient regime lasting a time $\sim 1/\kappa$ during which the average field energy adjusts to its equilibrium value, the photon number keeps jumping up and down randomly around $n_{\rm th}$.

Coherent states

Let us now describe the $T = 0$ K Monte Carlo trajectory starting from an initial coherent state $|\beta\rangle$. The properties of this trajectory, which may seem paradoxical at first sight, will explain the important features of coherent state relaxation: no entanglement with the environment and exponential decay of the field amplitude.

The probability for counting a photon in the first time interval is $p_1 = \kappa\tau\langle\beta|a^\dagger a\,|\beta\rangle = \kappa\tau|\beta|^2 = \kappa\tau\overline{n}$. If a photon is counted, the state is unchanged since $|\beta\rangle$ is an eigenstate of the jump operator $L_- = \sqrt{\kappa}a$. An evolution occurs, on the contrary, if no photon is recorded in this time bin. The imaginary frequency contribution to the effective Hamiltonian produces a decrease of the state complex amplitude, the field evolving, in the interaction picture with respect to its free Hamiltonian, according to:

$$|\beta\rangle \rightarrow \left|\beta e^{-\kappa\tau/2}\right\rangle \ . \tag{3.301}$$

This situation is quite paradoxical, since the field's state amplitude decreases only if no photon is recorded! How is this possible? First of all, how comes that the state does not change when we are sure that one photon has been lost? We have here the combination of two effects, which tend to change the photon number in opposite directions. On the one hand, the loss of a quantum reduces the average energy in the cavity. On the other hand, the registration of a photon click modifies our knowledge about the state in which the field was just before the photon was emitted, corresponding to an increase by precisely one unit of the photon number expectation at this time.

To understand this point, let us ask a question whose answer is a simple exercise in conditional probabilities: knowing the *a priori* Poissonian photon number distribution $p(n) = e^{-\overline{n}}\overline{n}^n/n!$ (centred at $n = \overline{n}$ at time t) *and* that a photon has been lost and detected as a 'click' c in the time interval $(t, t+\delta t)$, what is the *conditional* probability $p(n|c)$ that the field mode contained n photons at time

t? If the photon emission probability were n-independent, $p(n|c)$ would merely be equal to $p(n)$. The probability of losing a photon is however proportional to the expectation value of $a^\dagger a$, hence to n. Detecting a photon has thus the effect of shifting the probability distribution towards larger $n's$, since the corresponding states are more likely to lose quanta.

This result can be made quantitative by invoking Bayes law on conditional probabilities. The probability we seek, $p(n|c)$, is related to the reverse conditional probability $p(c|n)$ of detecting a click during the same time interval, *conditioned* to the prior existence of n photons. This probability is obviously $p(c|n) = \kappa n \delta t$. It is slightly different from the *a priori* probability $p_c = \kappa \overline{n} \delta t$ of detecting a click when the field is in the coherent state, a superposition of n states around the mean $\overline{n}$. We can then relate $p(n|c)$ and $p(c|n)$ by expressing in two different ways the *joint probability* $p(n, c)$ that a click is detected during the considered time interval *and* that the field contains n photons:

$$p(n, c) = p(c|n)p(n) = p(n|c)p_c \ , \tag{3.302}$$

which yields immediately the Bayes law result:

$$p(n|c) = p(n)\frac{p(c|n)}{p_c} = \frac{n}{\overline{n}}p(n) = e^{-\overline{n}}\frac{\overline{n}^{n-1}}{(n-1)!} = p(n-1) \ . \tag{3.303}$$

This formula shows that $p(n|c)$ is precisely equal to the *a priori* probability that the initial field contains $n-1$ photons. The maximum of $p(n-1)$, hence of $p(n|c)$, occurs for $n = \overline{n} + 1$. The knowledge that a click has occurred biases the photon number distribution before this click towards larger n values, with a photon number expectation exceeding the *a priori* average value by exactly one unit. The loss of the photon signalled by the click brings this number back down to $\overline{n}$. The two effects exactly cancel each other and the state of the field has not changed!

This is a very peculiar property of coherent states, a consequence of their Poissonian photon number distribution. For non-Poissonian fields with larger fluctuations, this effect could be even more counter-intuitive and result in an overall increase of the photon expectation number, just after the loss of a photon! We leave the reader to construct a photon number distribution leading to such a situation. Note finally that this counter-intuitive increase of the field energy upon loss of photons requires the existence of fluctuations in the initial energy distribution. The effect does not occur for a Fock state which jumps down the energy ladder at each click and loses its energy in a perfectly intuitive way.

We have now to understand the other side of the coherent state evolution paradox. Why are they decreasing in amplitude precisely during the time intervals when no photon clicks are registered? We have already encountered the same effect (continuous quantum state evolution without jump) when analysing the spontaneous emission of a single atom in a superposition of its emitting and non-emitting states. It is here again a matter of conditional probability. If no photon is detected in a time interval, it is more likely that the photon distribution has less photons that was *a priori* assumed.

To consider an extreme situation, a coherent field has a small probability, equal to $e^{-\overline{n}}$, to contain no photon at all. This is the probability that the detector will never click, however long one waits. The longer the time interval t without click, the more likely it becomes that the field is effectively in vacuum. Its wave function evolves continuously without jump under the effect of the non-hermitian operator $1 - i\kappa a^\dagger a/2$. If t becomes very long, the field ends up effectively in $|0\rangle$. This seems counter-intuitive, but we must not forget that this event has a very small probability of occurring. This example is once again a striking illustration of an important aspect of measurement theory. Even the absence of a click is information whose knowledge affects the wave function of the field.

In Monte Carlo simulations, the randomness is generated only by the jumps. The evolution between the jumps is continuous and deterministic. The insensitivity of a coherent state to jumps makes its Monte Carlo trajectory certain. To determine the state at time t of a field initially in state $|\beta\rangle$, we have to piece together its partial evolutions during the successive intervals between jumps t_1,

$t_2, \ldots, t_i, \ldots, t_N$ adding up to t. Whatever the distribution of these intervals, the final state is uniquely defined, in the interaction picture, as $\left|\beta e^{-\kappa(t_1+t_2+....+t_N)/2}\right\rangle = \left|\beta e^{-\kappa t/2}\right\rangle$. The field state remains pure, as already indicated by eqn. (3.301).

Chapitre 4

Coupling quantum field to matter

This Chapter completes our program. We now have quantum atoms and a quantum description of the field and we will couple these two systems. In a first Section of the Chapter, we will give the coupling Hamiltonians of charges with a quantum field in some simple situations. We will study the case of a classical macroscopic current and show that classical sources produce the most classical states, the coherent states of the field. We shall then give the general Hamiltonian coupling a quantum atom to the quantum field.

The next Section will be devoted to spontaneous emission. We will be able to compute from the first principles the spontaneous emission rate, through two complementary approaches. We will also touch the level shifts problems. The divergence of the Lamb shift is a clear indication that our simple approach to field quantization should be supplemented, for some problems, by the full renormalization of QED. Nevertheless, our approach leads to interesting results in simple cases.

The third Section will be devoted to a model of a field detector, an essential component in any quantum optics experiment. We will use this model to revisit some fundamental experiments, such as the intensity correlations observed for the first time by Hanbury-Brown and Twiss.

The final Section of this Chapter will be devoted to an in-depth description of Cavity Quantum Electrodynamics. This very active domain pushes the matter-field coupling to its simplest limits, with a single atom coupled to a single field mode containing a few photons. All the difficulties of the multi-mode problems disappear. The dynamics, in spite of being highly non-trivial, can be explicitly calculated and checked experimentally. The domain has provided a few key illustrations of quantum physics that we will shortly describe.

4.1 Interaction Hamiltonians

4.1.1 Quantum field and classical charges

We start by a short description of the last semi-classical model in these lectures. Instead of considering a quantum atom coupled to a classical field, we treat here the case of a quantum field coupled to a classical oscillating current, made of so many elementary charges that all its quantum features can be neglected. We write this current:

$$\mathbf{j}(\mathbf{r},t) = \mathbf{j}_0(\mathbf{r})e^{-i\omega_0 t} \ , \tag{4.1}$$

where the amplitude $\mathbf{j}_0$ may be complex.

We couple this current to all field modes. We will remove from the field Hamiltonian the constant energy offset of the vacuum state (we remove here an infinite quantity out of the Hamiltonian, but this is not a problem since we will treat separately all modes at the end).

The field Hamiltonian is thus

$$H_0' = \sum_\ell \hbar\omega_\ell a_\ell^\dagger a_\ell \ , \tag{4.2}$$

where we use a prime to distinguish it from the Hamiltonian including the vacuum energy contribution.

The classical interaction energy of the current with the field is the integral over all the space of the scalar product $-\mathbf{j}\cdot\mathbf{A}$ of the current with the vector potential. We will extend this and write the interaction Hamiltonian H_i as

$$H_i = -\int_{\mathcal{V}} \mathbf{j}(\mathbf{r},t)\cdot\mathbf{A}(\mathbf{r},t)\,d^3\mathbf{r}\ , \tag{4.3}$$

where

$$\mathbf{A}(\mathbf{r},t) = \sum_\ell \sqrt{\frac{\hbar}{2\epsilon_0\omega_\ell\mathcal{V}}}a_\ell\mathbf{f}_\ell(\mathbf{r}) + \text{c.c.}\ . \tag{4.4}$$

Note that all the dependence in $\mathbf{r}$ is in the classical parts of the vector potential. The interaction Hamiltonian is thus a combination of a_ℓ and $a_\ell^\dagger$ operators in the field's Hilbert space.

Before proceeding further, we will get rid of the free evolution of the modes by switching to an interaction representation with respect to H_0'. The state vector is then:

$$\left|\widetilde{\Psi}\right\rangle = U_0^\dagger\left|\Psi\right\rangle\ , \tag{4.5}$$

with

$$U_0 = e^{-iH_0't/\hbar}\ , \tag{4.6}$$

which factors in independent operators on each modes:

$$U_0 = \prod_\ell e^{-i\omega_\ell t a_\ell^\dagger a_\ell} \tag{4.7}$$

The new Hamiltonian is

$$\widetilde{H} = U_0^\dagger H_i U_0\ . \tag{4.8}$$

To get the Hamiltonian in the interaction representation, we need first to transform a_ℓ, a simple task since all modes transform independently:

$$\begin{aligned}\widetilde{a}_\ell &= e^{i\omega_\ell t a_\ell^\dagger a_\ell}a_\ell e^{-i\omega_\ell t a_\ell^\dagger a_\ell}\\ &= a_\ell - i\omega_\ell t a_\ell + \frac{(i\omega_\ell t)^2}{2}a_\ell + \dots\\ &= a_\ell e^{-i\omega_\ell t}\ ,\end{aligned} \tag{4.9}$$

where we have used the Baker Hausdorff Lemma and the fact that $[N_\ell, a_\ell] = -a_\ell$.

We inject that in the interaction Hamiltonian and get

$$\widetilde{H} = -\int d^3\mathbf{r}\,\left[\mathbf{j}_0(\mathbf{r})e^{-i\omega_0 t} + \mathbf{j}_0^*(\mathbf{r})e^{i\omega_0 t}\right]\cdot\left[\sum_\ell\sqrt{\frac{\hbar}{2\epsilon_0\omega_\ell\mathcal{V}}}\left(a_\ell e^{-i\omega_\ell t}\mathbf{f}_\ell(\mathbf{r}) + a_\ell^\dagger e^{i\omega_\ell t}\mathbf{f}_\ell^*(\mathbf{r})\right)\right]\ . \tag{4.10}$$

Obviously, we consider here only positive frequencies ω_ℓ and ω_0. The action of the current on the mode will be notable only if $\omega_\ell \approx \omega_0$. We can thus neglect all modes which are not close of the current frequency. For the remaining ones, we can again perform a variant of the rotating-wave approximation (RWA) by keeping in $\widetilde{H}$ only the terms evolving at slow frequencies and discarding those evolving close to $2\omega_0$. With this approximation and performing the integrals, we get finally:

$$\widetilde{H} = -\sum_\ell\sqrt{\frac{\hbar\mathcal{V}}{2\epsilon_0\omega_\ell}}J_0 a_\ell^\dagger e^{-i(\omega_0-\omega_\ell)t} + \text{h.c.}\ , \tag{4.11}$$

where the complex scalar J_0 is defined as:

$$J_0 = \frac{1}{\mathcal{V}}\int d^3\mathbf{r}\,\mathbf{j}_0(\mathbf{r})\cdot\mathbf{f}_\ell^*(\mathbf{r})\ . \tag{4.12}$$

Note that we have defined J_0 so that it has the dimension of a current density ($\mathbf{f}_\ell$ is dimensionless).

Since $\widetilde{H}$ is a sum of independent Hamiltonians for each mode, we can treat the dynamics of each mode separately. We will thus follow a single one and drop the mode index ℓ. Setting

$$K_0 = \sqrt{\frac{\hbar\mathcal{V}}{2\epsilon_0\omega}} J_0 \tag{4.13}$$

we can write the Hamiltonian in the simpler form

$$\widetilde{H} = -K_0 e^{-i\delta t} a^\dagger + \text{h.c.} \ , \tag{4.14}$$

where

$$\delta = \omega_0 - \omega \ , \tag{4.15}$$

is the detuning between the source and the mode.

We now compute the evolution under this Hamiltonian, starting from the initial vacuum state. It is important to note that the $\widetilde{H}$s taken at different times are non-commuting operators. The evolution operator is thus not simply the exponential of the integral of the Hamiltonian.

To cope with this problem, we consider the elementary evolution operator from time t to time $t + dt$. During this short time interval, the Hamiltonian can be taken as:

$$\widetilde{H} = -K_0 e^{-i\Phi} a^\dagger + \text{h.c.} \ , \tag{4.16}$$

where

$$\Phi = \delta t \ . \tag{4.17}$$

The elementary evolution operator $U(t, dt)$ is the exponential of this Hamiltonian, and is clearly of the form $\exp(\alpha a^\dagger - \alpha^* a)$, a displacement operator with the infinitesimal complex amplitude:

$$\alpha = \frac{iK_0}{\hbar} e^{-i\Phi} dt \ . \tag{4.18}$$

The total evolution operator is the product of all these elementary displacements. The product of two displacements is, within a phase, the displacement corresponding to the total displacement. Within a global phase (that we leave to the reader as an exercise), the final state at time t is thus a coherent state with an amplitude β:

$$\beta = \int_0^t \frac{iK_0}{\hbar} e^{-i\delta t'} \, dt' = -\frac{K_0}{\hbar\delta} \left[e^{-i\delta t} - 1 \right] \ . \tag{4.19}$$

When $\delta \neq 0$, the amplitude β propagates in phase space along a circle, a simple result. The field amplitude periodically goes back to zero, an reaches a maximum amplitude for $\delta t = k\pi$, where k is an odd integer. This periodic excitation and de-excitation of the field mode is a typical beating phenomenon.

The situation is different when $\delta = 0$. In this case, the amplitude β evolves linearly with time according to:

$$\beta = \frac{iK_0}{\hbar} t \ . \tag{4.20}$$

The number of photons in the mode, $|\beta|^2$ evolves quadratically. This runaway process is a direct consequence of the bosonic nature of the photons. The more photons in the field, the easier to add some new ones.

We have thus shown in this paragraph that a classical source produces a coherent state in each of the modes it is coupled to. These states are thus rather easily produced, be it with electronic oscillators in the radio-frequency domain or with lasers in the optical domain.

4.1.2 Quantum field and quantized atom

Writing the interaction Hamiltonian of a quantized atom with a quantized field is quite easy. We just replace in the different forms of the semi-classical Hamiltonian (obtained in the dipole approximation regime and neglecting the non-linear terms in the field) the fields or potentials by their classical counterparts.

We will use either

$$H_{ap} = -\frac{q}{m}\mathbf{P}\cdot\mathbf{A}(0)\ , \tag{4.21}$$

or

$$H_{de} = -\mathbf{D}\cdot\mathbf{E}(0)\ . \tag{4.22}$$

More specifically,

$$\mathbf{D} = d\boldsymbol{\epsilon}_d\left|g\right\rangle\left\langle e\right| + \text{h.c.}\ , \tag{4.23}$$

where d is the (possibly complex) dipole matrix element and ϵ_d a unit vector describing the polarization of the atomic transition. The electric field at the origin (where the atom is assumed to be located) is

$$\mathbf{E}(0) = i\sum_\ell \sqrt{\frac{\hbar\omega_\ell}{2\epsilon_0\mathcal{V}}}a_\ell\boldsymbol{\epsilon}_\ell + \text{h.c.}\ , \tag{4.24}$$

where we have used here for instance the plane wave mode expansion.

Developing the $\mathbf{D}\cdot\mathbf{E}$ scalar product, we find four types of terms. Two of them involve the operator $\sigma_- a^\dagger$ and its conjugate. They describe processes in which the atom gets excited (de-excited) while absorbing (emitting) a single photon. The two other types of terms involve $\sigma_+ a^\dagger$ and its conjugate. They correspond thus to counter-intuitive processes in which the atom gets excited while emitting a photon.

When the atom-field coupling is not too large, and for modes whose frequency is close to that of the atomic transitions, the two latter terms can be safely neglected. This is yet another variant of the Rotating Wave Approximation.

4.2 Spontaneous emission in free space

We apply first these Hamiltonians to the calculation of the spontaneous emission rate. We consider a single two-level atom initially in its upper state $|e\rangle$. The atom, coupled to the set of modes of a large (virtual) quantization box emits a photon when jumping in the ground state $|g\rangle$ (the $|e\rangle \to |g\rangle$ transition is at frequency ω_0).

We will use two complementary approaches to derive the spontaneous emission rate; The first, semi-qualitative one, makes use of a Fermi Golden Rule expression. The second, more detailed and predictive, reproduces the first calculations of Wigner and Weisskopf. It also puts in evidence the underlying difficulty of the diverging light shifts.

4.2.1 Fermi Golden Rule

We use the electric dipole form of the Hamiltonian. The field is expanded on the plane wave modes, in a very large quantization box. The initial state is $|e,0\rangle$ (atom in the upper state and no photon), the final state is obviously $|g,1_\ell\rangle$ (atom in the ground state with one photon in the mode indexed by ℓ. We have a discrete initial state coupled by the H_{de} Hamiltonian to a continuum of final states. The Fermi Golden Rule tells us that the evolution is irreversible, exponential, and proceeds at a rate proportional to the square of the coupling Hamiltonian matrix element times the density of final states.

The orientation of the outgoing photons will be important to compute the scalar products of the atomic and field polarization in the Hamiltonian. We must thus treat separately all final photon

directions. We assume that the quantization box is so large that there are still infinitely many modes with a wavevector pointing in a small solid angle $d\Omega$. Obviously, in the Fermi Golden Rule situation, the emission in separate sets of modes just add independently. We will thus add up the emission rates in all solid angles $d\Omega$. We should take care that, in $d\Omega$, all modes have nearly the same direction of propagation, but have two different possible polarizations (linear polarizations if we take linearly polarized mode basis).

We can thus write the spontaneous emission rate Γ as

$$\Gamma = \int d\Gamma d\Omega \ , \tag{4.25}$$

where $d\Gamma$ is the rate corresponding to an emission in $d\Omega$. It is given by the Fermi Golden Rule:

$$d\Gamma = \sum_{\boldsymbol{\epsilon}_\ell} \frac{2\pi}{\hbar} |W|^2 d\rho(E = \hbar\omega_0, d\Omega) \ , \tag{4.26}$$

where W is the coupling Hamiltonian matrix element and $d\rho$ the density of states in the solid angle $d\Omega$ at the atomic transition energy (the density of sates should be in energy terms for the Fermi Golden rule) and the sum runs over the two possible polarizations in this solid angle.

Let us first evaluate the density of states $d\rho$. An isotropy argument leads immediately to $d\rho = \rho d\Omega/4\pi$, where ρ is the total density of states per unit energy. We have already computed, in the first Section of the previous Chapter, the density of states in units of frequency[1]

$$\rho(\nu) = \frac{8\pi}{2c^3} \mathcal{V} \nu^2 d\nu \ . \tag{4.27}$$

Writing $\rho(E)dE = \rho(\nu)d\nu$ for $E = h\nu = \hbar\omega_0$, we arrive at

$$\rho(E) = \frac{\mathcal{V}}{2\pi^2 c^3} \frac{1}{\hbar} \left(\frac{E}{\hbar}\right)^2 \ , \tag{4.28}$$

and hence finally at

$$d\rho(E = \hbar\omega_0, d\Omega) = \frac{\mathcal{V}}{8\pi^3} \frac{\omega_0^2}{\hbar c^3} d\Omega \ . \tag{4.29}$$

Let us now evaluate the coupling term:

$$|W|^2 = |\left\langle g, 1_\ell \right| \mathbf{D} \cdot \mathbf{E} \left| e, 0 \right\rangle|^2 \ . \tag{4.30}$$

In order to simplify a bit the algebra, and without real loss of generality, we will set in this expression:

$$\boldsymbol{\epsilon}_d = \mathbf{u}_z \ , \tag{4.31}$$

i.e. we will use a linearly polarized atomic transition. Keeping only the RWA terms, the only term in the interaction Hamiltonian coupling the two states is that involving a and σ_+. Hence

$$|W|^2 = \left| d\mathbf{u}_z \cdot \boldsymbol{\epsilon}_\ell^* \sqrt{\frac{\hbar\omega_\ell}{2\epsilon_0 \mathcal{V}}} \right|^2 \ . \tag{4.32}$$

We can now fully evaluate $d\Gamma$ and we find, using $\omega_\ell = \omega_0$:

$$d\Gamma = \sum_{\boldsymbol{\epsilon}_\ell} \frac{1}{8\pi^2 \epsilon_0} \frac{\omega_0^3}{c^3} \frac{|d|^2}{\hbar} |\mathbf{u}_z \cdot \boldsymbol{\epsilon}_\ell^*|^2 d\Omega \ . \tag{4.33}$$

[1]Note that we use here a total density of states, not a volumic density (hence the factor $\mathcal{V}$. Moreover, we have a factor of two less than in the Planck's law calculation, since we will perform the sum over the two orthogonal polarizations later.

Calling $\boldsymbol{\epsilon}_1$ and $\boldsymbol{\epsilon}_2$ the two linear (hence real) orthogonal polarizations, we can expand $\mathbf{u}_z$ on the basis of these vectors, together with the unit vector in the direction of propagation, $\mathbf{u_k}$. Since all these vectors are unit vectors, we get

$$(\mathbf{u}_z \cdot \boldsymbol{\epsilon}_1^*)^2 + (\mathbf{u}_z \cdot \boldsymbol{\epsilon}_2^*)^2 = 1 - (\mathbf{u}_z \cdot \mathbf{u_k})^2 = 1 - \cos^2\theta = \sin^2\theta \ , \tag{4.34}$$

where the solid angle $d\Omega$ is defined by the spherical coordinates angles θ and ϕ.

We can now write the total emission rate by integrating over all solid angles:

$$\Gamma = \frac{1}{8\pi^2\epsilon_0}\frac{\omega_0^3}{c^3}\frac{|d|^2}{\hbar}\int_0^{2\pi}\int_0^{\pi} \sin^3\theta \, d\theta d\phi \tag{4.35}$$

The angular intergral is easy and simplifies to $8\pi/3$. We thus get the very important result, already announced a few times in these lecture notes:

$$\Gamma = \frac{\omega_0^3 |d|^2}{3\pi\omega_0\hbar c^3} \ . \tag{4.36}$$

4.2.2 Wigner-Weisskopf

We now give the more detailed Wigner-Weisskopf approach. It starts of course from the same hypotheses, but does not make use of the Fermi Golden rule. Instead, we shall write the explicit dynamics of the atom-field system in the Schrödinger picture. At time t, the complete state can be expanded as

$$|\Psi(t)\rangle = c_0(t)\,|e,0\rangle + \sum_\ell c_\ell(t)\,|g,1_\ell\rangle \ . \tag{4.37}$$

Letting

$$V_\ell = -\langle e,0|\,\mathbf{D}\cdot\mathbf{E}\,|g,1_\ell\rangle \ , \tag{4.38}$$

we can put the Schrödinger equation for $|\Psi\rangle$ under the form of an infinite set of coupled linear differential equations:

$$i\hbar\frac{dc_0}{dt} = \hbar\omega_0 c_0 + \sum_\ell V_\ell c_\ell \tag{4.39}$$

$$i\hbar\frac{dc_\ell}{dt} = \hbar\omega_\ell c_\ell + V_\ell^* c_0 \ , \tag{4.40}$$

with the initial conditions $c_0 = 1$, $c_\ell = 0$. We can formally integrate the second equation. Setting

$$b_\ell = c_\ell e^{i\omega_\ell t} \ , \tag{4.41}$$

we get the equation for b_ℓ as

$$i\hbar\frac{db_\ell}{dt} = e^{i\omega_\ell t}V_\ell^* c_0 \ , \tag{4.42}$$

and hence

$$b_\ell(t) = \frac{V_\ell^*}{i\hbar}\int_0^t c_0(t')e^{i\omega_\ell t'}\,dt' \tag{4.43}$$

or

$$c_\ell(t) = \frac{V_\ell^*}{i\hbar}\int_0^t c_0(t')e^{i\omega_\ell(t'-t)}\,dt' \tag{4.44}$$

We can inject this formal solution in the equation for c_0 and get rid of the simple term $-i\omega_0 c_0$ by setting

$$c_0 = e^{-i\omega_0 t}\alpha_0(t) \ . \tag{4.45}$$

We get

$$\frac{d\alpha_0}{dt} = -\sum_\ell \frac{|V_\ell|^2}{\hbar^2} e^{i\omega_0 t} \int_0^t e^{i\omega_\ell (t'-t)} e^{-i\omega_0 t'} \alpha_0 \, dt' \ . \tag{4.46}$$

Changing for the variable $\tau = t - t'$, we get

$$\frac{d\alpha_0}{dt} = -\int_0^t \mathcal{N}(\tau)\alpha(t-\tau)\, d\tau \ , \tag{4.47}$$

where the integral kernel $\mathcal{N}$ is:

$$\mathcal{N}(\tau) = \frac{1}{\hbar^2} \sum_\ell |V_\ell|^2 e^{i(\omega_0 - \omega_\ell)\tau} \ . \tag{4.48}$$

Using now the expression of the coupling Hamiltonian, we can make V_ℓ explicit as in the previous paragraph and get:

$$\mathcal{N}(\tau) = \frac{|d[^2}{\hbar^2} \left[\sum_\ell |\mathbf{u}_z \cdot \boldsymbol{\epsilon}_\ell|^2 \frac{\hbar\omega_\ell}{2\epsilon_0 \mathcal{V}} e^{-i\omega_\ell \tau} \right] e^{i\omega_0 \tau} \ . \tag{4.49}$$

It is quite clear from this expression than $\mathcal{N}(\tau)$ decays very rapidly versus τ. The sum over all the modes involves terms of similar orders of magnitude and vastly different frequencies, which very rapidly come out of phase with each other. In a time of the order of $1/\omega_0$, $\mathcal{N}$ practically vanishes. For all practical purposes, it can be considered as being proportional to a Dirac distribution. This is the Markov approximation, which holds as long as the reservoir has a wide enough spectrum to have basically a zero memory time.

Thus:

$$\int_0^t \mathcal{N}(\tau)\alpha(t-\tau)\, d\tau \approx \alpha_0(t) \int_0^\infty \mathcal{N}(\tau)\, d\tau = \left(\frac{\Gamma}{2} + i\Delta \right) \alpha_0(t) \ . \tag{4.50}$$

The equation of evolution of α_0 (remember than $\alpha - 0$ is, within a phase, identical to c_0 and thus that $|\alpha_0|^2$ is the probability for finding the system in its initial state) is thus:

$$\frac{d\alpha_0}{dt} = -\left(\frac{\Gamma}{2} + i\Delta \right) \alpha_0 \ . \tag{4.51}$$

In this equation, Γ clearly appears as the spontaneous emission rate and Δ as a frequency shift of the atomic transition.

The solution of this equation is obvious and, returning to the original coefficients, we finally find

$$c_0(t) = e^{-\Gamma t/2} e^{-i\omega_0 t} e^{-i\Delta t} \ , \tag{4.52}$$

and, injecting that in the formal solution of the equation for c_ℓ:

$$c_\ell(t) = \frac{V_\ell}{i\hbar} \frac{1 - e^{-\Gamma t/2} e^{i(\omega_\ell - \omega_0 - \Delta)t}}{(\Gamma/2) - i(\omega_\ell - \omega_0 - \Delta)} \ . \tag{4.53}$$

Taking the square modulus of this coefficient in the limit of large times:

$$|c_\ell|^2 = \frac{|V_\ell|^2}{\hbar^2} \frac{1}{(\Gamma^2/4) + (\omega_\ell - \omega_0 - \Delta)^2} \ , \tag{4.54}$$

we get the final probability for having a photon in mode ℓ i.e. the spectrum of the spontaneous emission. Not surprisingly, we find a Lorentzian spectrum with a width Γ centred at the atomic frequency ω_0 shifted by Δ.

The last step to complete the calculation is thus to integrate the kernel $\mathcal{N}$ and to find its real and imaginary parts. We get:

$$\left(\frac{\Gamma}{2}+i\Delta\right)=\frac{|d|^2}{\hbar^2}\sum_\ell(\mathbf{u}_z\cdot\boldsymbol{\epsilon}_\ell)^2\frac{\hbar\omega_\ell}{2\epsilon_0\mathcal{V}}\int_0^\infty e^{i(\omega_0-\omega_\ell)\tau}\,d\tau\ . \tag{4.55}$$

Using the distribution identity

$$\int_0^\infty e^{i\omega t}\,dt=\pi\delta(t)+i\mathcal{P}\mathcal{P}\frac{1}{\omega}\ , \tag{4.56}$$

we can separate easily the Γ and Δ parts.

For Γ , we get

$$\Gamma=\frac{2\pi|d|^2}{\hbar^2}\sum_\ell(\mathbf{u}_z\cdot\boldsymbol{\epsilon}_\ell)^2\frac{\hbar\omega_\ell}{2\epsilon_0\mathcal{V}}\delta(\omega_0-\omega_\ell)\ , \tag{4.57}$$

which is exactly the expression of the Fermi golden rule if we replace the sum by an integral over a density of modes. We leave it to the reader to check the exact identity with the result of the previous paragraph.

What about Δ now? We will not enter into the details, but the calculation merely diverges, due in particular to the contribution of the infinite frequency modes. The atomic transitions should be shifted by an infinite amount, a quite non-physical result.

This problem plagued the early days of quantum electrodynamics. The solution cam rather late, during the Shelter island congress of 1947. Lamb had experimentally observed the slight shift between the energies of the $2S$ and $2P$ levels. This shift results from the coupling to the vacuum modes. Computing it was thus a really important problem. It implied the development of renormalization theory.

We will not treat it here of course. Suffice it to say that it provides a consistent way to compute finite energy level shifts. We can nevertheless continue our exploration of the atom-field coupling. Most interesting phenomena, be it only the spontaneous emission, rely on the coupling with a few nearly resonant modes. For these processes, the infinitely many high frequency modes play no role. We can thus simply take into account the effect of these modes as (measurable) shifts of the energy levels and compute the finite effect of the resonant modes without any mathematical problem.

4.3 Photodetection

Photodetection is a key ingredient in quantum optics. After all, any quantum optics experiment finally ends up in detecting photons. We propose in this Section a simple model of a photodetector and apply it to some interesting quantum experiments, such as the Hanbury-Brown and Twiss intensity correlations.

4.3.1 Photodetector model

We need to model a broadband photodetector, such as a photomultiplier or a photodiode. It is quite clear that a two-level atom will not do. We thus consider instead a system with a ground state $|g\rangle$ and a continuum of excited states $|e_i\rangle$, coupled to the ground state by electric dipole transitions. We consider that the detector has 'clicked' when it has made a transition from its lower state to any of its excited states. Note that our model, though simple, is a rather good description of a detector based on photo-ionisation.

The detector Hamiltonian is:

$$H_d=\sum_i\hbar\omega_i\,|e_i\rangle\langle e_i|\ , \tag{4.58}$$

where ω_i is the transition frequency from $|g\rangle$ to $|e_i\rangle$. The detector-field coupling H_i is the $-\mathbf{D}\cdot\mathbf{E}$ Hamiltonian, where, with a simple generalization of the two-level model:

$$\mathbf{D} = \sum_i d_i(\boldsymbol{\epsilon}_i |g\rangle\langle e_i| + \boldsymbol{\epsilon}_i^* |e_i\rangle\langle g|) \ . \tag{4.59}$$

We are interested here in the qualitative behaviour of the model. We will thus neglect most of the factors and keep only the essentially important terms. We can thus rewrite the interaction Hamiltonian as:

$$H_i = \sum_i \kappa_i |e_i\rangle\langle g| E^+ + \text{h.c.} \ , \tag{4.60}$$

where E^+ is the positive frequency part of the proper polarization component of the electric field. The factor κ_i encapsulates the dipole matrix elements and all numerical factors. We assume here, for the sake of simplicity, that the detector system is located at the origin.

We switch now to an interaction representation with respect to the detector and field free Hamiltonians. This interaction representation amounts simply into replacing $|e_i\rangle\langle g|$ by $\exp(i\omega_i t)|e_i\rangle\langle g|$ and all the a_ℓ operators in E^+ by $a_\ell \exp(-i\omega_\ell t)$, making E^+ a time-dependent operator. Finally, the Hamiltonian reduces in this interaction representation to

$$\widetilde{H}_i = \sum_i \kappa_i e^{i\omega_i t} |e_i\rangle\langle g| E^+(t) + \text{h.c.} \ , \tag{4.61}$$

We now write the Schrödinger equation for the sate vector of the detector+field system and solve it with the initial condition

$$|\Psi(0)\rangle = |g\rangle \otimes |\Psi_f\rangle \ , \tag{4.62}$$

where $|\Psi_f\rangle$ is the field state to detect. The formal solution of the evolution equation is

$$|\Psi(t)\rangle = |g\rangle \otimes |\Psi_f\rangle + \frac{1}{i\hbar}\int_0^t \widetilde{H}_i(t')|\Psi(t')\rangle \, dt' \ . \tag{4.63}$$

We cannot solve this integro-differential equation, but we can find a perturbative solution at the first order in the field-detector coupling. We assume that the time is short enough so that the detector is still mainly in state $|g\rangle$ and replace, in the integral, $|\Psi(t')\rangle$ by $|\Psi(0)\rangle = |g\rangle \otimes |\Psi_f\rangle$.

Noting furthermore that, in $\widetilde{H}_i$, the $|g\rangle\langle e_i| E^-$ part gives zero when applied to the initial state, we have

$$|\Psi(t)\rangle = |g\rangle \otimes |\Psi_f\rangle + \frac{1}{i\hbar}\sum_i \kappa_i \left[\int_0^t dt' \, e^{i\omega_i t'} E^+(t')|\Psi_f\rangle\right] \otimes |e_i\rangle \ . \tag{4.64}$$

The probability p_e for having observed a 'count' at time t is simply:

$$p_e = \sum_i |\langle e_i|\Psi\rangle|^2 = \sum_i \langle\Psi|e_i\rangle\langle e_i|\Psi\rangle \ . \tag{4.65}$$

Injecting in this expression the first-order solution of the Schrödinger equation, we get:

$$p_e = \frac{1}{\hbar^2}\sum_i |\kappa_i|^2 \int_0^t dt' \int_0^{t'} dt'' \, e^{i\omega_i(t'-t'')} \langle\Psi_f| E^-(t'')E^+(t')|\Psi_f\rangle \ . \tag{4.66}$$

For a high enough density of states (this is certainly the case for any practical detector) the sum over the final states can be replaced by an integral with the introduction of a density of states:

$$\sum_i \longrightarrow \int d\omega \rho(\omega) \ . \tag{4.67}$$

The relevant levels for the detector are nearly resonant with the incoming field. In this narrow spectral region, we can furthermore assume that the coupling κ, a priori a function of ω is nearly constant.

The double integral giving p_e contains then an integral over the final state frequency:

$$\int d\omega e^{i\omega(t'-t'')} = \pi\delta(t'-t'') \ . \tag{4.68}$$

Only one time integral is left and we finally arrive at

$$p_e(t) \propto \int_0^t dt' \ \langle\Psi_f| \, E^-(t')E^+(t') \, |\Psi_f\rangle \ . \tag{4.69}$$

If we consider now a detector made of very many such systems (located at the same point of course), the 'intensity' of the signal, I, is proportional to dp_e/dt. Hence, the 'photocurrent' is:

$$I(t) = \langle\Psi_f| \, E^-(t)E^+(t) \, |\Psi_f\rangle \ . \tag{4.70}$$

The detected signal is proportional at any time to the average value of the E^-E^+ term in the field state, a very simple result, quite compatible with the expectations from classical photodetection theory (intensity proportional to the square modulus of the field). Note also that the field operator product is here in the normal order (involving the photon number operator $a^\dagger a$), so that the vacuum field corresponds to a zero detected intensity.

4.3.2 Intensity correlations

The interference effects are not limited to the classical (or quantum) addition of the field amplitudes. They can also be directly evidenced on the intensity of the photodetection signal itself, even if the fields are treated in the classical formalism. The realization of this fact by Hanbury-Brown and Twiss has first provided an interesting method for high resolution astronomy, but is has also played a key role in the development of quantum optics, since the intensity correlation signal directly reveals the statistical properties of the quantum state.

Classical Hanbury-Brown and Twiss experiments

We shall first consider a simpler version of the HBT experiment which provides without calculations an insight into the intensity correlations already in the classical field domain.

The classical light produced by a source is split in two equal parts by a beamsplitter and sent to two detectors recording the intensity. The source may be for instance a spectral lamp emitting trains of exponentially damped field pulses, with a correlation time τ_c. A system records the intensities $I_1(t)$ and $I_2(t)$ and computes their correlation function:

$$G_2(\tau) = \overline{I_1(t)I_2(t+\tau)} \ , \tag{4.71}$$

where the overline describes an average over a long time period or over very many realizations. The correlation function G_2 is independent of t if we make the hypothesis of a stationary phenomenon. If we think, for a short while, in terms of photons, G_2 is proportional to the probability for detecting a photon at $t+\tau$ knowing that a photon has been detected at t. The (for the time being) classical correlation function gives thus a detailed insight into the field statistical properties.

For a very large time difference τ, the signals recorded by the two detectors are independent, since the source has a short memory time τ_c. Hence,

$$G_2(\infty) = (\overline{I})^2 \ , \tag{4.72}$$

where $\overline{I}$ is half of the mean intensity sent by the source.

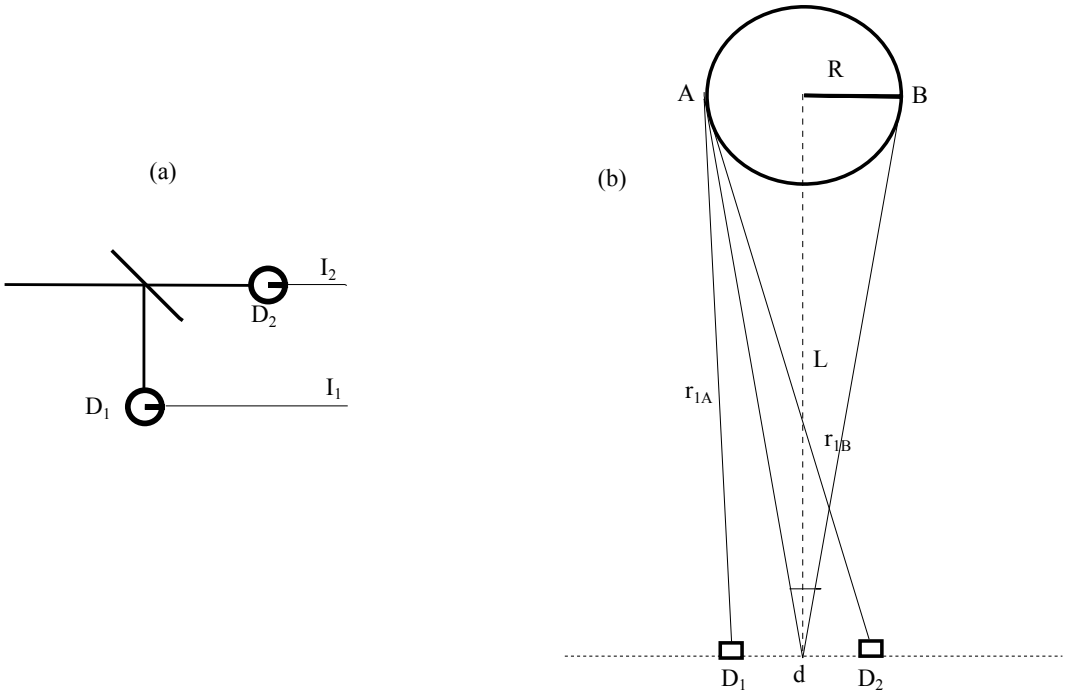

Figure 4.1: (a) An autocorrelation experiment for a simple source. (b) Geometry of the HBT experiment for the determination of stellar diameters.

At short times, and particularly for $\tau = 0$, the two recorded intensities are not independent. Indeed

$$G_2(0) = \overline{I^2} \ , \tag{4.73}$$

the average of the square intensity. Since

$$\overline{I^2} - (\overline{I})^2 = \overline{(I - \overline{I})^2} \geq 0 \ , \tag{4.74}$$

it follows that, for any classical source:

$$G_2(0) \geq G_2(\infty) \ . \tag{4.75}$$

The intensity autocorrelation function is a decreasing function of time. This can be interpreted simply. When the source has an intensity fluctuation above the average (simultaneous emission of two pulses for instance), this surge is equally split between the two detectors, recorded by both of them. The correlation is thus maximal for short times and the width of the maximum of the correlation function is clearly of the order of τ_c.

HBT in their Nature paper (**178**, 1046) had a different purpose. They wanted to measure the angular diameters of stars too small to be resolved by conventional astronomy. They thus installed two small telescopes at a distance d apart, pointing at the same star at a huge distance L (that we will assume to be at the zenith) (figure 4.1). They measured the intensities correlation function for a zero delay τ as a function of d. Why is it that it contains information about the star size? For that, we need to make a more precise calculation, yet in the classical framework.

Let us consider two emitting points on the extremities of a diameter of the star, A and B. Since the star is a quite classical source, these two points emit totally uncorrelated fields, with random instantaneous phases.

The envelope field received by D_1 is thus of the form:

$$E_1 = \alpha e^{ikr_{1A}} e^{i\phi_A} + \beta e^{ikr_{1B}} e^{i\phi_B} \ , \tag{4.76}$$

where r_{1A} and r_{1B} are the distances of the detector with the two emitting points, k is the wavevector of light and ϕ_A and ϕ_B are the time-dependent random phases of the field pulses emitted on both sides, which have an extremely short mutual correlation time τ_c. The factors α and β encapsulate all the geometrical and dimensional factors. Note that, since the phases are random,

$$\overline{I_1} = \overline{|E_1|^2} = |\alpha|^2 + |\beta|^2 \ . \tag{4.77}$$

A similar expression holds for E_2 of course

$$E_2 = \alpha e^{ikr_{2A}} e^{i\phi_A} + \beta e^{ikr_{2B}} e^{i\phi_B} \ . \tag{4.78}$$

Let us now compute the measured intensity correlation function at zero delay, $\overline{I_1(t)I_2(t)}$. By expressing it in terms of the instantaneous electric fields, replacing the fields by their detailed expression and expanding all squares and products, we do find a rather complex expression.

However, since we average on time, we should keep only those terms which do not involve a random phase. The computation is painful, but one gets at the end

$$\overline{I_1(t)I_2(t)} = \overline{I_1}\ \overline{I_2} + |\alpha|^2|\beta|^2 \cos\, k\,[r_{1A} + r_{2B} - r_{1B} - r_{2A}] \ . \tag{4.79}$$

For a symmetric configuration, when A and B are symmetric with respect to the mediating segment $D_1 - D_2$, $r_{1A} - r_{2A} = r_{2B} - r_{1B}$ and

$$\overline{I_1(t)I_2(t)} = \overline{I_1}\ \overline{I_2} + |\alpha|^2|\beta|^2 \cos\, 2k(r_{1A} - r_{2A}) = \overline{I_1}\ \overline{I_2} + |\alpha|^2|\beta|^2 \cos\, 2\frac{\omega}{c}(r_{1A} - r_{2A}) \ , \tag{4.80}$$

where ω is the field pulsation.

The zero-time intensity correlation signal thus varies simply (as a cosine) as a function of the difference of the light's flight time from A to detectors 1 and 2, a very simple result indeed. Calling R the star radius, Θ its angular diameter (see figure 4.1), we get

$$\overline{I_1(t)I_2(t)} = \overline{I_1}\ \overline{I_2} + |\alpha|^2|\beta|^2 \cos kd\Theta \ . \tag{4.81}$$

A measurement of the correlation function versus d thus provides a direct measurement of the star's diameter. The resolution is excellent and equivalent to the diffraction limit of an ideal telescope with a diameter d. In fact, the intensity correlation directly measures the difference between the time of flight of light from the star to the two detectors. The method is thus quite impervious to atmospheric perturbations. The only condition is that the time of flight perturbations induced by the atmospheric turbulence are less than the source correlation time. This is always the case, even at a low altitude.

Quantum intensity correlations

Let us now interpret the intensity correlation experiments from the quantum side. The single photodetector current is the average value of the product $E^- E^+$. We extend that to the correlation functions of the intensity received at time t in point $\mathbf{r}_1$ with the intensity received at time $t + \tau$ at point $\mathbf{r}_2$. Without further justification, let us admit that this correlation function writes

$$G_2(\mathbf{r}_1, \mathbf{r}_2, t, \tau) = \langle \Psi_f |\, \hat{G}_2\, | \Psi_f \rangle \ , \tag{4.82}$$

where we defined

$$\hat{G}_2 = E^-(\mathbf{r}_1, t) E^-(\mathbf{r}_2, t+\tau) E^+(\mathbf{r}_2, t+\tau) E^+(\mathbf{r}_1, t) \ . \tag{4.83}$$

If we take $\tau = 0$ and $\mathbf{r}_1 = \mathbf{r}_2$, it is clear for a single mode situation that $\hat{G}_2$ is proportional to $(a^\dagger)^2 a^2$.

We shall also define a normalized correlation function by

$$g_2 = \frac{G_2}{\overline{I_1}\ \overline{I_2}} \ , \tag{4.84}$$

where the denominator is made up of the product of the average intensities in $\mathbf{r}_1$ and $\mathbf{r}_2$.

Two field modes

Let us consider first the simple situation of two field modes, labelled 1 and 2 impinging at once on two detectors D_A and D_B located in $\mathbf{r}_A$ and $\mathbf{r}_B$[2]. This is the quantum version of the classical HBT experiment. The two modes correspond to the positive frequency fields (projected over the common polarization direction of the two detectors:

$$E_i^+ = \mathcal{E}_i e^{i(\mathbf{k}_1\cdot\mathbf{r}-\omega_i t)} a_i \ , \tag{4.85}$$

where the index i stands for 1 or 2. The total positive frequency component of the electric field is thus

$$E^+ = E_1^+ + E_2^+ \ . \tag{4.86}$$

We will assume that the field state is a tensor product of Fock states in each mode, $|\Psi\rangle = |N_1, N_2\rangle$.

We will consider two photo-detection signals: the simple photo-current detected at one of the detectors:

$$G_1(\mathbf{r}_A, t) = \langle\Psi| E^-(\mathbf{r}_A, t)E^+(\mathbf{r}_A, t) |\Psi\rangle \ , \tag{4.87}$$

and the two-point two-times correlation $G_2(\mathbf{r}_A, t_A, \mathbf{r}_B, t_B)$ defined above.

Let us first show that there can be no interference effect in the single-point single-time detection. Expanding in the expression of G_1 the fields in their components, we find four terms. Due to the orthogonality of the Fock states, these terms give a non-vanishing contribution to G_1 only when they conserve the photon number in each mode. The only surviving terms are proportional to $a_1^\dagger a_1$ and $a_2^\dagger a_2$. They give a contribution proportional to $N_1\mathcal{E}_1^2$ and $N_2\mathcal{E}_2^2$ respectively, and all phase factors cancel out. The total detection probability is thus merely the sum of the intensities of the two modes and there are no interference effect (this is due to the fact that the field state is a product of photon-number states, which contain no phase information).

Let us now write explicitly the G_2 correlation function. Once again, the only remaining terms in the expansion of the field operators must conserve the number of photons in each mode. Only four terms survive (with their obvious hermitian conjugates), with field operators proportional to $a_1^\dagger a_1^\dagger a_1 a_1$, $a_2^\dagger a_2^\dagger a_2 a_2$, $a_1^\dagger a_2^\dagger a_1 a_2$ and $a_2^\dagger a_1^\dagger a_2 a_1$. The first two terms have no phase factors and are proportional to $N_i(N_i-1)\mathcal{E}_i^4$. Only the two last terms can contribute to an interference effect. Indeed,

$$\langle\Psi| a_1^\dagger a_2^\dagger a_1 a_2 |\Psi\rangle + \text{h.c.} = 2\mathcal{E}_1^2\mathcal{E}_2^2 N_1 N_2 \text{Re}\left[e^{i[(\mathbf{k}_2-\mathbf{k}_1)\cdot(\mathbf{r}_A-\mathbf{r}_B)-(\omega_2-\omega_1)(t_A-t_B))]}\right] \ . \tag{4.88}$$

The other term has a similar expression. This term is obviously an interference one, sensitive to the phase difference of the relative mode phases at the two points of interest. One can check easily that the phase differences here are identical to those involved in the classical HBT experiment discussion. In fact, any quantum interference results from the coherent addition of the probability amplitudes linked to two indistinguishable quantum paths. Here, they correspond to one photon of mode 1 being detected in A while a photon of 2 is detected in B on the one hand, and one photon of 1 detected in B and one photon of 2 detected in A on the other hand. From an experimenter's perspective, those two paths cannot be distinguished if the frequency of the photons is not measured, and they interfere. See the Cohen-Tannoudji-Guéry-Odelin for an in-depth discussion.

Single emitter: anti-bunching

We now consider the spontaneous emission by a single atom and compute the two points and two times field correlation function. We will not give a fully detailed calculation, but only a qualitative discussion, which, nevertheless, captures all the essential phenomena. The experiment we have in mind is thus a single atom placed at the source location in the elementary HBT experiment.

[2]This discussion is derived from the Cohen-Tannoudji, Guéry-Odelin book.

Let us thus compute the correlation:

$$G_2(\mathbf{r}, 0, \mathbf{r}, \tau) \equiv G_2(\tau) \ , \tag{4.89}$$

which is clearly proportional to the probability for detecting a photon in $\mathbf{r}$ at time τ knowing that a photon has already been detected at the same point at time zero. Of course, this function would be identically zero if the atom is not excited by an external source. If this is not the case, it will emit a single photon, and there is no room for a second emission. We thus assume that there is some coherent pumping mechanism (continuous laser or trains of laser pulses) which repeatedly re-excites the atom.

We will use for this semi-qualitative computation an Heisenberg picture in which the operators depend upon time, the state being constant. We thus need the field operator $E^+(\tau)$ as a function of time. This field is produced by the atom through the $\mathbf{D} \cdot \mathbf{E}$ electric dipole coupling term. In the classical realm, the field radiated is proportional to the atomic dipole. In the quantum realm, we will thus admit that the positive frequency electric field operator E^+, which freely evolves as $\exp(-i\omega t)$ in the Heisenberg picture is proportional to the atomic dipole (which evolves at a similar frequency) or, more simply, to the operator $\sigma_-(\tau)$. Hence, the correlation is proportional to

$$G_2(\tau) = \langle \sigma_+(0)\sigma_+(\tau)\sigma_-(\tau)\sigma_-(0) \rangle \tag{4.90}$$

At the origin of time, $\sigma_-(0) = |g\rangle \langle e|$ and $\sigma_+(0) = |e\rangle \langle g|$. At time τ, $\sigma_\pm(\tau) = U^\dagger \sigma_\pm(0) U$, where U is the atomic evolution operator describing the pumping process. We can thus write

$$G_2 = \Big\langle |e\rangle \langle g| \, [U^\dagger \, |e\rangle \langle g| \, U][U^\dagger \, |g\rangle \langle e| \, U] \, |g\rangle \langle e| \Big\rangle \ . \tag{4.91}$$

We must here evaluate the average value in the initial atomic state, which is clearly $|e\rangle$(since a photon will be detected at time zero, the atom must be excited at that time). We thus have:

$$G_2(\tau) = | \langle e| \, U(\tau) \, |g\rangle \, |^2 \ , \tag{4.92}$$

a quite simple result (of course, computing U might be a more difficult problem, but we do not enter in it.

For $\tau = 0$, $U = \mathbb{1}$ and $G_2 = 0$. We get here the main result of this discussion. When a single atom is used as emitter, the field correlation at zero time is also zero. This is quite different from the classical HBT case, in which the correlation was always maximal at short times. The interpretation of the phenomenon is trivial. Once the atom has emitted a photon, it is in the ground state and cannot emit another photon before the pumping process (described by the evolution operator U) has promoted it again into $|e\rangle$. The photons emitted by an individual quantum emitter are thus 'anti-bunched' whereas the photons emitted by a classical source tend to be 'bunched' and to exhibit positive correlation at short times.

For longer times τ the evolution leads back to level $|e\rangle$ and the probability for observing the second photon raises. The correlation function raises and reaches, perhaps after some damped oscillations reflecting the Rabi oscillations of the atom in the pumping field, the asymptotic value of uncorrelated events.

The observation of this effect by Kimble and Mandel in 1977 (PRL 39, 691) is, together with the Hong Ou Mandel photon bunching on a beamsplitter one of the founding experiments of modern quantum optics. The anti-bunching effect is still widely used to assess the single-emitter nature of a quantum source.

4.4 The dressed atom model

We now examine an important situation, that of a single two-level atom strongly coupled to a single field mode. This ideal situation describes quite well the Cavity Quantum Electrodynamics (CQED)

experiments, as explained in the next Section. It is also a fair description of the coupling of an atom to a strong single-mode laser field, so strong that the coherent atom-field coupling overwhelms the dissipative processes, due for instance to spontaneous emission from the atomic exited levels.

We will see in this Section that this simple problem can be approached by an explicit, exact diagonalization of the atom-field Hamiltonian, introducing the so-called 'dressed states'. Proposed in the 60s by Claude Cohen-Tannoudji, they have been widely used since then. They are a mandatory step to treat the Cavity Quantum electrodynamics situation, in which the field mode only contains a few photons. They are also quite useful in the large field limit, since they lead to a simpler and more insightful solution than the Optical Bloch equations.

4.4.1 The atom-field eigenstates

Hamiltonian

The atom-field Hamiltonian simply reads:

$$H = H_a + H'_c + H_{ac} \ , \tag{4.93}$$

where H_a and $H'_c = \hbar\omega_c N$ are the atom and field Hamiltonians.[3]

Performing the rotating-wave approximation, the atom–cavity coupling term reduces to:

$$H_{ac} = -i\hbar\frac{\Omega_0}{2}\left[a\sigma_+ - a^\dagger\sigma_-\right] \ , \tag{4.94}$$

where we introduce the 'vacuum Rabi frequency' Ω_0:

$$\Omega_0 = 2\frac{d\mathcal{E}_0\boldsymbol{\epsilon}_d^*\cdot\boldsymbol{\epsilon}_c}{\hbar} \ , \tag{4.95}$$

where $\boldsymbol{\epsilon}_c$ is the field mode polarization unit vector. We assume, for the sake of simplicity, that $\boldsymbol{\epsilon}_d^*\cdot\boldsymbol{\epsilon}_c$ is real and positive, hence Ω_0.[4] The frequency Ω_0 measures the strength of the atom–field coupling. It is proportional to the interaction energy of the atomic dipole with a classical field having the r.m.s. amplitude of the vacuum.

Let us examine briefly the 'uncoupled' eigenstates of $H_a + H'_c$. They are the tensor products $|e,n\rangle$ and $|g,n\rangle$ of atomic and field energy states. Their energies are $\hbar(\omega_{eg}/2 + n\omega_c)$ and $\hbar(-\omega_{eg}/2 + n\omega_c)$. When the atom–field detuning:

$$\Delta_c = \omega_{eg} - \omega_c \ , \tag{4.96}$$

is equal to 0 or small compared to ω_c, the uncoupled states $|e,n\rangle$ and $|g,n+1\rangle$ are degenerate or nearly degenerate. The excited states of $H_a + H'_c$ are thus organized as a ladder of doublets, separated from each other by the energy $\hbar\omega_c$ (Fig. 4.2). The ground state $|g,0\rangle$, representing the atom in its lower state in the cavity vacuum, is the only unpaired state at the bottom of this ladder.

The nth excited doublet stores $n+1$ elementary excitations either as $n+1$ field quanta ($|g,n+1\rangle$) or as the sum of n photons added to one atomic excitation ($|e,n\rangle$). The operator $M = a^\dagger a + \sigma_+\sigma_-$, representing the total number of atomic and field excitations, commutes with H and is a constant of motion. The excitation number being conserved, the atom–field coupling H_{af} connects only states inside each doublet. The diagonalization of the full Hamiltonian, discussed in the next paragraph thus amounts to solving separate two-level problems.

[3] We take the vacuum as the zero energy for the field, getting rid of the $\hbar\omega_c/2$ offset. The field quantities are indexed with a c in anticipation of the Section on cavity quantum electrodynamics.

[4] If this is not the case, we can always make Ω_0 real positive by multiplying it by a proper phase term.

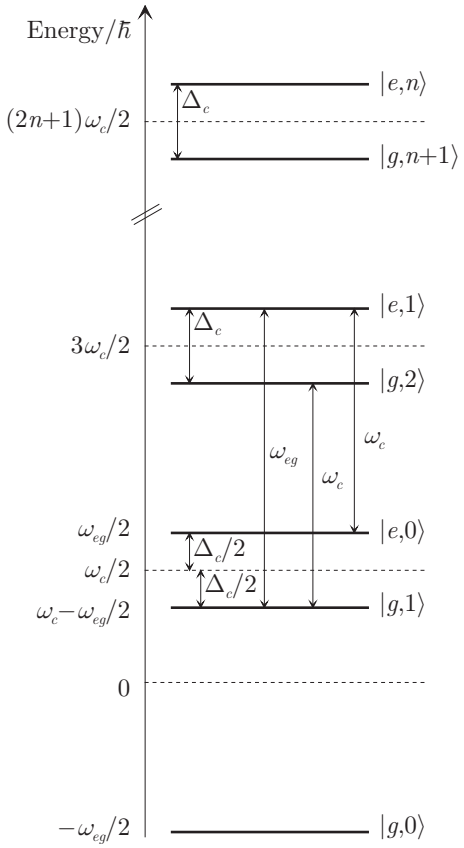

Figure 4.2: Uncoupled atom–cavity energy states in the case $\Delta_c > 0$. Apart from the ground state $|g, 0\rangle$, they form an infinite ladder of two-level manifolds separated by the field frequency ω_c. In each manifold, the states $|e, n\rangle$ and $|g, n + 1\rangle$ are separated by $\hbar\Delta_c$.

Eigenenergies and eigenvectors

Let us call H_n the restriction of the total Jaynes–Cummings Hamiltonian to the nth doublet. Introducing the 'n-photon Rabi frequency':

$$\Omega_n = \Omega_0\sqrt{n+1}\ , \tag{4.97}$$

we can write H_n in matrix form as:

$$H_n = \hbar\omega_c\,(n+1/2)\,\mathbb{1} + V_n\ , \tag{4.98}$$

with:

$$V_n = \frac{\hbar}{2}\begin{pmatrix}\Delta_c & -i\Omega_n\\ i\Omega_n & -\Delta_c\end{pmatrix} = \frac{\hbar}{2}[\Delta_c\sigma_Z + \Omega_n\sigma_Y]\ . \tag{4.99}$$

The diagonalization of H_n is thus formally identical to the determination of the eigenstates of a spin placed in a magnetic field whose components along OZ and OY are proportional to Δ_c and Ω_n. This fictitious field makes with Z the angle θ_n defined by:

$$\tan\theta_n = \Omega_n/\Delta_c\ . \tag{4.100}$$

This 'mixing angle', varying between 0 and π, is useful to express in a simple form the eigenstates of the atom–field system, which are represented in the $\{|e,n\rangle\,,|g,n+1\rangle\}$ basis by the same amplitudes as the $|0,1\rangle_{\theta_n,\varphi}$ spin states whose Bloch vectors point along the θ_n, $\varphi=\pi/2$ direction on the Bloch sphere. From this simple analogy, we deduce immediately that the eigenvalues of H_n are:

$$E_n^{\pm} = (n+1/2)\,\hbar\omega_c \pm \frac{\hbar}{2}\sqrt{\Delta_c^2+\Omega_n^2}\ , \tag{4.101}$$

with the corresponding eigenvectors:

$$\begin{aligned}|+,n\rangle &= \cos(\theta_n/2)\,|e,n\rangle + i\sin(\theta_n/2)\,|g,n+1\rangle\ ;\\ |-,n\rangle &= \sin(\theta_n/2)\,|e,n\rangle - i\cos(\theta_n/2)\,|g,n+1\rangle\ .\end{aligned} \tag{4.102}$$

These states, which are generally entangled, are called the 'dressed states' of the atom–field system.

The variation of the dressed energies as a function of Δ_c is represented in Fig. 4.3. For very large detunings, the dressed energies almost coincide with the uncoupled state energies $(n+1/2)\hbar\omega_c \pm \hbar\Delta_c/2$. At zero detuning, the uncoupled energy levels cross. The atom–cavity coupling transforms this crossing into an avoided crossing, the minimum distance between the dressed states being the coupling energy $\hbar\Omega_n$. We examine now in more detail two interesting limiting cases: the resonant case ($\Delta_c = 0$) and the 'large detuning case' ($\Delta_c \gg \Omega_n$).

4.4.2 Resonant case: Rabi oscillation induced by n photons

In the resonant case, the mixing angle is $\theta_n = \pi/2$ for all n values. The dressed states, separated by $\hbar\Omega_n$, are:

$$|\pm,n\rangle = [|e,n\rangle \pm i\,|g,n+1\rangle]\,/\sqrt{2}\ . \tag{4.103}$$

We have here a situation similar to two coupled degenerate oscillators, whose eigenmodes are the symmetric and anti-symmetric superpositions of the independent free modes. The eigenmode frequency difference corresponds then to the beating note in the correlated motion of the two oscillators. Here, the separation of the dressed states at resonance corresponds to the frequency of the reversible energy exchange between the atom and the field.

To be more specific, let us consider the simple case of an atom initially ($t=0$) in state $|e\rangle$, inside a cavity containing n photons. The initial state, $|\Psi_e(0)\rangle = |e,n\rangle$, expanded on the dressed states basis is:

$$|\Psi_e(0)\rangle = [|+,n\rangle + |-,n\rangle]\,/\sqrt{2}\ . \tag{4.104}$$

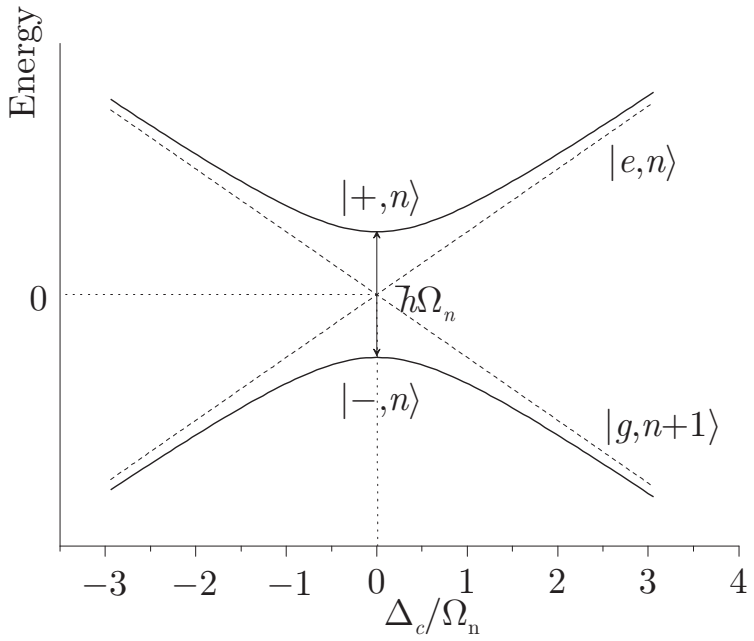

Figure 4.3: Dressed state energies as a function of the atom–cavity detuning Δ_c. The uncoupled state energies are represented as dotted lines.

We will describe the evolution of this state in the interaction representation with respect to the constant term $\hbar\omega_c(n+1/2)\mathbb{1}$ in eqn. (4.98). At time t, $|\Psi_e(0)\rangle$ becomes:

$$\left|\widetilde{\Psi}_e(t)\right\rangle = \left[|+,n\rangle\, e^{-i\Omega_n t/2} + |-,n\rangle\, e^{i\Omega_n t/2}\right]/\sqrt{2}\ . \tag{4.105}$$

The probabilities of finding the atom in $|e\rangle$ or $|g\rangle$ are obtained by reverting to the uncoupled basis:

$$\left|\widetilde{\Psi}_e(t)\right\rangle = \cos\frac{\Omega_n t}{2}\,|e,n\rangle + \sin\frac{\Omega_n t}{2}\,|g,n+1\rangle\ . \tag{4.106}$$

Similarly, if the atom is initially in state $|g\rangle$ in a cavity containing $n+1$ photons,[5] the combined atom–field state at time t is:

$$\left|\widetilde{\Psi}_g(t)\right\rangle = -\sin\frac{\Omega_n t}{2}\,|e,n\rangle + \cos\frac{\Omega_n t}{2}\,|g,n+1\rangle\ . \tag{4.107}$$

The atom–field coupling results in a reversible energy exchange between $|e,n\rangle$ and $|g,n+1\rangle$ at frequency Ω_n. This is the quantum version of the Rabi oscillation phenomenon which can be understood as a 'quantum beat' between the two dressed states.

For the initial state $|e,0\rangle$ (or $|g,1\rangle$), this oscillation occurs at the frequency Ω_0, hence the name of vacuum Rabi frequency coined for this parameter. This situation will be described in details in the next Section about CQED As the coupling of two field modes by a beam-splitter, the Rabi oscillation produces in general an entanglement (eqns. 4.106 and 4.107).

For a mesoscopic coherent field, with an average photon number $\overline{n}$ of a few units, the Rabi oscillations signal involves a sum of components at the frequencies Ω_n. The resulting signal is surprisingly complex, with a collapse of the oscillations due to the field amplitude dispersion, and a revival at long times due to the quantization of the amplitude. These phenomena will be discussed in the next Section also.

[5]Note that an atom in $|g\rangle$ does not evolve in the cavity vacuum since the state $|g,0\rangle$ is an eigenstate of the full atom–field Hamiltonian.

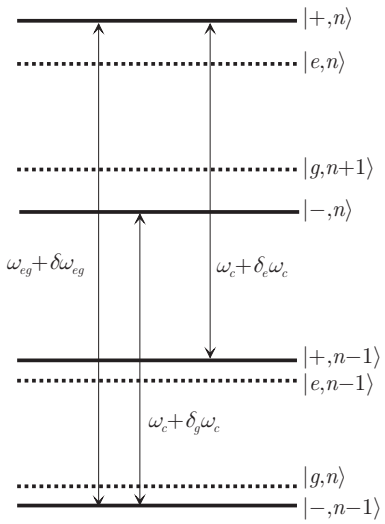

Figure 4.4: Dressed state energies in the far-detuned case for two adjacent manifolds. The effect of the non-resonant interaction is a slight shift of the atom–field energy levels. This results in atomic transition and field mode frequency shifts, illustrated by the vertical arrows.

Let us examine the case of a large classical field, represented by a coherent state with a very large average photon number $\overline{n}$. The relative dispersion of the photon number, $1/\sqrt{\overline{n}}$ is the extremely small, and all dressed atoms multiplicities have nearly equal splitting, $\Omega_{\overline{n}} = \Omega_0\sqrt{\overline{n}}$ (we can safely neglect 1 in front of $\overline{n}$). All evolutions in all the nth doublets are exactly the same and we recover the classical result, a simple sinusoidal Rabi oscillation between $|e\rangle$ and $|g\rangle$ at the frequency $\Omega_{\overline{n}}$. In other words, for all practical purposes and as far as only the Rabi oscillation is concerned, a large coherent state can be assimilated to a Fock state.

Of course, even in a large Fock state, the Rabi oscillation would entangle the atom and the field ($|n\rangle$ and $|n+1\rangle$ are always orthogonal). This entanglement is an artefact of assimilating the coherent state with a Fock state. Adding or subtracting a single photon to a large coherent state does not appreciably modify it. The field can thus be taken out of the dynamics evolution, and the dressed states are reduced to two atomic superposition states, $(|e\rangle \pm i\,|g\rangle)\sqrt{2}$, eigenstates of the coupling Hamiltonian with the classical field. We obviously retrieve in this way the formalism of Chapter 2.

4.4.3 Non-resonant coupling and single-atom index effects

Remarkable phenomena, which can be interpreted as single-atom refractive index effects, are also expected when the atom and the field are not at resonance. Exact expressions of the atom–field eigenstates and energies are given by eqns. (4.101) and (4.102) for an arbitrary detuning Δ_c. Rather than discussing these general expressions, we focus here on the large detuning case, for which a perturbative treatment leads to simple formulas with a clear physical interpretation. A mere inspection of Fig. 4.3 shows that for $|\Delta_c| \gg \Omega_n$ the dressed levels tend towards the uncoupled ones. When $\Delta_c \to +\infty$, we deduce from eqn. (4.100) that $\theta_n \to 0$, entailing that $|+,n\rangle \to |e,n\rangle$ and $|-,n\rangle \to -i\,|g,n+1\rangle$ (eqn. 4.102). These conclusions are reversed for large negative detunings: when $\theta_n \to \pi$, $|+,n\rangle \to i\,|g,n+1\rangle$ and $|-,n\rangle \to |e,n\rangle$.

Since the dressed states almost coincide with the uncoupled ones, the probability of an atomic transition accompanied by photon absorption or emission is negligible, as expected from an energy conservation argument in this off-resonant situation. The energies of the dressed states are however slightly different from the uncoupled ones, as seen on Fig. 4.3. These energies can be expressed

by expanding eqn. (4.101) to lowest order in powers of the small parameter Ω_n/Δ_c (for the sake of definiteness, we assume from now on $\Delta_c > 0$):

$$E_n^{\pm} = (n + 1/2)\,\hbar\omega_c \pm \hbar\left(\frac{\Delta_c}{2} + \frac{\Omega_n^2}{4\Delta_c}\right) . \tag{4.108}$$

Figure 4.4 shows the effect of this energy shift on two adjacent doublets of the atom–field system. In each doublet the level spacing is slightly increased, the effect being larger in the upper one. More quantitatively, the shifts $\Delta_{e,n}$ and $\Delta_{g,n}$ of the states $|e, n\rangle$ and $|g, n\rangle$ are:

$$\Delta_{e,n} = \hbar(n + 1)s_0 \; ; \qquad \Delta_{g,n} = -\hbar n s_0 \; , \tag{4.109}$$

with:

$$s_0 = \frac{\Omega_0^2}{4\Delta_c} . \tag{4.110}$$

These shifts, which affect globally the atom–field states, can be given complementary physical interpretations, depending upon which of the two interacting subsystems we are observing. They correspond to reciprocal changes of the atomic transition and field mode frequencies.

The atomic transition frequency measured in a field containing n photons is equal to $1/\hbar$ times the energy splitting between levels $|g, n\rangle$ and $|e, n\rangle$ (Fig. 4.4). It is thus shifted from its free-space value by:

$$\delta\omega_{eg} = (2n + 1)s_0 . \tag{4.111}$$

This shift is the sum of two contributions. The first one, $2ns_0$, is proportional to the photon number n. It corresponds to the so-called light shift. The second contribution in eqn. (4.111), equivalent to the light shift produced by 'half a photon', is observed in the vacuum. It is a Lamb shift effect, due to the coupling of the excited atomic level to the vacuum fluctuations in the mode.

The Lamb shift effect is usually very weak and can be observed only in the CQED context. The light shifts in intense laser fields are much larger. They are the basis for the so-called 'dipole force' trapping of cold atoms. An intense laser beam, detuned on the red of the atomic resonance, is tightly focused on cold atoms in their ground state $|g\rangle$. The light shift of this level is negative. The energy is thus minimum at the maximum of the field intensity. The light shift is an effective conservative potential for the atomic motion. In simple terms, the atoms in the ground state are attracted and trapped near a field intensity maximum, hence at the focal spot of the laser beam. The trapping depth can reach rather high values, well in the mK range. Dipole traps are widely used for atomic sample manipulations and Bose Einstein condensation. Note that the phenomenon is reversed for a blue-detuned laser, the atoms being then expelled from the high-field regions. Proper combinations of red and blue detuned fields can be used to tailor interesting potentials, in particular in the immediate vicinity of very thin optical fibres.

Optical lattices are a variant. Atoms in a three-dimensional standing wave light field experience a periodic trapping potential. The atoms thus behave as particles in solid state, also subjected to a 3d periodic potential. In this respect, optical lattices can be viewed as a quantum simulator for the exploration of complex quantum phenomena.

The dressed levels shifts, viewed from the field perspective, correspond to a change of the field mode frequency. When an atom in level $|e\rangle$ interacts non-resonantly with the field, the $|e, n\rangle$ levels corresponding to different n values are equidistant, with a spacing $\hbar(\omega_c + s_0)$ (Fig. 4.4). This means that the field frequency is offset from ω_c by:

$$\delta_e\omega_c = s_0 . \tag{4.112}$$

For an atom in level $|g\rangle$, the $|g, n\rangle$ to $|g, n + 1\rangle$ spacings are $\hbar(\omega_c - s_0)$, independent of n. The mode frequency is thus displaced by an opposite amount:

$$\delta_g\omega_c = -\delta_e\omega_c = -s_0 . \tag{4.113}$$

These shifts have a transparent interpretation in terms of refractive index. The atom, which cannot absorb or emit light in the detuned mode, behaves as a piece of transparent dielectric. It plays the same role as the dielectric plungers used to tune cavities in microwave equipment. The atomic index changes the mode frequency. This effect is dispersive (frequency dependent) and s_0 has the same sign as Δ_c.

Standard optical index of refraction is certainly rooted in these shift effects. It is nevertheless a much more complex phenomenon, since it involves dense matter (interatomic interactions are non negligible) and since the atoms can barely be considered as two-level systems. However, again, the CQED context allows one to observe and use these dispersive effects.

4.4.4 Two applications

Autler-Townes splitting

We return here to the discussion of Section 2.6.3. We consider a three-level system, with two long-lived levels $|g\rangle$ and $|f\rangle$, both connected to an excited state $|e\rangle$ by two electric dipole transitions with quite different frequencies. The $|g\rangle \to |e\rangle$ transition is addressed by a strong resonant laser. A much weaker probe beam explores the spectrum of the $|f\rangle \to |e\rangle$ transition dressed by the intense laser. Obviously, the $|f\rangle$ level is not affected by the dressing laser (which is far from resonance with the $|f\rangle \to |e\rangle$ transition).

The strong dressing laser is in a coherent state with a large average photon number. As shown above, it can be assimilated to some extent to a Fock state $|n\rangle$. The uncoupled levels are thus replaced by the dressed states $|\pm, n\rangle$, superpositions with equal weight of $|e, n\rangle$ and $|g, n+1\rangle$, separated in energy by $\hbar\Omega_n$. The level $|f, n\rangle$ (atom in level $|f\rangle$ with n photons in the dressing laser) is coupled to the level $|e, n\rangle$ by the probe laser (which can change the atomic level, but not the photon number in the dressing laser). Hence, both the dressed states $|\pm, n\rangle$ are coupled to $|f, n\rangle$ by the probe laser (albeit with a matrix element reduced by a factor $1/\sqrt{2}$).

The spectrum of the $|f\rangle \to |e\rangle$ transition, instead of a single line at the naked atomic frequency, is thus made of two (ideally infinitely narrow) lines separated by the dressing Rabi frequency Ω_n and centered on the naked atomic frequency. This is the Autler-Townes splitting, which can be viewed as a direct spectral counterpart of the temporal Rabi oscillation. Of course, this spectrum can be computed from the solution of the optical Bloch equations, as mentioned in Chapter 2. However, the dressed atom approach in much simpler.

We predict here infinitely narrow lines, since we have not included any relaxation process. A proper treatment of spontaneous emission in the dressed atom picture will be outlined in the next paragraph. We leave to the reader as an exercise to extend it to the present situation and to show that the two components of the Autler-Townes splitting are equally widened by spontaneous emission.

Mollow fluorescence triplet

We are interested here in the spectrum of the fluorescence emitted by the atom under a strong laser drive, observed for instance by collecting the light emitted in a direction different from that of the dressing mode.

We thus clearly need to incorporate spontaneous emission in the picture. As for a free atom, the jump operator in the Lindblad equation must be $\sqrt{\Gamma}\sigma_-$, where Γ is the spontaneous emission rate and $\sigma_- = |g\rangle\langle e|$, which transforms $|e, n\rangle$ into $|g, n\rangle$. The atomic lowering operator thus acts on the dressed states as $\sigma_- |\pm, n\rangle = |g, n\rangle$. Since both dressed levels $|\pm, n-1\rangle$ involve the uncoupled level $|g, n\rangle$, fluorescence-induced quantum jumps may occur on all four transitions between $|\pm, n\rangle$ and $|\pm, n-1\rangle$. The transitions between the two + and the two − levels are at the naked atomic frequency ω_{eg}. The 'crossed' transitions $|\pm, n\rangle \to |\mp, n-1\rangle$ are at $\omega_{eg} \pm \Omega_n$ (we can neglect the variation of the Rabi frequency between the two adjacent multiplicities).

The dressed atom spontaneous emission can thus be viewed as a sequential cascade through the ladder of dressed states (which can be viewed as infinite since the photon number dispersion is much larger than unity in a strong coherent field and also since the laser source renews constantly the photons in the dressing mode as they are scattered by the atom).

The spectrum of fluorescence is thus made of three lines (hence the name Mollow triplet), one at the naked frequency and two sidebands. It is quite clear from the above discussion that the central line is about twice more intense than the sidebands. A detailed calculation of the weights and widths of the three Mollow triplet lines can be performed based on the Lindblad equations. We refer the interested reader to the Cohen-Tannoudji's textbook *Photons and atoms*.

Another effect can be readily predicted from the dressed atom picture. Once the atom has emitted a photon on the lower sideband, it is left for sure in the $|+, n-1\rangle$ level. From there, the next photon can never be emitted in the lower sideband again since this sideband originates from the $-$ dressed states. The photons in the two sidebands have thus a negative time correlation (anti-bunching). This effect is very easily predicted in the dressed atom picture and can be exactly computed. It is considerably less evident in the optical Bloch equations frame.

We have discussed in this section two applications of the dressed atom picture. There are many others, and this approach is most certainly the most fruitful one in quantum optics.

4.5 Cavity Quantum electrodynamics

The final Section of this Chapter deals with the Jaynes and Cummings model (1963), a fair and precise description of a Cavity Quatum Electrodynamics situation, when an atom is placed inside a high-quality nearly resonant cavity. The coherent interaction of the atom with the field can then overwhelm the dissipative processes. This very active domain is interesting, for its applications, but also because it leads to direct illustrations of the quantum postulates and to new light shed onto the quantum nature of the fields.

The large number of experimental figures and of schemes and drawings makes it easier to give the lectures as a slides presentation. These lectures notes will thus be replaced, for this final section, by the handouts of the slides.